Morphological models for IRM

Rhine branches 1D

Deltares

Morphological models for IRM
Rhine branches 1D

Authors

Victor Chavarrias

Marcela Busnelli

Kees Sloff

Deltares

Morphological models for IRM
Rhine branches 1D

Client	Rijkswaterstaat Water, Verkeer en Leefomgeving
Contact	Ralph Schielen
Reference	11203684-015-ZWS-0011_v1.0
Keywords	Rijntakken, morphodynamic model, one-dimensional

Document control

Version	0.1
Date	2020-12-11
Project number	11203684-015
Document ID	11203684-015-ZWS-0011
Pages	175
Status	Final

Author(s)

	Victor Chavarrias	Deltares
	Marcela Busnelli	RHDKV
	Kees Sloff	Deltares

Doc. version	Author	Reviewer	Approver	Publish
0.1	Victor Chavarrias	Willem Otte-vanger		
	Marcela Busnelli			
	Kees Sloff			
1.0	Victor Chavarrias	Willem Otte-vanger	Johan Boon	
	Marcela Busnelli		Gerard Blom	
	Kees Sloff			

Deltares

Executive summary

The Dutch Rhine River branches (*Rijntakken*) provide, among other things, for drinking water to millions of citizens and with a means of transportation. At the same time, the rivers pose a continuous threat to life in the Netherlands. *Rijkswaterstaat* is responsible for managing the river system and facilitating all of its functions. This is a difficult task that *Rijkswaterstaat* has done for centuries.

Until recently, river maintenance was mainly concerned with single-function interventions to, for instance, improve the river's navigability or reduce flood risk. This type of interventions framework has the negative consequence that an improvement in one function may not be beneficial for another function or service. For this reason and having in mind the long-term impact of interventions, *Rijkswaterstaat* has devised an Integral River Management (IRM) programme. This programme develops the necessary policy for providing both short-term and long-term solution to river problems from a multidimensional and multidisciplinary point of view, contrary to past single-function interventions.

The IRM programme requires a tool to evaluate the long-term and large-scale morphological effects of river interventions as well as the impact of different future scenarios related, for instance, to climate change. To help *Rijkswaterstaat* in gaining insight into the morphological impact of river interventions, a numerical model of the *Rijntakken* is built.

The model is one-dimensional and uses the D-HYDRO SUITE . It comprises the Dutch Rhine River branches and downstream part of the German Rhine. The upstream end of the domain is found at the confluence of the Lippe with the Rhine at Wesel (Germany, Rhine kilometre 815). The downstream ends of the domain are found at Hardinxveld, Krimpen aan de Lek, and the Ketelmeer. The model stems from combining the official SOBEK 3 schematizations of the *Rijntakken* and an existing model, also in SOBEK 3 , of the German Rhine. These models have been built for hydrodynamic studies and need to be adjusted for being suitable to predict morphodynamic changes.

In a first step, the hydrodynamic parameters of the models are calibrated. This is done by comparing water level, velocity at the main channel, and discharge partitioning at the bifurcations with WAQUA two-dimensional results on steady-state hydrodynamic simulations. The calibrated model is extended with morphodynamic parameters based on the SOBEK-RE schematization by Sloff (2006). The morphodynamic parameters are then calibrated by comparing bed-level changes in the period 1995-2011. Afterwards, the model is validated against morphodynamic development between 2011 and 2019.

Deltares

Contents

Morphological models for IRM
11203684-015-ZWS-0011_v1.0, Version 0.1, 2020-12-11, Final

Deltares

List of Figures

Deltares

Deltares

Deltares

Deltares

Deltares

Deltares

1   Introduction

1.1   Background

The Integral River Management programme (IRM) requires a tool to evaluate the long-term and large-scale morphological effects of proposed interventions and changes in forcings in the Rhine branches in the Netherlands (*Rijntakken*), such as climate change, and changes in upstream sediment composition. *Rijkswaterstaat* has commissioned Deltares to develop a morphological model using the one-dimensional version of the D-HYDRO SUITE (D-FLOW FM 1D). The immediate use of the model is for the PlanMER phase of the IRM program, where interventions are tested and evaluated for policy decisions regarding erosion and sedimentation of the river bed and discharge capacity of the river. The time scale of these developments is in the order of 30 years (until 2050), considering spatial scale in the order of several or tens of kilometers. The model is only meant for morphodynamics of the main- channel of the Rijntakken. For hydrodynamic assessments the current SOBEK 3 or WAQUA model is currently still the model which can best be used. This document describes the construction, calibration and verification of the morphodynamic model.

1.2   Outline

The document is organized as follows. In Section 2, the methodology is explained. The methodology consists of three steps: model set-up (Section 3), hydrodynamic step (Section 4), and the morphodynamic step (Section 5). In Section 6 we conduct a sensitivity analysis of the results. The discussion of the results and obtained conclusions are presented in sections 7 and 8, respectively.

1.3   Software

DELFT3D FM SUITE refers to the software integrating all modules for modelling hydrodynamics, morphodynamics, water quality, real time control of structures, etcetera, in 1D, 2D, and 3D on unstructured grids. An unstructured grid can be curvilinear, as it is necessary for using the predecessor DELFT3D 4 . D-HYDRO SUITE is equivalent to DELFT3D FM SUITE and it is the preferred naming in the Netherlands.

D-FLOW FM, D-MORPHOLOGY, and D-REAL TIME CONTROL (shortened as D-RTC) are the modules in D-HYDRO SUITE for water flow, morphodynamics, and real time control of structures, respectively.

The model described in this report is developed using the one-dimensional features available in D-HYDRO SUITE and it uses the modules D-FLOW FM, D-MORPHOLOGY, and D-REAL TIME CONTROL. For the sake of simplifying the naming, in the rest of the report we will refer to it as D-FLOW FM 1D software system.

Previous 1D morphology models for the Rhine branches were developed about 15 years ago (Sloff, 2006) and used the SOBEK-RE (River-Estuary) modelling system. SOBEK-RE is not to be confused with the similarly named SOBEK-RUR software systems, which have been further developed for hydrodynamic simulations over the past decades ultimately resulting in SOBEK 3 . From the numerical point of view,

Deltares

SOBEK-RE and D-FLOW FM 1D are completely different. For instance, the grid in SOBEK-RE is collocated while staggered in D-FLOW FM 1D . A key difference between SOBEK-RE and SOBEK-RUR (and by extension SOBEK 3 and D-FLOW FM 1D) is that SOBEK-RE has an implicit steady-state flow solver in which the time step is not restricted by the flow celerities. On the contrary, the explicit scheme employed in D-FLOW FM 1D causes the time step to be limited by the fastest flow celerity. When modelling morphodynamic changes, the timescale of interest is related to changes in the bed, which are orders of magnitude smaller than change in flow. Hence, an efficient steady-state solver is useful for reducing the computational time. Moreover, the numerical scheme of the morphodynamic equations in SOBEK-RE is of higher order than the one in D-FLOW FM 1D , which implies that less cells are needed for obtaining the same accuracy. While D-FLOW FM 1D does not have the advanced morphological module of SOBEK-RE , SOBEK-RE cannot be coupled to two-dimensional models, as it is possible in D-HYDRO SUITE .

At present (2020), all 1D, 2D and 3D modelling tools at Deltares are migrated to D-HYDRO SUITE , which will contain identical solvers and GUI for the 1D as well as for the 2D/3D software. All operational models of *Rijkswaterstaat* will operate in D-HYDRO SUITE software in the future. The morphology module of D-HYDRO SUITE (i.e., the one used in this report) is identical to that of DELFT3D 4 , with a much more extensive functionality than SOBEK-RE . However, during this project the support for the morphology module was in "alpha status", and much development has been done.

In this report, the final simulations have been conducted using the DIMR set 2.12.01 (version 66638) which runs the D-Flow FM version 1.2.102.66429M, and FBC version 1186 on a Windows operating system using a single core.

1.4   New models developed within this project

This report covers the construction and test results of the following models:
•   `dflowfm1d_dmor-Rijn-j19-v1`
•   `dflowfm1d_dmor-Rijn-j11-v1`
•   `dflowfm1d_dmor-Rijn-j95-v1`

The naming convention is `<software system>-<region>-<schematisation>-<version>`:
•   `dflowfm1d_dmor`: The models are constructed using the 1D component of D-HYDRO SUITE in combination with the D-MORPHOLOGY and D-RTC modules. As the main purpose of the model is morphodynamic prediction, `dmor` is added to the name.
•   `Rijn`: The river system for which they are developed.
•   `j19, j11, j95`: Each model is built using the geometry describing the state of the river system in the high water season of a certain year. E.g., j19 refers to the high water season 2019-2020.The exception is j95 which refers to the geometry during the high discharge in January/February 1995.
•   `v1`: This is the first version of the models. Subsequent changes to the model will be given a new version number. Changes to the previous version will be documented separately.

Deltares

1.5 Data sources used in this project

The following sources of data have been used during the project:

- Hydraulic measured data for the period 1995-2020 obtained from Rijkswaterstaat (waterinfo website):
  - Time series of discharges at Lobith.
  - Time series of water elevation at Hardinxveld, Krimpen, Keteldiep, Kattendiep,
- Flow velocities and water levels derived from WAQUA simulations.
- Bed topography schematisations of the years 1995, 2011, and 2019 converted from the SOBEK 3 schematisations that have been transferred from BASELINE and WAQUA using WAQ2PROF .
- Grain size distribution from the SOBEK-RE schematization (Sloff, 2006). Data for the Dutch part of the river system is derived from measurements made in 1995 by averaging the measurements in a cross-section and window-average in the streamwise direction using a 20 km long window. The date of the data for the German part of the River system is unspecified and required processing by assuming a lognormal distribution.
- Estimated annual sediment transport load from Frings et al. (2019).

1.6 Application disclaimer

Each of these models are developed for simulation of long-term morphological evolution of the channel bed, which includes the simulation of sediment transport, erosional and depositional trends with a length scale of more than a few kilometres. Accuracy of simulation results is strictly limited to the conditions and data-accuracy under which the model was tested, or can be reasonably expected, as described in this report.

The models are not developed for hydraulic applications (flow routing, water depths, water levels), detailed local morphological studies (scale in the order of hundred meters or less) or floodplain sedimentation.

1.7 Team composition

The project has been carried out by dr. ir. V. Chavarrias, dr. ir. M. Busnelli (RHDHV), and dr. ir. C. J. Sloff. Dr. ir. W. Ottevanger had a reviewer role and dr. ir. A. Spruyt has been the project leader.

The client was represented by dr. R. M. J. Schielen (*Rijkswaterstaat*, WVL).

Deltares

2 Methodology

For the sake of predicting hydrodynamics (water levels, flow velocities, discharges, etc.), *Rijkswaterstaat* possesses hydrodynamic models of the *Rijntakken* in 2D and 1D. These models are built using WAQUA and SOBEK 3 , respectively. The starting point of the final morphodynamic model is the most recent SOBEK 3 schematisation of 2019 `sobek-rijn-j19`.

In a first step, the schematisation is converted to D-FLOW FM 1D . Several adjustments are necessary, which are described in Section 3.

For an accurate prediction of morphodynamic development it is necessary to capture only hydrodynamic features that are essential for sediment transport and sediment-transport gradients in space and time. The flow velocity in the main channel and the discharge distribution in the main channel are of high importance for modelling the morphological developments with varying discharges. For this reason, our objective is not to calibrate the model following the standard (time consuming) procedure using OpenDA but to obtain a model that captures the essential hydrodynamic components. The evaluation of the D-FLOW FM 1D model results is done by comparing results to the WAQUA 2019 results for constant discharges, as there are expected to be the most accurate results available. This hydrodynamic step is conducted in Section 4.

In order to develop the morphological component of the model, we make use of the latest one-dimensional morphodynamic model of the *Rijntakken* developed by Sloff (2006) using SOBEK-RE . This study provides grain size dependent morphodynamic parameters starting from the confluence between the Ruhr and the Rhine (Rhine kilometre 781). There are three SOBEK 3 model schematisations available for this study representing the state of the years 1995, 2011, and 2019. The upstream boundary of the models is situated in the Boven-Rijn (Rhine kilometre 862). This location is too close to the area of interest. For this reason, the models need to be extended. This is done by coupling the models to an exiting SOBEK 3 model from the German Rhine (Becker, 2017). The bed level of the main channel approximately represents the situation in 2012, although the year slightly varies along the reach depending on the availability of data.

Ideally, one would select independent and sufficiently long calibration and verification periods of time. However, there are some limitations in following this approach. The first limitation is that large river interventions (e.g., Room for the River, RvR) have been carried out. The second limitation is that there exist a SOBEK 3 schematisation representing the state in 1995 but the next one available represents the state in 2011. Due to these limitations, it has been decided to differentiate between long-term morphological trends and local impact of interventions in the calibration and verification:

- First set of simulations for long-term morphology (16 years) using the flow hydrograph of the period 1995 - 2011.
  - Simulation with initial cross-section schematisation 1995.
  - Simulation with initial cross-section schematisation 2011.
- Second set of simulations for local impact of interventions using the flow hydrograph of the period 2011-2019.
  - Simulation with initial cross-section schematisation 2011.

Deltares

– Simulation with initial cross-section schematisation 2019.

The first simulations will be used to calibrate the large-scale trends as obtained from recent analyses (for periods of 10 to 20 years). It is not possible to introduce the major Room for the River interventions gradually into the schematisation during the period between 1995 and 2011, as these imply a change of the cross-sectional shape. Therefore, it has been chosen to run simulations without the measures (1995 cross-sections) and with all the measures (2011 cross-sections) to be able to separate the effects of these measures from the large-scale (autonomous) trends. The analysis should account for additional uncertainties from the transition from single beam to multibeam measurements (around 2000) and gradual changes in trends at branches between 1995-2011 (bed-level degradation has reduced at the end of this period). Note that, besides closed-balance dredging (maintenance dredging with dumping in a nearby location) there has not been any dredging for sediment removal in this period in the considered reaches, except for the Beneden Waal and Merwedes.

The second simulations will provide an opportunity to verify the trends and can be used to fine tune local developments related to RvR measures. As the impacts of measures after 2011 (such as longitudinal dams and groyne lowering) cannot be captured in the run using the schematisation of 2011, there is a need to run a simulation using the schematisation of 2019 and analyse the results in a similar manner as in the first step. The morphodynamic step is shown in Section 5.

Deltares

3 Model setup

As explained in the methodology (Section 2), four SOBEK 3 schematisations need to be converted to D-FLOW FM 1D that represent the *Rijntakken* in 1995, 2011, and 2019 and the German Rhine. The steps to convert the simulations are:
- Simplification of the SOBEK 3 schematisations.
- Merging of the German Rhine to *Rijntakken* models.
- Conversion from SOBEK 3 to D-FLOW FM 1D .
- Model straightening.
- Friction adjustment.
- Main channel width adjustment.
- Storage area adjustment.

These steps are described in the following sections.

3.1 Simplification of the SOBEK 3 schematisations

All SOBEK 3 schematisations are converted to version 3.19.39355. Various changes to the official SOBEK 3 versions of the German and *Rijntakken* are conducted for the sake of simplifying the models. Moreover, certain features in SOBEK 3 are not available in D-FLOW FM 1D . In particular, the changes are:
- A single branch has been left in the German Rhine.
- The space step of the German Rhine has been increased to approximately 500 m, as in the *Rijntakken*.
- High-water channels (*Hoogwater geulen*) and its structures have been removed.
- The features "extra resistance" have been removed.
- The Amsterdam-Rijn Kanaal has been removed.
- Retention areas have been removed.
- The real time control (RTC) parameters for the steering of weirs are corrected. It appears that the parameters of the 2011 schematisation were not correct. The RTC control of 2019 has been used in all models.

3.2 Merging of the German Rhine to *Rijntakken* models

The merge of the models is done in SOBEK 3 . First, the German Rhine is converted to the same coordinate system as the *Rijntakken*, this is RD New Amersfoort (EPSG: 28992). A node is added in the German Rhine at the location of the upstream end of the *Rijntakken*. The branch of the German Rhine downstream of that node is removed. The branches of the German Rhine upstream from the confluence of the Lippe and the Rhine (Rhine kilometre 815) are removed and the models are merged (Figure 1).

Deltares
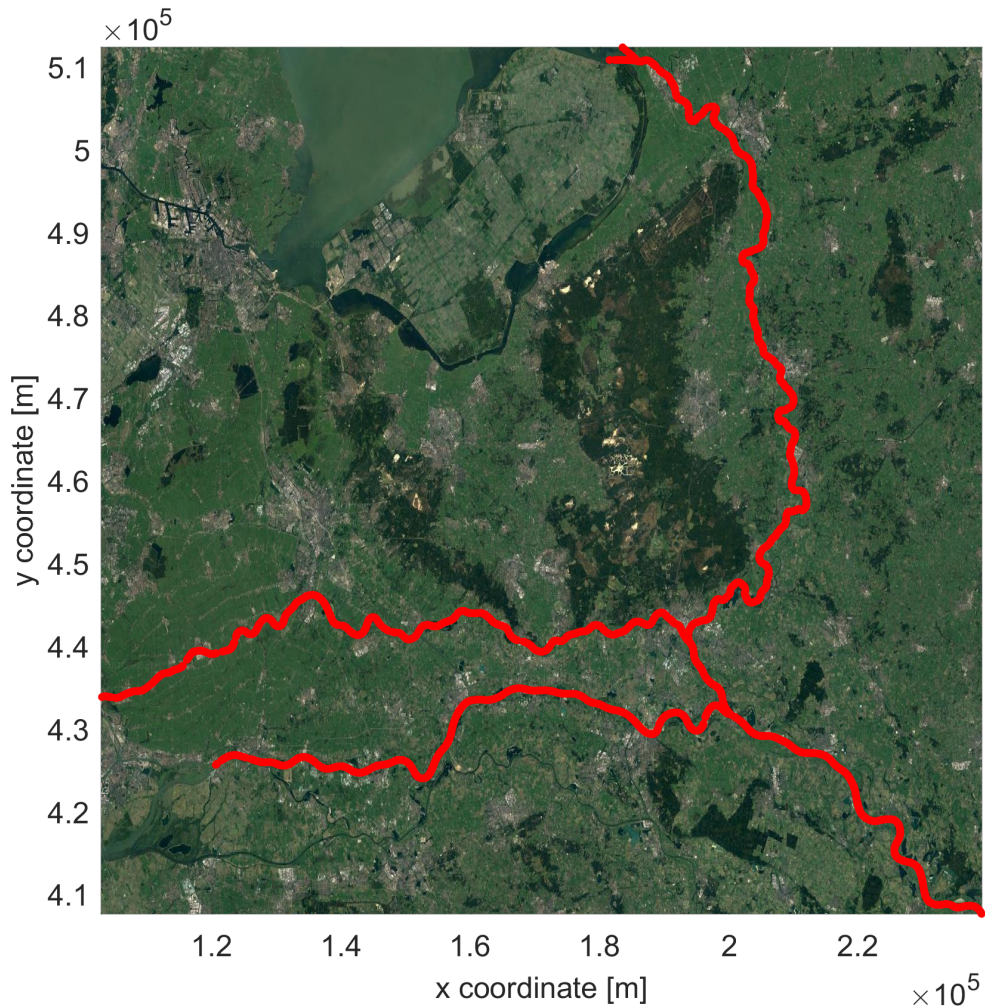
Figure 1 Resulting network.

3.3 Conversion from SOBEK 3 to D-FLOW FM 1D

The SOBEK 3 model is an integrated model, which consist of a flow model and an RTC model. The RTC model can be copied without conversion from SOBEK 3 . The flow model and integrated model (configuration xml file) needs to be converted to D-FLOW FM 1D .

The conversion of the flow model from the SOBEK 3 model is performed using the conversion script which is found in the repository https://svn.oss.deltares.nl/repos/openearthtools/trunk/python/applications/delft3dfm/convert_to_dflowfm. Manual adjustments are needed for:

- Changing the definition of laterals to D-FLOW FM 1D standards.
- Changing boundary conditions and computation period.
- The keyword `gateLowerEdgeLevel` D-FLOW FM 1D structures was taken as equal to `crestLevel+openLevel` in SOBEK 3 . However, this should be the `openLevel` in SOBEK 3 . This is important for computing the discharge of the Lek branch under low discharges.

Deltares

3.4 Model straightening

D-FLOW FM 1D uses a 2D numerical solver, which causes energy losses due to curvature of the streamlines. While being physically correct, it requires of a detailed representation of the curvature (i.e., a substantial amount of grid cells per bend) for not causing unrealistically large energy loses. In preventing both unrealistic energy loses and a small space step, the domain is straightened by using a conversion script found in the repository
https://svn.oss.deltares.nl/repos/openearthtools/trunk/matlab/applications/vtools.

3.5 Friction adjustment

The friction coefficient in SOBEK 3 and WAQUA is constant between water level measuring stations as a result of the original calibration procedure, where a sudden jump between values exists. While using a piecewise friction coefficient in a hydrodynamic simulation in the Dutch Rhine branches is acceptable, this strategy cannot be followed when the simulation includes morphodynamic changes. The sudden changes in friction coefficient yield sudden changes in sediment transport which eventually cause unrealistic bed level development. In this study a constant roughness coefficient along the branches is calibrated. However, this coefficient might change depending only on the discharge level.

3.6 Main channel width adjustment

In the SOBEK 3 schematisations, the main channel is defined between the *normaallijnen* which is the line over the toes of the groynes separating the main channel from the groyne fields. This is problematic in morphodynamic models with D-FLOW FM 1D . The reason is that the elevation of the main channel must remain below the minimum elevation of the floodplains (which include the groyne toes). In other words, the function between width and elevation must be monotonic. Hence, aggradation is very limited. For allowing aggradation, the main channel width must be increased.

A first methodology for increasing the width based on automatically finding the location of the groyne crests was followed. This is described in details in Appendix B of Berends and Daggenvoorde (2020). However, the main channel presented abrupt changes along the longitudinal profile (see figures in Appendix A). The main channel width is relevant to the sediment transport and sediment transport gradient and therefore has a large influence on the bed level changes. In order to preserve the original main channel width gradient, a constant factor of 1.1 for the widening is applied based on the inspection of the original and new profiles. It is recommended further checking the main channel width generated from the 2D bed elevation in BASELINE .

Deltares

3.7 Storage area adjustment

The storage area in the cross sections is removed, as there appears to be an issue with the advection scheme in the presence of storage in DFlow-FM 1D. Storage is not relevant for the current model.

This can be shown in the following manner. The timing of a flood wave is slightly modified when storage areas are removed. Nevertheless, although we intend to use real data, we intend to use daily series. Assuming a prismatic channel with constant section and slope, a flood wave travels at a celerity equal to $B^{-1} \cdot \partial Q_\mathrm{u} / \partial h$, where B is the total width, Q_u is the discharge under uniform flow conditions, and h is the flow depth. Assuming a Manning friction relation, a flow velocity equal to 2 m/s, a conveyance width equal to 300 m and a total width equal to 600 m, the celerity is equal to 1.67 m/s. Consider now, for instance, the distance between Lobith and Tiel (roughly 60 km). A flood wave takes approximately 10 h to travel this distance. Removing storage will slightly modify this 10 h. However, given that we use daily discharge series (i.e., we have the same discharge for 24 h), 10 h is irrelevant. Thus, a fraction of 10 h is completely negligible. Overall, it is important to remember that we are going to calibrate and verify based on morphodynamic changes on the scale of several years. Individual flood events are outside the scope of the model.

Details of effect of storage in the propagation of a flood wave are described in Appendix B

Deltares

4 Hydrodynamic step

4.1 Calibration procedure

The original SOBEK 3 models were calibrated on measured water levels at observation stations, by modifying main channel roughness (Manning) coefficients. For morphodynamic simulation, correct flow velocities are more important, as this is crucial for proper prediction of sediment transport rates. The cross-section in the SOBEK 3 models were derived from these WAQUA models. Though WAQUA models have also been calibrated to reproduce water level measurements, WAQUA (2D model) results are considered the best approximation of actual flow conditions currently available for the calibration of the DELFT3D FM SUITE models.

The calibration is based on the comparison of D-FLOW FM 1D and WAQUA models using the 2019 model schematisation for four representative constant discharges at Lobith: 2000 m^3/s, 4000 m^3/s, 6000 m^3/s and 8000 m^3/s. Also the OLA (*Overeengekomen Lage Afvoer*) of 1020 m^3/s is considered. Although this discharge is not relevant for morphodynamic development, it is important to test the ability of the model in reproducing the conditions for this discharge as the water level is indicative of the reference plane used for dredging operations.

The downstream water level boundary conditions for these discharges are defined based on WAQUA results at the D-FLOW FM 1D boundary locations: Krimpen (Lek), Kattendiep and Keteldiep (IJssel) and Hardinxveldboven (Waal). Furthermore the same constant lateral discharges in WAQUA are applied in D-FLOW FM 1D .

The 1D simulations are carried out for a period of 20 days and it is checked that the steady state has been reached (i.e., results are not changing in time).

We compare D-FLOW FM 1D results with WAQUA along the river axis on the following model output:
• Water levels.
• Main channel velocity.
• Main channel discharge.
• Total discharge per branch (discharge distribution at bifurcations).

WAQUA results at the river axis for these output variables is obtained in the following way (applying GIS and MATLAB® scripts):
• Water levels are available at water level stations (history output) (SDS WAQUA files). These stations are located on the river axis with a spatial interval of one kilometre.
• Main channel flow velocities and discharges are derived from the map output (SDS WAQUA files). Discharges and depth-averaged flow velocities are available on every grid line. To transform these grid line variables to main channel variables the following steps are required:
  – Use the main channel shape from BASELINE to select all main channel grid lines.
  – Determine the streamwise position of the grid lines perpendicular to river axis.
  – Average the flow velocities and sum the discharges per grid line to get main channel variables along the river.
• Total discharges are available at discharge stations (history output) (SDS

Deltares

WAQUA files). These stations are located on the river axis with a spatial interval of one kilometre. To compare the discharges we applied the total discharge at the first kilometre of the river branch.

Several computations were carried with constant roughness. First constant Manning friction values equal to $0.025\,\text{m}^{-1/3}\text{s}$, $0.030\,\text{m}^{-1/3}\text{s}$, $0.035\,\text{m}^{-1/3}\text{s}$, and $0.040\,\text{m}^{-1/3}\text{s}$ were simulated for a discharge equal to $2000\,\text{m}^3/\text{s}$, $4000\,\text{m}^3/\text{s}$, $6000\,\text{m}^3/\text{s}$ and $8000\,\text{m}^3/\text{s}$. After evaluating the results, the constant roughness values were refined per discharge. Finally the most appropriate constant roughness is recommended on the basis of the best reproduction of the velocities in all the branches also taking into account the water levels and discharge distribution within the branches.

For OLA (discharge at Lobith equal to $1020\,\text{m}^3/\text{s}$) the roughness might be considered as variable along the reaches in order to reproduce the OLR (*Overeengekomen Lage Rivierstand*, the water level associated to the OLA) accurately, since for this discharge level the morphological developments are not significant. The results for a discharge equal to $1020\,\text{m}^3/\text{s}$ with original roughness are also presented and analysed. However, a detail calibration has not taken place to more accurate reproduce the OLR. This is only of importance when dredging is activated in the model. The dredging module can be used to calculate the necessary dredging volume as function of the available navigation depth at OLR.

4.2 Calibration results

Appendices E, F, G, H, present the comparison of the water levels, flow velocities and discharges in the main channel between WAQUA and D-Flow FM 1D for the selected Manning friction coefficient for a discharge equal to $2000\,\text{m}^3/\text{s}$, $4000\,\text{m}^3/\text{s}$, $6000\,\text{m}^3/\text{s}$, and $8000\,\text{m}^3/\text{s}$, respectively.

The summarized results are shown in boxplots with the bias between D-Flow FM 1D and WAQUA and its standard deviation per branch and discharge for the variables: water levels, velocity in the main channel and discharge in the main channel (Figures 2, 3, 4, 5, 6, and 7). The figures also show the case with the original roughness from the Sobek 3 schematization ("original").

The elements shown in the figures are:
- Average biases (coloured bars).
- Different Manning roughness values (each value has a different colour).
- Error bars displaying the range from one standard deviation below the average error till on standard deviation above.
- Columns with different variables.
- Rows with different discharge levels.

Furthermore, it is important to analyse the discharge distribution within the branches. The discharges deviate from the one in WAQUA as shown in the figures with total discharges and difference in percentage with WAQUA (shown in Figures 8, 9, 10 and 11). However, the discharge distribution also deviates for the original roughness. A discussion about discharge accuracy is given in Section 7.

The selection is mainly based on the assessment of the flow velocities in the main channel, as this is the main driver of morphodynamic changes, and on limiting the differences in water levels between WAQUA and D-Flow FM 1D . Depending on the branch the bias and standard deviation in the water levels increases or decreases with

Deltares

the friction value. The velocity has the opposite behaviour as the water level. Worded differently, if the water-level performance increases with friction, the flow-velocity performance decreases. For instance, the optimum friction coefficient for the water level in the Pannerdensch Kanaal is approximately $0.032\,\text{m}^{-1/3}\text{s}$ while for velocity is closer to $0.038\,\text{m}^{-1/3}\text{s}$. We considering that a friction coefficient larger than $0.039\,\text{m}^{-1/3}\text{s}$ seems not realistic and will not reduce the bias and standard deviation in the flow velocities. Besides, a larger friction coefficient increases the difference in discharge distribution without significantly improving the flow velocities in the main channel. Reducing the friction value improves the flow velocity slightly in branches such as the Waal affecting negatively to other branches such as the IJssel.

Even only considering the data in the summarized figures, the amount of variables to be considered in the calibration is large. Moreover, one has to consider that, for instance, the lengths of the branches are different, and hence the impact of an error in flow velocity along the Waal is different than along the Pannerdensch Kanaal. Rather than searching for complex metrics which require subjective input in any case (such as the impact of the error in each branch), expert judgement and discussion by all the team members also considering the longitudinal profiles (Appendices E - I) is preferred, arriving to the conclusion that a compromise in all branches and discharges is found by selecting a constant friction Manning coefficient of $0.031\,\text{m}^{-1/3}\text{s}$ for discharges lower or equal to $2000\,\text{m}^3/\text{s}$ and of $0.036\,\text{m}^{-1/3}\text{s}$ for discharges higher than $4000\,\text{m}^3/\text{s}$. In between $2000\,\text{m}^3/\text{s}$ and $4000\,\text{m}^3/\text{s}$, friction values are interpolated.

It is recommended to check the influence of this constant friction factor on sediment transport and morphological developments when a flood hydrograph is applied. The friction coefficient is associated to the bed shear stresses which are relevant in the determination of the sediment transported and therefore on the celerity of the bed disturbances.

For the OLA discharge of $1020\,\text{m}^3/\text{s}$ the water levels are fairly reproduced by the model (Appendix I) without any changes in the friction. However further calibration is needed to accurate computed OLR when the dredging module is applied.

Deltares
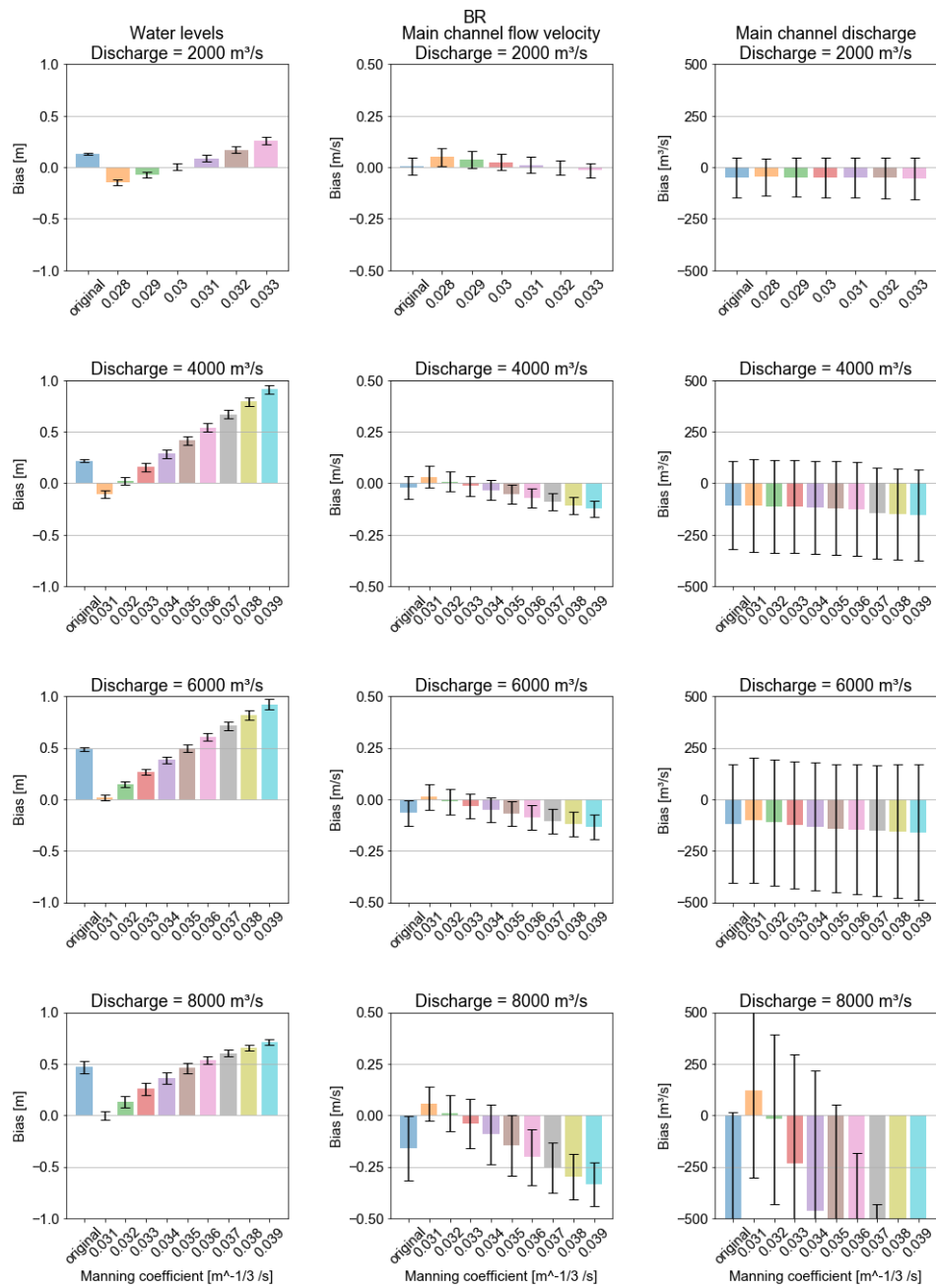
Figure 2 Boxplots of the biases for four different manning values and four different discharge levels - Boven-Rijn
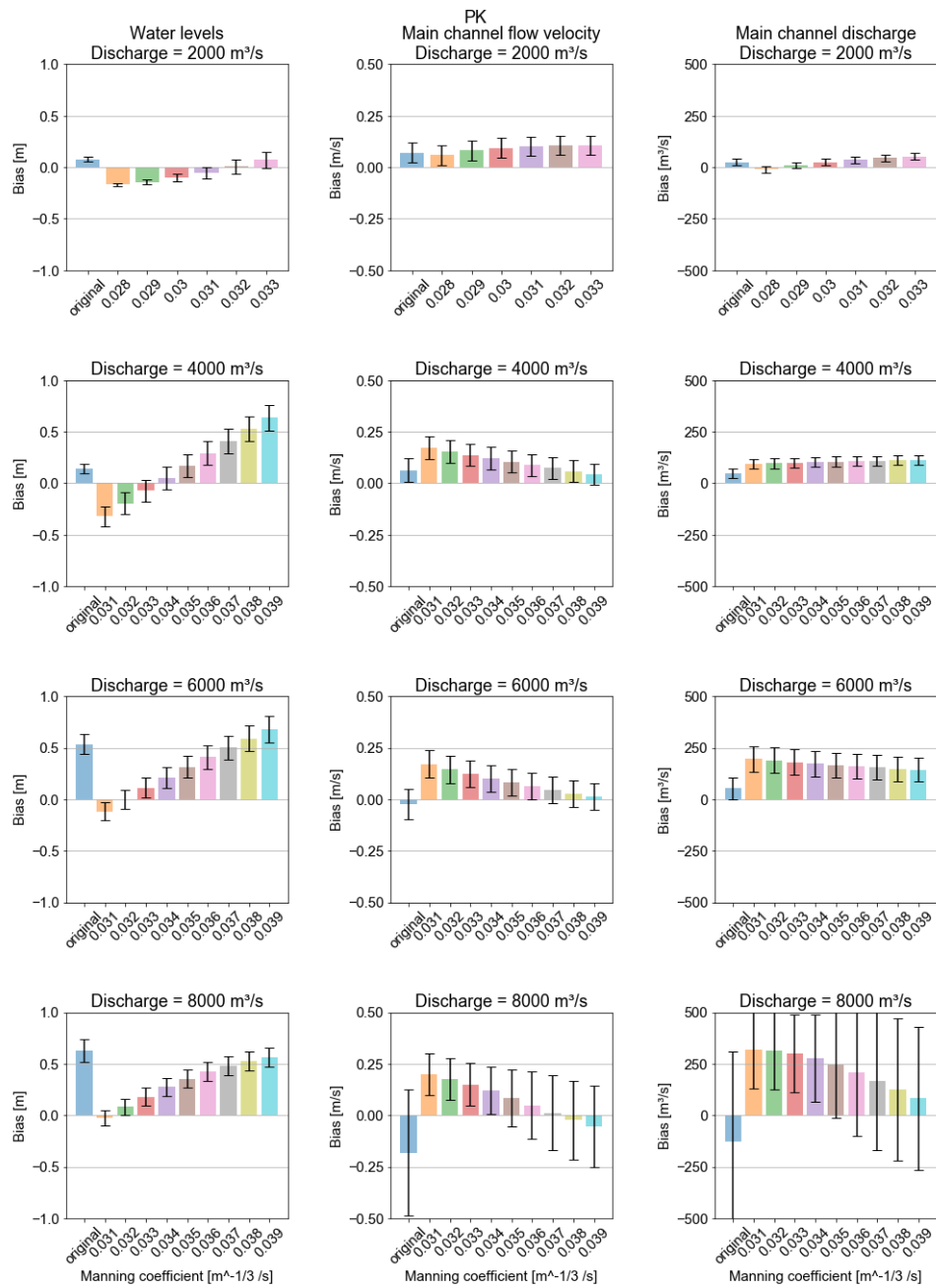
Figure 3 Boxplots of the biases for four different manning values and four different discharge levels - Pannerdensch Kanaal

Morphological models for IRM
11203684-015-ZWS-0011_v1.0, Version 0.1, 2020-12-11, Final

Deltares
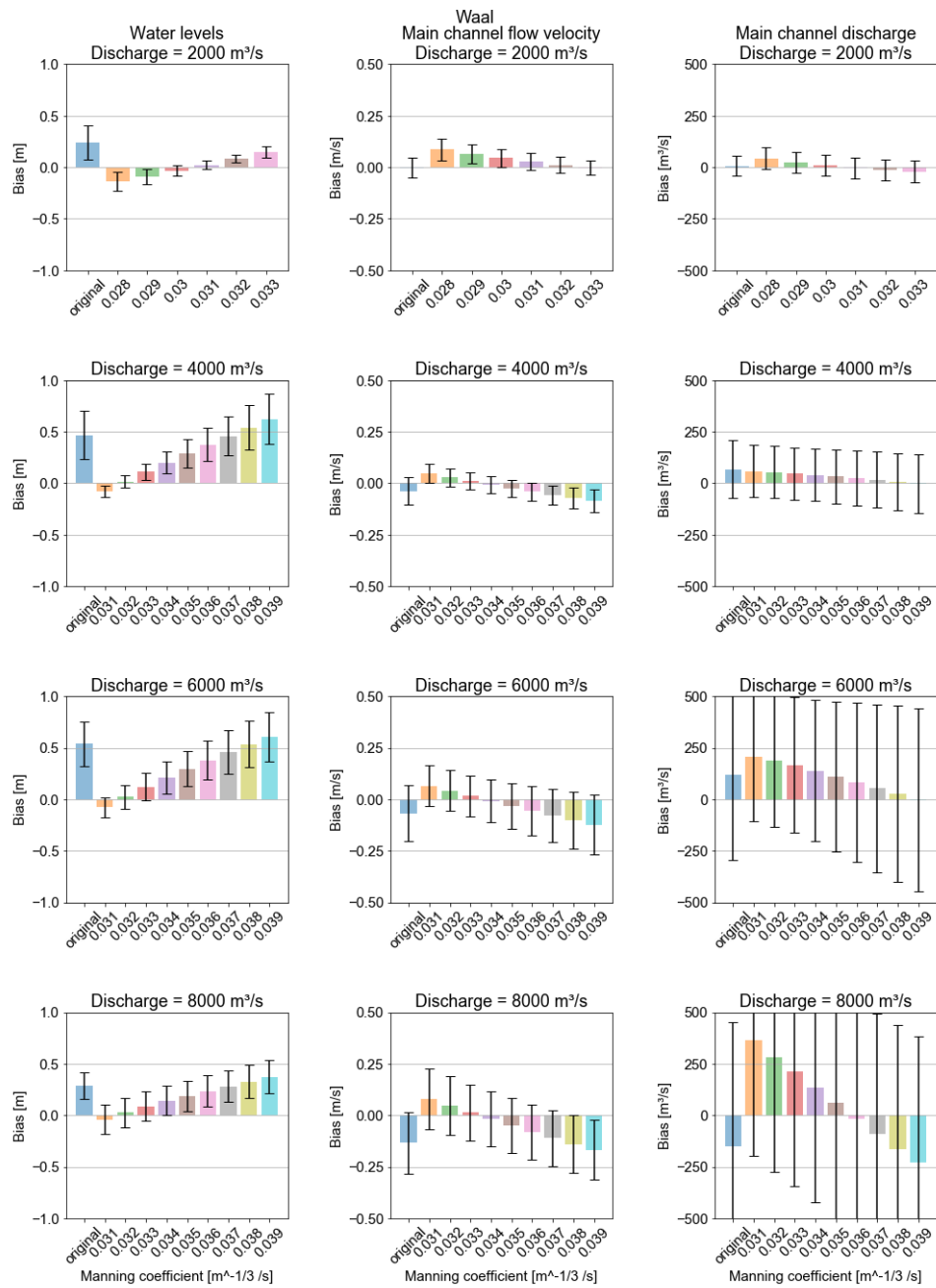
Figure 4 Boxplots of the biases for four different manning values and four different discharge levels - Waal

Morphological models for IRM
11203684-015-ZWS-0011_v1.0, Version 0.1, 2020-12-11, Final

Deltares
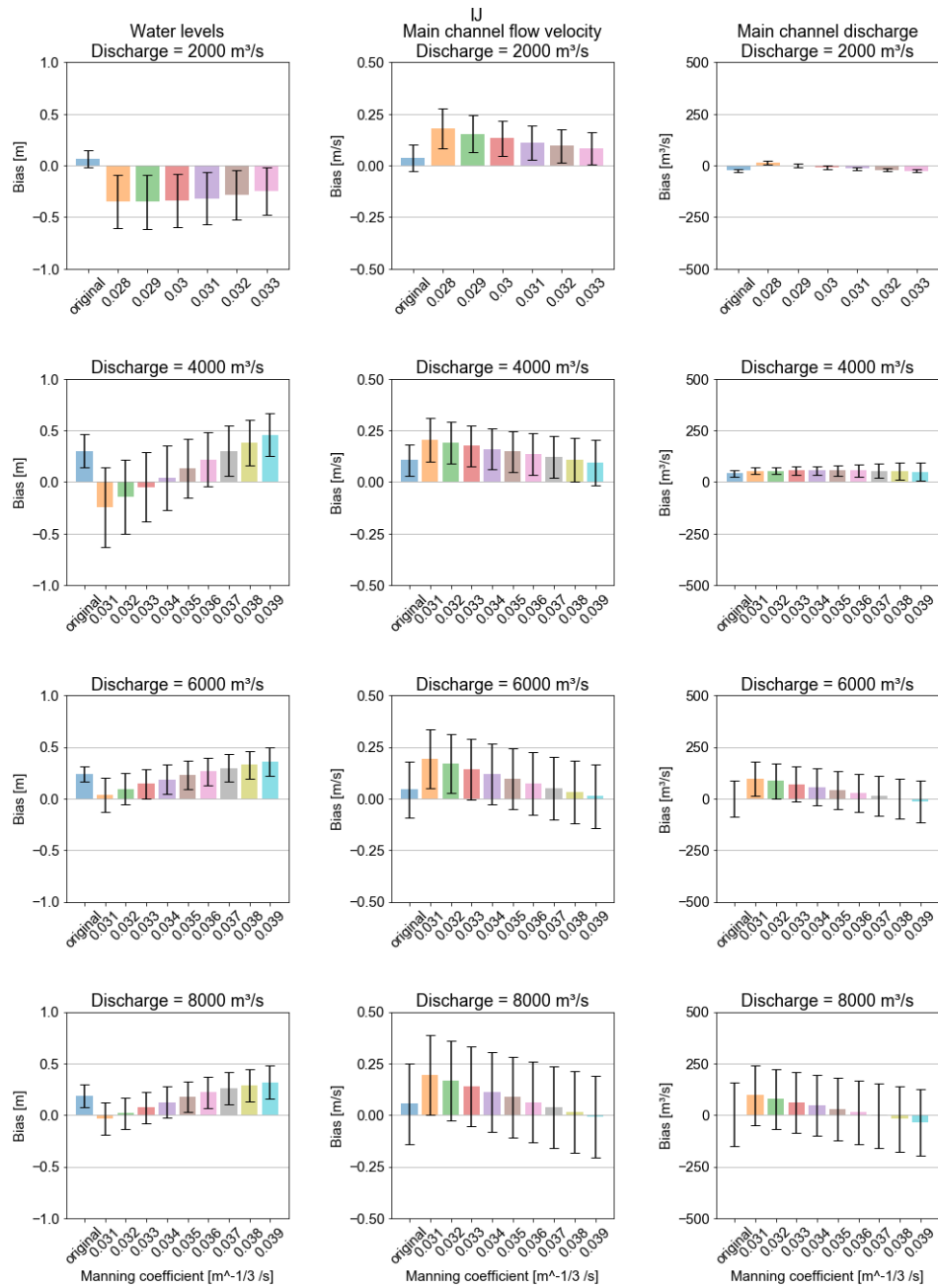
Figure 5 Boxplots of the biases for four different manning values and four different discharge levels - IJssel

Deltares
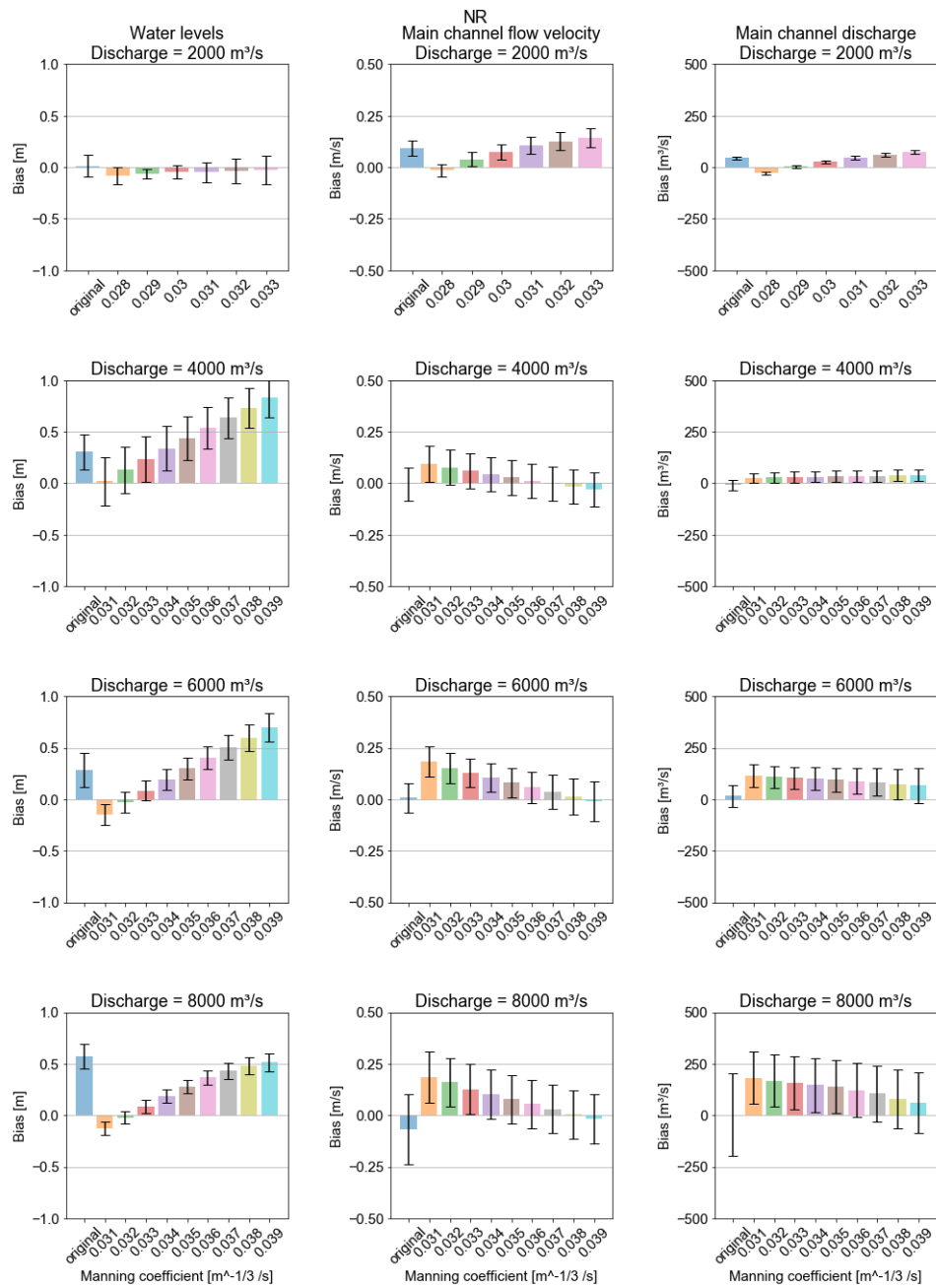
Figure 6 Boxplots of the biases for four different manning values and four different discharge levels - Nederrijn

Morphological models for IRM
11203684-015-ZWS-0011_v1.0, Version 0.1, 2020-12-11, Final

Deltares
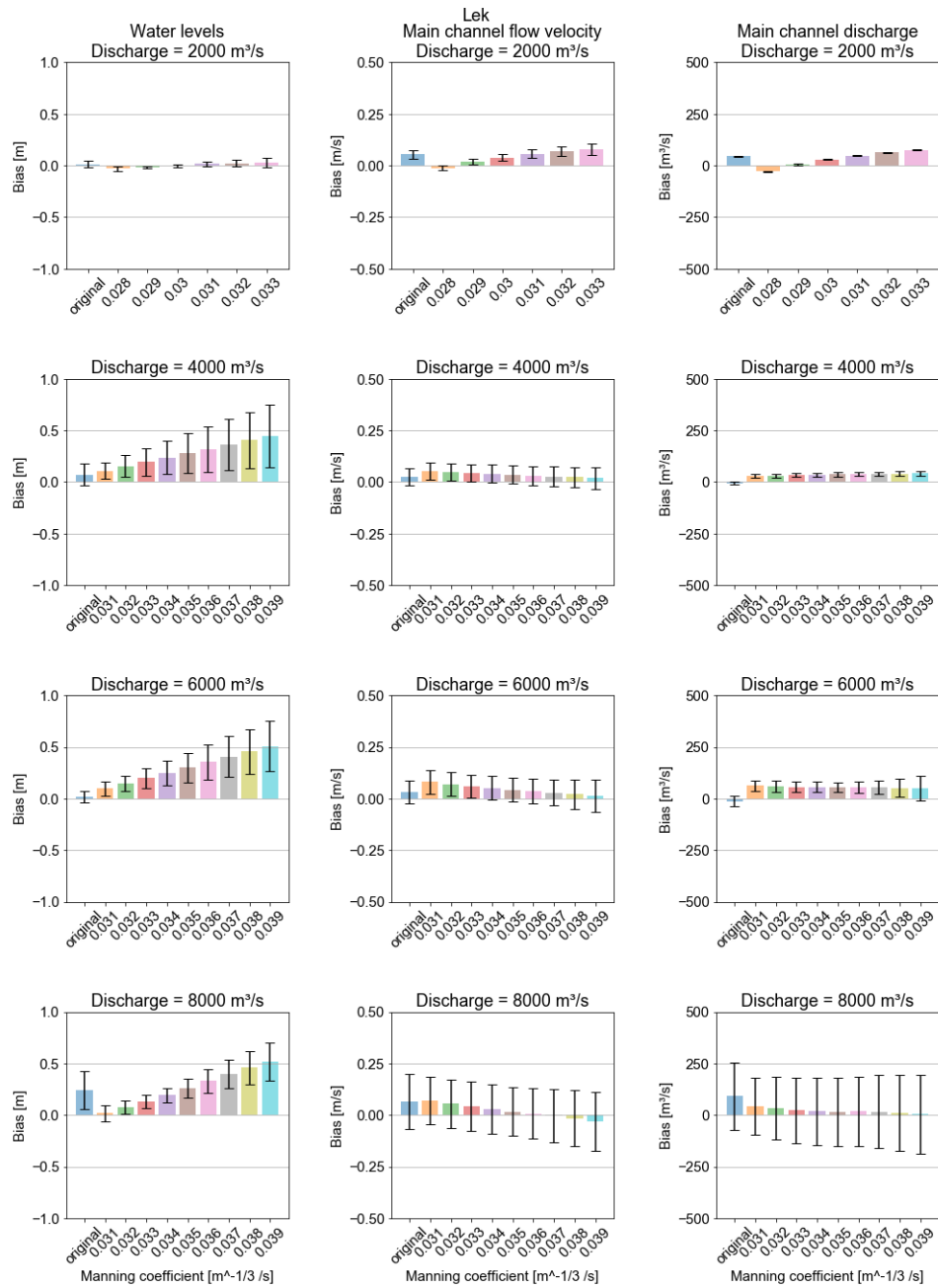
Figure 7 Boxplots of the biases for four different manning values and four different discharge levels - Lek

Morphological models for IRM
11203684-015-ZWS-0011_v1.0, Version 0.1, 2020-12-11, Final

Deltares
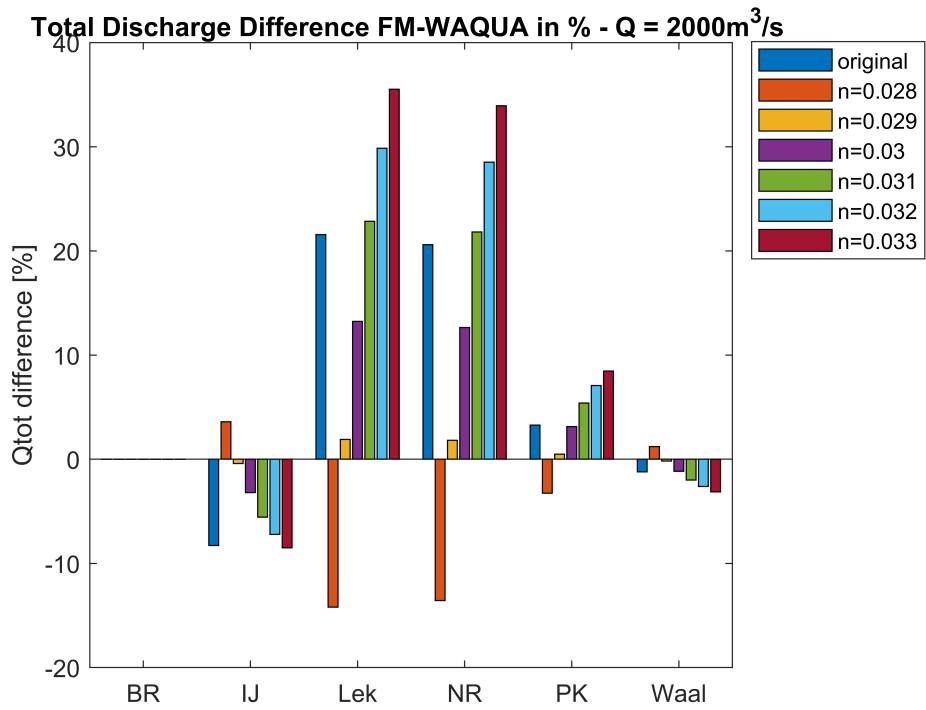
Figure 8 Difference in percentage total discharges for different manning Q=2000 m^3/s
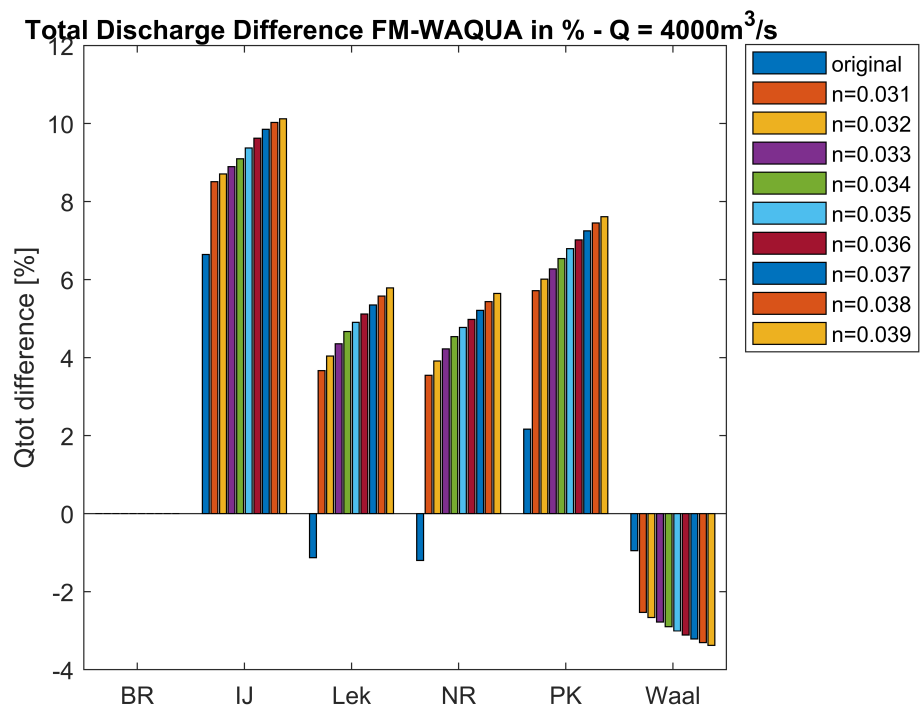
Figure 9 Difference in percentage total discharges for different manning Q=4000 m^3/s

Deltares
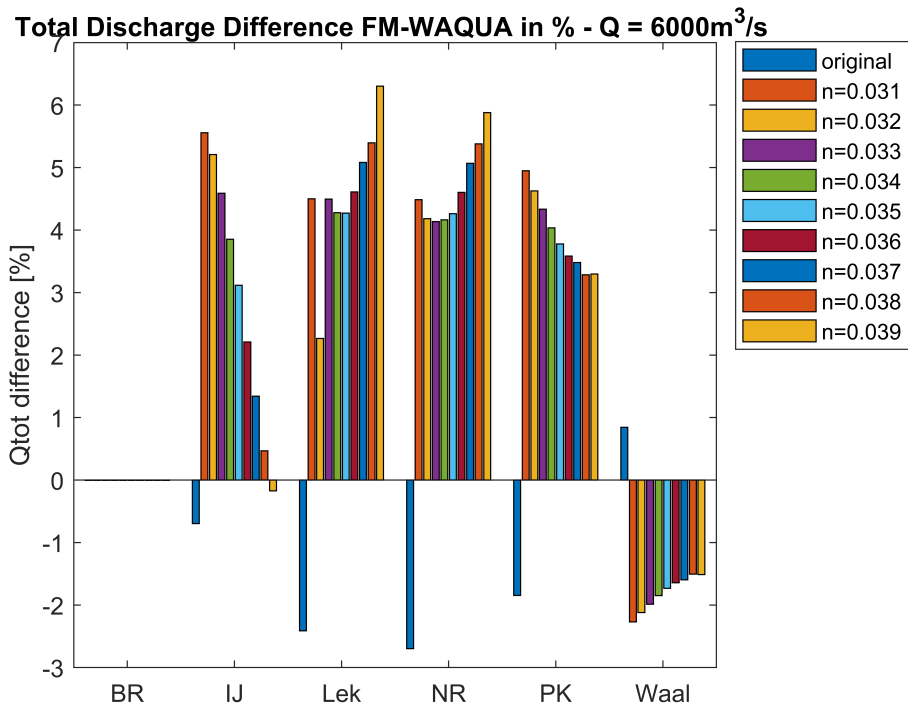
Figure 10 Difference in percentage total discharges for different manning Q=6000 m³/s
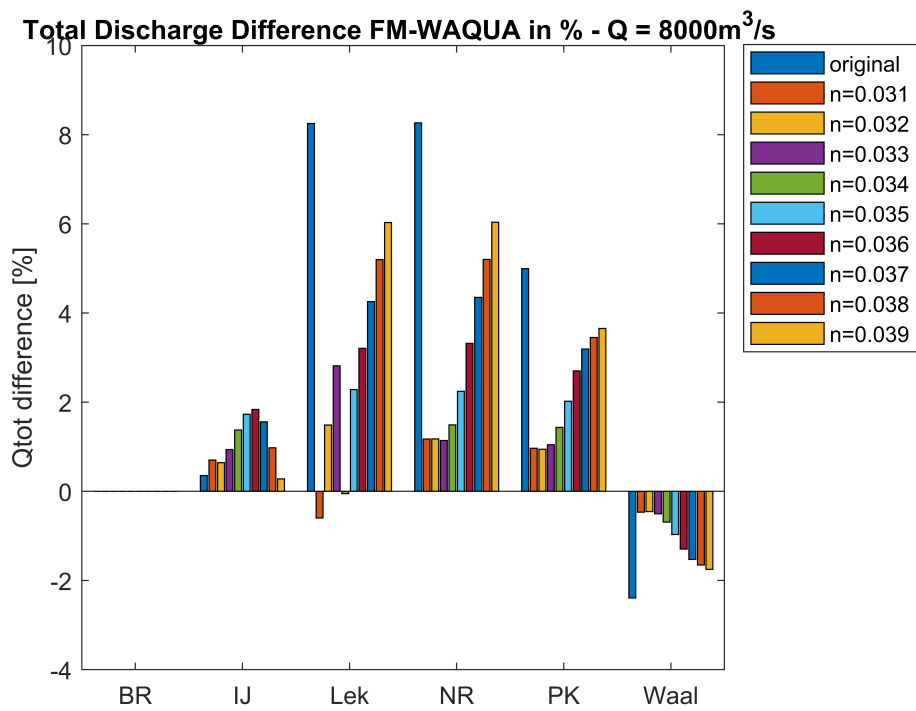
Figure 11 Difference in percentage total discharges for different manning Q=8000 m³/s

Deltares

5 Morphodynamic step

In this section we describe the extension of the hydrodynamic model to predict morphodynamic changes (Section 5.1). The model is calibrated (Section 5.2) and verified (Section 5.4).

5.1 Model extension and calibration parameters

The basis of the model extension is the latest morphodynamic model of the *Rijntakken* developed by Sloff (2006).

The morphodynamic items and main parameters added to the hydrodynamic model are:
- Characteristic grain sizes,
- initial grain size distribution,
- active-layer thickness,
- sediment transport relation,
- nodal-point relation.

Given the above items and parameters in each item, the calibration of the model is an underdetermined problem, meaning that there are several combinations of parameters that provide the same results, or results equally valid. For this reason, it is assumed that the uncertainty in the initial grain size distribution is low compared to the parameters of the sediment transport and nodal-point relations. Similarly, the active-layer thickness is not treated as a calibration parameter.

Each of the items above is discussed in the following sections.

5.1.1 Characteristic grain sizes

The model by Sloff (2006) discretized the sediment mixture into 17 grain sizes. Their smallest grain size is on the silt range. The interest of the current model is to predict morphodynamic change in the main channel. Floodplain depositional processes remain outside the scope of this project. Hence, all sediment is modelled as bed load and the smallest size fraction is removed. The characteristic grain sizes of the model are shown in table 1.

5.1.2 Initial grain size distribution

The initial grain size distribution is based on the model by Sloff (2006). As in the current model the finest fraction is removed with respect to the model by Sloff (2006), the finest fraction of the current model contains the volume fraction content of the finest fraction of the model by Sloff (2006). In other words, Fraction 1 in the current model is the sum of Fraction 1 and Fraction 2 in the model by Sloff (2006).

The geometric (d_g) and arithmetic (d_m) mean grain size for each branch is shown in Figures 12, 13, 14, 15, and 16. Data provided by Roy Frings is added for comparison when available.

As data about the substrate is unavailable, the substrate is assumed to have the same grain size distribution as the bed surface. The changes in substrate grain size distribution are modelled by means of a maximum number of 10 layers with a maximum thickness equal to 0.4 m. We note that there was a measurement campaign

Deltares

Fraction	Grain size [m]	Type
1	7.529×10^{-5}	sand
2	1.060×10^{-4}	sand
3	1.500×10^{-4}	sand
4	2.121×10^{-4}	sand
5	2.979×10^{-4}	sand
6	4.213×10^{-4}	sand
7	7.071×10^{-4}	sand
8	1.414×10^{-3}	sand
9	2.366×10^{-3}	gravel
10	3.346×10^{-3}	gravel
11	5.656×10^{-3}	gravel
12	1.131×10^{-2}	gravel
13	2.262×10^{-2}	gravel
14	4.525×10^{-2}	gravel
15	9.050×10^{-2}	gravel
16	1.810×10^{-1}	gravel

Table 1 Characteristic grain sizes.

of the substrate in the Pannerdensche Kop area (Gruijters *et al.*, 2001). This is, however, insufficient for developing the model of the entire Rhine branches. This point is further discussed in Section 7.

The model by Sloff (2006) is built in SOBEK-RE . Fixed layers are flagged by setting the composition of the substrate to 100 % of the coarsest fraction. In DELFT3D FM SUITE , fixed layers are prescribed by lack of sediment. Hence, at the locations in which the substrate of the SOBEK-RE model is composed of coarse sediment only, the thickness of the substrate layers is set equal to 0.

In SOBEK-RE , the initial grain size distribution is prescribed at each cell centre. In DELFT3D FM SUITE , the input data is spatial (i.e., values are are given at x and y locations) and interpolated. For preventing interpolation issues, data is input not only at cell centres but also at points perpendicular to the river axis.

Deltares
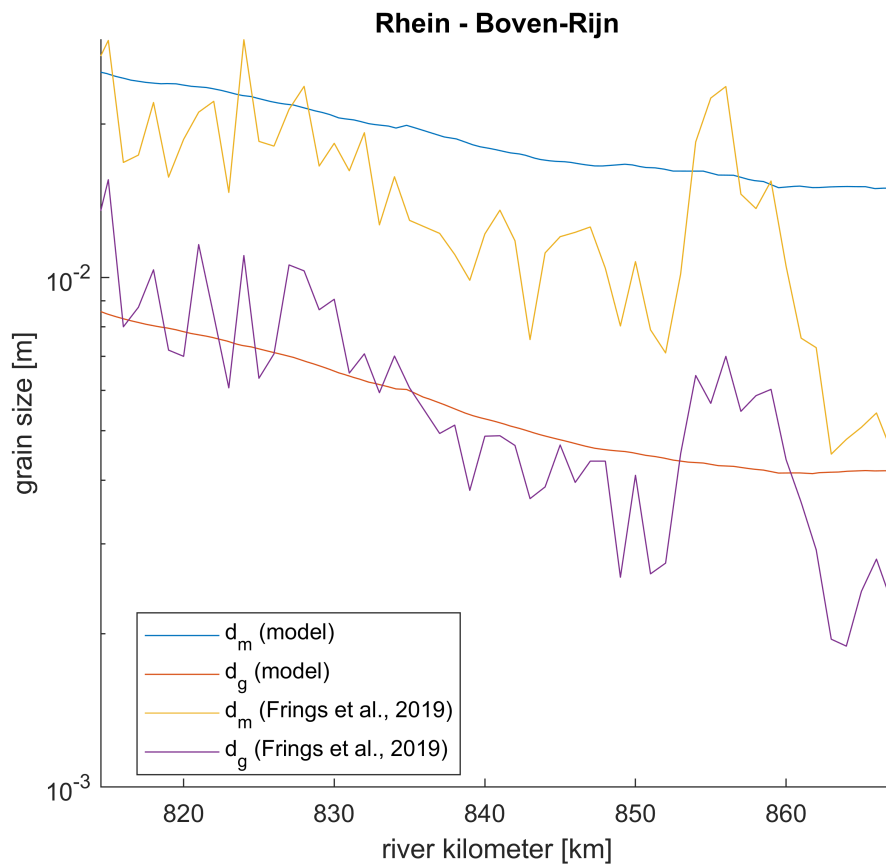
Figure 12 Geometric (d_g) and arithmetic (d_m) mean grain size along the Rhein - Boven-Rijn.

Deltares
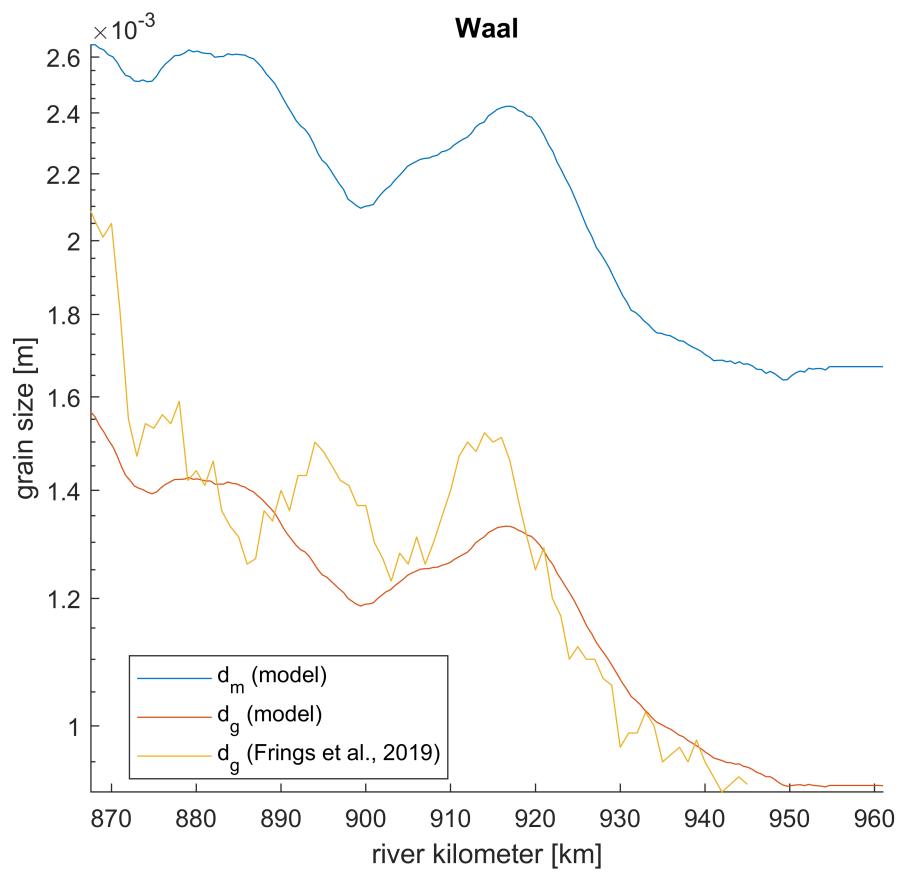
Figure 13 Geometric (d_g) and arithmetic (d_m) mean grain size along the Waal.

Deltares
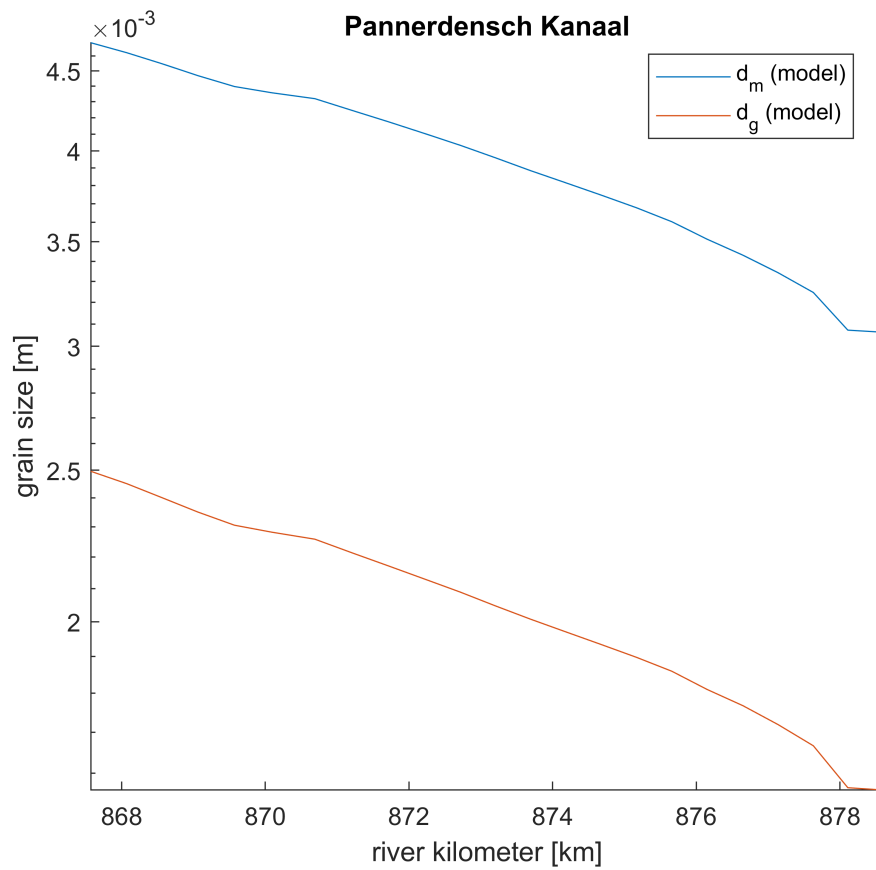
Figure 14 Geometric (d_g) and arithmetic (d_m) mean grain size along the Pannerdensch Kanaal.
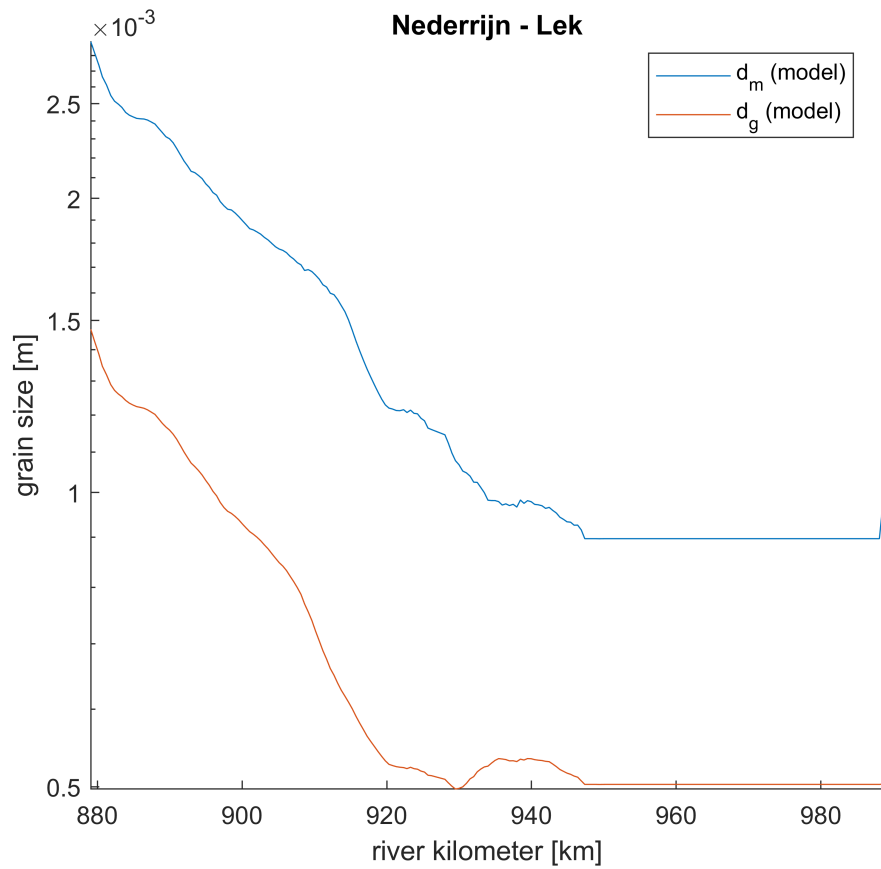
Figure 15 Geometric (d_g) and arithmetic (d_m) mean grain size along the Nederrijn - Lek.

Deltares
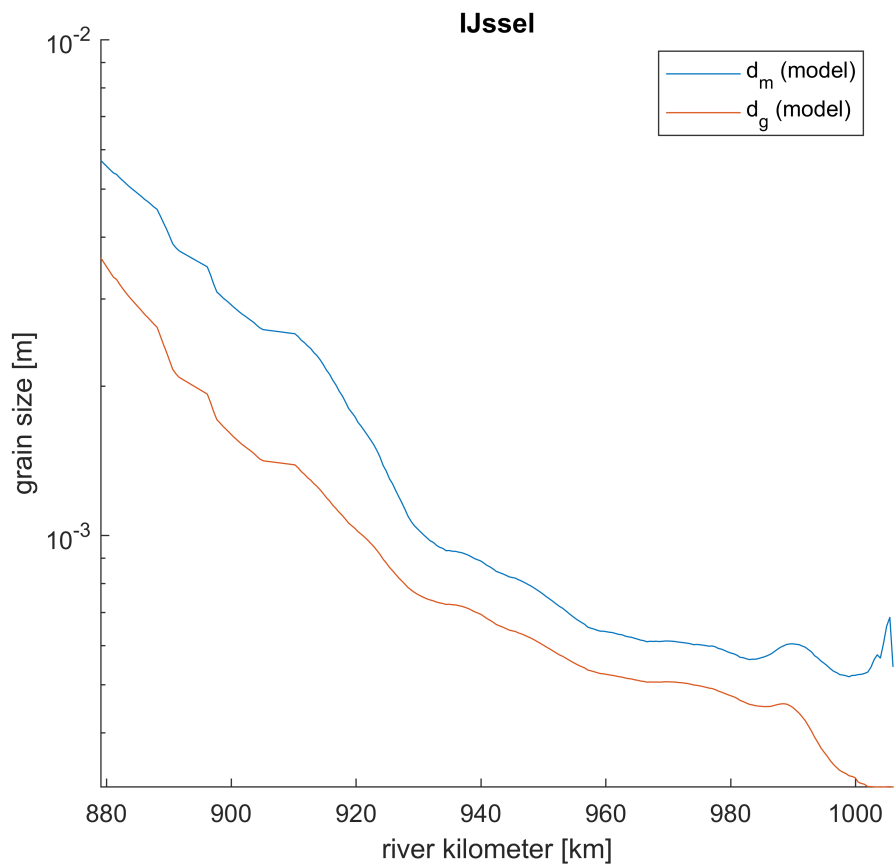
Figure 16 Geometric (d_g) and arithmetic (d_m) mean grain size along the IJssel.

Deltares

5.1.3 Active-layer thickness

Morphodynamic changes accounting for mixed-size sediment are modelled using the active-layer model (Hirano, 1971). The active layer represents the part of the bed that interacts with the flow. Only sediment in the active layer can be set into transport. Sediment in the active layer is perfectly mixed.

The only source of vertical mixing in the active-layer model is a change in mean bed elevation (i.e., averaged over the passage of several bedforms). For this reason, sediment in the active layer represents an average over the passage of several bedforms of the composition of the bed surface and the active-layer thickness represents the scale of the mixing bedforms (e.g., Parker *et al.*, 2000).

It is possible to consider a spatially and temporally varying active-layer thickness that models changes in dune height. Nevertheless, it is opted to reduce the model complexity and over-parametrization by setting a constant active-layer thickness in both space and time. Given than most changes occur during high-flow events, an active-layer thickness equal to 1 m is chosen. The effects of varying this parameter are shown in the discussion section.

5.1.4 Sediment transport relation

The sediment transport relation has been used as a calibration parameter. Here we state the final result and in Section 5.2 the procedure to find it is explained.

The sand fractions (see Table 1) are modelled using the relation by Engelund and Hansen (1967):

$$q_{\mathrm{b}k}^{*} = \alpha \frac{0.05}{C_{\mathrm{f}}} (\theta_k)^{5/2} \ , \tag{5.1}$$

where α [-] is a calibration parameter, $q_{\mathrm{b}k}^{*}$ [-] is the non-dimensional sediment transport rate:

$$q_{\mathrm{b}k}^{*} = \frac{q_{\mathrm{b}k}}{F_{\mathrm{a}k}\sqrt{g\Delta d_k^3}} \ , \tag{5.2}$$

where $q_{\mathrm{b}k}$ [m^2/s], $F_{\mathrm{a}k}$ [-] is the volume of sediment of size fraction k in the active layer, g [m/s^2] is the acceleration due to gravity, $\Delta = 1.65$ is the submerged specific density, d_k is the characteristic grain size of size fraction k, C_{f} is the non-dimensional friction coefficient:

$$C_{\mathrm{f}} = \frac{n^2 g}{R_{\mathrm{h}}^{1/3}} \ , \tag{5.3}$$

where n [s/m$^{1/3}$] is the Manning friction coefficient, R_h [m] is the hydraulic radius, and θ_k [-] is the Shields (1936) stress on size fraction k:

$$\theta_k = \frac{\tau_b}{\rho g \Delta d_k} \ , \tag{5.4}$$

where τ_{b} [N/m^2] is the bed shear stress:

$$\tau_{\mathrm{b}} = \rho g R_{\mathrm{h}} S_{\mathrm{f}} \ , \tag{5.5}$$

where S_{f} is the friction slope:

$$S_{\mathrm{f}} = \frac{C_{\mathrm{f}} u^2}{g R_{\mathrm{h}}} \ , \tag{5.6}$$

Deltares

Branch	α sand fractions [-]	α gravel fractions [-]
Rhein - Boven-Rijn	0.47	0.60
Waal	0.18	0.32
Pannerdensch Kanaal	0.22	0.12
Nederrijn – Lek	0.10	0.10
IJssel	0.10	0.10

Table 2 Calibration parameter of the sediment transport relation.

where u [m/s] is the main channel flow velocity.

The gravel fractions are modelled using the sediment transport relation by Meyer-Peter and Müller (1948):

$$q_{bk}^* = \alpha A(\theta_k - \xi_k \theta_c)^B \, , \tag{5.7}$$

where ξ_k [-] is the hiding-exposure relation by Ashida and Michiue (1971):

$$\xi_k = \begin{cases} 0.843 \left(\frac{d_k}{D_m}\right)^{-1} & \text{for} \frac{d_k}{D_m} \leq 0.4 \\ \left(\frac{\log_{10}(19)}{\log_{10}(19\frac{d_k}{D_m})}\right)^2 & \text{for} \frac{d_k}{D_m} > 0.4 \end{cases} \, , \tag{5.8}$$

where D_m [m] is the arithmetic mean grain size, $\theta_c = 0.025$ [-] is the critical bed shear stress, $A = 8$ and $B = 3/2$. The use of the arithmetic mean grain size is treated in the discussion section.

The calibration parameter α varies per size fraction (sand or gravel fraction) and per river branch (Table 2).

5.1.5 Nodal-point relation

In the model developed by Sloff (2006), the nodal-point relation used in both bifurcations is of the form:

$$\frac{Q_{bk1}}{Q_{bk2}} = \beta_k \frac{Q_1}{Q_2} \, , \tag{5.9}$$

where Q_{bkj} [m³/s] is the sediment transport rate of size fraction k on the outgoing branch j, Q_j is the water discharge on the outgoing branch j, and β_k is a calibration parameter. In this model the same functional relationship is used. It is to be noted that this relationship yields an unstable bifurcation for a constant discharge Wang *et al.* (1995); Schielen and Blom (2018). The effect of a different nodal-point relation is treated in the discussion section.

The calibration parameter vary per size fraction and bifurcation (Table 3) and the calibration procedure is explained in Section 5.2.

Deltares

Bifurcation (Outgoing branch 1/Outgoing branch 2)	β sand fractions [-]	β gravel fractions [-]
Pannerdensche Kop (Waal/Pannerdensche Kanaal)	1.79	1.79
IJssel Kop (Nederrijn/IJssel)	1.35	0.99

Table 3 Calibration parameter of the nodal-point relation.

5.2 Calibration procedure

The schematization with cross-sections from 1995 in the period 1995-2011 was used for calibration (see Section 2 for reasoning and explanation). The daily hydrograph at Lobith for this period of time was used as the upstream boundary condition. We are aware that the the upstream end of the domain is situated upstream from Lobith. Nevertheless, the distance is not significant considering that we are using daily values of the water discharge (i.e., flood-wave propagation is not accurately modelled) and the interest of the model is on morphodynamic development. Using values at Lobith facilitates future uses and applications of the model. Time series of water elevation at Hardinxveld, Krimpen, Kettendiep, and Kattendiep are imposed as downstream hydrodynamic boundary conditions. The time series are shown in Appendix C. The main locations where water is extracted or input along branches (i.e., laterals) are included in the model. The time series of discharges per location are shown in Appendix D.

The upstream morphodynamic boundary condition is fixed bed and composition. The upstream end is sufficiently far from the domain of interest (i.e., the Dutch part of the river system) such that it is guaranteed that the influence of this boundary condition does not reach in the simulation time. This choice is later discussed (Section 7).

The first data source available for calibration is the sediment transport rates estimated by Frings *et al.* (2019) (Table 4). These are average values derived from a long term analysis (1991-2010) that provide values that the model should reasonably reproduce. Their data discerns between sand and gravel.

The second data-set used for calibrating the model are the bed elevation of 2011 as existing in the SOBEK 3 model. This bed elevation is derived from BASELINE , which contains the measured bed elevation. BASELINE data is processed using the WAQ2PROF protocol for converting two-dimensional data into representative one-dimensional values. Hence, by using the bed elevation of the SOBEK 3 model as a calibration target we are using the measured bed level, already processed for obtaining a characteristic cross-sectional value.

Initially, several sediment transport relations (Wilcock and Crowe (e.g. 2003); Ashida and Michiue (e.g. 1971)) were used for computing the mean sediment load. As the interest was on the mean sediment transport only, rather than running a simulation, the processed was speeded-up by postprocessing the hydrodynamic results of one simulation. In other words, the annual sediment transport was computed without modelling morphodynamic changes. It was realized that it was not possible to accurately predict both the sand and the gravel transport for all branches using the same load relation (Appendix J). Moreover, when comparing with simulations considering morphodynamic change, it was seen that the initial estimation of the annual sediment transport rate neglecting morphodynamic change was not sufficiently accurate.

Deltares

Branch	gravel load (without pores) [m³/y]	sand load (without pores) [m³/y]
Rhein	41×10^3	204×10^3
Boven-Rijn	39×10^3	232×10^3
Boven-Waal	23×10^3	208×10^3
Midden-Waal	16×10^3	198×10^3
Beneden-Waal	6×10^3	185×10^3
Pannerdensch Kanaal	13×10^3	36×10^3
Boven-IJssel	2×10^3	17×10^3
Midden-IJssel	1×10^3	15×10^3
Beneden-IJssel	1×10^3	15×10^3
Boven-Nederrijn	10×10^3	26×10^3
Beneden-Nederrijn	7×10^3	26×10^3
Lek	3×10^3	26×10^3

Table 4 Annual sediment loads per branch estimated by Frings *et al.* (2019).

It was decided to use the relation by Engelund and Hansen (1967) for the sand fractions and the relation by Meyer-Peter and Müller (1948) with a critical bed shear stress equal to 0.025 for the gravel fractions, as these were the most accurate for each of the fractions individually. Calibration was further reduced by using the same prefactor α for all size fractions that are sand or gravel (Equations ((5.1)) and ((5.7))), although one could technically calibrate each size fraction independently. Furthermore, calibration was reduced to a whole river branch (i.e., Rhein - Boven-Rijn, Waal, Pannerdensch Kanaal, Nederrijn - Lek, and IJssel).

Morphodynamic simulations were conducted where the calibration factors of the sediment transport relation of the Rhine (i.e., until the Pannerdensche Kop) were varied such that the mean annual load reaching the Pannerdensche Kop was as close as possible to the measured values. Worded differently, the calibration target was the mean annual load at the last observation station in the Rhein - Boven-Rijn branch. Unrealistic parameters of the nodal-point relation and the calibration factors along the downstream branches caused unrealistic changes in the Rhein - Boven-Rijn branch. Hence, calibration required iteration. Modification of the calibration parameters along the downstream branches and the nodal-point relation was necessary when changing the calibration parameters of the upstream branch. Due to the computational time, it was not possible to conduct a wide variation of the calibration factors and it is possible that further adjustments reduces the difference with measured values. Nevertheless, the agreement is satisfactory, also considering the uncertainty in the measured values.

Once the calibration factors of the Rhein - Boven-Rijn branch were correct, the parameters of the nodal-point relation of the Pannerdensche Kop were calibrated such that the sediment distribution to the downstream branches was as close as possible to the measured values. In other words, the calibration target of the nodal-point relation was the mean annual load in the first observation station in the Waal and the Pannerdensch Kanaal. Similarly, the process was iterative given that the sediment transport relation parameters of the downstream branches influences the development in the bifurcation.

Deltares

The process continued downstream and it was repeated for each of the river branches. In total, 115 simulations were run for calibration of the sediment transport parameters. The simulation time of each run was 8.2 h on a single core in a Intel Xeon Gold 6144 at 3.5 GHz with 16 GB of RAM memory. The diagnosis file of the final run where all parameters can be found, as well details concerning the computational time can be found in Appendix K. The final schematization can be found in the RiverLab (https://oss.deltares.nl/web/riverlab-models)

5.3 Calibration results

5.3.1 Mean annual load at bifurcations

Figures 17 and 18 present the total (gravel and sand) sediment transport rates at the Pannerdensche Kop and the IJssel Kop, respectively. Values are within acceptable range (around 10% error) when compared to those by Frings *et al.* (2019) (Tables 5 and 6).
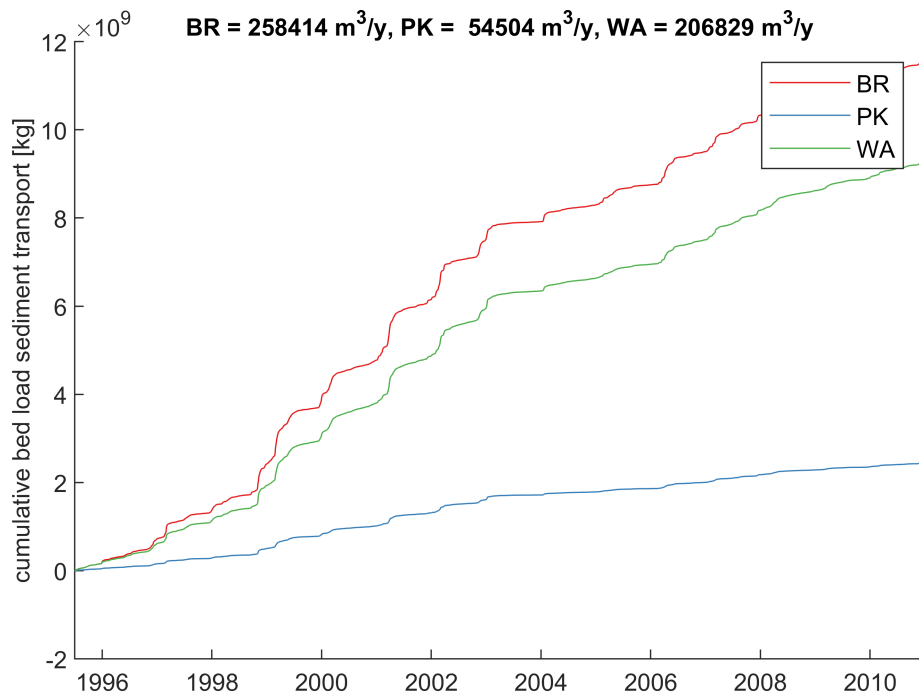
Figure 17 Total (gravel and sand) sediment transport at the Pannerdensche Kop

Branch	Model [m^3/y]	Frings *et al.* (2019) [m^3/y]	% [-]
Boven-Rijn	258×10^3	271×10^3	-4.8
Pannerdensche Kanaal	55×10^3	49×10^3	12.2
Waal	207×10^3	231×10^3	-10.4

Table 5 Comparison between the total load predicted by the model and the estimation by Frings *et al.* (2019) in the Pannerdensche Kop.

Branch	Model [m³/y]	Frings *et al.* (2019) [m³/y]	% [-]
Pannerdensche Kanaal	56×10^3	49×10^3	14.2
IJssel	22×10^3	19×10^3	15.7
Nederrijn	34×10^3	36×10^3	-5.6

Table 6 Comparison between the total load predicted by the model and the estimation by Frings *et al.* (2019) in the IJssel Kop.
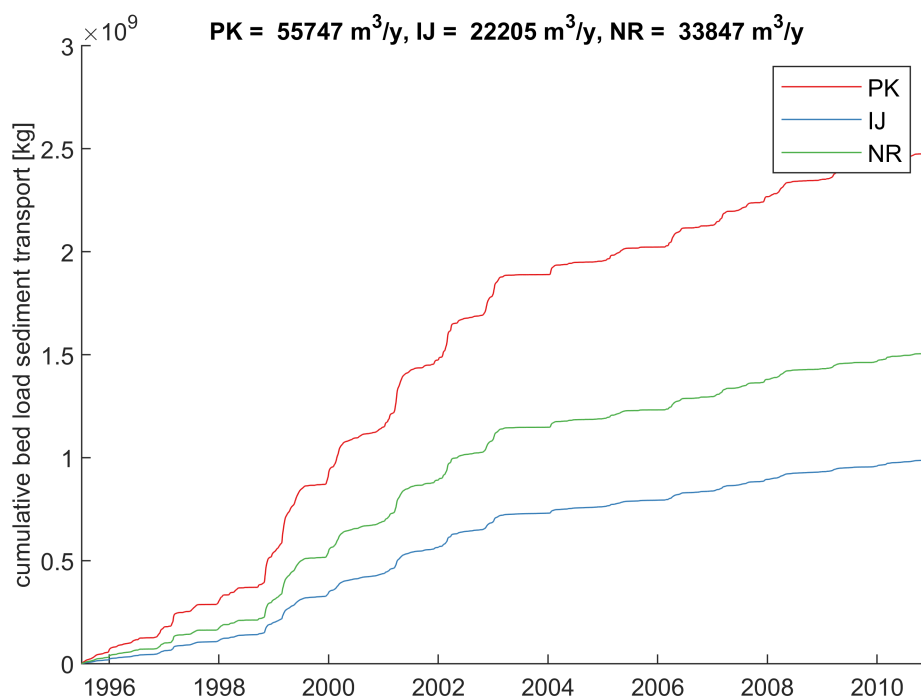
Figure 18 Total (gravel and sand) sediment transport at the IJssel Kop

5.3.2 Bed elevation changes

Figures 19, 20, 21, 22, 23 show the measured and modelled bed level changes in the period 1995-2011 along the Rhein - Boven-Rijn , Waal , Pannerdensch Kanaal , Nederrijn - Lek , and IJssel , respectively. The essential features are captured. In Figure 19 the measured change in the Rhein is equal to zero because the same schematization of the Rhein is used in both the 1995 and 2011 schematizations. The ongoing degradation of the most downstream section of the Boven-Rijn is correctly modelled. Degradation of the Boven Waal is correctly modelled. The aggradation in the downstream section of the Waal which is not measured is due to the fact that dredging in the Merwedes counteracting aggradation in the Waal that occurred in this area is not modelled. In the Pannerdensch Kanaal , degradation of the upstream part is correctly modelled, although aggradation in the centre part is predicted, which is not measured. This aggradational feature is associated to a coarsening wave that forms during the flood of 1999. Changes are nevertheless acceptable. Along the Nederrijn - Lek , no clear aggradational or degradational trend is observed, similarly to measured values. The changes along this branch are somehow larger in the model than in the measured data. Changes in bed elevation along the IJssel are also reasonable when compared to measured values.

Deltares
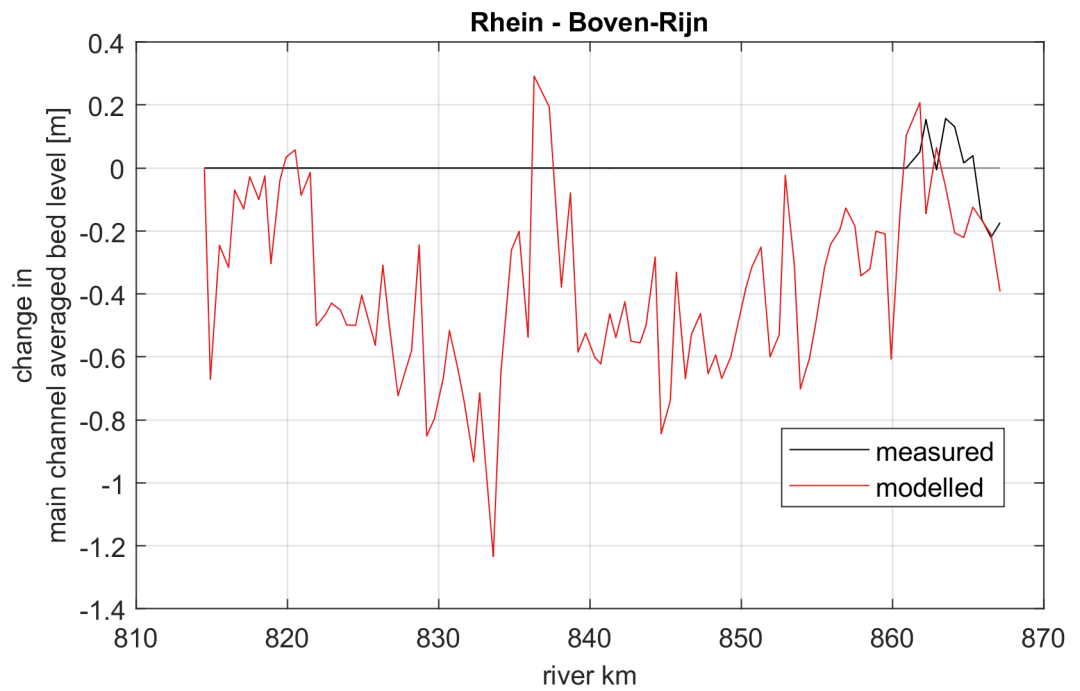
Figure 19 Bed level change along the Rhein - Boven-Rijn in the calibrated run in the period 1995-2011.
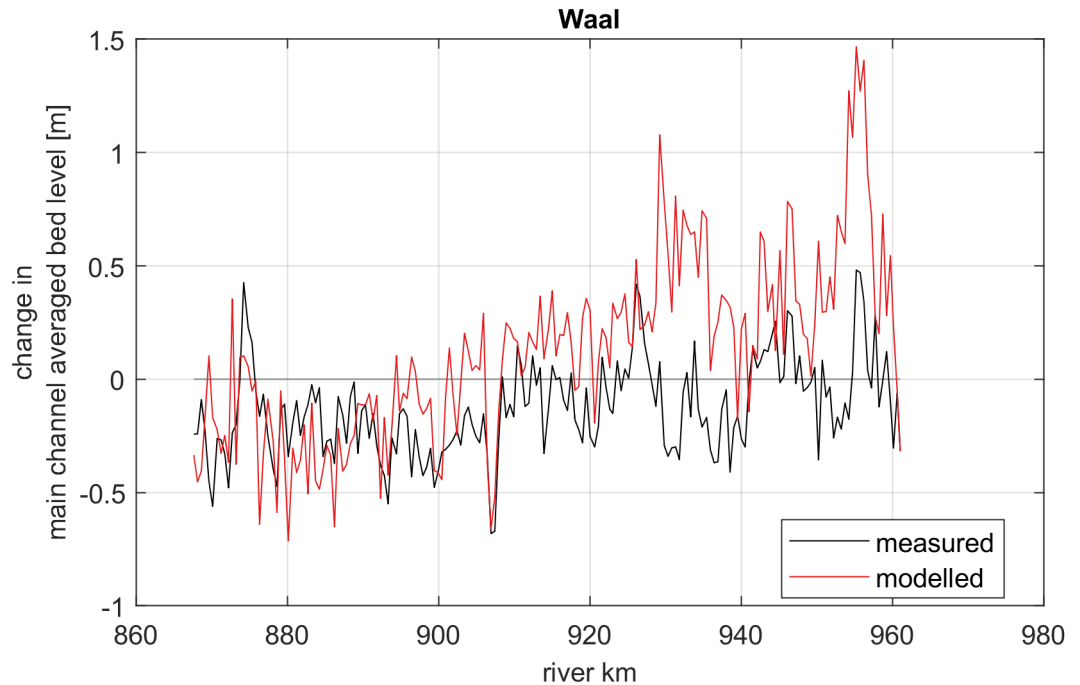
Figure 20 Bed level change along the Waal in the calibrated run in the period 1995-2011.

Deltares
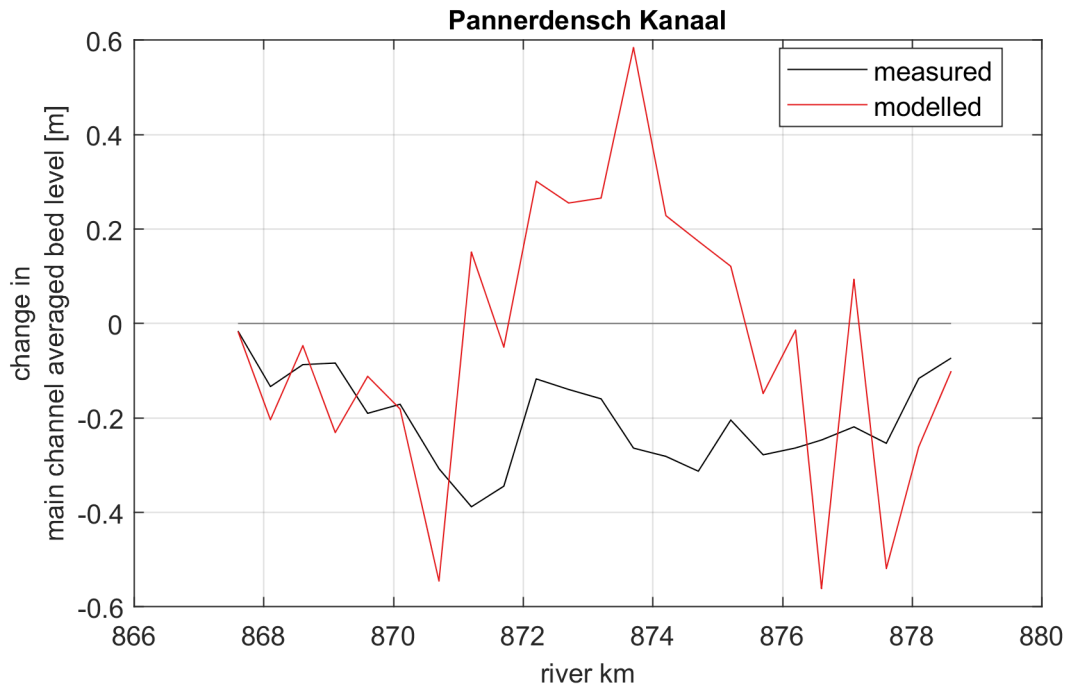
Figure 21 Bed level change along the Pannerdensch Kanaal in the calibrated run in the period 1995-2011.
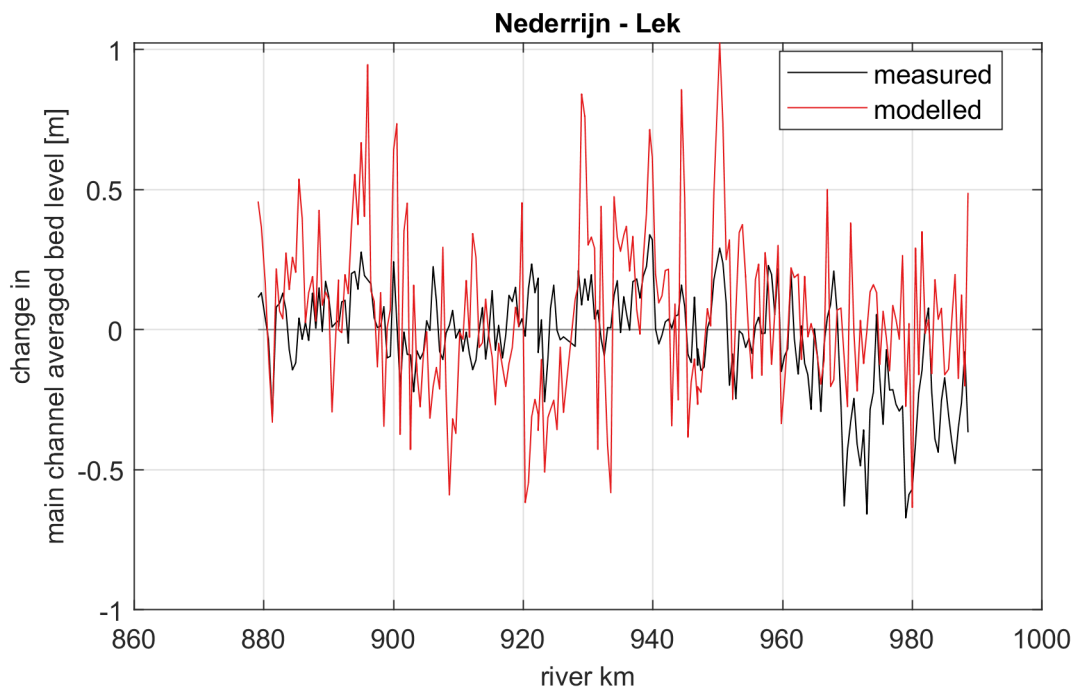
Figure 22 Bed level change along the Nederrijn - Lek in the calibrated run in the period 1995-2011.

Morphological models for IRM
11203684-015-ZWS-0011_v1.0, Version 0.1, 2020-12-11, Final

Deltares
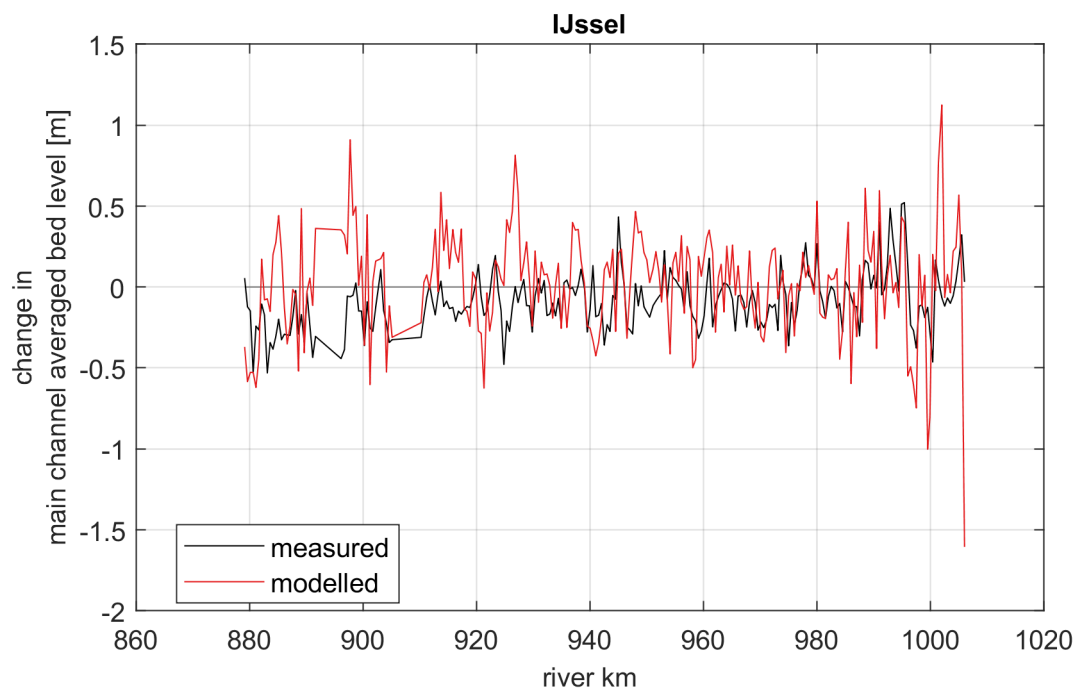
Figure 23 Bed level change along the IJssel in the calibrated run in the period 1995-2011.

Deltares

5.3.3 Grain size distribution changes

Figures 24, 25, 26, 27,28 present the changes in mean grain size along the branches. In this case, it is not possible to compare to measured data, as data of 2011 are not available. It is also relevant to consider that, even if data would be available, the frequency in time (in average the are measurements every decade) and in space (there are measurements every kilometre) is low compared to the time and space scale of local changes and fluctuation due to, for instance, flood events or the presence of bed forms. Hence, comparing to measurements representing one year is inadequate and a long term trend is preferred. As this is not available, changes with respect to the initial condition are shown. A slight coarsening of the Rhein is visible. Variation is, nevertheless, within the data scatter. A coarsening wave is present in the Pannerdensch Kanaal, that forms during a flood event. The upstream part of the IJssel becomes finer with time. This could indicate that less coarse sediment enters the IJssel in the model than in reality. However, the load estimation is correct. Calibration of the sediment transport rate at that location could prevent the slight fining, but this is constrained from the fact that it was decided to use the same calibration parameters for the whole branch.
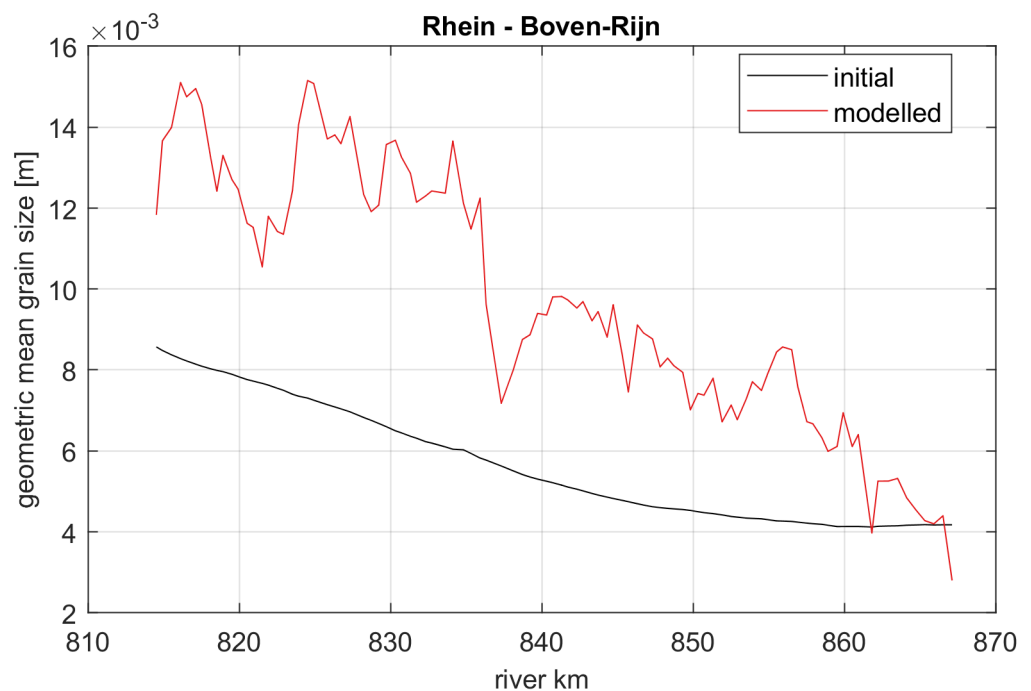
Figure 24 Grain size-initial cross-section 1995 after calibration-Boven-Rijn

Deltares
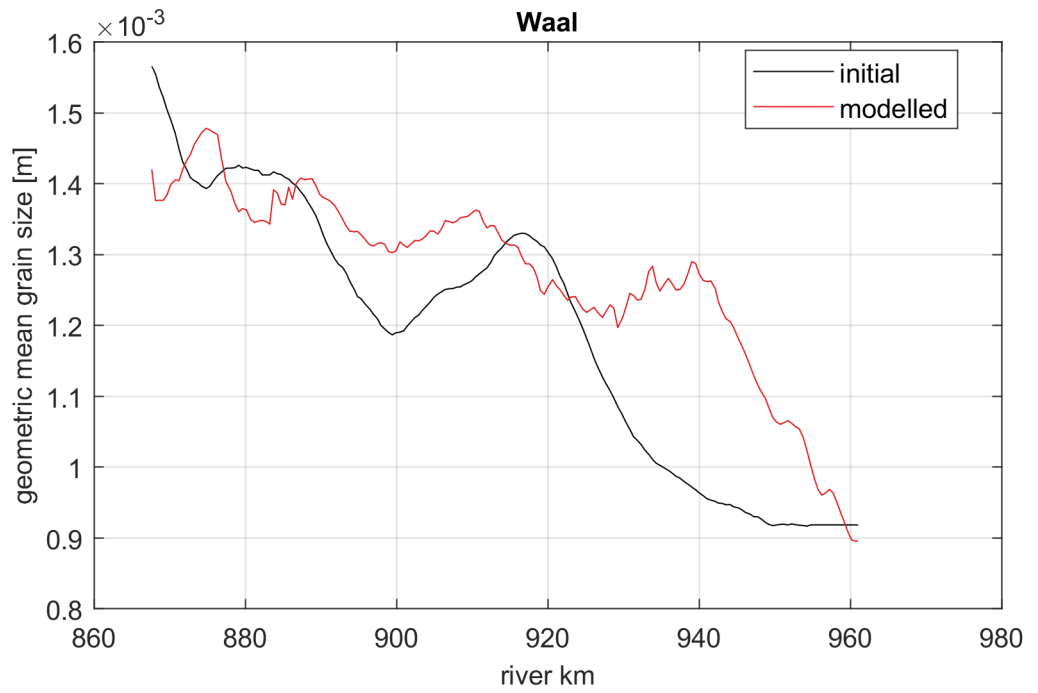
Figure 25 Grain size-initial cross-section 1995 after calibration-Waal
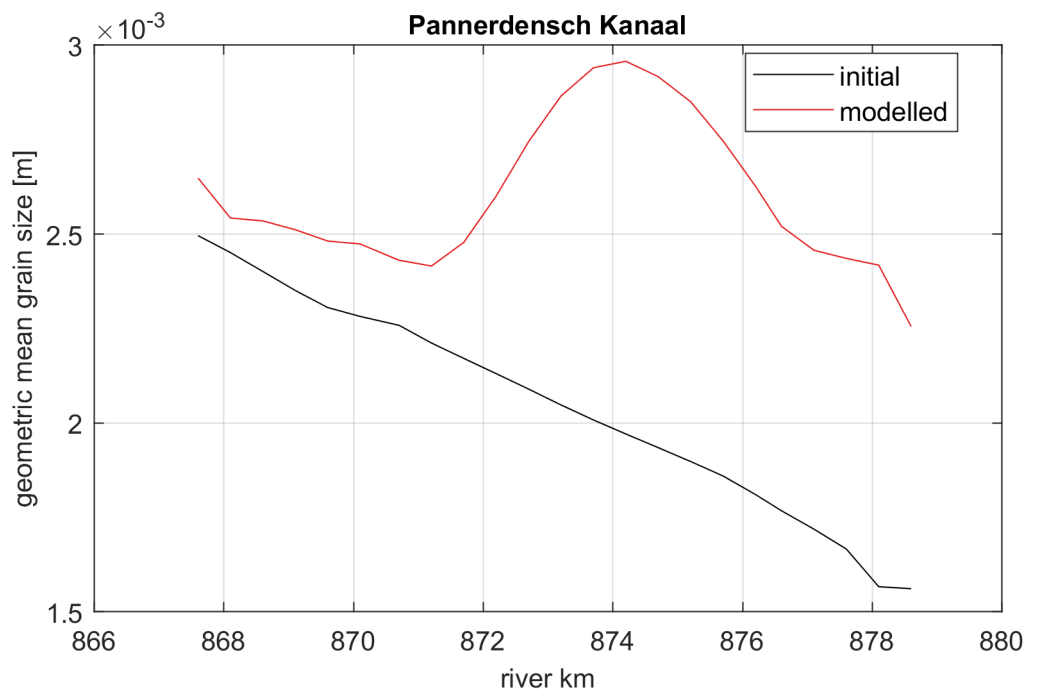
Figure 26 Grain size-initial cross-section 1995 after calibration-Pannerdensch Kanaal

Deltares
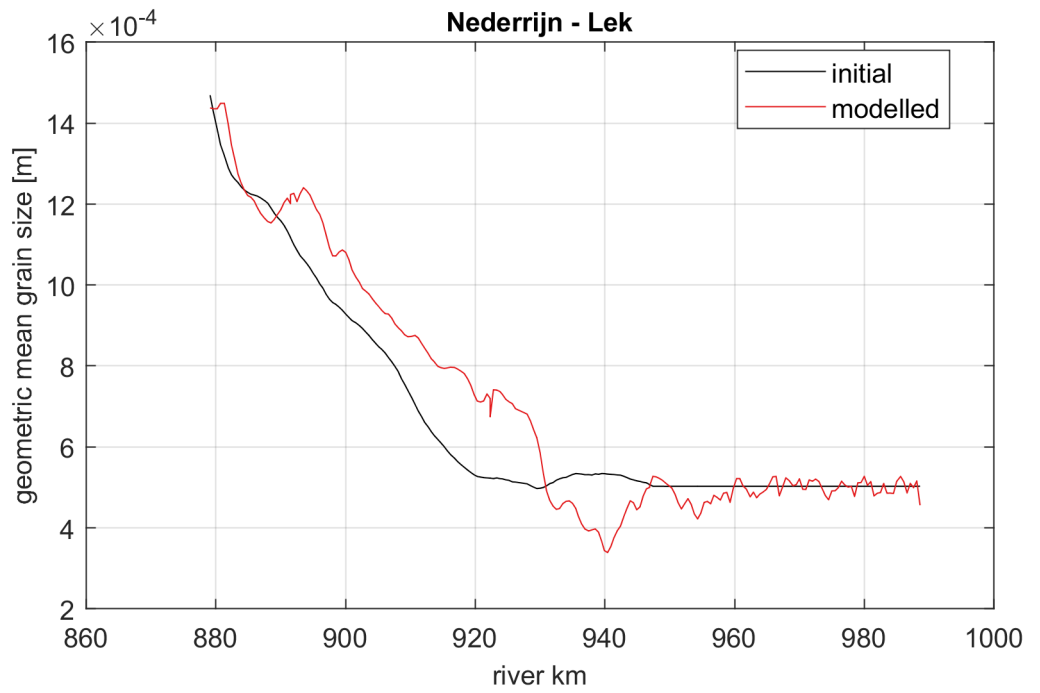
Figure 27 Grain size-initial cross-section 1995 after calibration-Nederrijn-Lek
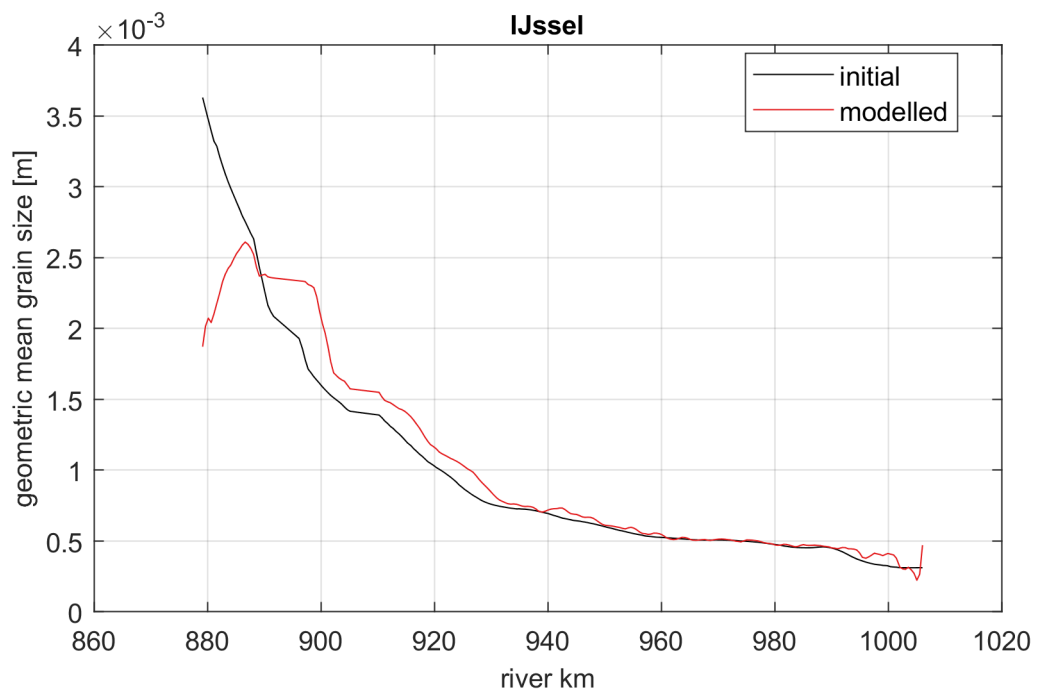
Figure 28 Grain size-initial cross-section 1995 after calibration-IJssel

Morphological models for IRM
11203684-015-ZWS-0011_v1.0, Version 0.1, 2020-12-11, Final

Deltares

5.3.4 Celerity of perturbations

Figures 29 and 30 shows the changes in geometric mean grain size with respect to the intial conditions and changes in bed elevation with respect to the previous output time along the Waal, respectively. It is possible to observe that changes propagate at, approximately, 1 km/y, as shown by Sieben *et al.* (2005).
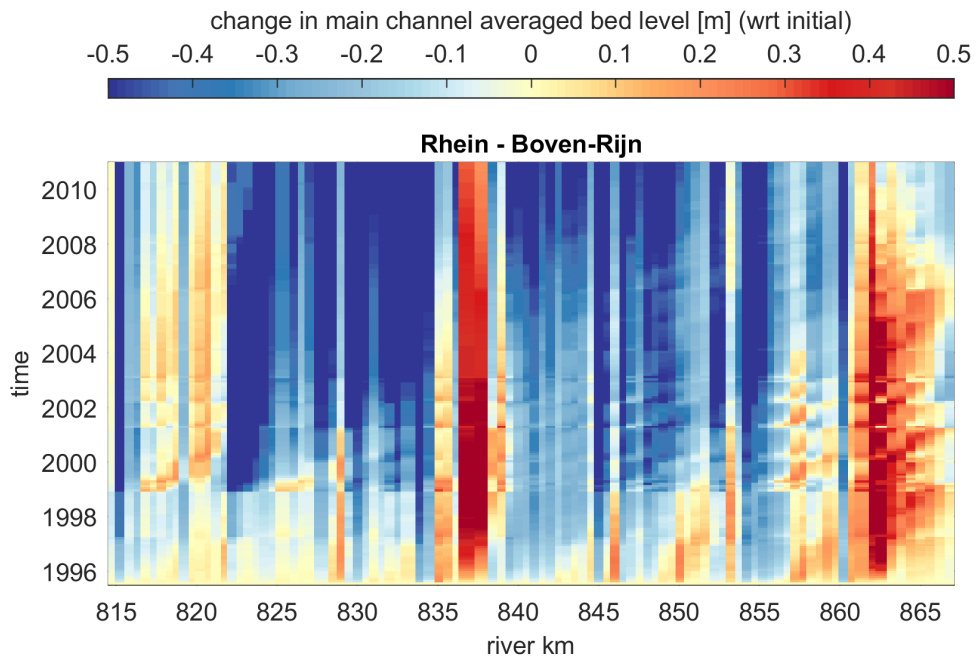
Figure 29 Bed level changes in time with respect to the initial conditions along the Rhein - Boven-Rijn

All figures showing changes with time are in Appendix L.
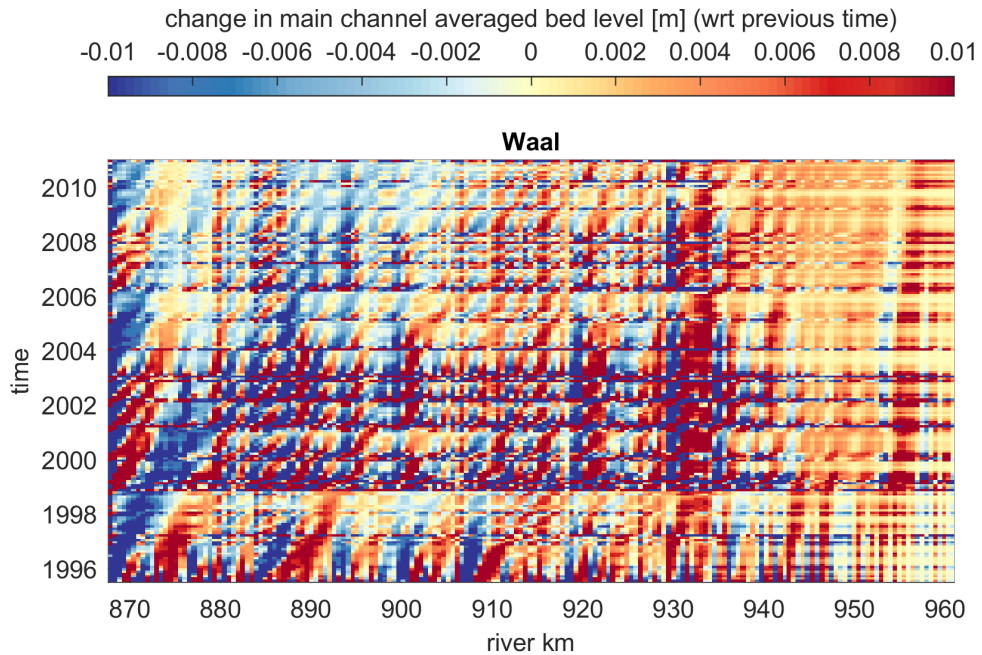
Figure 30 Bed level changes in time with respect to the initial conditions along the Rhein - Boven-Rijn

5.4 Verification

Three simulations are conducted to verify the morphological model:
1   Simulation with initial schematization of 2011 period 1 July 1995 - 1 January 2011,
2   Simulation with initial schematization of 2011 period 1 January 2011 - 1 January 2020, and
3   Simulation with initial schematization of 2019 period 1 January 2011 - 1 January 2020.

The same parameters as in the calibration runs are used in the verification runs. The initial composition of the bed is also the same as in the calibration runs.

Appendices M and N present the figures with the results of the period 1995-2011 and 2011-2019, respectively. In general all the results are within acceptable terms. The mean annual load in the period 2011-2019 is lower than in the period 1995-2011, which can be explained from the fact that there exist less high-flow events. The general patterns described in the calibration section are found in the validation runs. Interestingly, the aggradational pattern in the Pannerdensch Kanaal found in the calibration run but not in the measured data appears both in the runs and in the data of the period 2011-2019. This may indicate that the aggradational pattern at that location is realistic and the fact that it does not appear in the data of 2011 is due to the timing of the bed elevation measurements. The bed level comes from BASELINE , which comes from yearly multibeam measurements that reflect the situation at one particular instant. Hence, depending on the timing, features associated to, for instance, flood events may or may not be captured in the measured data. Moreover, not all bed-level data represents the same instant, further hampering comparison to model results at one particular time.

Deltares

6 Sensitivity analysis

The calibration has been conducted on the parameters of the sediment transport relation and the nodal-point relation only. Nevertheless, these are not the only two sets of parameters that strongly influence a morphodynamic simulation accounting for mixed-size sediment. In particular, the active layer thickness has an important impact as regards to the celerity at which changes in the grain size distribution propagate and it has been shown to be a crucial parameter for accurate calibration of morphodynamic runs. The type of nodal point relation influences the behaviour of a bifurcations and impacts its stability. In this section we show the effect of varying the active-layer thickness 6.1 and using a different nodal-point relation 6.2.

6.1 Variation of the active-layer thickness

The active-layer thickness is inversely related to the propagation celerity of perturbations in grain size distribution Chavarrías *et al.* (2019). Thus, a smaller active-layer thickness causes faster changes in grain size distribution and vice versa. Changes in grain size affect the bed elevation changes in turn.

We conduct two simulations of the calibration run changing the active-layer thickness to 0.5 m and 2.0 m. Figures 31, and 32 present the changes in grain size at the bed surface in these two cases, respectively. One observes that, indeed, changes in grain size occur faster for a thinner active layer. The slower changes in grain size cause less changes in bed elevation (Figure 33). The differences between runs diminish in the downstream part of the Waal, in which grain size distribution becomes more uniform.

All simulation results are within an acceptable band and, by calibration of the sediment transport relation, one could improve the performance given a particular active-layer thickness. It is recommended to base the value of the active layer thickness on the height of perturbations to the mean bed elevation and to calibrate the sediment transport relation, rather than having both as calibration values. This is because a higher control of the simulation results is achieved by the sediment transport relation and the physical constrains of the active-layer thickness allow for less variation.

Deltares
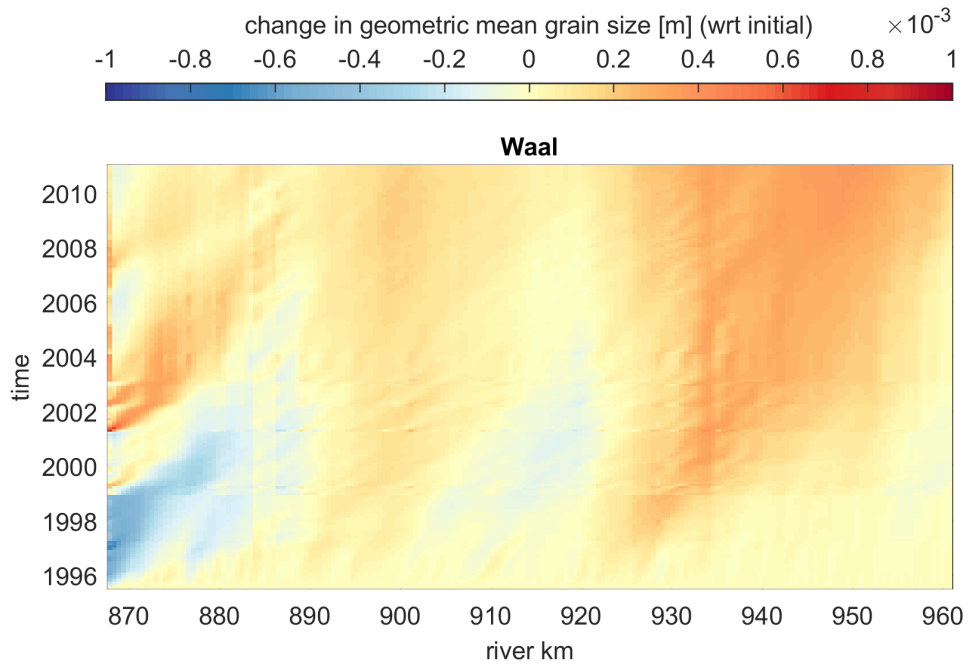
Figure 31 Change in geometric mean grain size at the bed surface with respect to the initial situation for the calibration run but with the active-layer thickness equal to 0.5 m.
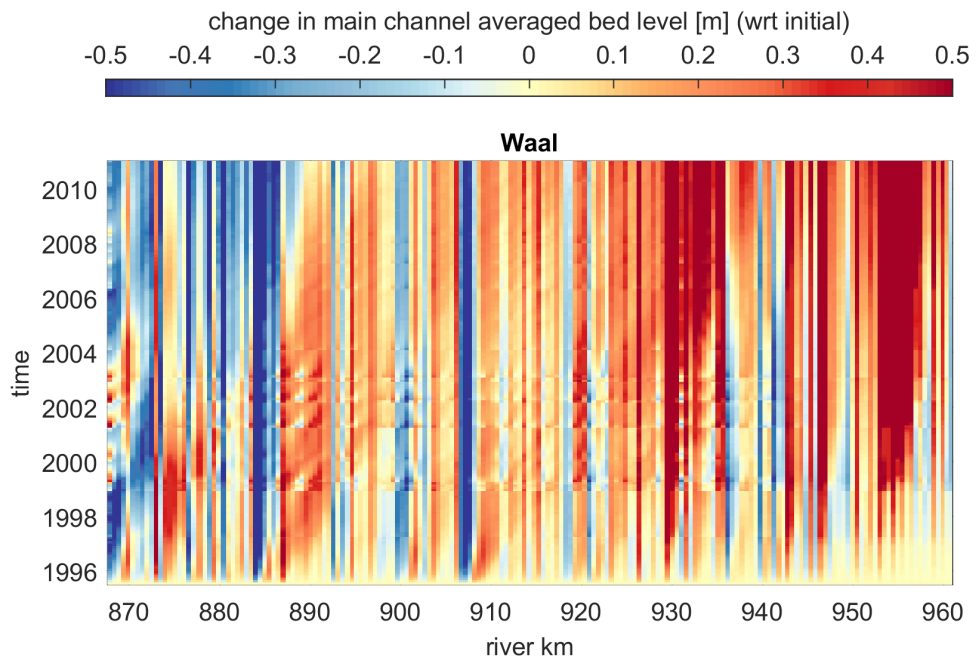
Figure 32 Change in geometric mean grain size at the bed surface with respect to the initial situation for the calibration run but with the active-layer thickness equal to 2.0 m.

Deltares
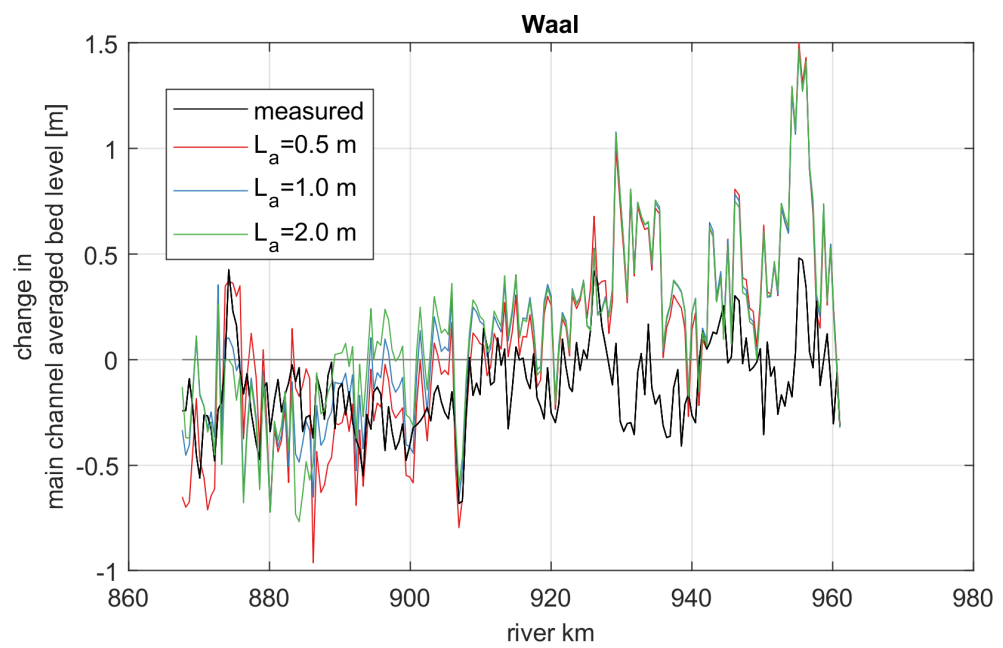
Figure 33 Change in bed elevation in the calibration run for a varying active-layer thickness.

Deltares

6.2 Variation of the nodal-point relation

The model uses a nodal-point relation that is intrinsically unstable for a constant discharge 5.1.5. Nevertheless, the fact that one of the downstream branches does not close during the simulation period and the results are realistic is not surprising. This is first due to the unsteadiness of the flow, which is not considered in the theoretical analysis. Flow variability may cause an unstable bifurcation to become stable, specially considering the complex dynamics of the *Rijntakken*. For instance, when the discharge is low, the weir at Driel changes the flow pattern deviating a larger amount of water towards the Waal.

Second, the classical theory of bifurcations stability is derived under unisize sediment conditions (Wang *et al.*, 1995). This theory has been extended to a mixture of two sediment size fractions by Schielen and Blom (2018), but the dynamics of a bifurcation system with an undetermined number of size fractions remains elusive.

Third, previous studies require the use of the sediment transport relation by Engelund and Hansen (1967) for obtaining an analytical solution. In this case, the power of the discharge ratio must be larger than $b/3$, being b the degree of non-linearity of the sediment transport relation (Mosselman, 2013). Assuming that the result is valid when using the sediment transport relation by Meyer-Peter and Müller (1948), the degree of non-linearity in this case varies between infinite, for a bed shear stress close to incipient motion, to 3, for an infinitely large bed shear stress. Hence, for a large bed shear stress, a bifurcation would be stable when the power of the discharge ratio is 1, and would always be unstable regardless of the power for a small bed shear stress.

Fourth, the effect of combining two different transport relations has never been studied and the situation further complicates when considering that the sediment transport relation has different calibration coefficients in each of the branches of the bifurcation.

Last, the morphodynamic time scale associated to changes in a bifurcating system is significantly longer than the simulation time of the runs we have conducted. For this reason, it is not expected that one will be able to discern between a stable or an unstable system in the runs we conducted.

In order to show the effect of a different power in the discharge ratio, we conduct one numerical run using the following nodal point relation:

$$\frac{Q_{\mathrm{b}k1}}{Q_{\mathrm{b}k2}} = \left(\frac{B_1}{B_2}\right)^m \left(\frac{Q_1}{Q_2}\right)^k , \tag{6.1}$$

where power of the discharge ratio $k = 5/3$, in this way guaranteeing stability according to the classical theory, B_j [m] is the width of outgoing branch j, and m [-] is a constant computed such that, for a discharge ratio $R_{\mathrm{q}} = 2$, which is the standard water distribution in both bifurcations for a high discharge, the sediment ratio is the same as it is in the calibration run:

$$m = \frac{\log \beta_k R_{\mathrm{q}}^{1-k}}{\log \frac{B_1}{B_2}} . \tag{6.2}$$

Considering that in the model, the upstream widths of the Waal is 280.5 m, the Pannerdensche Kanaal is 143 m, the Nederrijn is 110.6 m, and the IJssel is 81 m, we compute the powers in Table 7. The results for the Waal branch are shown in Figure 34. As expected, the differences between the calibration run and the one using a stable value of the discharge ratio are minimal and restricted to the upstream part of

Deltares

Bifurcation (Outgoing branch 1/Outgoing branch 2)	m sand fractions [-]	m gravel fractions [-]
Pannerdensche Kop (Waal/Pannerdensche Kanaal)	0.1745	0.1745
IJssel Kop (Nederrijn/IJssel)	-0.5201	-1.5159

Table 7 Parameters of the nodal-point relation in a stable case.

the domain, as information travels at approximately 1 km/y. Appendix O presents the figures of all the river branches.
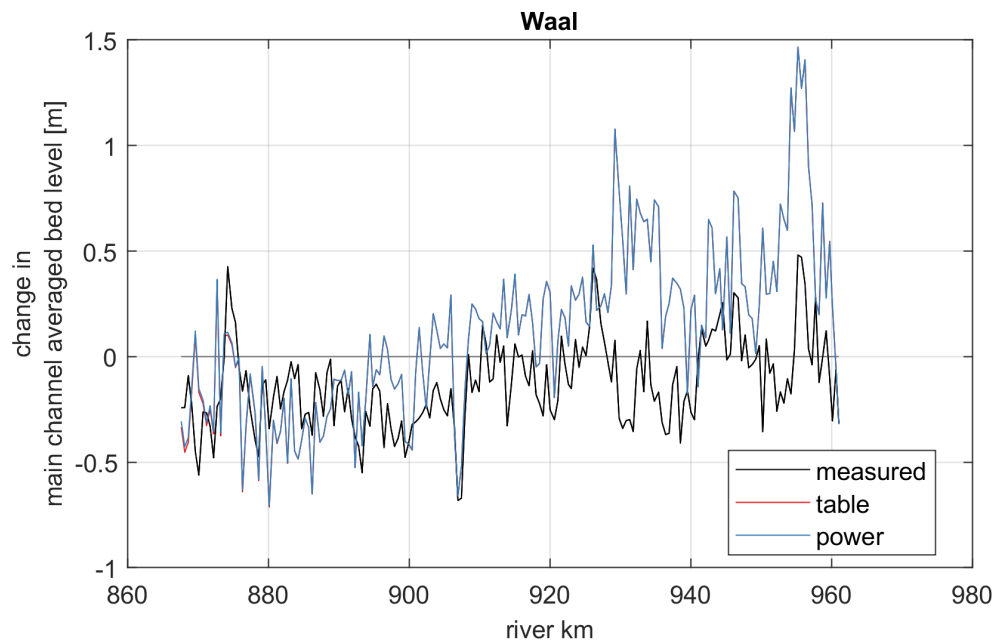
Figure 34 Bed elevation changes of the calibration run along the Waal using an unstable nodal-point relation ("table") and a stable one ("power").

Deltares

7 Discussion

The morphodynamic model we have developed is based on the SOBEK 3 hydrodynamic model, which is in turn based on the WAQUA model via the WAQ2PROF procedure. This is an important limitation, as the WAQUA model and WAQ2PROF procedure have been developed for preserving the hydrodynamic properties of interested, which do not need to be the properties one aims at preserving in a morphodynamic model. For instance, the width presents large variations in streamwise direction which do not seem realistic in a morphodynamic model in which the transport of sediment occurs only in the main channel. The gradients in width are found to be acceptable for prevention of large gradients in the velocity in the main channel and floodplains in the one-dimensional SOBEK 3 model as in the WAQUA 2D model, but still cause unrealistic sediment transport gradients, as the sediment transport rate is restricted to the main channel.

Moreover, the SOBEK 3 and WAQUA models have not been validated for situations after Room for the River interventions (*T.C. Vos, Rijkswaterstaat ON*, personal communication), which limit the application extent. Furthermore, only the main-channel roughness of the SOBEK 3 model has been calibrated, assuming that the roughness of the floodplains is correct. In a 1D model only cross-section average quantities are simulated. The separation between main channel, groyne fields and flood plains is artificially added through assumptions that only allows for a rough approximation of the real hydrodynamics of each section. Besides, several other 2D and 3D processes are parametrized or simplified in the 1D model. Furthermore, the choice of which part of the cross section is considered main channel is inconsistent and leads to gradients in flow velocity and discharge distribution along the branches. As a consequence, the calibrated roughness is used to compensate for these missing or inconsistency effects, and does not have a link to the physical state of the river bed. Unfortunately, because of the choice to calibrate the models only on main-channel roughness, all imperfections have to be concentrated through this roughness. In the morphological model this is partially repaired by choosing a reasonable and physically sound main-channel roughness, but at the costs of water level predictability. The hydrodynamic calibration results show that there are errors in water level of the order of centimetres and up to a decimetre. The model is therefore not to be used for assessment of hydraulic impacts. The model is applicable for studying the long term impact of large scale human interventions (Section 1.6).

The model has been thoroughly calibrated. Nevertheless, it is important to realize the limitations of the measured data in which the calibration has been based. For instance, the water discharge distribution along the Pannerdensche Kop of the last 10 years presents large inaccuracies, as it is based on water elevation measurements that require update (*T.C. Vos, 2020, Rijkswaterstaat ON*, personal communication). As regards to the morphodynamic component, the sediment load has been used to calibrate the model. This is highly uncertain and presents large variations in time and in space. Accurate measurements of the load (also bedload) in both space and time are needed for correctly calibrating the model. Furthermore, the spatial and temporal frequency of the measurements of the bed surface grain size distribution are not high enough for properly assessing its changes (Chavarrías and Ottevanger, 2019).

The schematizations we have used provide the bed elevation and the river situation in 1995, 2011, and 2019. Nevertheless, there is a difference between the measured bed

Deltares

elevation with single and multi beam, and the bed elevation in the model. This is because the measured two-dimensional bed elevation data is first input into the *Rijkswaterstaat* ArcGIS application and database BASELINE and then converted into representative one-dimensional values characteristic of a certain river section (i.e., *SOBEKvakken*). Werner *et al.* (2000) shows an example of the generation of cross-sectional data. Attention needs to be paid when comparing these two.

The morphodynamic development in the presence of fixed layers is characterized by an intrinsic two-dimensional effect. While in reality one of the sides of the cross-section is fixed and the other is not, in the model the bed elevation of the whole cross-section is fixed. For this reason, the elevation of the fixed layer in the model does not need to be the bed elevation in the field, but it needs to capture the essential morphodynamic development. In long term simulations, it is important to judge the results having in mind these limitations.

The same schematization of the German Rhine has been used in combination with all schematizations of the *Rijntaken*. Given that the interest of the model is in the Dutch part of the River system, the effect of inaccuracies in the German Rhine is limited. However, for long term simulations, the system is dominated by the load and changes in the German Rhine, and further attention needs to be paid. In this regards, the boundary condition that has been imposed at the upstream end of the domain is a fixed bed level and composition. This implies that the conditions of the first node, which appears to have relatively low flow velocities, are driving the dynamics of the river. For long term simulations, the upstream part of the domain should be moved even further upstream. A different approach would be to feed the annual load rather than fixing the bed, although this would not prevent the need to have the domain of interest sufficiently far from the upstream boundary.

The hiding-exposure relation that has been used only affects gravel, as sand has been modelled with a load relation that does not have a critical bed shear stress. While this has provided acceptable results, there is a discussion about the physical interpretation of such a relation. In essence, sand particles are affecting the mobility of gravel particles, but gravel particles are not affecting the mobility of sand particles. Moreover, the hiding-exposure function as it is implemented in DELFT3D FM SUITE depends on the arithmetic mean grain size, while it would be more reasonable that it depends on the geometric mean grain size given that the distribution is closer to a logarithm than to a linear function.

The current model is one of the first one-dimensional morphodynamic models developed using D-FLOW FM 1D . There are clear advantages of using this software, as are the fact that it can be extended to include two and three-dimensional features, and the large number of processes that can be included in future model extensions. Nevertheless, there are three main shortcomings to tackle in future development. First, the lack of a steady-state solver implies that the unsteady flow equations are solved, although the unsteadiness of the flow is irrelevant for our purpose. Hence, the simulation time is considerably increased and the calibration possibilities reduced.

Second, the "bend effect" is prevented by artificially straightening the domain. While this proves to be an acceptable solution, it prevents further extension to two-dimensional models and increases the work-flow complexity considerably. Moreover, even in purely one-dimensional models, straightening does not solve the "bend effect" problem if flow is reversed, as it happens in a tidal environment such as the Rijn-Maas estuarine area. In this case, straightening the domain does not only not solve the problem but it actually enhances it, as a bifurcation angle close to zero

Deltares

during ebb becomes close to 180 degrees during flow.

Last, morphodynamic development in the presence of structures needs to be assessed. In the SOBEK 3 schematization, the node immediately downstream of a structure is situated close to the structure. This does not limit the simulation time in a hydrodynamic run using D-FLOW FM 1D , as the advection scheme in the presence of a structure does not take into account the downstream information in the stencil. However, in a morphodynamic simulation, this small cell close to a structure may be the limiting factor and cause crash of a simulation, as the morphodynamic celerities are not taken into account in the automatic time-stepping. In fact, we had to considerably reduce the time step in some of the simulations to prevent this issue from arising [1].

---

[1] The model developed in this project is currently being used by HKV for conducting a project committed by *Rijkswaterstaat* consisting on estimating bed level changes over 100 years. They have encountered the same unstable behaviour at structures and in their case it was not solved by reducing the time step. This may indicate that the problem is not associated to morphodynamic CFL, although a thorough test and analysis has not been conducted. In solving this problem we considered that a pragmatic as well as realistic solution was to prevent bed elevation changes in the cells immediately upstream and downstream of the structures. This was achieved by the so-called MORPHOPOL option, in which a polygon inside which morphodynamic changes are allowed is defined. One can interpret the lack of morphodynamic changes around structures in several ways. One interpretation is that *Rijkswaterstaat* will dredge or dump the necessary amount of sediment that keeps the bed elevation equal to its initial value. Contrary to the actual dredging operations along the river, dredged material is not deposited somewhere else in the river and this interpretation implies that there is a net gain or loss of sediment in the river.

Deltares

8 Conclusions and recommendations

8.1 Conclusions

In this report, the development, calibration, and verification of a one-dimensional morphodynamic model of the Dutch Rhine branches *(Rijntakken)* and downstream part of the German Rhine using D-Flow FM 1D is described. The upstream end of the domain is found at the confluence of the Lippe with the Rhine at Wesel (Germany, Rhine kilometer 815). The downstream ends of the domain are found at Hardinxveld, Krimpen aan de Lek, and the Ketelmeer.

The starting point of the schematization is the existing Sobek 3 one-dimensional models of the *Rijntakken* and the German Rhine. These models have been built for hydrodynamic studies and need to adjusted for being suitable to predict morphodynamic changes. Adjustment includes, among other thing, removing of sections not relevant for morphodynamic studies, increasing the main channel width for allowing aggradation above the initial groyne toe, setting a single friction coefficient per branch for preventing unrealistic changes in sediment transport rate, straightening of the model schematization for preventing spurious energy loses. Once adjusted, the models are combined into one single model and converted to D-Flow FM 1D .

In a first step, the hydrodynamic parameters of the models are calibrated. This is done by comparing water level, velocity at the main channel, and discharge partitioning at the bifurcations with WAQUA results on steady-state hydrodynamic simulations. It is found that the hydrodynamic variables are correctly reproduced for morphodynamic purposes using a single friction coefficient for the entire river system. The coefficient varies with discharge. Two values are proposed, one for discharges below 2000 m^3/s and one for discharges above 4000 m^3/s. Values in between are interpolated.

The calibrated model is extended with morphodynamic parameters based on the Sobek-RE model schematization by Sloff (2006). In the current schematization, 16 sediment size fractions are modelled from which 8 are sand and the 8 are gravel. Several sediment transport relations are tried arriving to the conclusion that the most promising approach is to consider the relation by Engelund and Hansen (1967) for the sand fractions and the one by Meyer-Peter and Müller (1948) considering the hiding-exposure effect for the gravel fractions. The prefactor of the load relations and the nodal-point-relation coefficients that model the sediment distribution in the river bifurcations are calibrated by comparing the mean annual load at the bifurcations with estimated values by Frings *et al.* (2019) and the bed level along the branches with the bed level in the Sobek 3 official schematizations, which is derived from measured data. It is found that it is necessary to modify the prefactor per branch to achieve realistic results. The calibration process requires iterative solving and is done for the period 1995-2011. Afterwards, the model is validated against morphodynamic development between 2011 and 2019.

Deltares

8.2 Recommendations for future model development

As regards to the model schematization, it is recommended to review it with special attention to the parameters from the hydrodynamic model that have not been assessed in detail. In particular, the role of the main channel width.

As regards to the data used in developing the model, it is recommended to carefully assess the sediment transport and grain size distribution of the bed surface of the *Rijntakken*. Detailed measurements of both, and a project with the specific objective of modelling this is recommended.

As regards to the software, it is recommended to implement a steady-state solver and to solve the limitations of the "bend effect", as well as to carefully assess the role of structures in the presence of morphodynamic development. A detailed profiling of the computational time should be conducted for identifying bottlenecks.

Deltares

9   References

Ashida, K. and M. Michiue, 1971. "An investigation of river bed degradation downstream of a dam." In *Proc. of the 14th IAHR World Congress, 29 August–3 September, Paris, France*, vol. 3, pages 247–255.

Ashida, K. and M. Michiue, 1972. "Study on hydraulic resistance and bed-load transport rate in alluvial streams." *Proc. Jpn. Soc. Civ. Eng.* 206: 59–69. DOI: 10.2208/jscej1969.1972.206_59.

Becker, A., 2017. *1D2D model of the Lower Rhine and the upper Dutch Rhine branches between Andernach and Nijmegen, Arnhem and Zutphen*. Tech. Rep. 11203685-002, Deltares, Delft, the Netherlands.

Berends, K. and R. Daggenvoorde, 2020. *1D morphodynamic model for the Maas*. Tech. Rep. 1203684-015-ZWS-0001, Deltares, Delft, the Netherlands.

Chavarrías, V. and W. Ottevanger, 2019. *Morphological development of the bifurcation at Pannerden: Measurements, simulations and improving of graded-sediment modelling*. Tech. Rep. 11203682-007-ZWS-0005, Deltares, Delft, the Netherlands.

Chavarrías, V., G. Stecca, A. Siviglia and A. Blom, 2019. "A Regularization Strategy for Modeling Mixed-Sediment River Morphodynamics." *Adv. Water Resour.* 127: 291–309. DOI: 10.1016/j.advwatres.2019.04.001.

Engelund, F. and E. Hansen, 1967. *Monograph on sediment transport in alluvial streams*. Tech. Rep., Hydraulics Laboratory, Technical University of Denmark, Copenhagen, Denmark.

Frings, R., G. Hillebrand, N. Gehres, K. Banhold, S. Schriever and T. Hoffmann, 2019. "From source to mouth: Basin-scale morphodynamics of the Rhine River." *Earth Sci. Rev.* 196. DOI: 10.1016/j.earscirev.2019.04.002, ISSN 0012-8252, URL http://www.sciencedirect.com/science/article/pii/S0012825216304585.

Gruijters, S., J. Veldkamp, J. Gunnink and J. Bosch, 2001. *The lithological and sedimentological structure of the Pannerdensche Kop bifurcation*. Tech. rep., Geological Survey of the Netherlands (TNO).

Hirano, M., 1971. "River bed degradation with armoring." *Proc. Jpn. Soc. Civ. Eng.* 195: 55–65. DOI: 10.2208/jscej1969.1971.195_55.

Meyer-Peter, E. and R. Müller, 1948. "Formulas for bed-load transport." In *Proc. 2nd IAHR World Congress, 6–9 June, Stockholm, Sweden*, pages 39–64.

Mosselman, E., 2013. *Gravel-bed Rivers: Processes, Tools, Environments,*, chap. 9, Modelling Sediment Transport and Morphodynamics of Gravel-bed Rivers, pages 101–115. John Wiley & Sons, Chichester, United Kingdom.

Parker, G., C. Paola and S. Leclair, 2000. "Probabilistic Exner Sediment Continuity Equation for Mixtures with No Active Layer." *J. Hydraul. Eng.* 126 (11): 818–826. DOI: 10.1061/(ASCE)0733-9429(2000)126:11(818), URL http://ascelibrary.org/doi/abs/10.1061/%28ASCE%290733-9429%282000%29126%3A11%28818%29.

Schielen, R. M. and A. Blom, 2018. "A reduced complexity model of a gravel-sand river bifurcation: Equilibrium states and their stability." *Adv. Water Resour.* 121: 9–21. DOI: 10.1016/j.advwatres.2018.07.010, ISSN 0309-1708, URL http://www.sciencedirect.com/science/article/pii/S0309170818300162.

Deltares

Shields, A., 1936. *Anwendung der Ähnlichkeitsmechanik und Turbulenzforschung auf die Geschiebebewegung*. Ph.D. thesis, Versuchsanstalt für Wasserbau und Schiffbau, 26, Berlin, Germany. (in German).

Sieben, J., R. van der Veen, D. F. Kroekenstoel and M. Schropp, 2005. *Morfologische effecten Ruimte voor de Rivier in het Bovenrivierengebied*. Tech. Rep. 2005.044X, RIZA, Directoraat-Generaal Rijkswaterstaa, Arnhem, the Netherlands. (in Dutch).

Sloff, C. J., 2006. *Uitbreiding SOBEK-RT model naar niet-uniform sediment*. Tech. Rep. Q4130.10, Delft Hydraulics Laboratory, Delft, the Netherlands.

Wang, Z., M. D. Vries, R. Fokkink and A. Langerak, 1995. "Stability of river bifurcations in ID morphodynamic models." *J. Hydraul. Res.* 33 (6): 739–750. DOI: 10.1080/00221689509498549.

Werner, M. G. F., M. Ververs, C. van, Haselen, U. Pakes., K. Daamen and M. Muerlebach, 2000. "A comparison of methods for generating cross sections for flood modelling using detailed floorplain elevation models." In A. Bronstert and C. Bismuth, eds., *Proceedings of the European conference on advances in flood research, 1-11 November*, vol. 1, pages 73–83. Potsdam institute for climate impact research.

Wilcock, P. R. and J. C. Crowe, 2003. "Surface-based Transport Model for Mixed-Size Sediment." *J. Hydraul. Eng.* 129 (2): 120–128. DOI: 10.1061/(ASCE)0733-9429(2003)129:2(120), URL http://ascelibrary.org/doi/abs/10.1061/%28ASCE%290733-9429%282003%29129%3A2%28120%29.

A   Main channel width
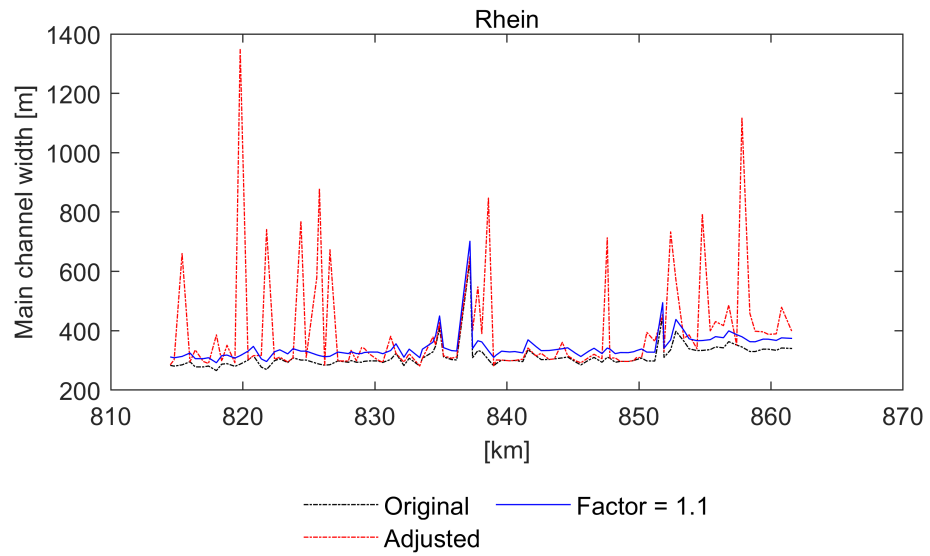
Figure 35 Main channel width - Rhein.
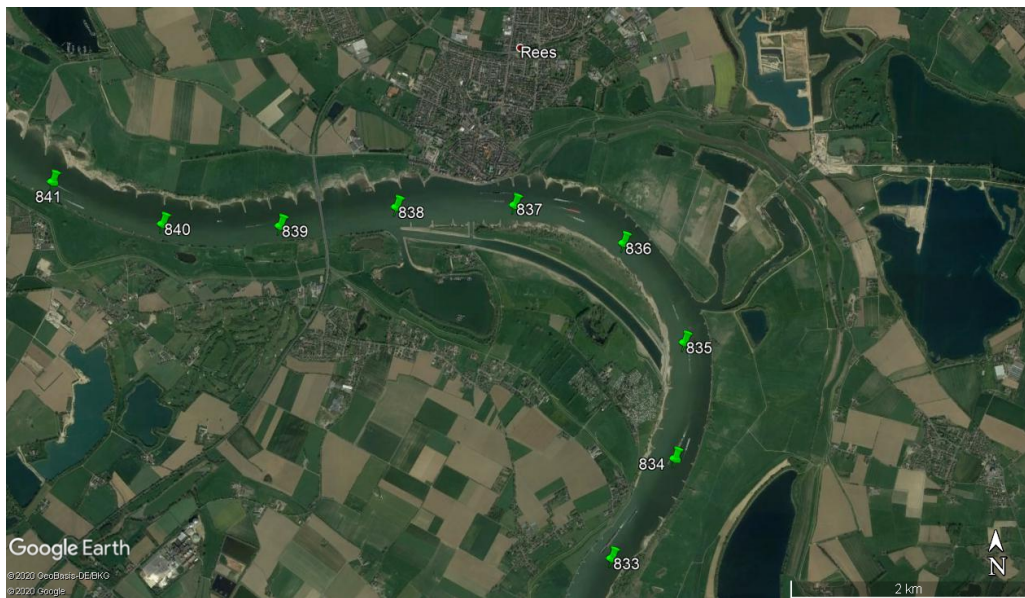
Figure 36 Cross-section issue example
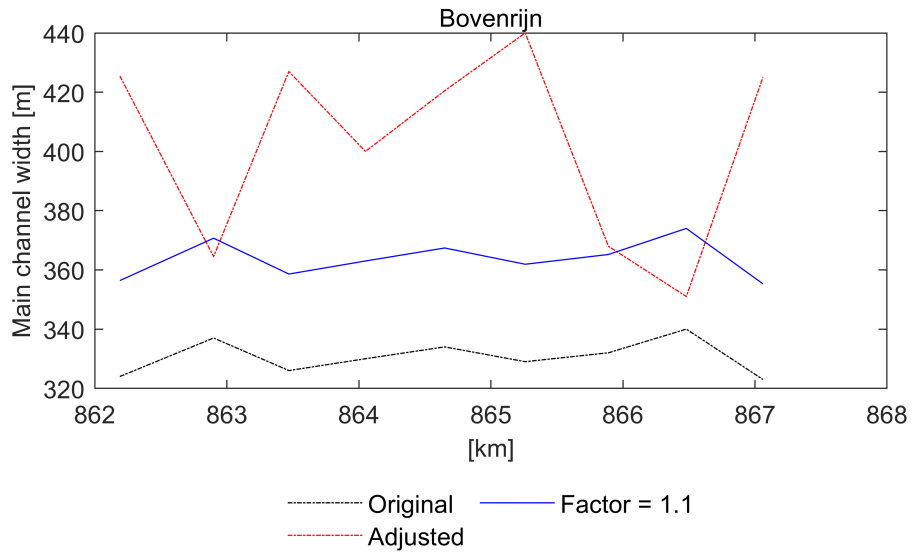
Figure 37 Main channel width - Boven-Rijn.
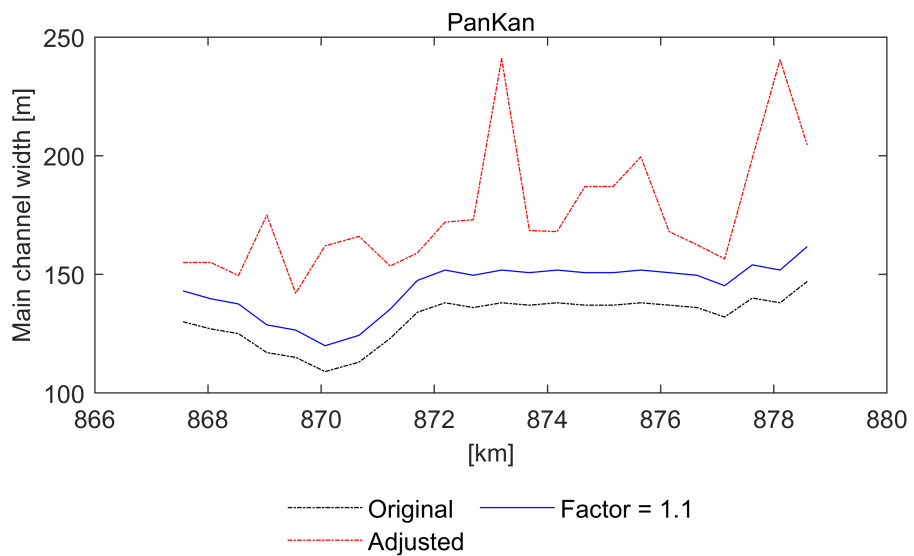
Figure 38 Main channel width - Pannerdensch Kanaal.

Deltares
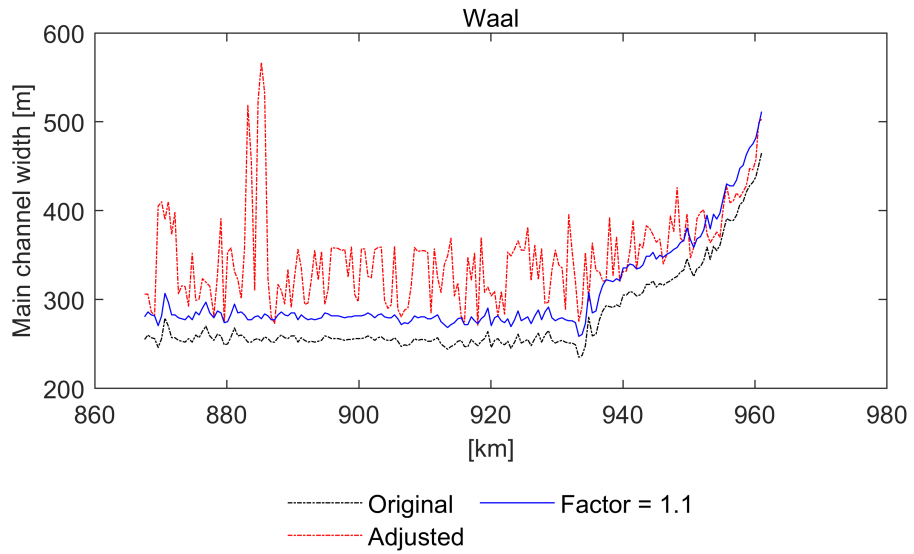
Figure 39 Main channel width - Waal.
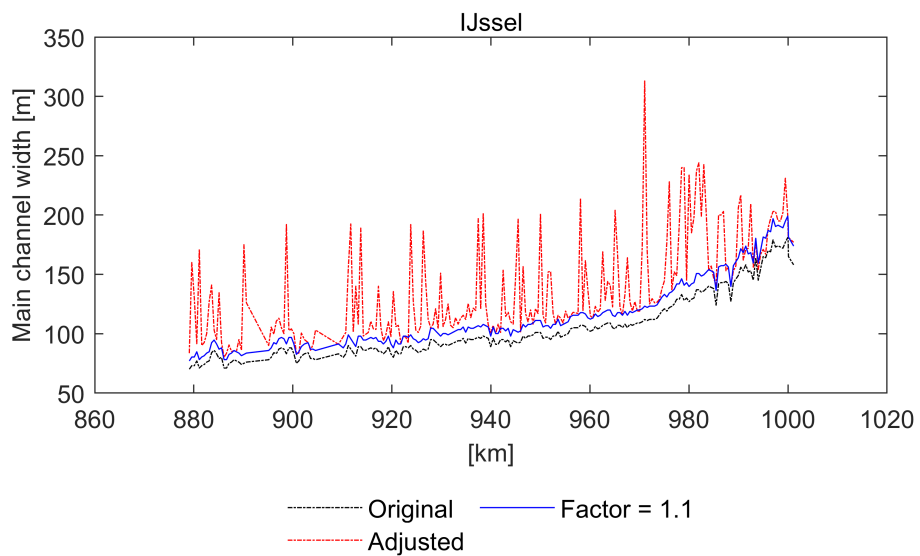
Figure 40 Main channel width - IJssel.
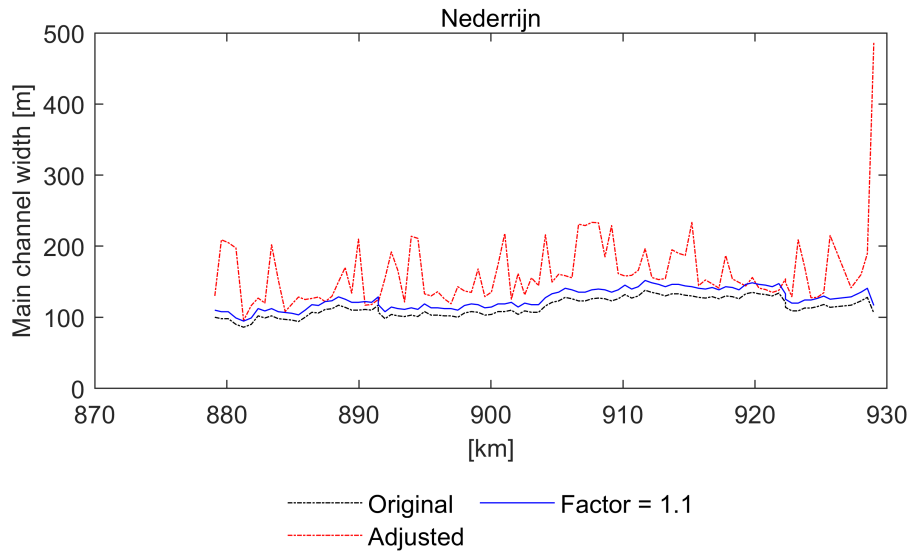
Figure 41 Main channel width - Nederrijn.
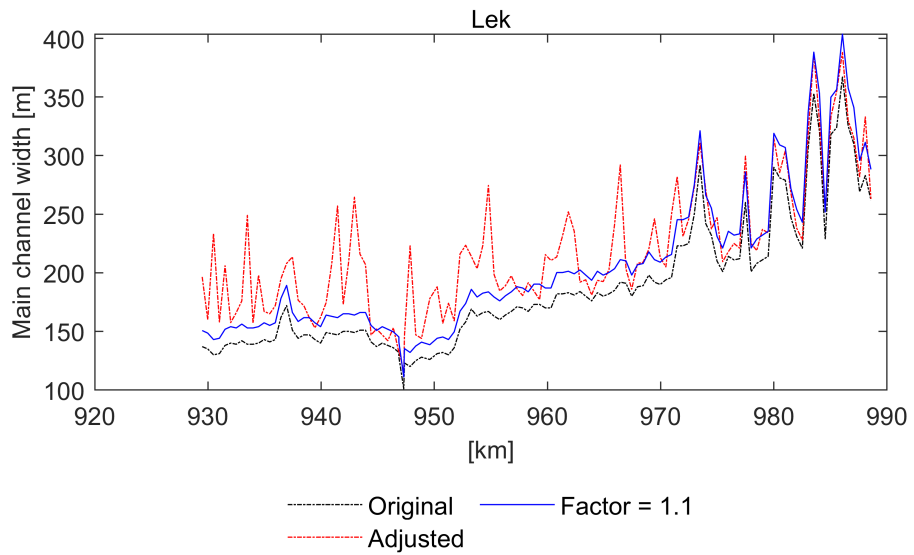
Figure 42 Main channel width - Lek.

Deltares

B   Effect of removing storage width

In converting the model to D-Flow FM 1D , and subsequently to run it for morphodynamics, the storage are of the cross-sections have been removed from the schematization. This is necessary to prevent undesired numerical behaviour that has been observed with including the storage terms in the numerical solution. It is relevant to mention that the exclusion of storage terms has various relevant benefits for morphological simulations and has therefore been removed (or ignored) in all previous morphodynamic simulations for the Rijntakken and Maas (these used SOBEK-RE with a quasi-steady approach, in which storage does not have any relevance, as the flow is steady). The main advantages are:

- Behaviour of models with quasi-steady morphology (including 2D DVR) is similar;
- The use of large morphological factors is less problematic (given the necessary stretching of flood waves in case of unsteady flow).

Storage primarily affects the damping and celerity of flood waves. To illustrate the impact of removing storage on the morphodynamic simulation of flood waves the theoretical and simulated impacts are presented in this section.

The propagation speed of a flood wave is roughly estimated as (for a model with Manning friction and wide rectangular cross-section):

$$c = \frac{5}{3} \frac{B_f}{B} u \; , \tag{B.1}$$

with B_f being flow width, and B the total width at the water surface (including storage width). For $B = B_f$ it can be found that the speed of the flood wave is $5/3u$, and is therefore faster than the flow velocity u. For $B_f < 3/5B$ the flood wave will move slower than the flow velocity. For a situation with tabulated cross-section and flood plain the following relation can be used:

$$c = \frac{5}{3} \frac{1}{B} \left(B_{f,m} u_m + B_{f,w} u_w \right) \; . \tag{B.2}$$

Here index m relates to main channel, and index w relates to flood plain (*winterbed*).

The damping of the wave can be roughly estimated as (sine-shaped wave in rectangular channel):

$$\frac{\mathrm{d}Q_{\max}}{\mathrm{d}s} = -5.8 \frac{(B/B_f)^2}{C^2 S_0^2} \cdot \frac{a_0}{T^2} \; , \tag{B.3}$$

where a_0 [m] is the amplitude, C [m$^{1/2}$/s] is the Chézy coefficient for hydraulic roughness, S_0 is the slope, and T is the period. The equation shows that with increasing B/B_f (i.e., more storage) the damping also increases. Also an increasing roughness (decreasing C) or reduced bed slope will provide more damping. Finally, also for a high amplitude or a shorter wave, a stronger damping will occur.

For example, in the Waal the ratio B_f/B is approximately 0.9 for the main channel, and about 0.75 for the width at the highest water levels. In this example we consider the reduction of the discharge peak (and the associated water level difference) between the Pannerdensche Kop and Tiel (distance about 62 km). The numbers

Deltares

Parameter	High water level	Main channel	No storage
B_f/B [-]	0.75	0.9	1.0
C [m$^{1/2}$/s]	45	45	45
S_0 [-]	1×10^{-4}	1×10^{-4}	1×10^{-4}
a_0 [m^3/s]	5000	5000	5000
T [s]	2592000	2592000	2592000
$\mathrm{d}Q_{\max}/\mathrm{d}s$	-0.000307	-0.0002132	-0.000173
ΔQ over 60 km [m^3/s]	-18	-13	-10
$\Delta Q/Q$ over 60 km [%]	-0.4	-0.3	-0.2

Table 8 Effect of storage in cross-section.

corresponding to the damping of a 5000 m^3/s flood peak and a period $T = 30\,days$ (a typical duration for the Rhine) are shown in Table 8:

When compared to $B_f/B = 1$ (no storage) the additional damping of the flood peak for $B_f/B = 0.75$ (maximum storage) is approximately 8 m^3/s, which gives a water-level difference of roughly 1 cm.

Using the formula for the celerity it can be found that, with an average flow velocity of 1.2 m/s in these conditions, the flood peak takes about 12 h hours to travel over 62 km from Pannerdensche Kop until Tiel.

These estimates have been compared to outcomes of simulations with the SOBEK-RE model for the Rhine branches (Waal branch) (Figures 43 to 45). When computed with $B_f/B = 1$ (no storage, including removal of weirs) the damping of the flood peak released at the Pannerdensche Kop (inflow boundary) is expected to be in the order of 14 m^3/s at Tiel (Rhine-km 930). Effectively this corresponds to the damping for $B_f/B = 0.9$, which is explained since only the storage from the tabulated cross-sections were removed in the model, but not the storage areas of the summer-dike sections. If storage is fully eliminated, the damping of the initially released flood wave is reduced from –18 m^3/s ($B_f/B = 0.75$, confirmed in the table and in the figure) to –10 m^3/s. This means 8 m^3/s less damping on a flood peak of 5000 m^3/s in the Waal.

Additionally we plot the results for a long series and relative to the discharge at the Pannerdensche Kop (Figures 46 and 47). Note that for the relation curve (relation discharge Pannerdensche Kop and Rhine-km 930) a time shift of 13 hours has been applied. The effects of damping of the flood wave disappear in the additional band width, both for water levels and for flow velocities.

Deltares
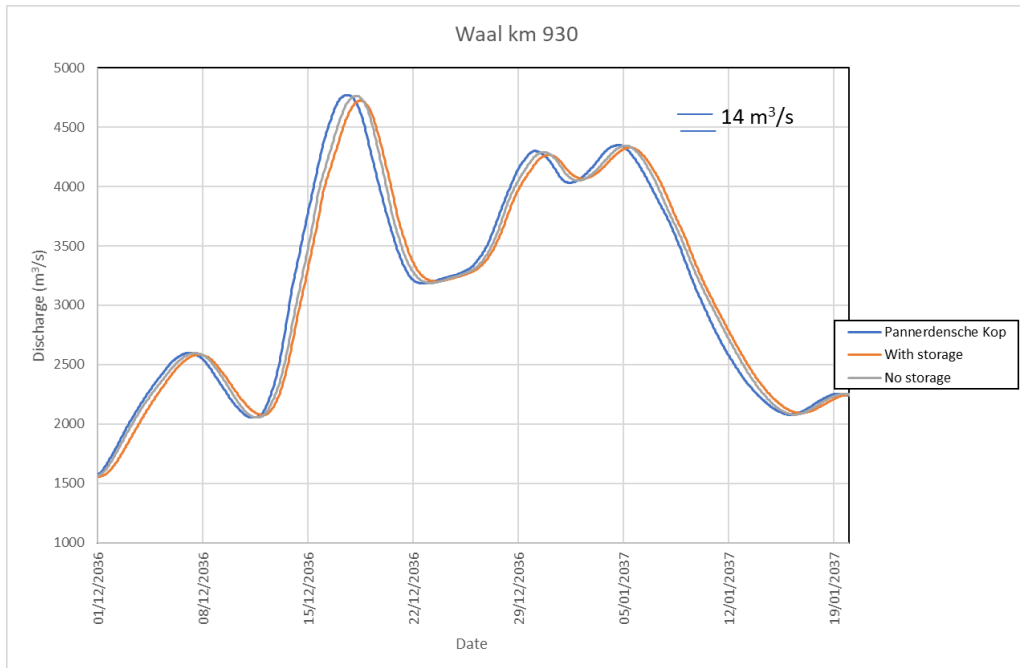
Figure 43 Computed discharge as function of time for a flood peak, at Pannerdensche Kop and at Tiel (Rhine-km 930), for simulations with storage, without storage, and without storage and weirs.
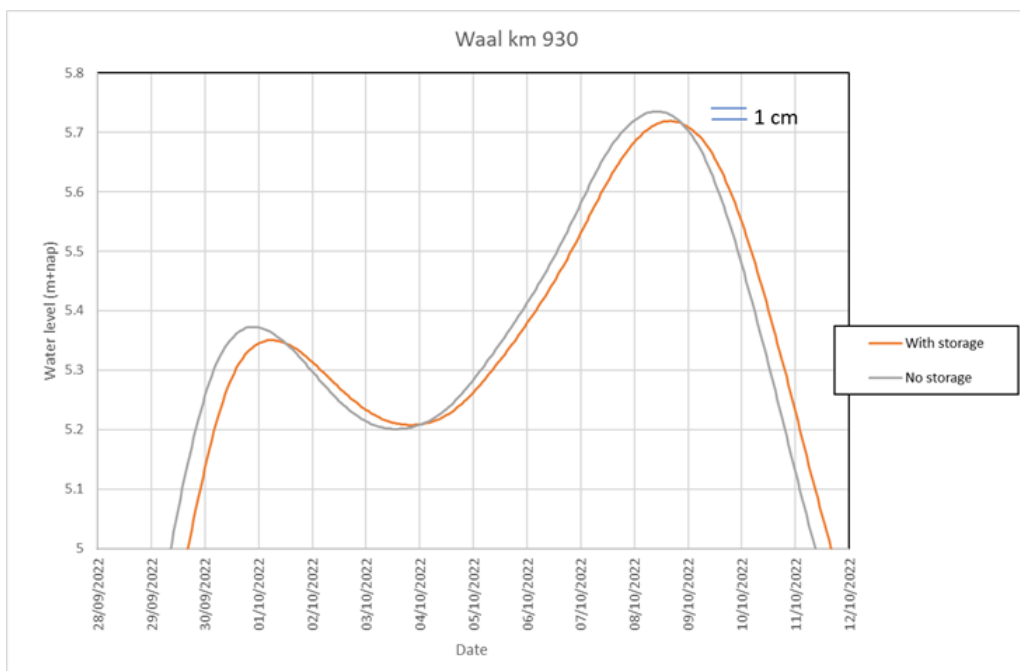
Figure 44 Computed water level as function of time for a flood peak, at Pannerdensche Kop and at Tiel (Rhine-km 930), for simulations with storage, without storage, and without storage and weirs.

Deltares
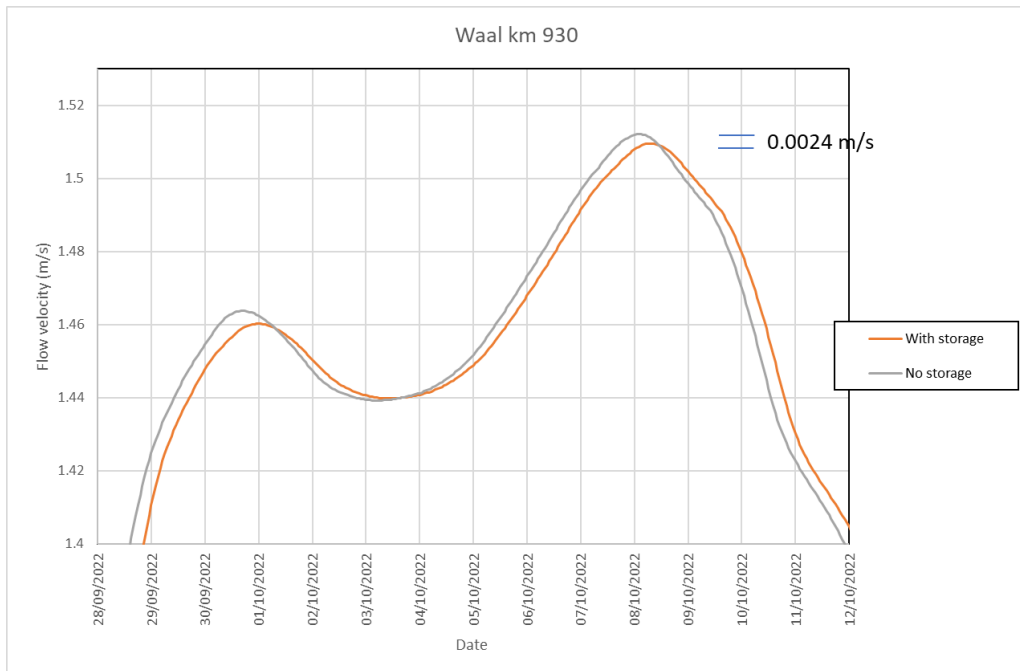
Figure 45 Computed flow velocity as function of time for a flood peak, at Pannerdensche Kop and at Tiel (Rhine-km 930), for simulations with storage, without storage, and without storage and weirs.
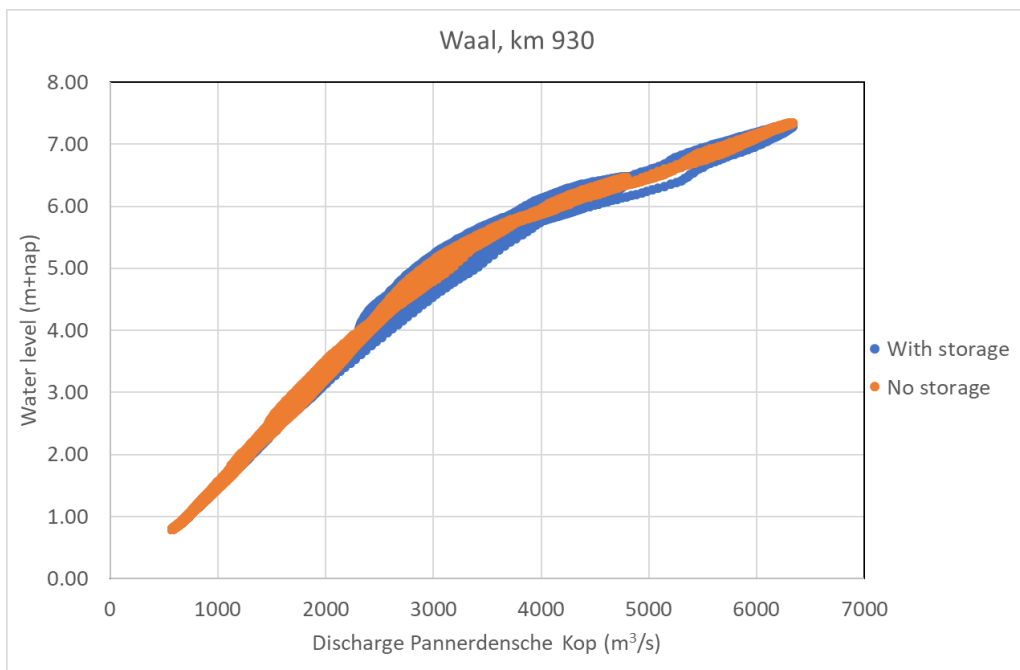
Figure 46 Computed water levels (SOBEK-RE Rhine branches), as function of discharge at the Pannerdensche Kop for an unsteady-flow simulation with and without storage width.

Deltares
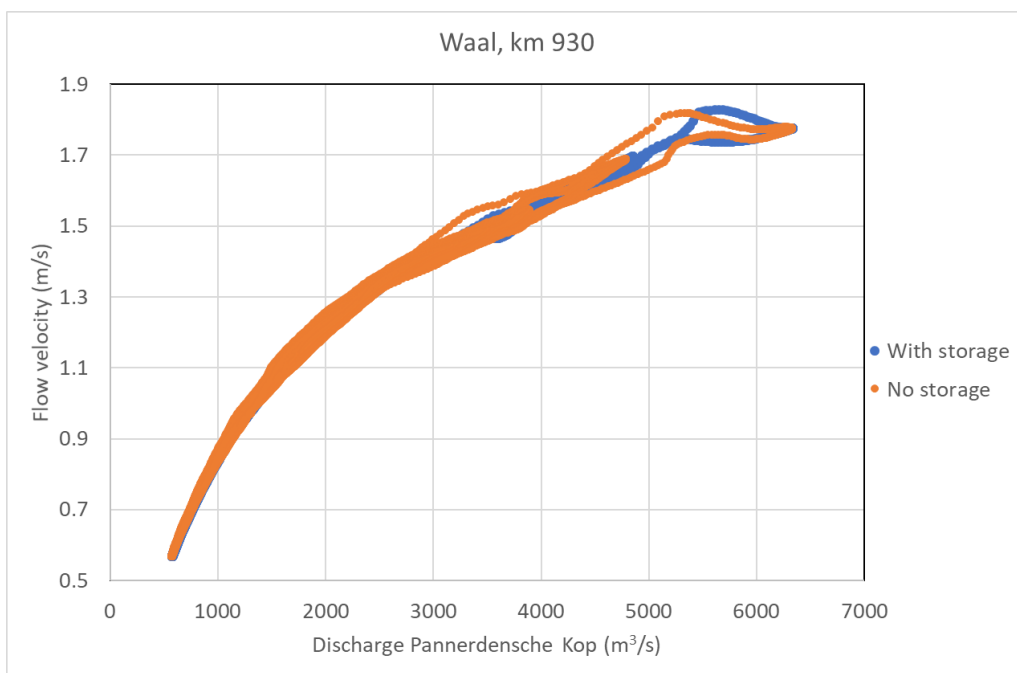
Figure 47 Computed flow velocities (SOBEK-RE Rhine branches), as function of discharge at the Pannerdensche Kop for an unsteady-flow simulation with and without storage width.

Morphological models for IRM
11203684-015-ZWS-0011_v1.0, Version 0.1, 2020-12-11, Final

C   Boundary conditions
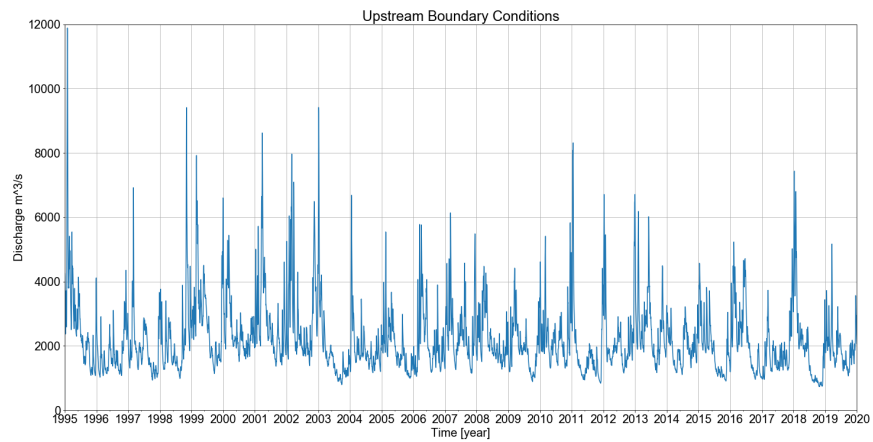
Figure 48 Time series of the upstream input discharge Lobith.
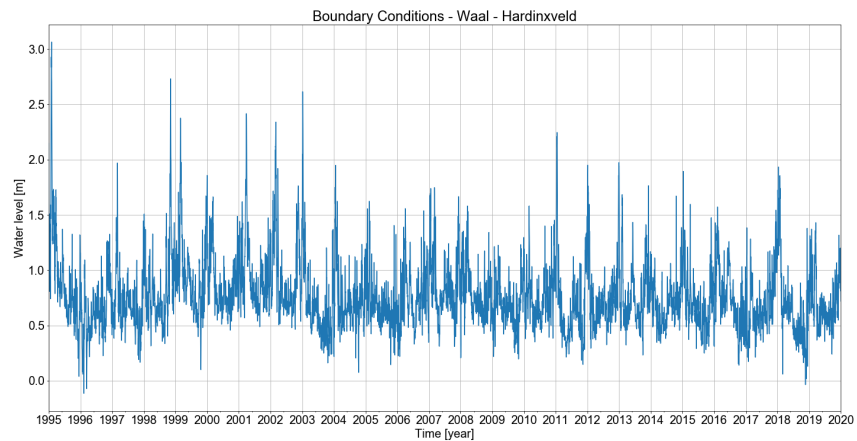
Figure 49 Time series of the downstream water levels Waal - Hardinxveld.

Morphological models for IRM
11203684-015-ZWS-0011_v1.0, Version 0.1, 2020-12-11, Final
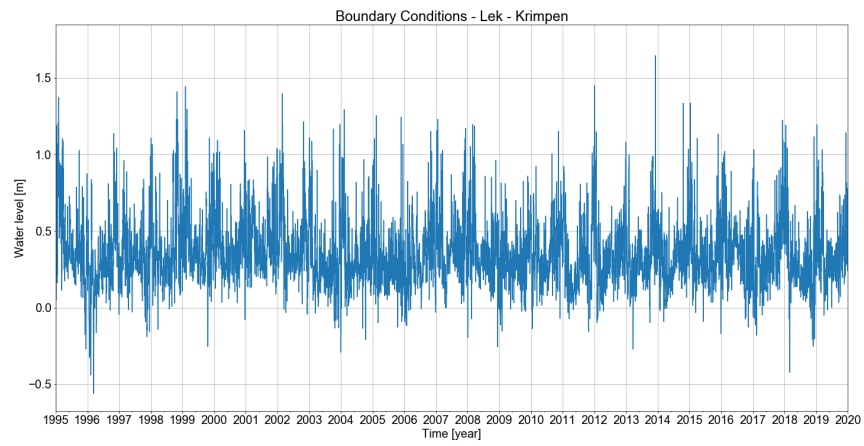
Figure 50 Time series of the downstream water levels Lek - Krimpen.
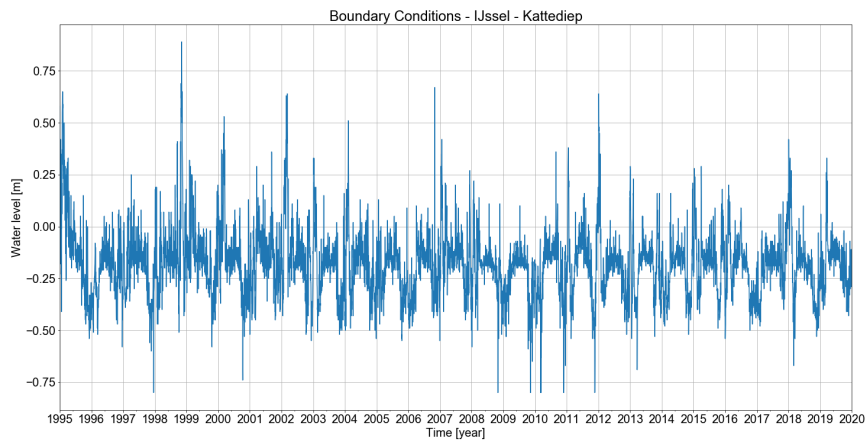
Figure 51 Time series of the downstream water levels IJssel - Kattendiep.
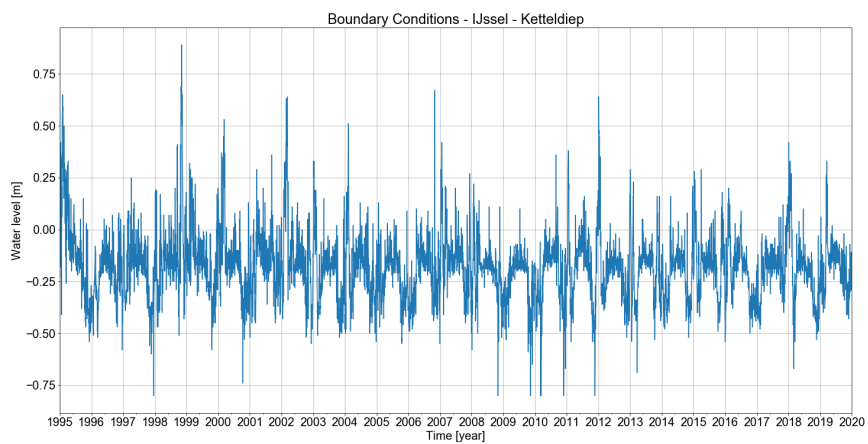
Figure 52 Time series of the downstream water levels IJssel - Keteldiep.

Morphological models for IRM
11203684-015-ZWS-0011_v1.0, Version 0.1, 2020-12-11, Final

Deltares
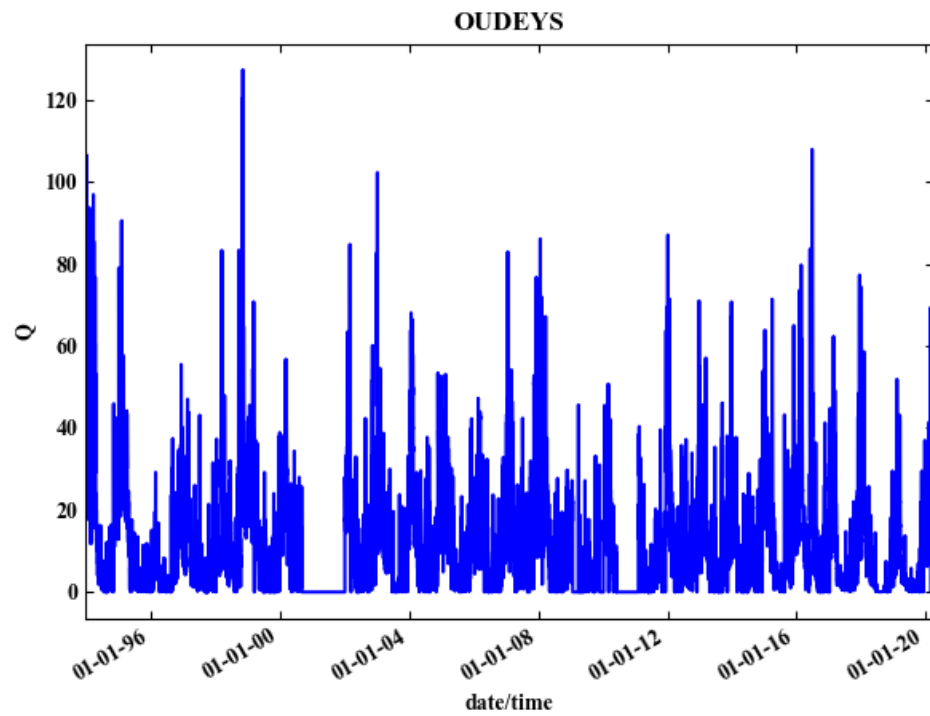
D   Laterals

Figure 53 Time series of the input discharge "Oude IJssel".

Deltares
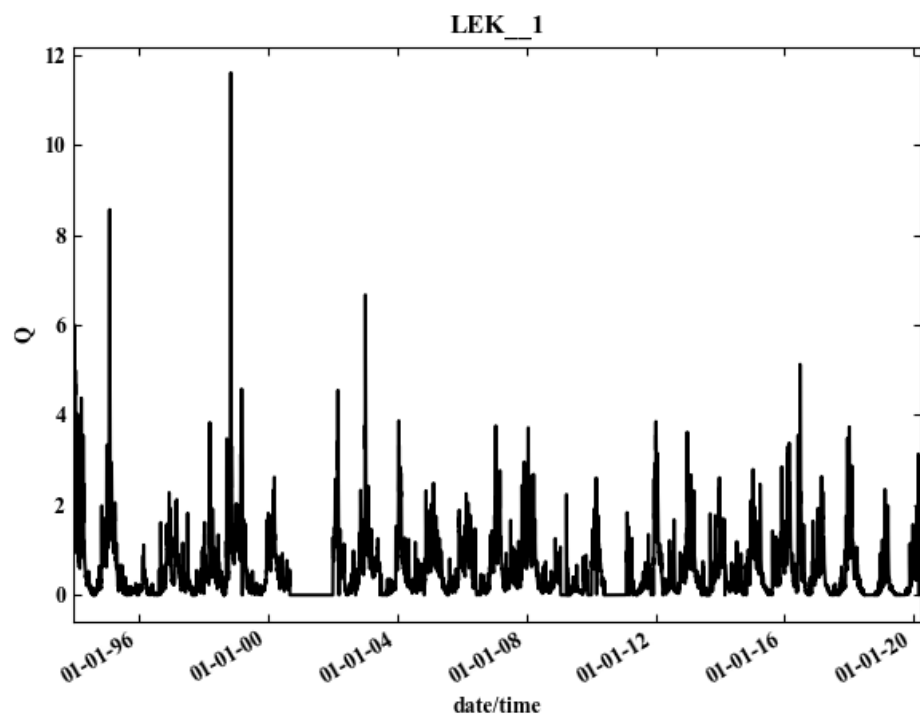
Figure 54 Time series of the lateral discharge "Lek 1".
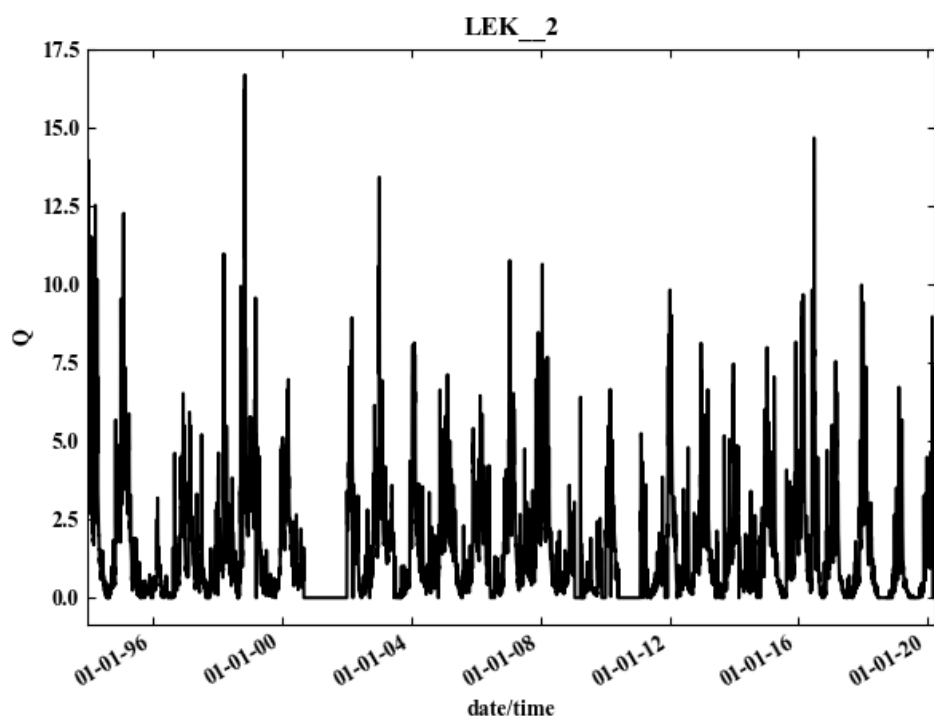
Figure 55 Time series of the lateral discharge "Lek 2".

Morphological models for IRM
11203684-015-ZWS-0011_v1.0, Version 0.1, 2020-12-11, Final

Deltares
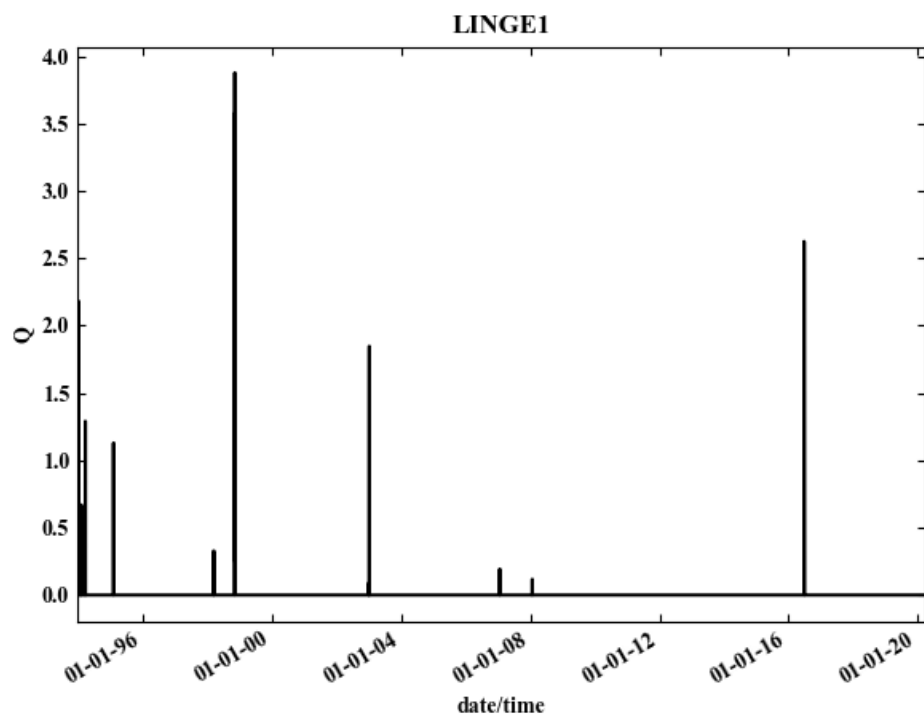
Figure 56 Time series of the lateral discharge "Linge 1".
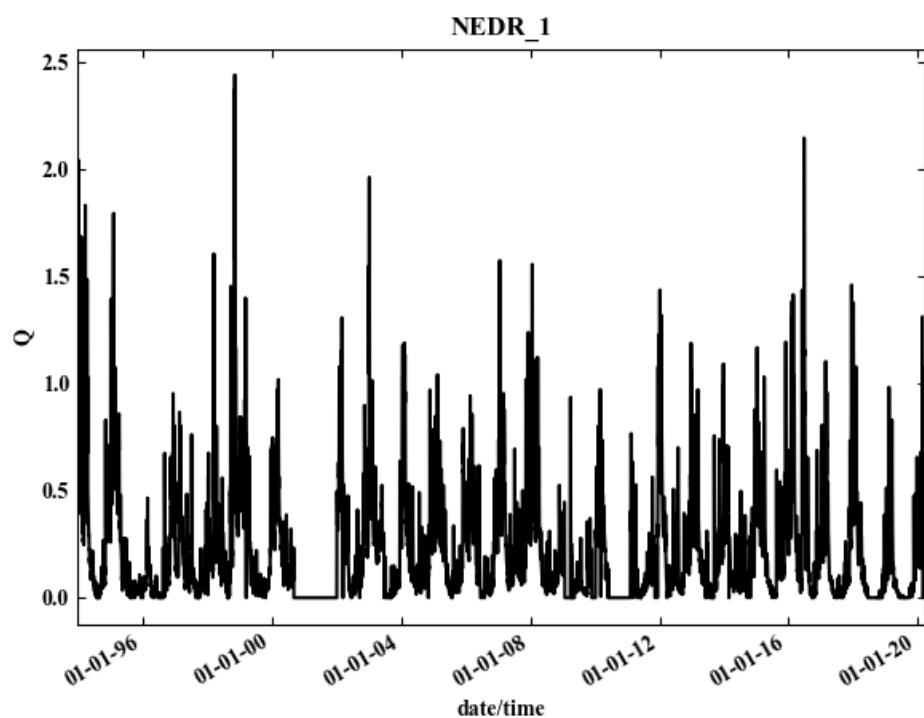
Figure 57 Time series of the lateral discharge "Nederijn 1".

Morphological models for IRM
11203684-015-ZWS-0011_v1.0, Version 0.1, 2020-12-11, Final

Deltares
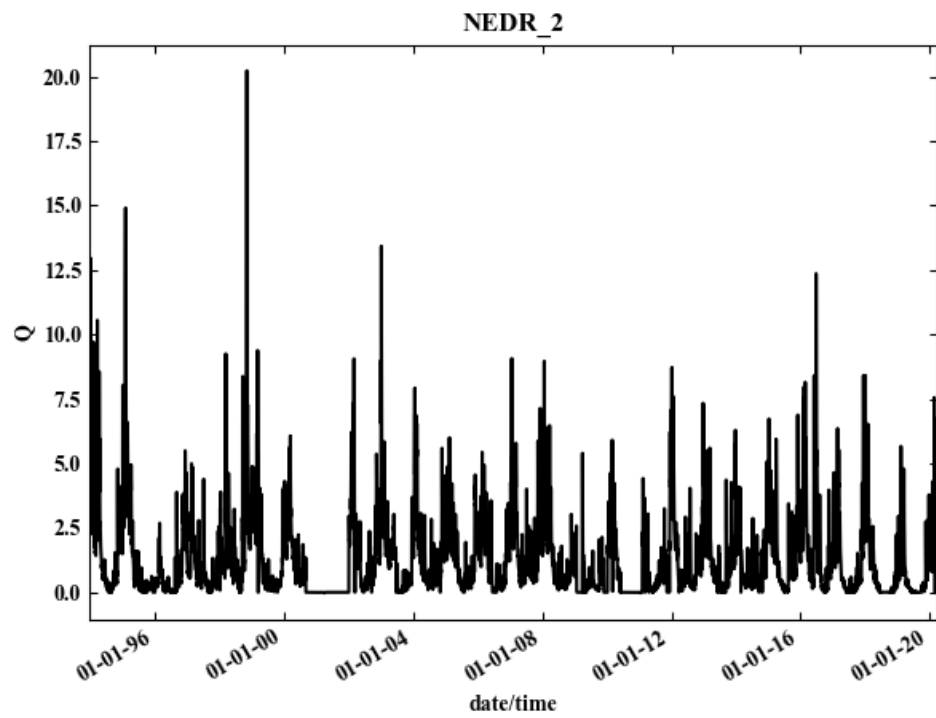
Figure 58 Time series of the lateral discharge "Nederijn 2".
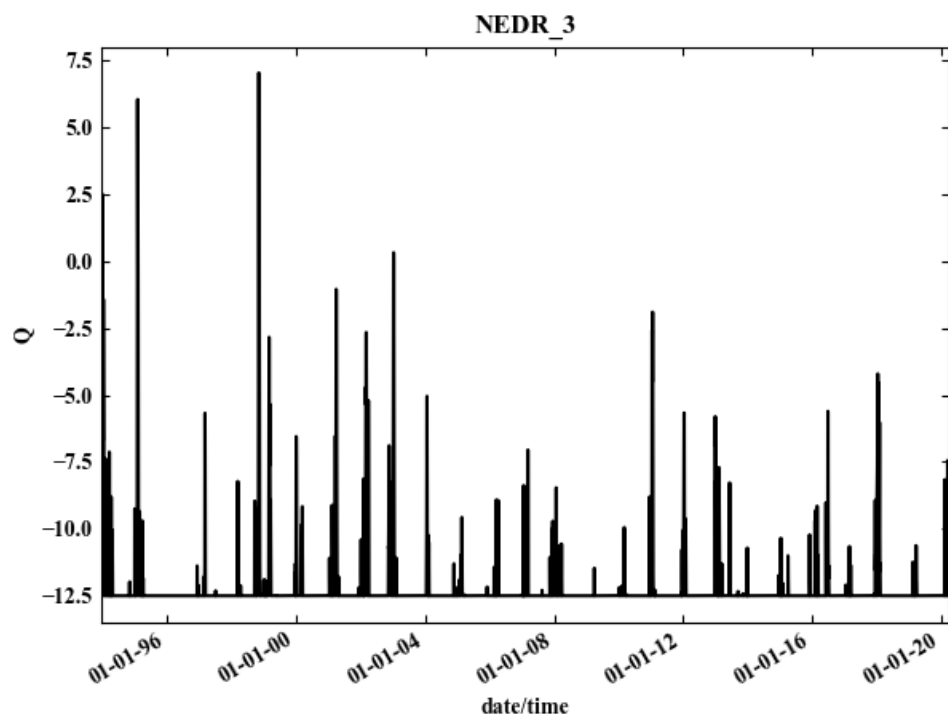
Figure 59 Time series of the lateral discharge "Nederijn 3".

Deltares

PANKAN
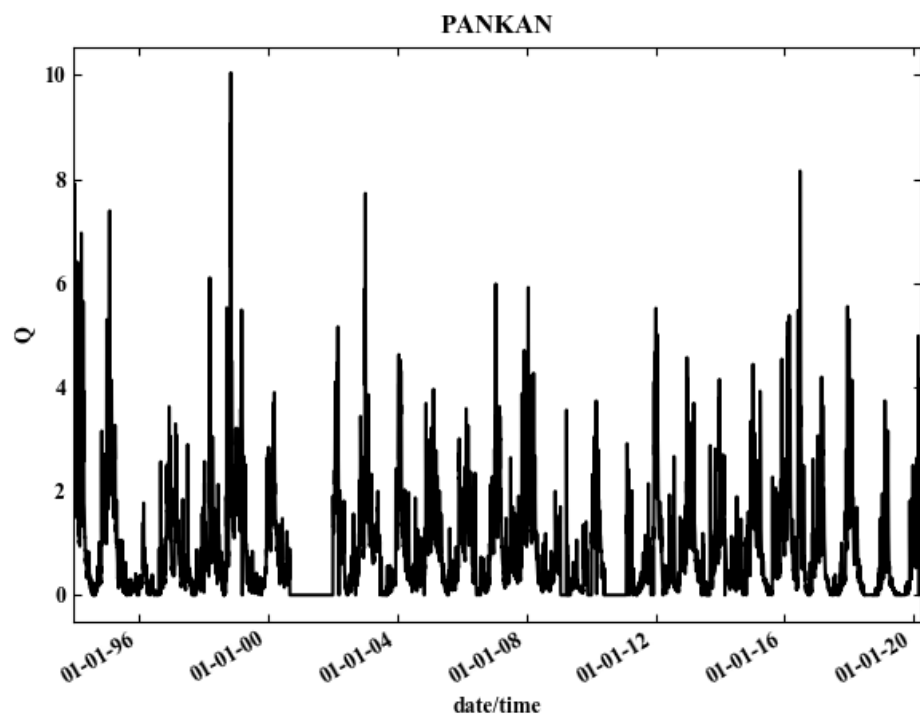
Figure 60 Time series of the lateral discharge "Pannerdensch Kanaal".
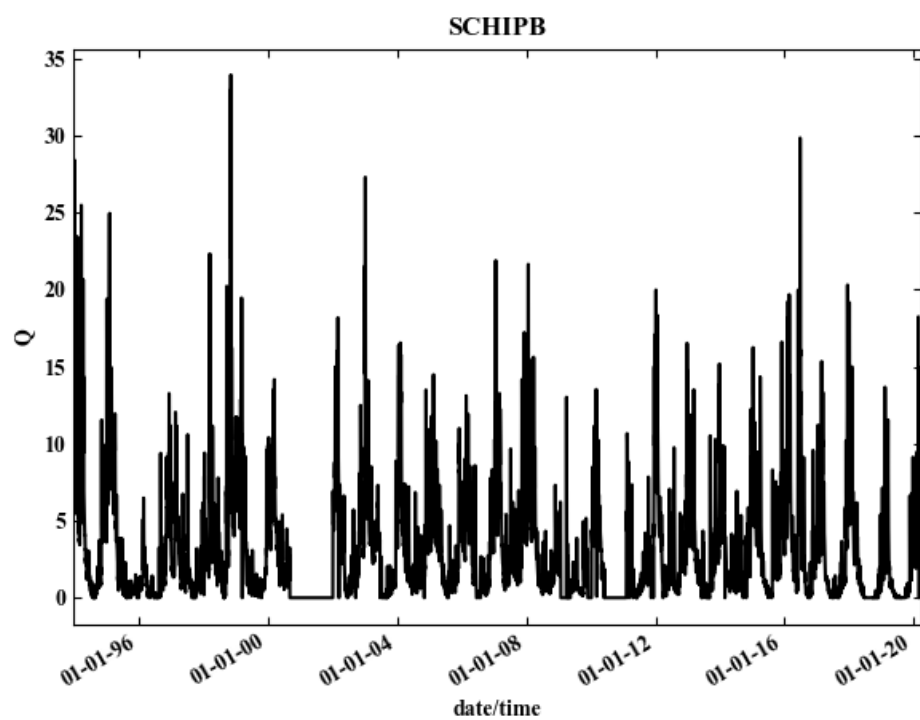
SCHIPB

Figure 61 Time series of the lateral discharge "Schipb".

Morphological models for IRM
11203684-015-ZWS-0011_v1.0, Version 0.1, 2020-12-11, Final

Deltares
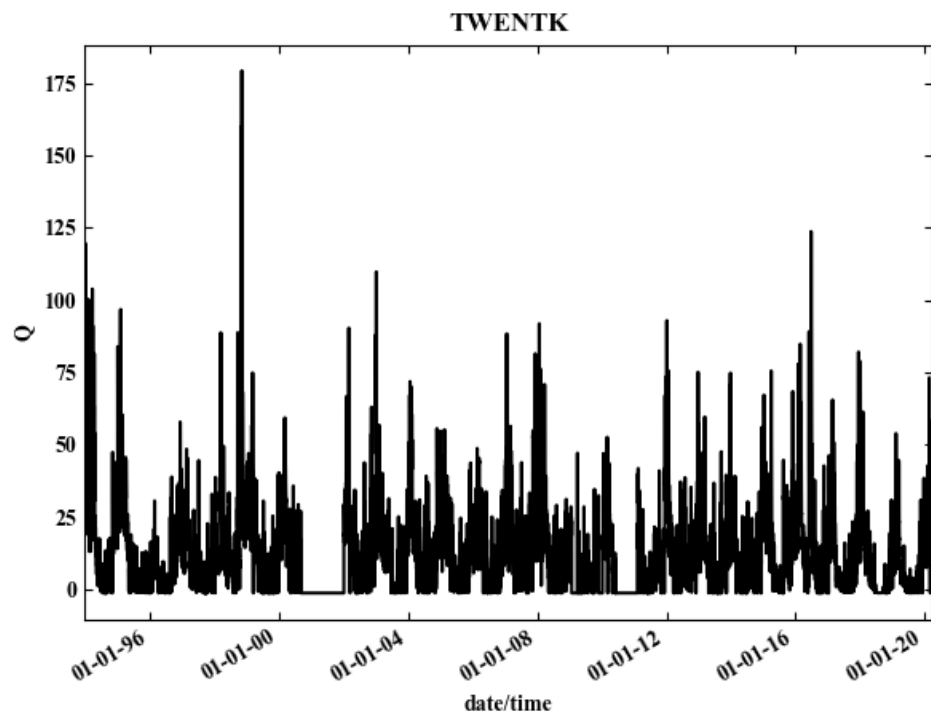
TWENTK

Figure 62 Time series of the lateral discharge "Twente Kanaal".
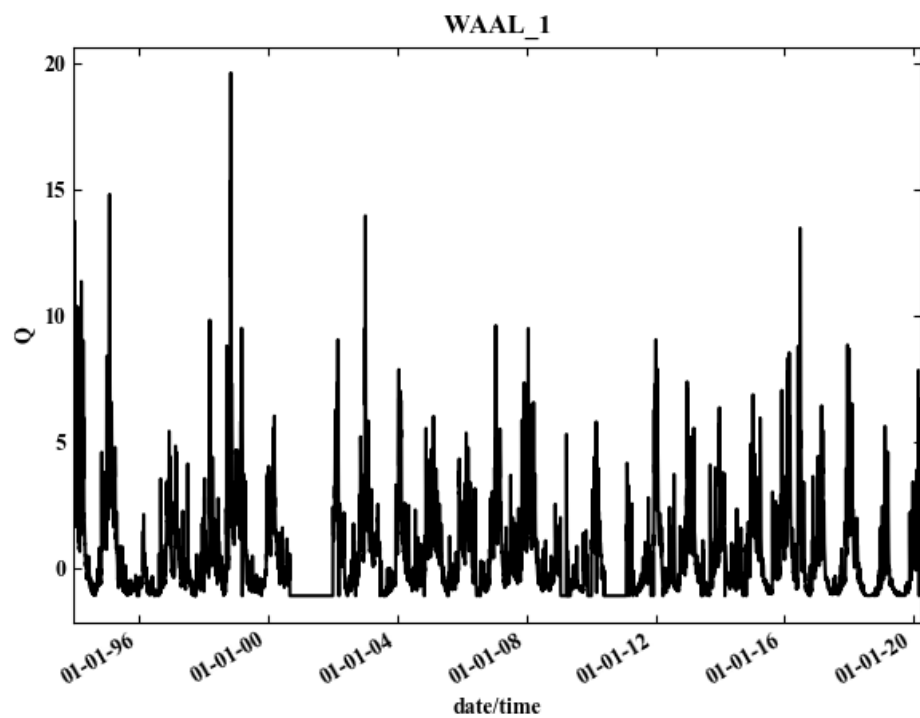
WAAL_1

Figure 63 Time series of the lateral discharge "Waal 1".

Morphological models for IRM
11203684-015-ZWS-0011_v1.0, Version 0.1, 2020-12-11, Final

Deltares
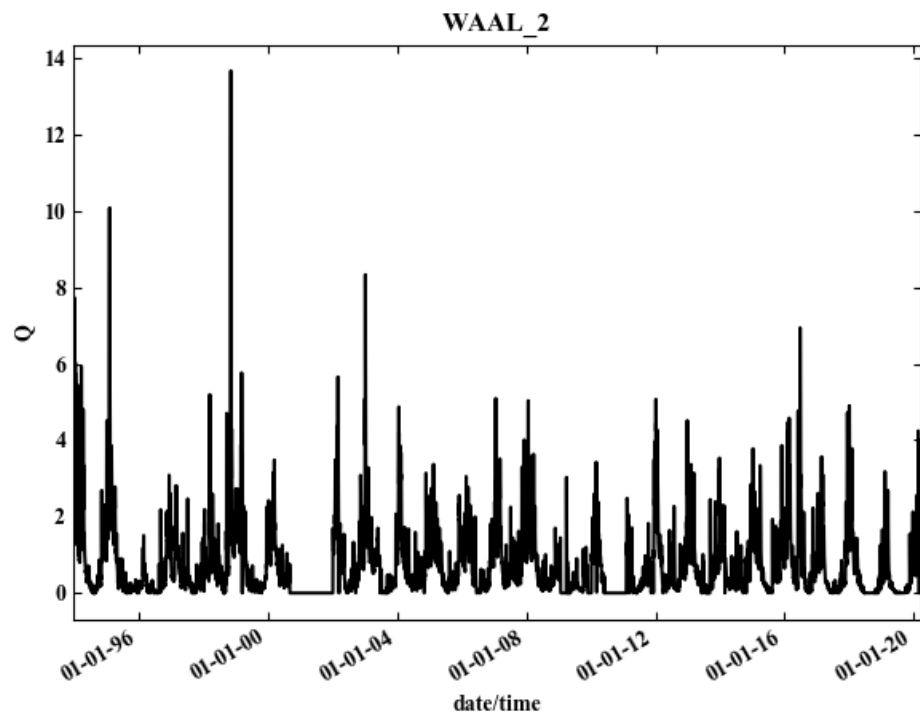
WAAL_2

Figure 64 Time series of the lateral discharge "Waal 2".
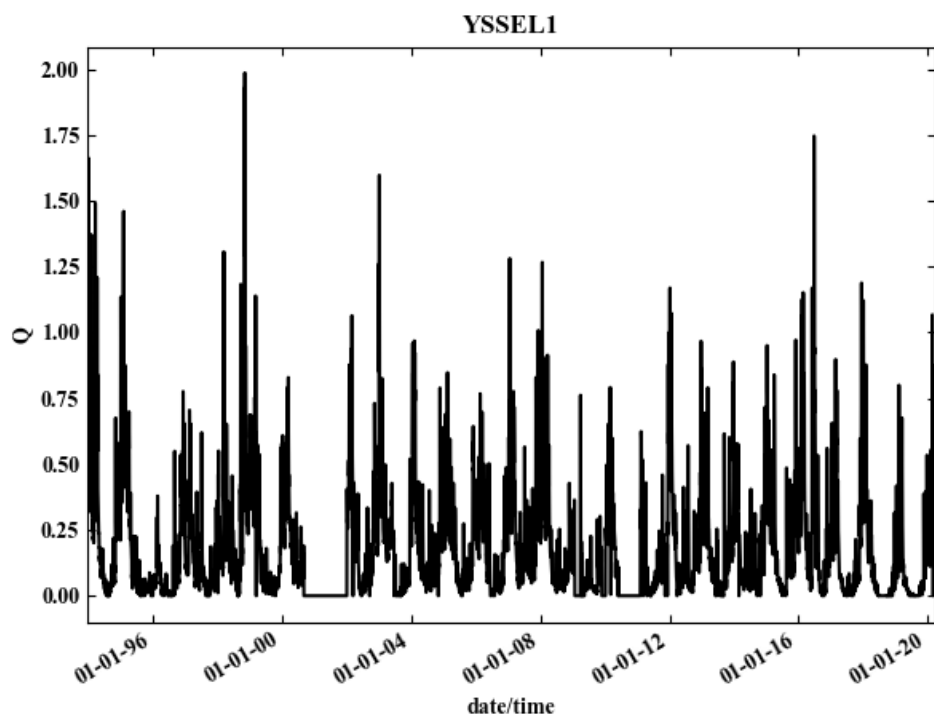
YSSEL1

Figure 65 Time series of the lateral discharge "IJssel 1".

Deltares
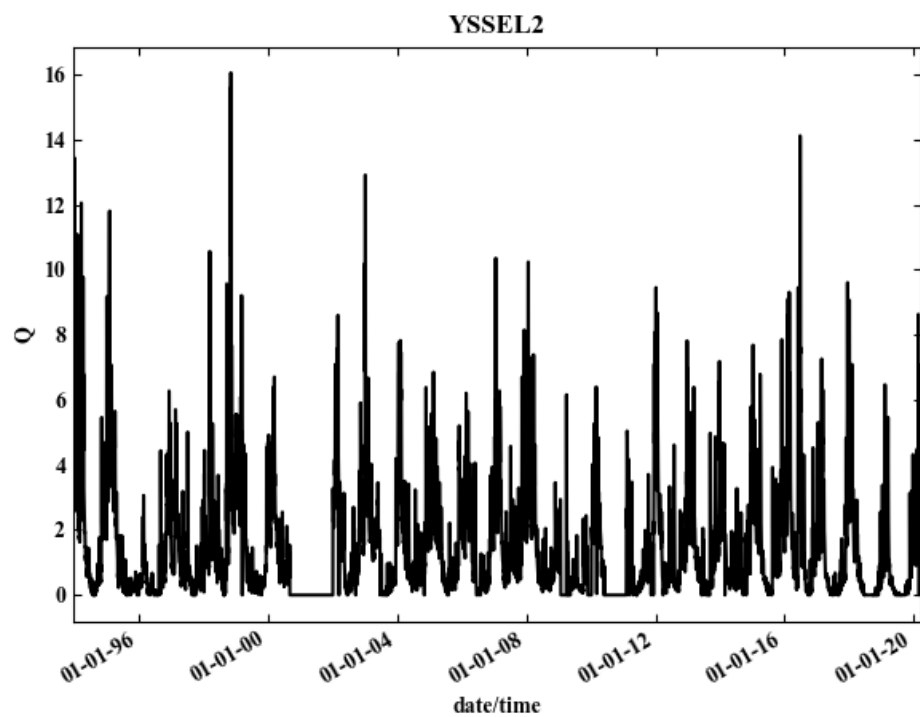
Figure 66 Time series of the lateral discharge "IJssel 2".
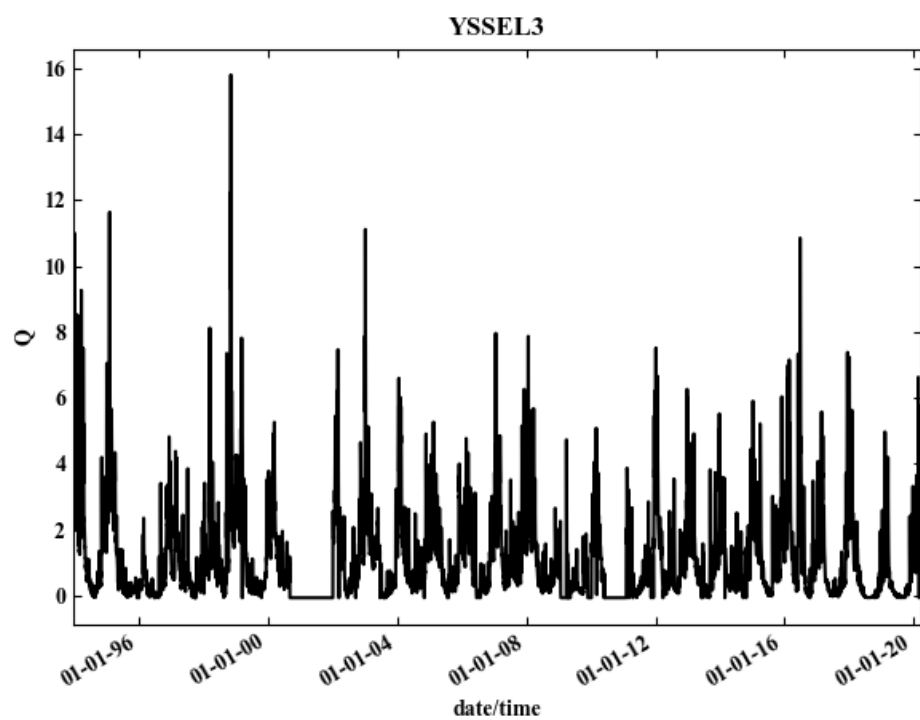
Figure 67 Time series of the lateral discharge "IJssel 3".

Morphological models for IRM
11203684-015-ZWS-0011_v1.0, Version 0.1, 2020-12-11, Final

Deltares
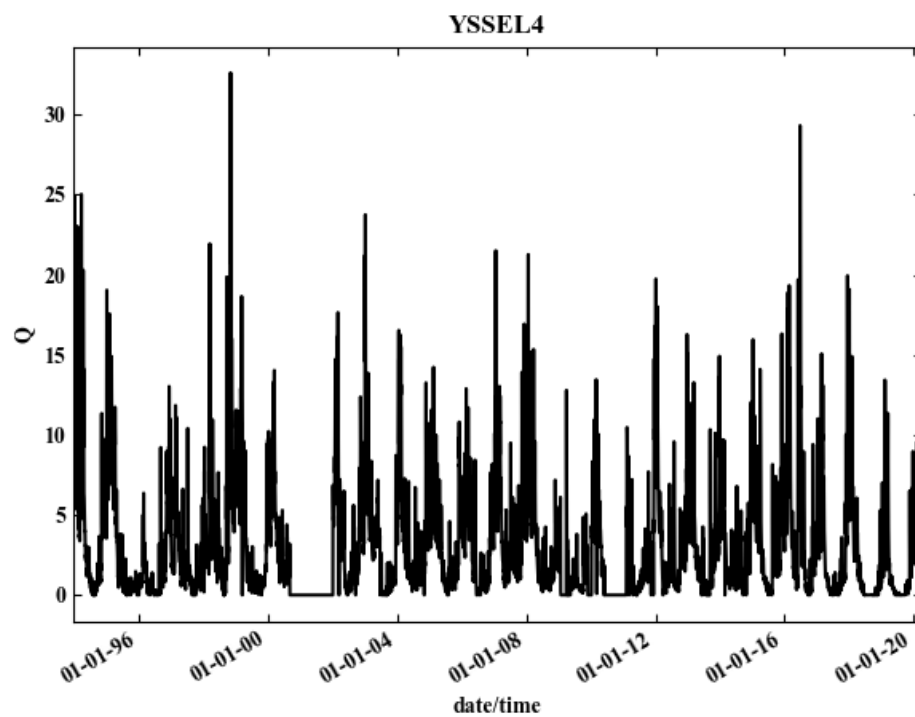
Figure 68 Time series of the lateral discharge "IJssel 4".
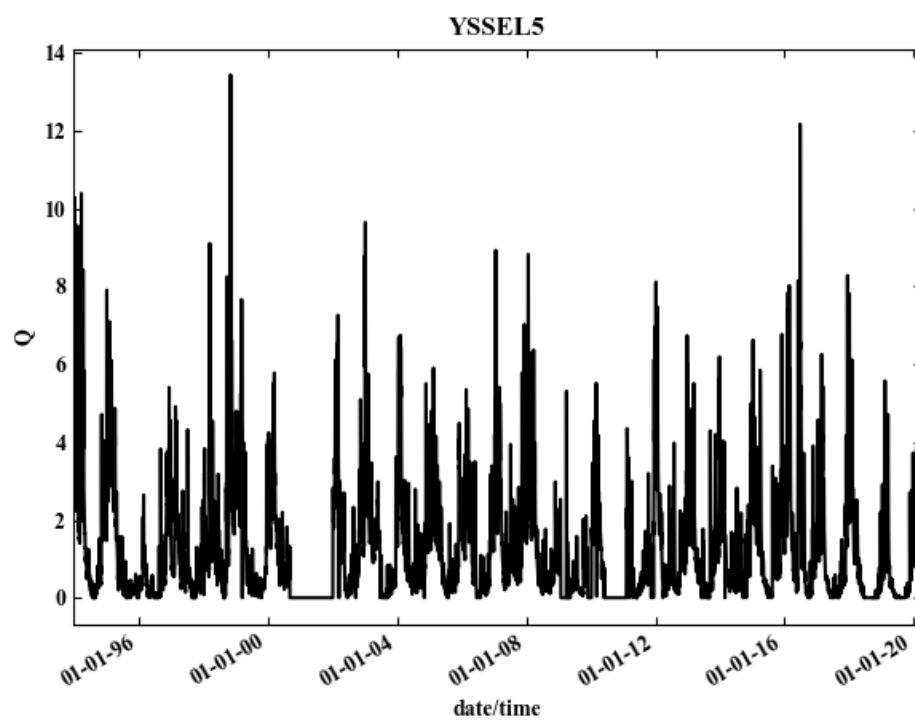
Figure 69 Time series of the lateral discharge "IJssel 5".

Deltares
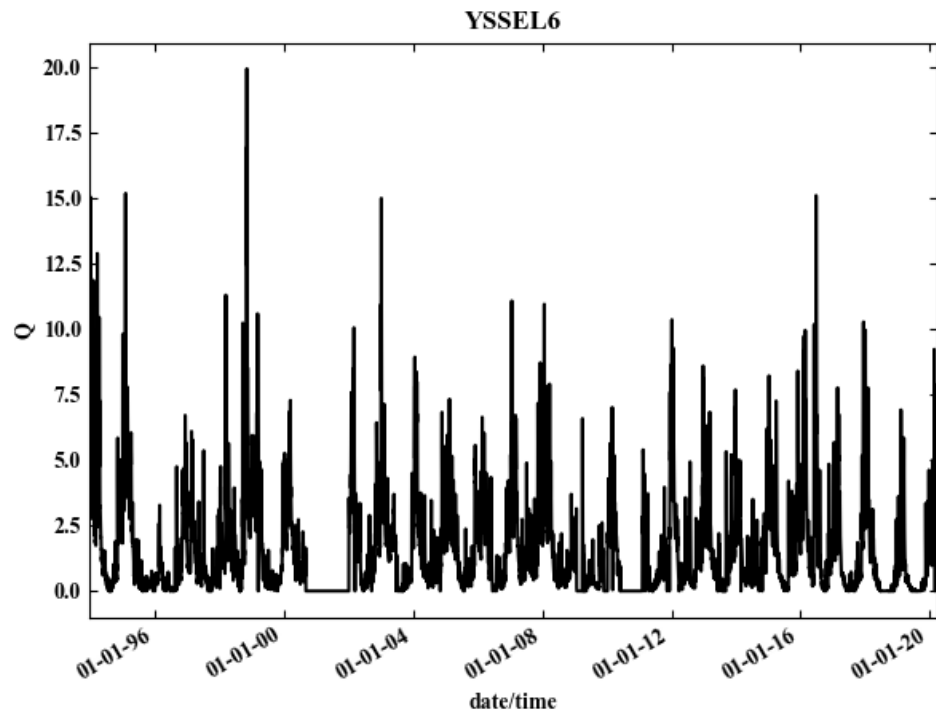
Figure 70 Time series of the lateral discharge "IJssel 6".
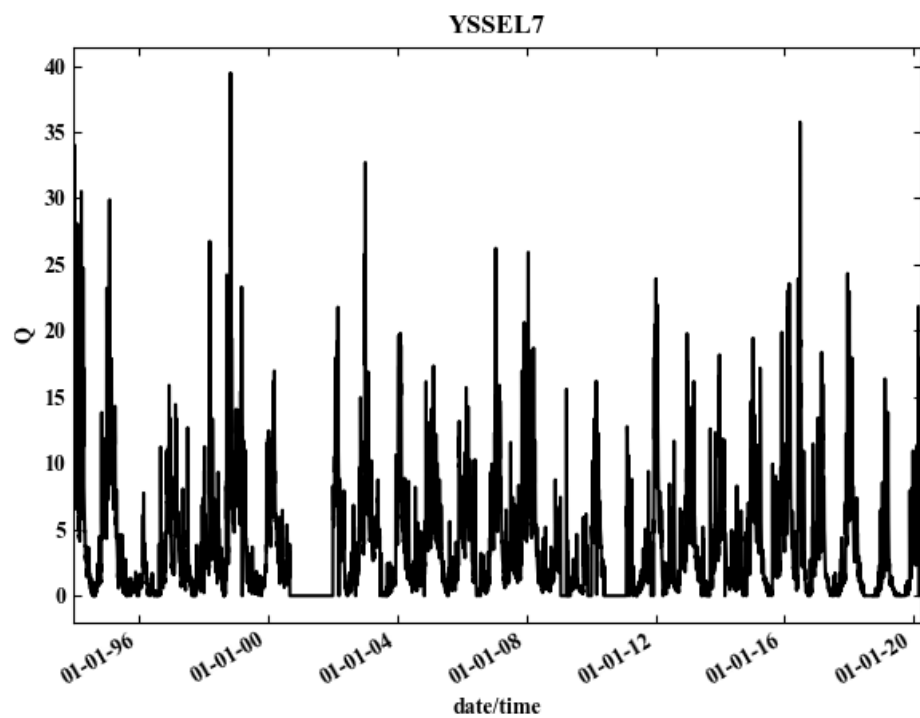
Figure 71 Time series of the lateral discharge "IJssel 7".

Morphological models for IRM
11203684-015-ZWS-0011_v1.0, Version 0.1, 2020-12-11, Final

Deltares
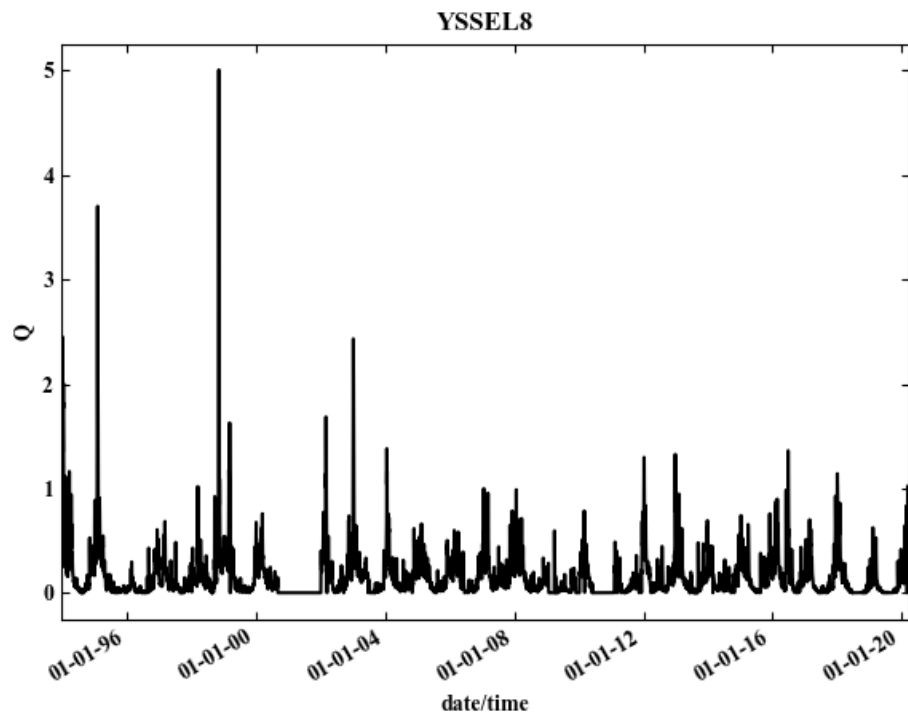
Figure 72 Time series of the lateral discharge "IJssel 8".

Deltares

E Comparison between WAQUA and D-Flow FM 1D for a discharge equal to 2000 m³/s

Figure 73 Comparison water level D-Flow FM 1D - WAQUA - Boven-Rijn - Q=2000

Figure 74 Comparison main channel flow velocity D-Flow FM 1D - WAQUA - Boven-Rijn - Q=2000

Figure 75 Comparison main channel discharge D-Flow FM 1D - WAQUA - Boven-Rijn - Q=2000

Figure 76 Comparison water level D-Flow FM 1D - WAQUA - Pannerdensch Kanaal - Q=2000

Morphological models for IRM
11203684-015-ZWS-0011_v1.0, Version 0.1, 2020-12-11, Final

Deltares
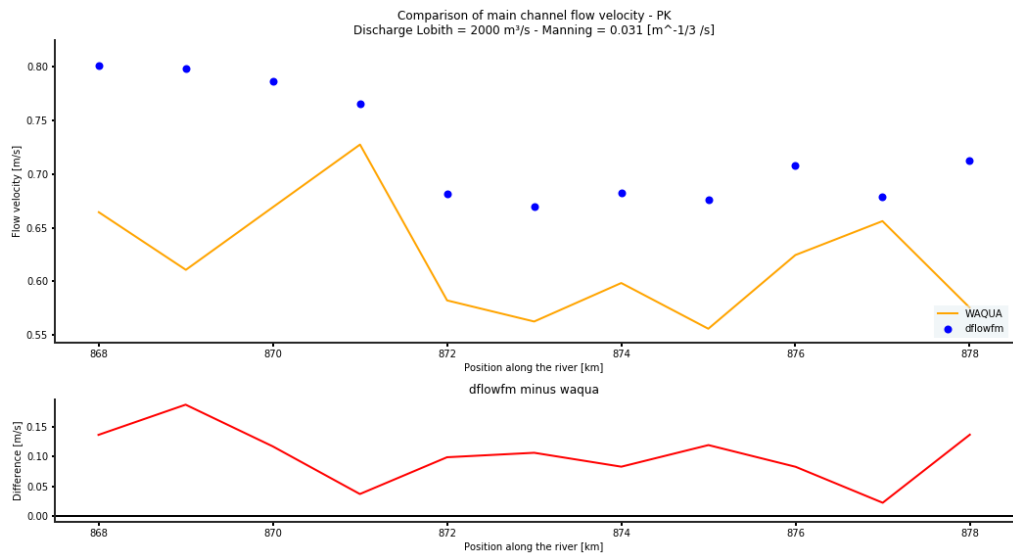
Figure 77 Comparison main channel flow velocity D-Flow FM 1D - WAQUA - Pannerdensch Kanaal - Q=2000
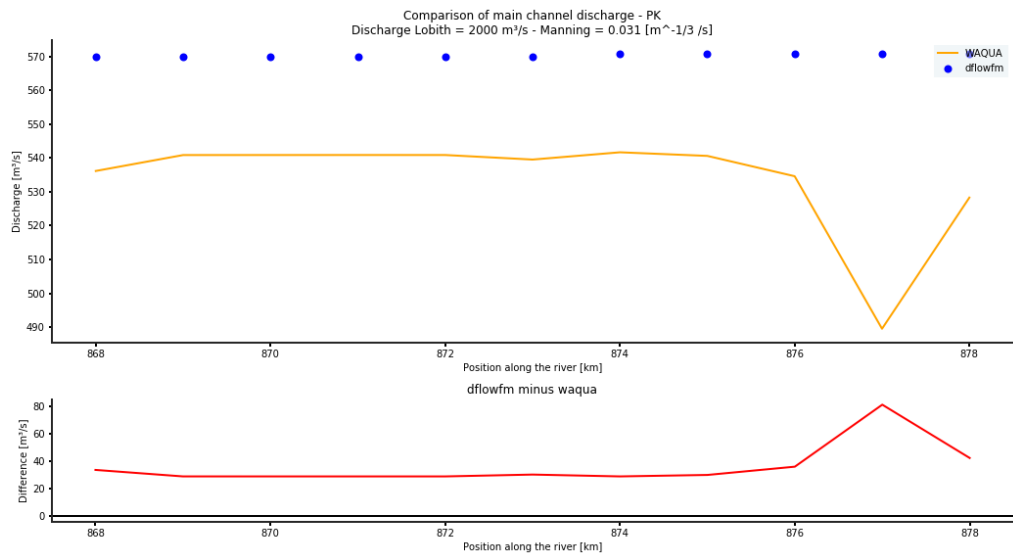
Figure 78 Comparison main channel discharge D-Flow FM 1D - WAQUA - Pannerdensch Kanaal - Q=2000

Deltares
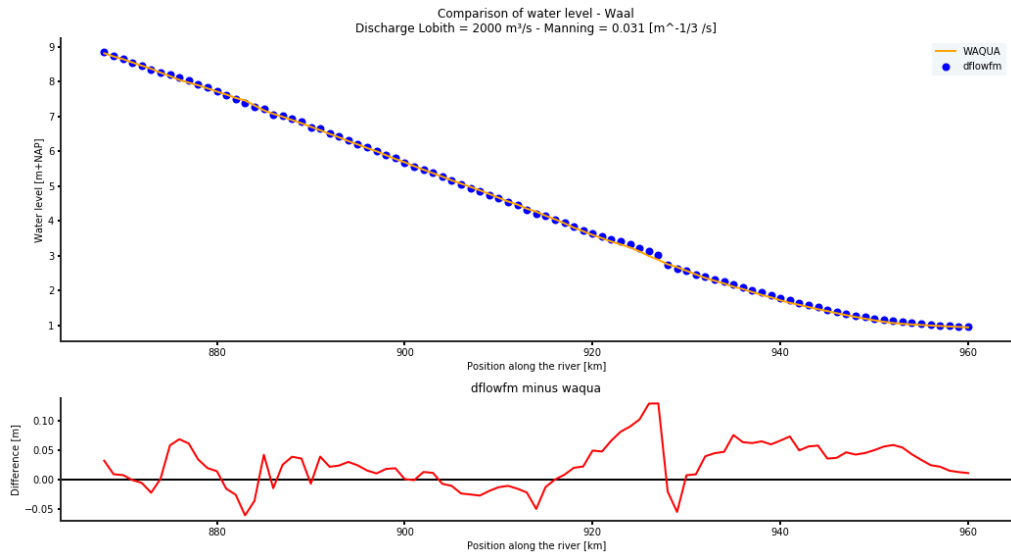
Figure 79 Comparison water level D-Fʟᴏᴡ FM 1D - WAQUA - Waal - Q=2000
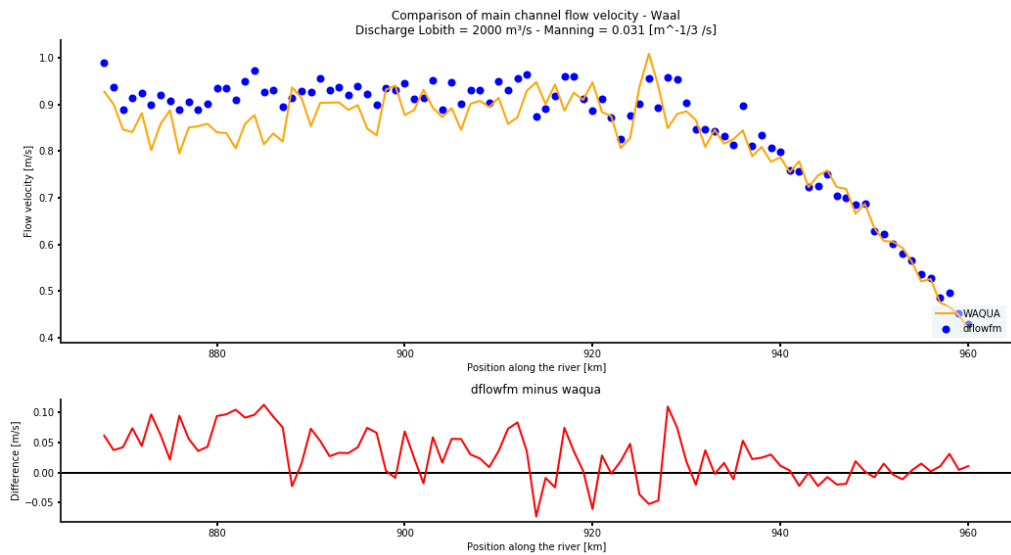
Figure 80 Comparison main channel flow velocity D-Fʟᴏᴡ FM 1D - WAQUA - Waal - Q=2000

Morphological models for IRM
11203684-015-ZWS-0011_v1.0, Version 0.1, 2020-12-11, Final

Deltares
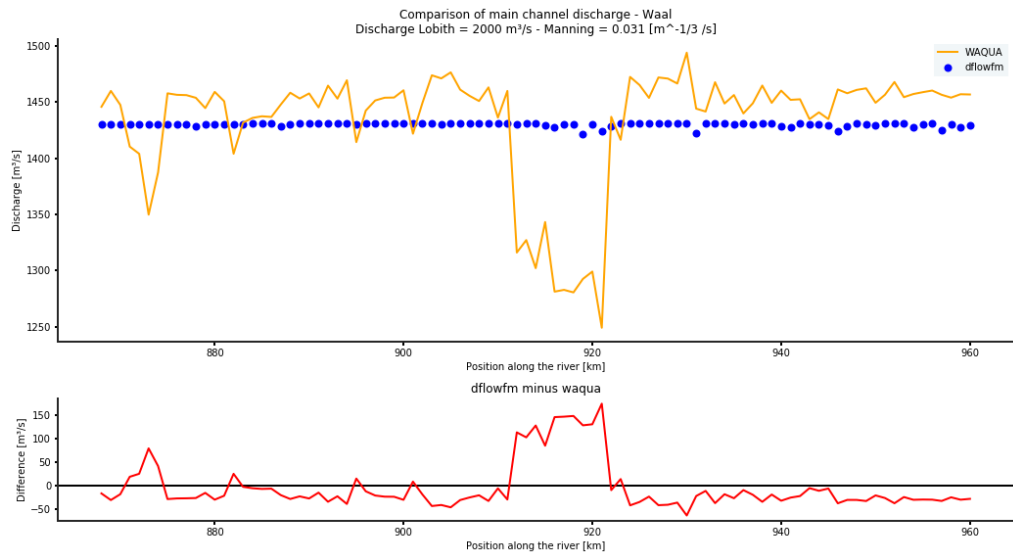
Figure 81 Comparison main channel discharge D-Flow FM 1D - WAQUA - Waal - Q=2000
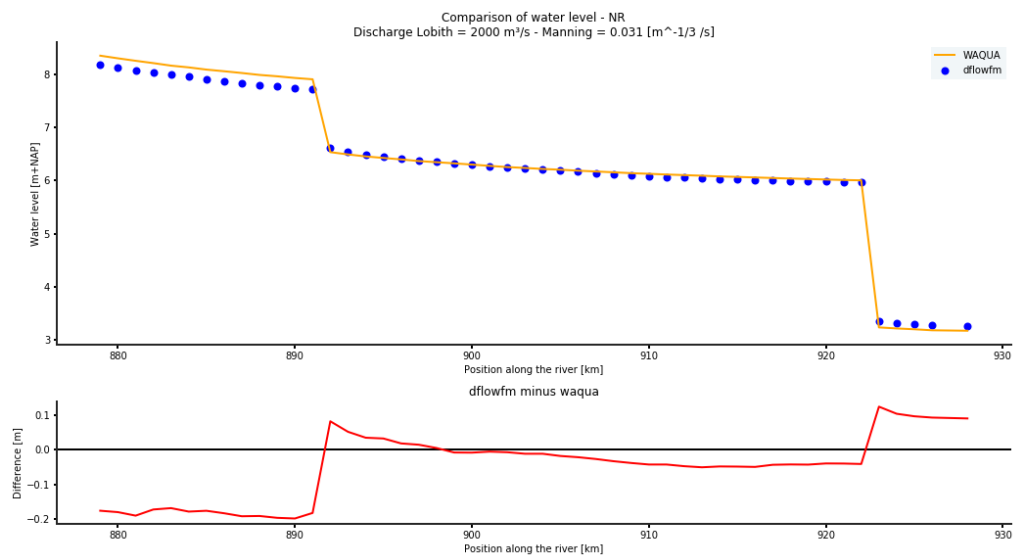
Figure 82 Comparison water level D-Flow FM 1D - WAQUA - Nederrijn - Q=2000

Deltares
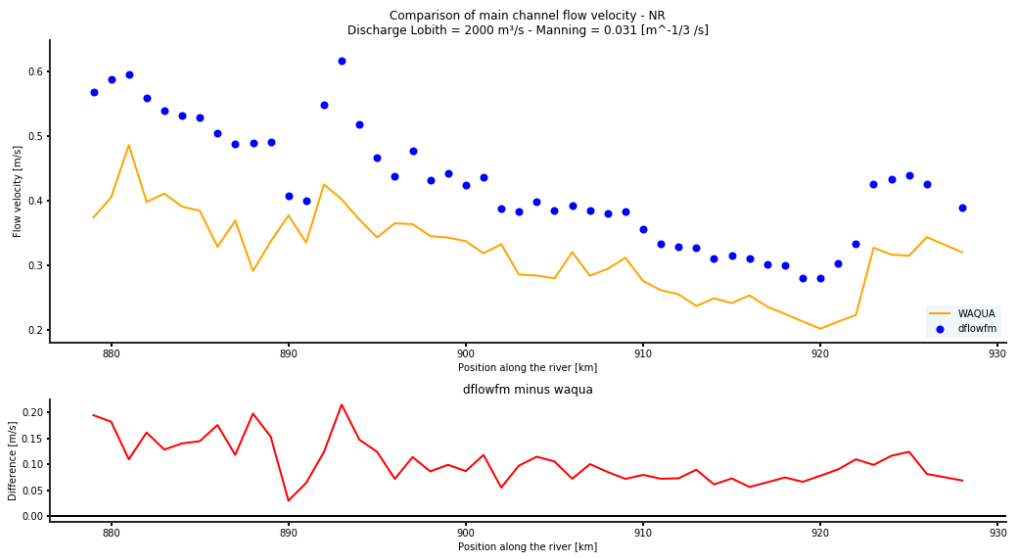
Figure 83 Comparison main channel flow velocity D-FLOW FM 1D - WAQUA - Nederrijn - Q=2000
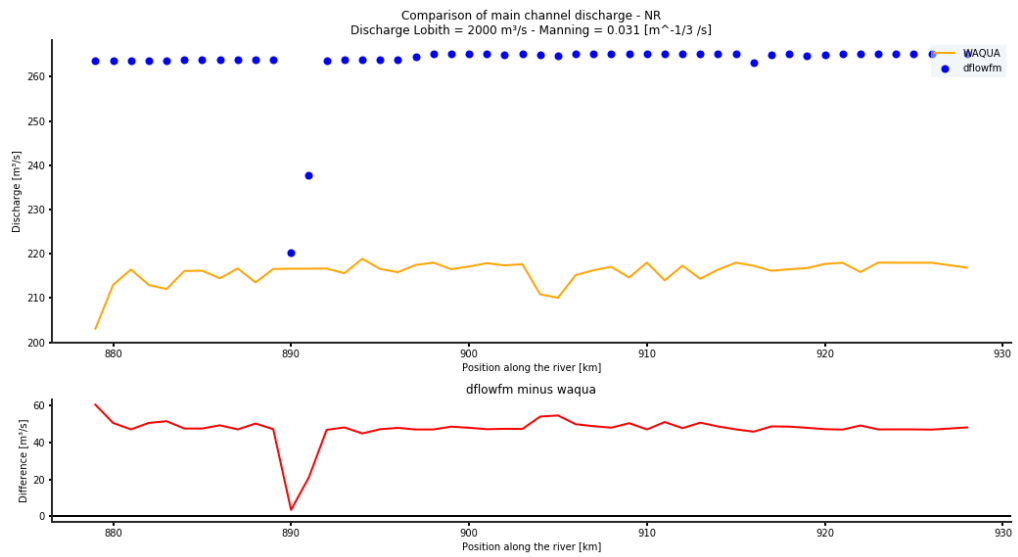
Figure 84 Comparison main channel discharge D-FLOW FM 1D - WAQUA - Nederrijn - Q=2000

Morphological models for IRM
11203684-015-ZWS-0011_v1.0, Version 0.1, 2020-12-11, Final

Deltares
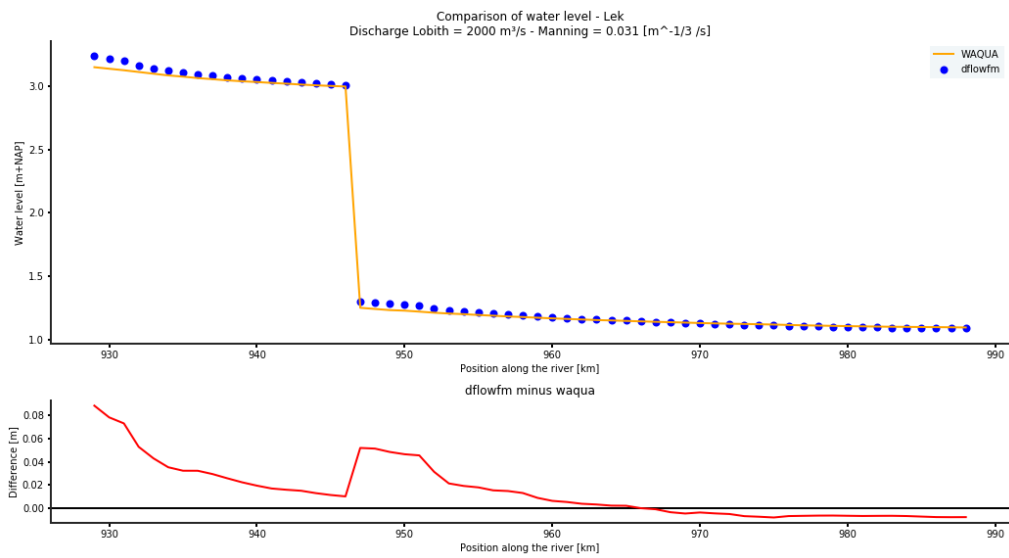
Figure 85 Comparison water level D-Fʟᴏᴡ FM 1D - WAQUA - Lek - Q=2000
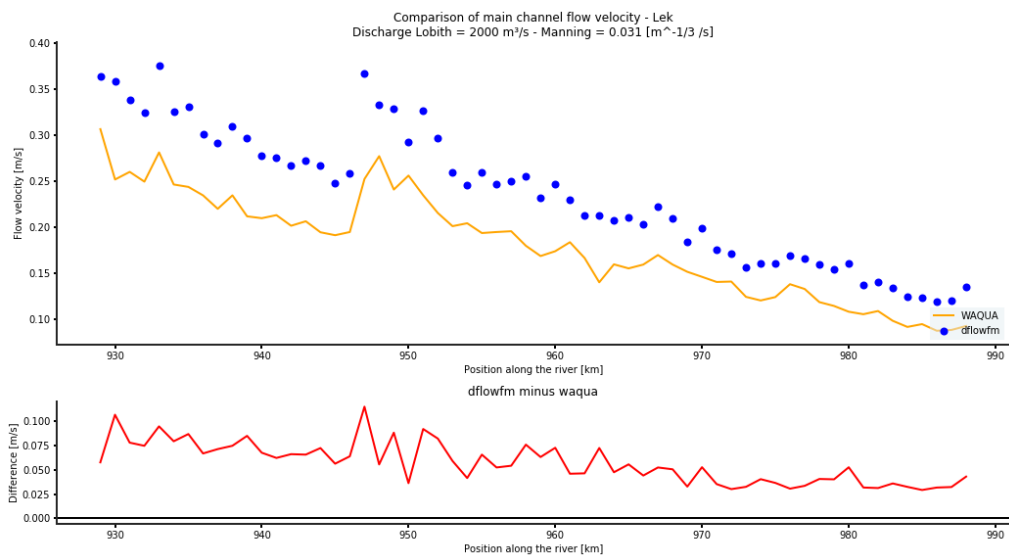
Figure 86 Comparison main channel flow velocity D-Fʟᴏᴡ FM 1D - WAQUA - Lek - Q=2000

Morphological models for IRM
11203684-015-ZWS-0011_v1.0, Version 0.1, 2020-12-11, Final

Deltares
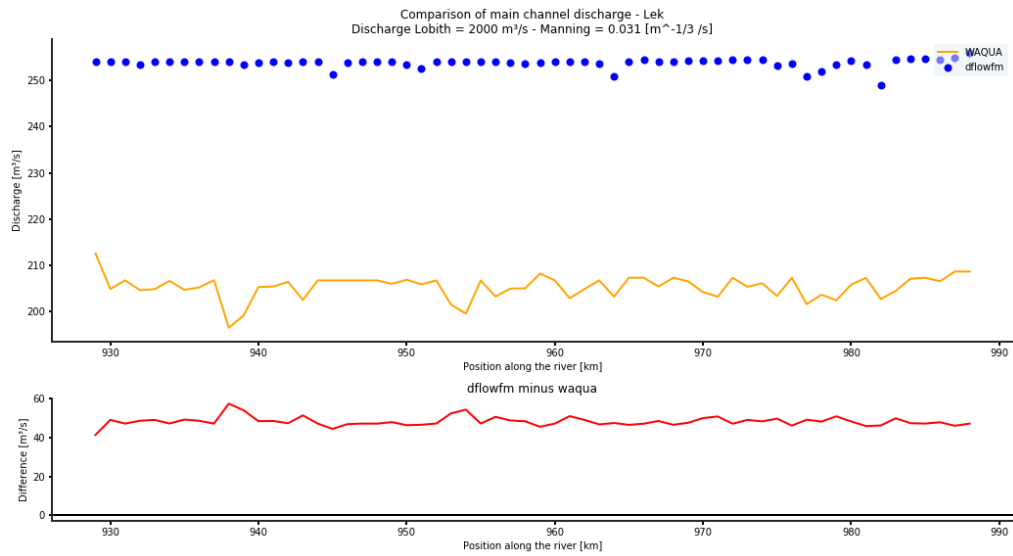
Figure 87 Comparison main channel discharge D-Flow FM 1D - WAQUA - Lek - Q=2000
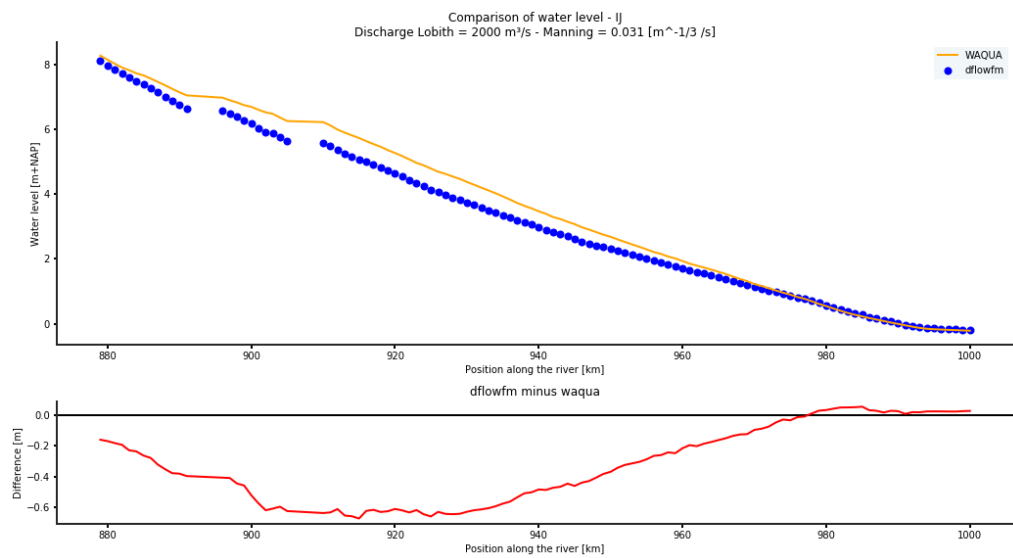
Figure 88 Comparison water level D-Flow FM 1D - WAQUA - IJssel - Q=2000

Morphological models for IRM
11203684-015-ZWS-0011_v1.0, Version 0.1, 2020-12-11, Final

Deltares
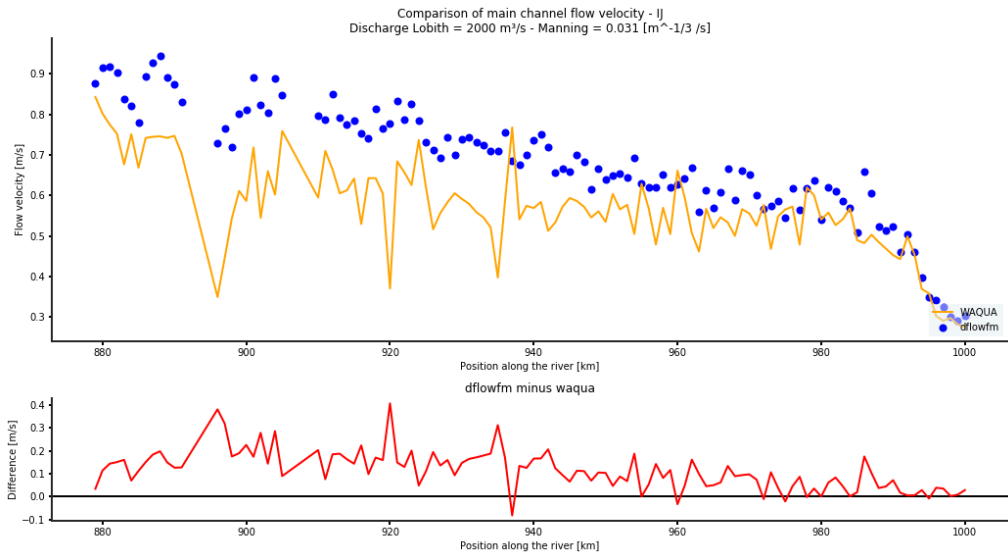
Figure 89 Comparison main channel flow velocity D-Flow FM 1D - WAQUA - IJssel - Q=2000
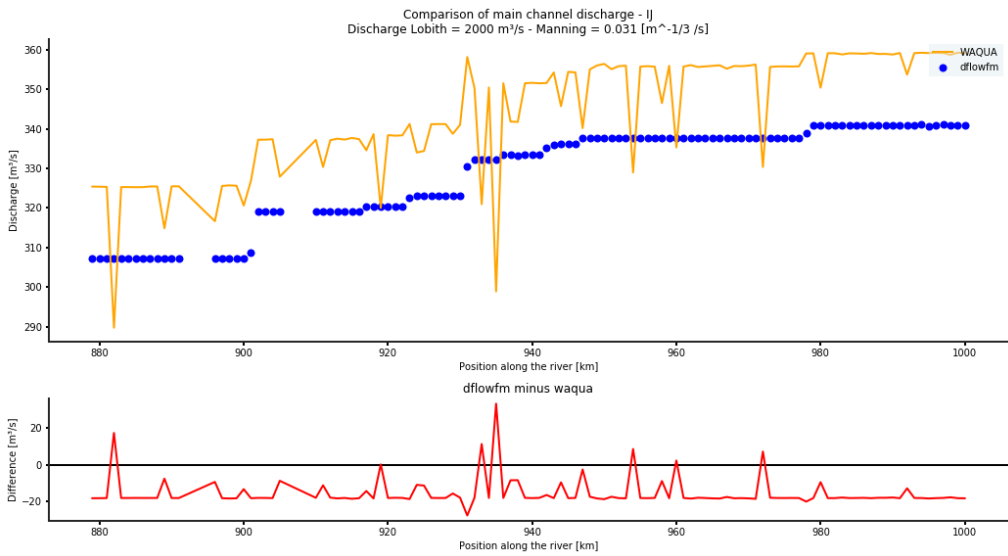
Figure 90 Comparison main channel discharge D-Flow FM 1D - WAQUA - IJssel - Q=2000

Morphological models for IRM
11203684-015-ZWS-0011_v1.0, Version 0.1, 2020-12-11, Final

Deltares

F   Comparison between WAQUA and D-FLOW FM 1D for a discharge equal to 4000 m³/s

Comparison of water level - BR
Discharge Lobith = 4000 m³/s - Manning = 0.036 [m^-1/3 /s]
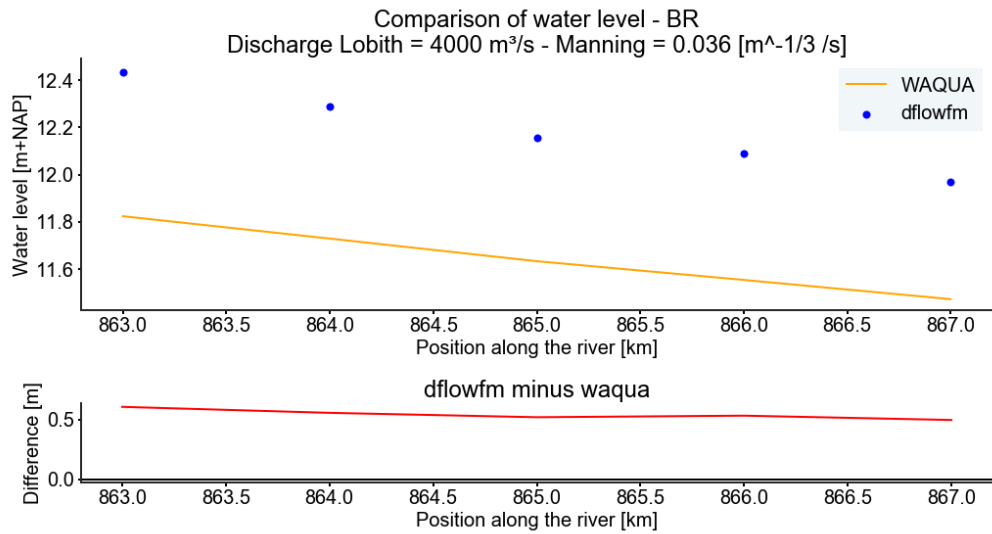
Figure 91 Comparison water level D-FLOW FM 1D - WAQUA - Boven-Rijn - Q=4000

Comparison of main channel flow velocity - BR
Discharge Lobith = 4000 m³/s - Manning = 0.036 [m^-1/3 /s]
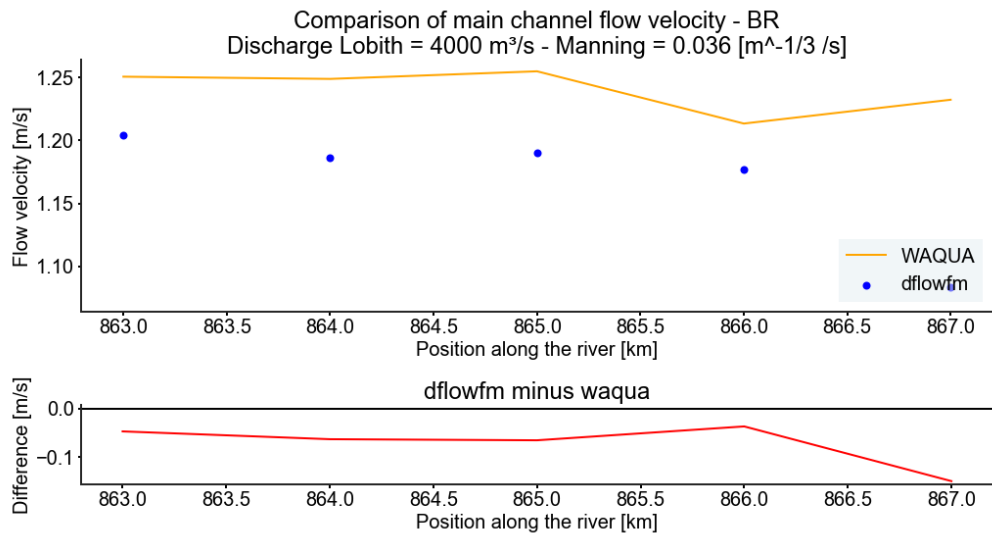
Figure 92 Comparison main channel flow velocity D-FLOW FM 1D - WAQUA - Boven-Rijn - Q=4000

Morphological models for IRM
11203684-015-ZWS-0011_v1.0, Version 0.1, 2020-12-11, Final

Deltares
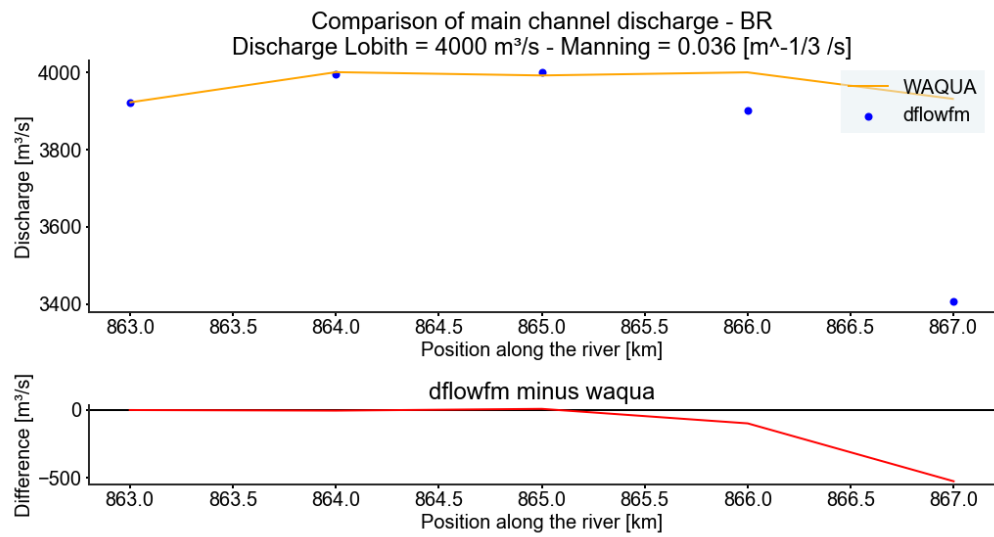
Figure 93 Comparison main channel discharge D-Fʟᴏᴡ FM 1D - WAQUA - Boven-Rijn -
Q=4000
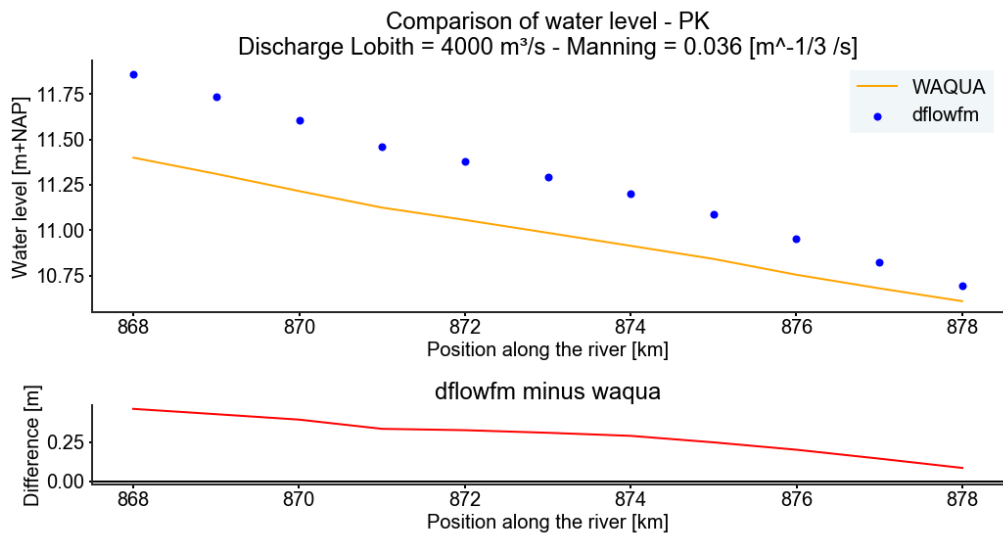
Figure 94 Comparison water level D-Fʟᴏᴡ FM 1D - WAQUA - Pannerdensch Kanaal -
Q=4000
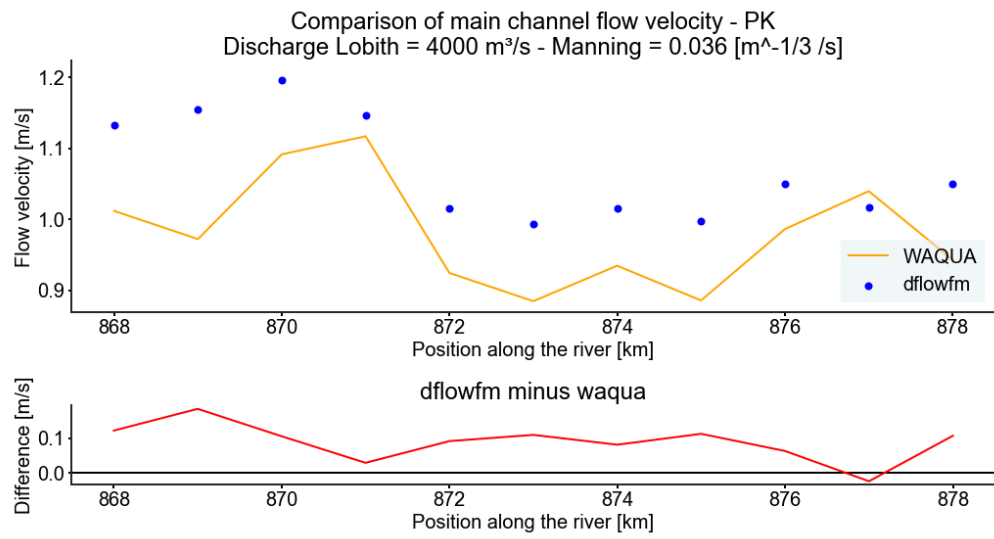
Figure 95 Comparison main channel flow velocity D-FLOW FM 1D - WAQUA - Pannerdensch Kanaal - Q=4000
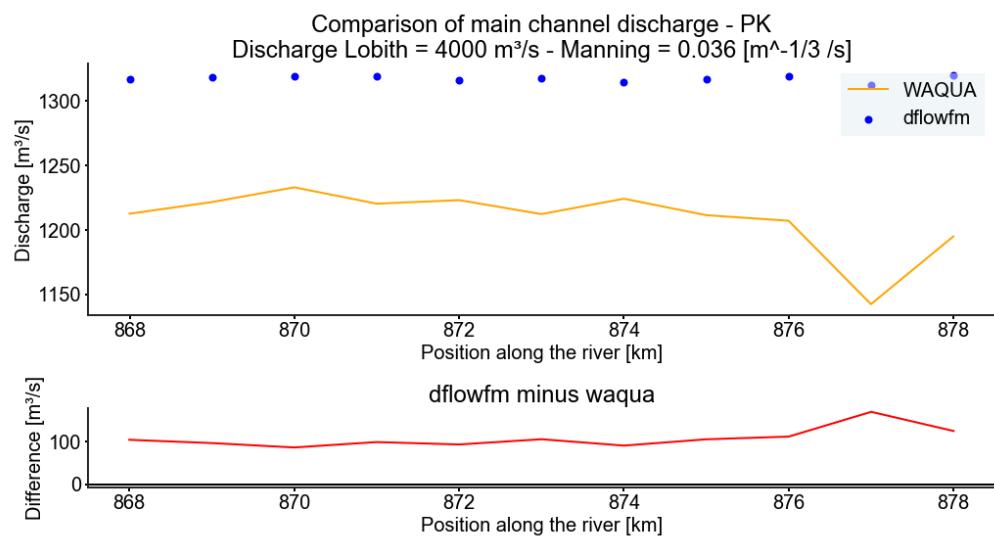
Figure 96 Comparison main channel discharge D-FLOW FM 1D - WAQUA - Pannerdensch Kanaal - Q=4000

Morphological models for IRM
11203684-015-ZWS-0011_v1.0, Version 0.1, 2020-12-11, Final

Deltares
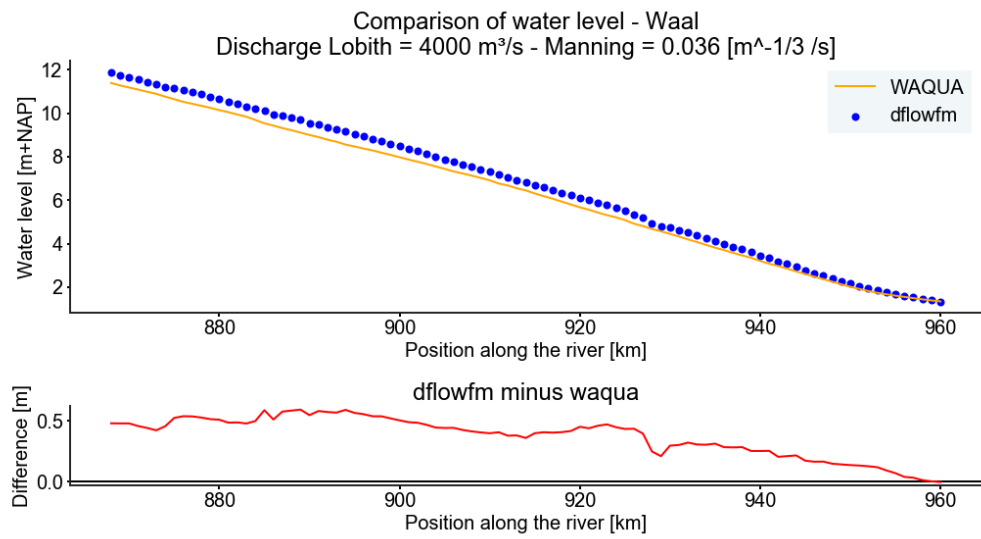
Figure 97 Comparison water level D-Fʟᴏᴡ FM 1D - WAQUA - Waal - Q=4000
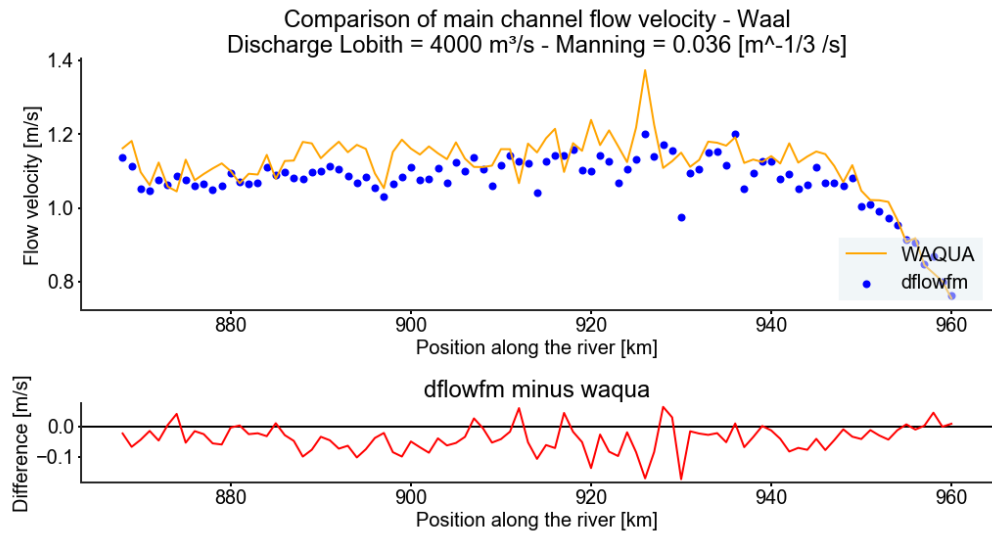
Figure 98 Comparison main channel flow velocity D-Fʟᴏᴡ FM 1D - WAQUA - Waal - Q=4000

Deltares

Figure 99 Comparison main channel discharge D-Flow FM 1D - WAQUA - Waal - Q=4000
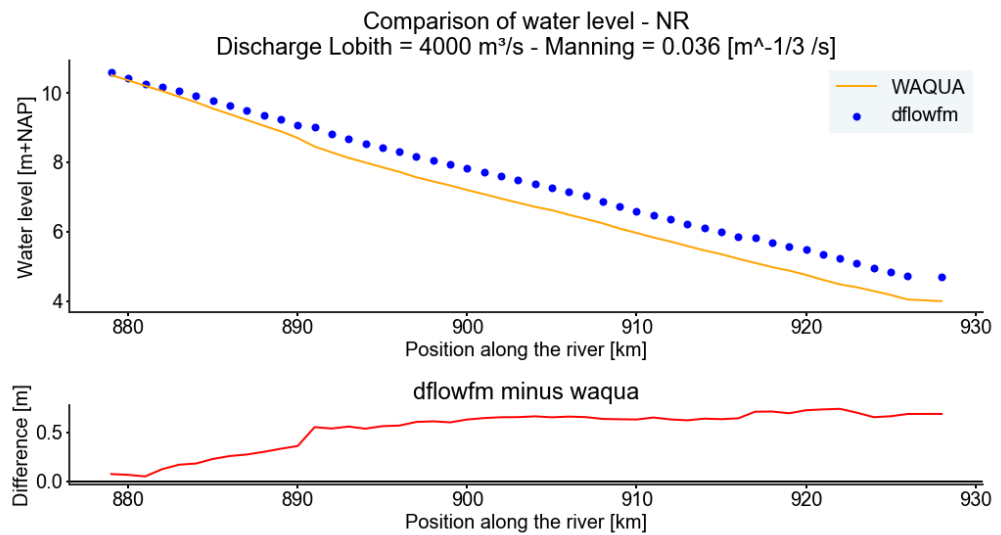
Figure 100 Comparison water level D-Flow FM 1D - WAQUA - Nederrijn - Q=4000

Deltares
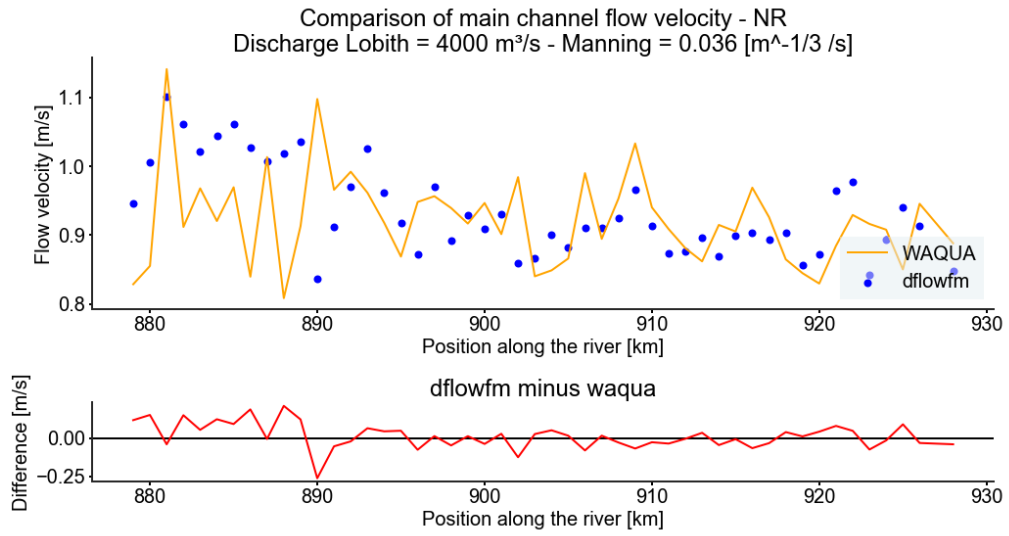
Figure 101 Comparison main channel flow velocity D-Flow FM 1D - WAQUA - Nederrijn - Q=4000
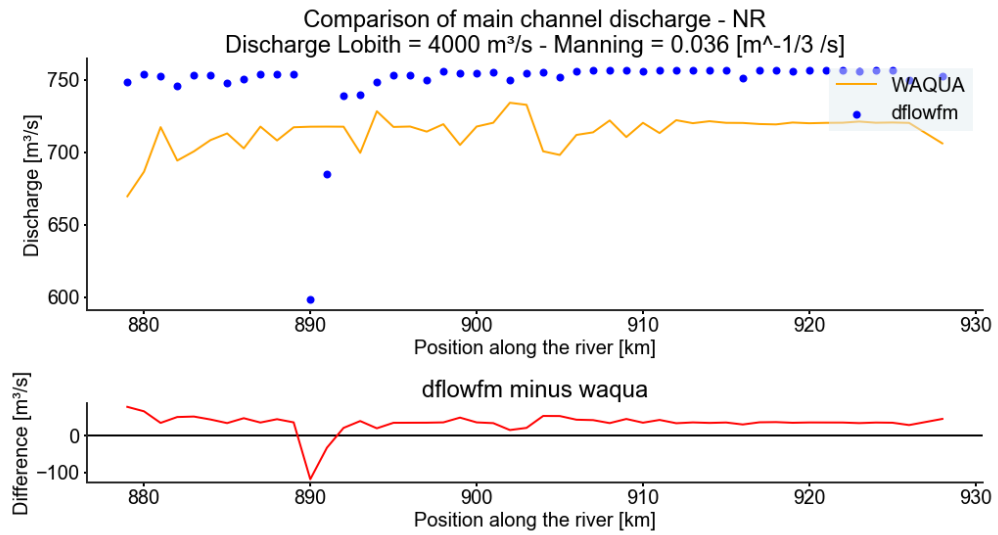
Figure 102 Comparison main channel discharge D-Flow FM 1D - WAQUA - Nederrijn - Q=4000

Deltares
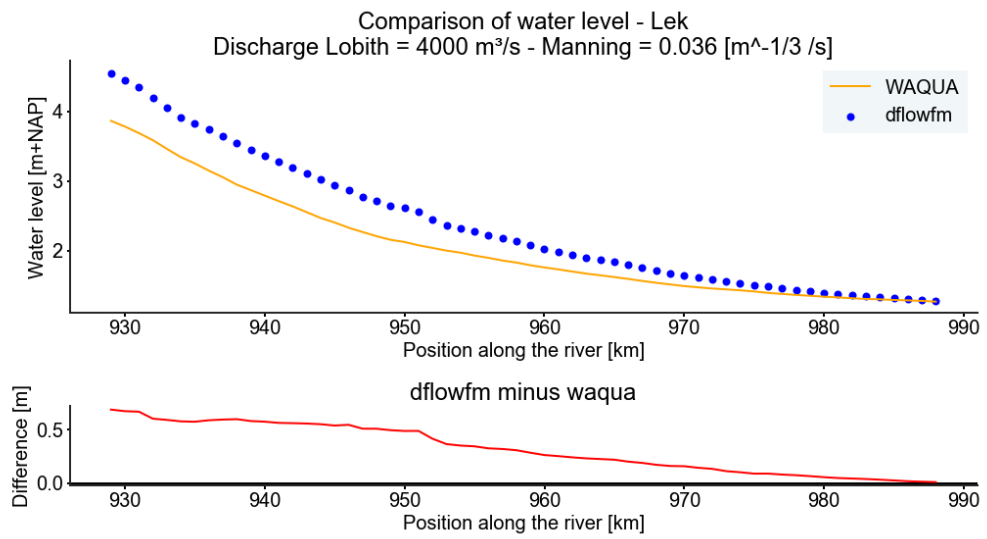
Figure 103 Comparison water level D-Flow FM 1D - WAQUA - Lek - Q=4000
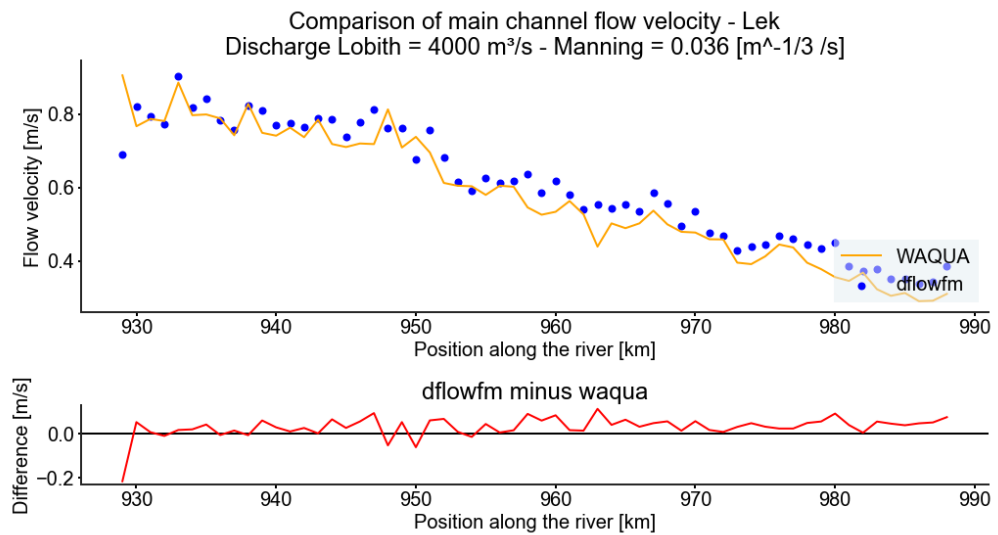
Figure 104 Comparison main channel flow velocity D-Flow FM 1D - WAQUA - Lek - Q=4000

Deltares
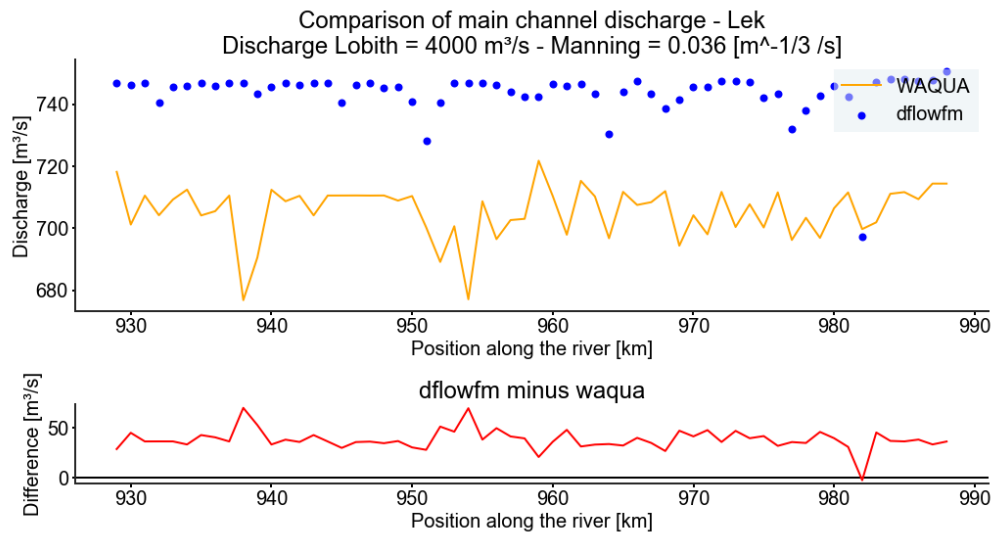
Figure 105 Comparison main channel discharge D-Flow FM 1D - WAQUA - Lek - Q=4000
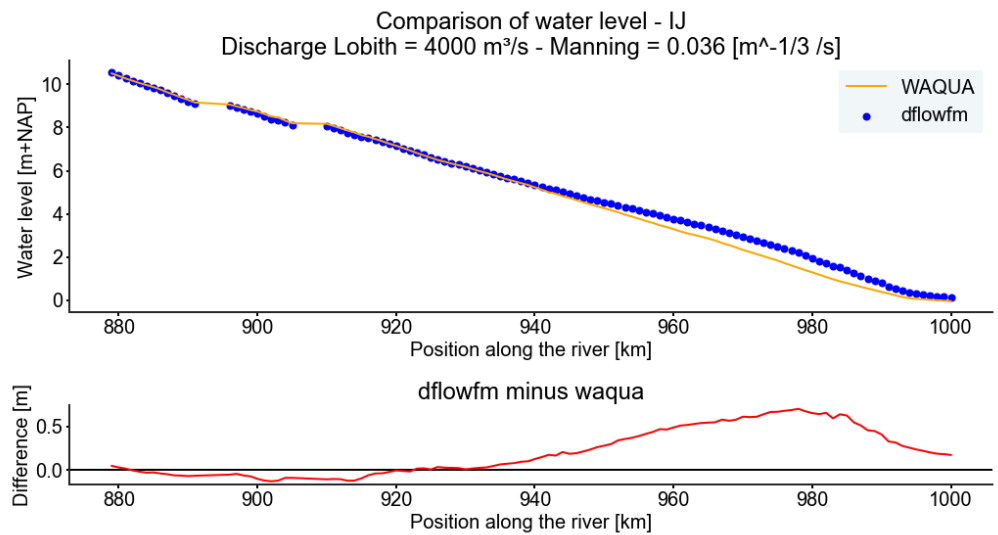
Figure 106 Comparison water level D-Flow FM 1D - WAQUA - IJssel - Q=4000

Deltares
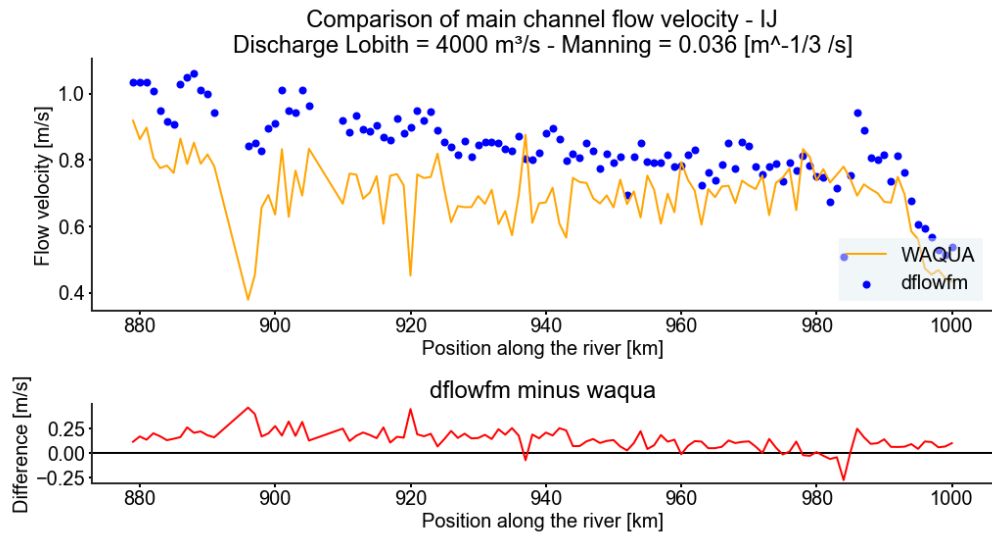
Figure 107 Comparison main channel flow velocity D-Flᴏᴡ FM 1D - WAQUA - IJssel - Q=4000
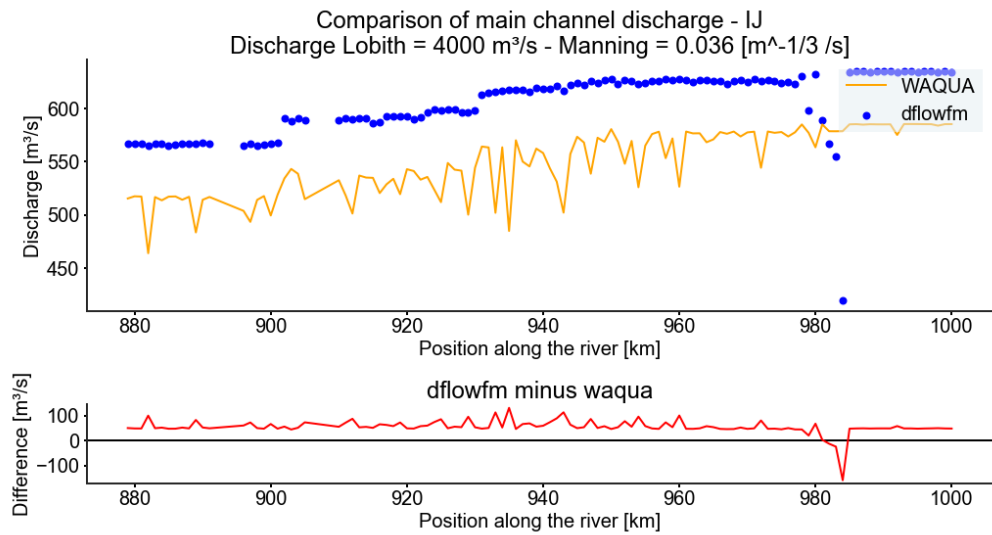
Figure 108 Comparison main channel discharge D-Flᴏᴡ FM 1D - WAQUA - IJssel - Q=4000

G   Comparison between WAQUA and D-F<small>LOW</small> FM 1D for a discharge equal to 6000 m³/s
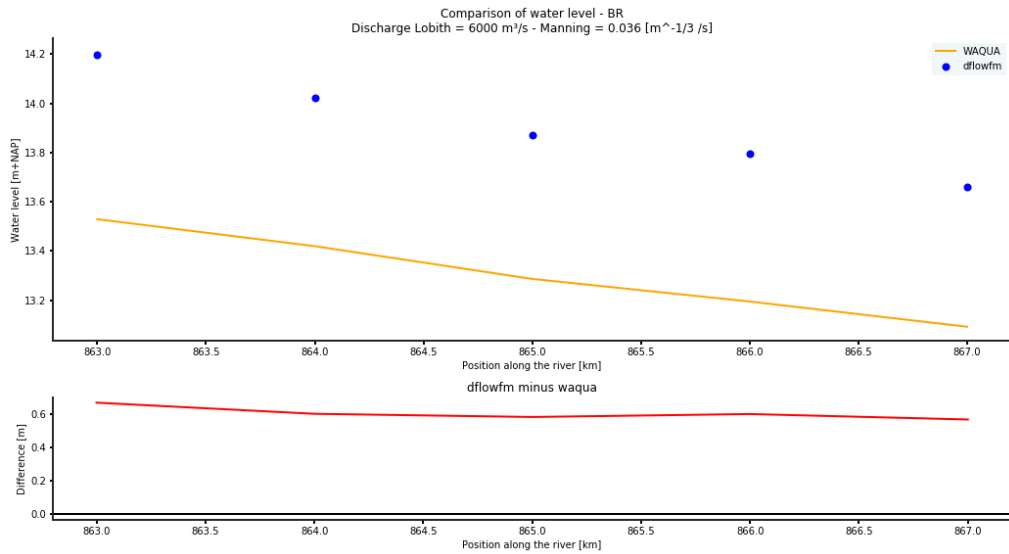
Figure 109 Comparison water level D-F<small>LOW</small> FM 1D - WAQUA - Boven-Rijn - Q=6000
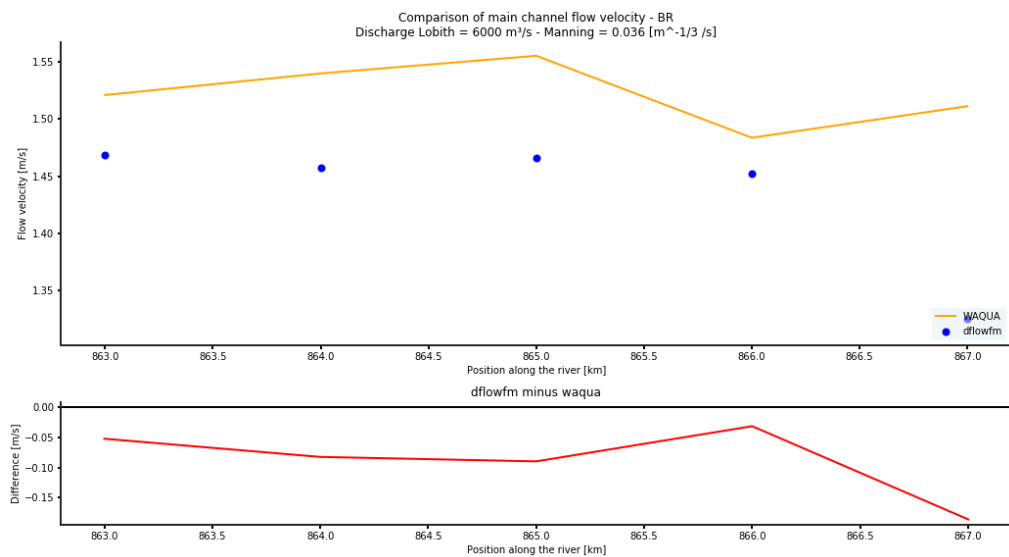
Figure 110 Comparison main channel flow velocity D-F<small>LOW</small> FM 1D - WAQUA - Boven-Rijn - Q=6000
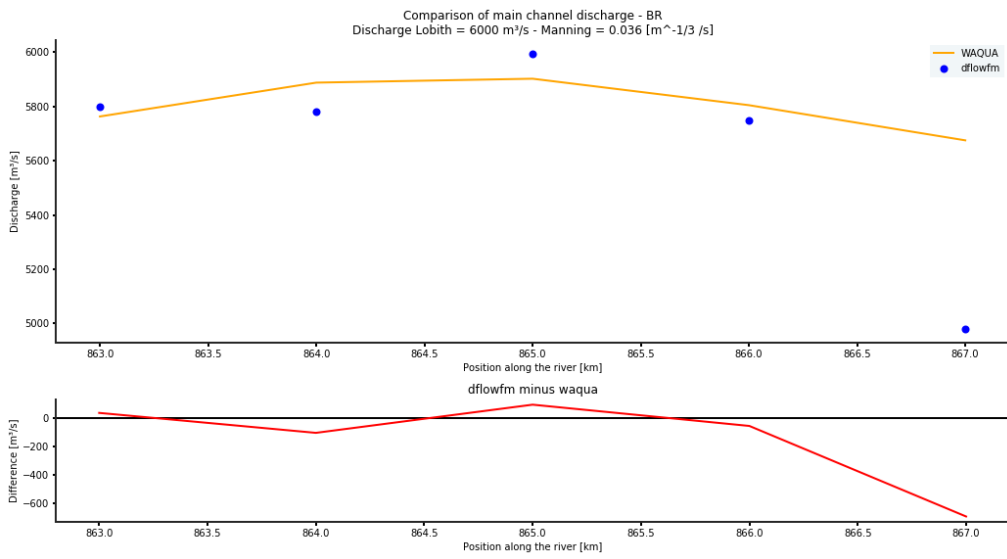
Figure 111 Comparison main channel discharge D-FLOW FM 1D - WAQUA - Boven-Rijn - Q=6000
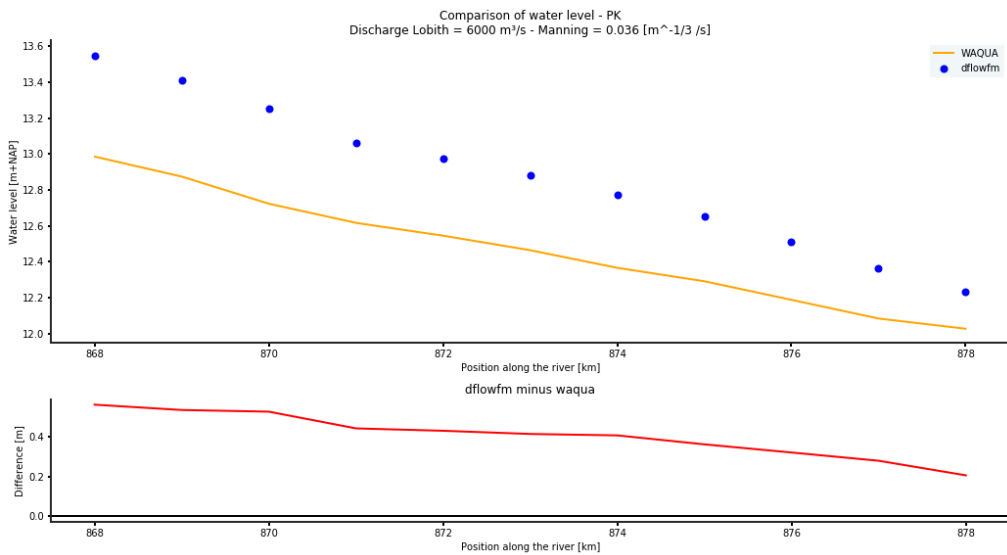
Figure 112 Comparison water level D-FLOW FM 1D - WAQUA - Pannerdensch Kanaal - Q=6000

Morphological models for IRM
11203684-015-ZWS-0011_v1.0, Version 0.1, 2020-12-11, Final

Deltares
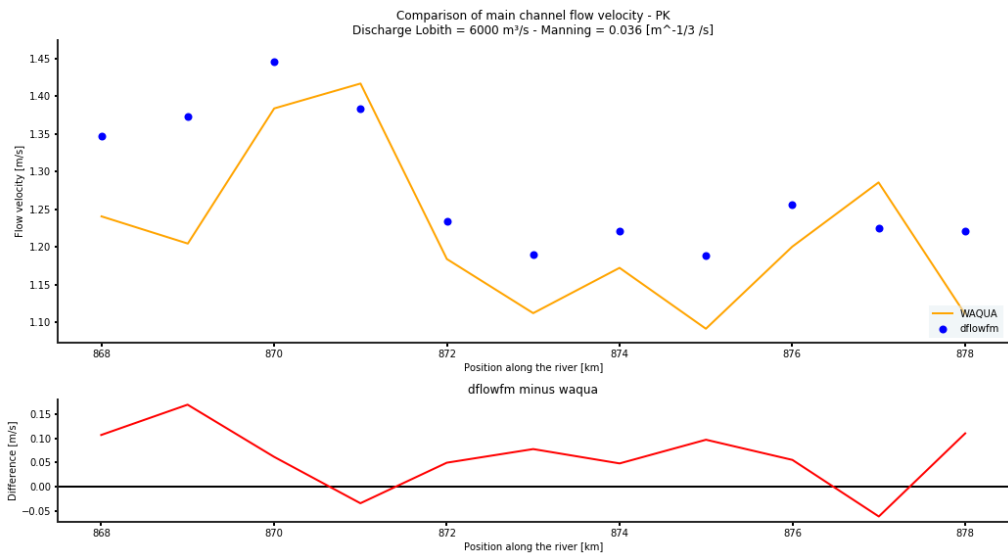
Figure 113 Comparison main channel flow velocity D-Flow FM 1D - WAQUA - Pannerden-sch Kanaal - Q=6000
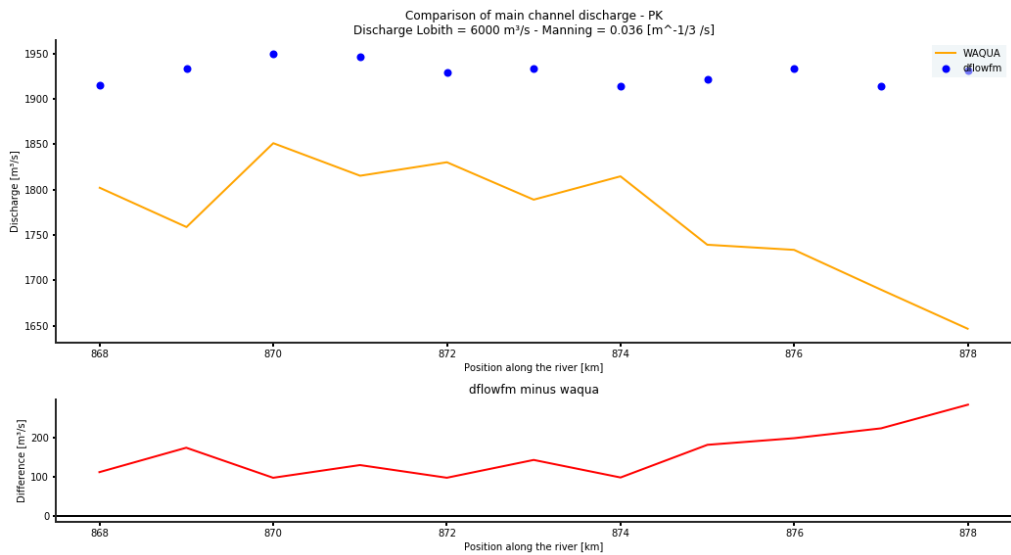
Figure 114 Comparison main channel discharge D-Flow FM 1D - WAQUA - Pannerdensch Kanaal - Q=6000
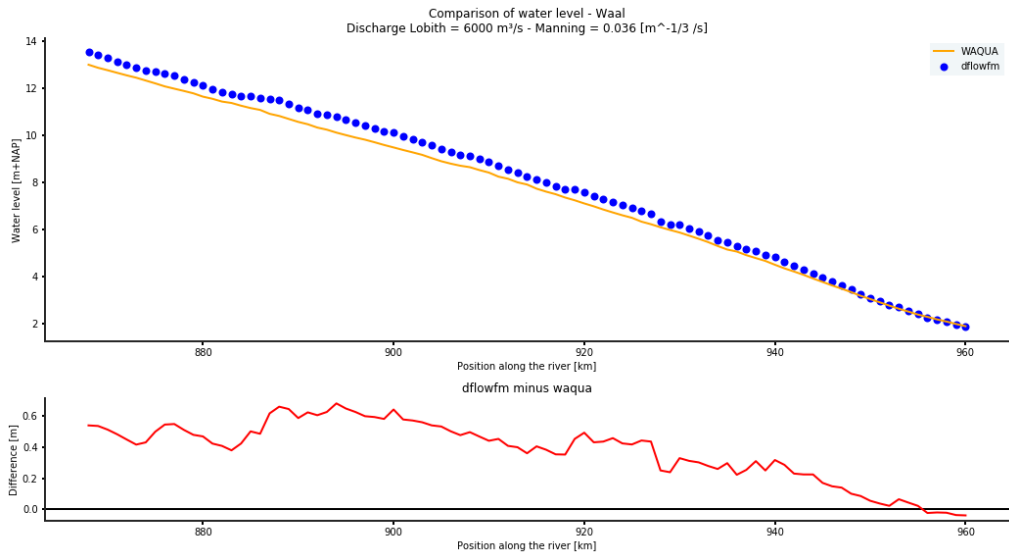
Figure 115 Comparison water level D-Flow FM 1D - WAQUA - Waal - Q=6000
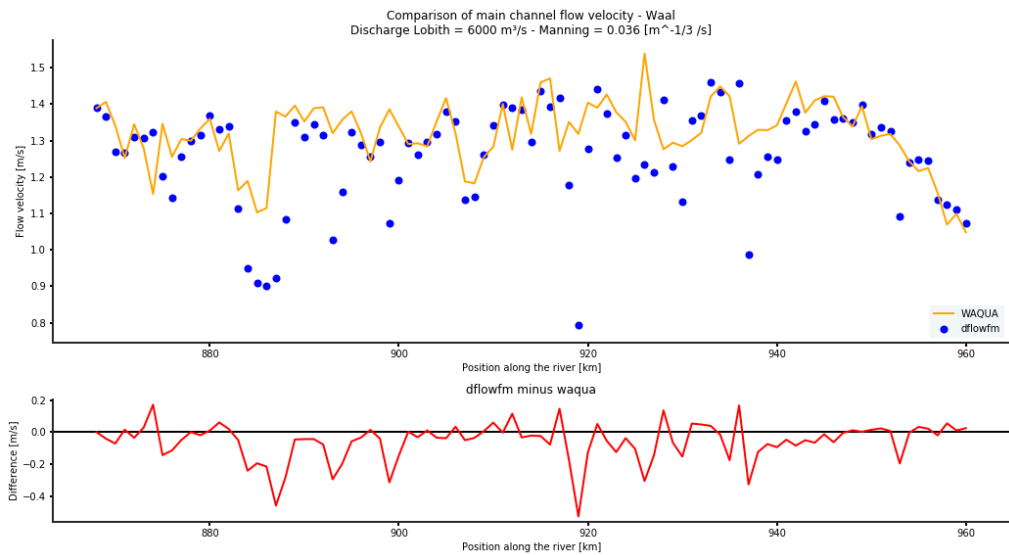
Figure 116 Comparison main channel flow velocity D-Flow FM 1D - WAQUA - Waal - Q=6000

Morphological models for IRM
11203684-015-ZWS-0011_v1.0, Version 0.1, 2020-12-11, Final

Deltares
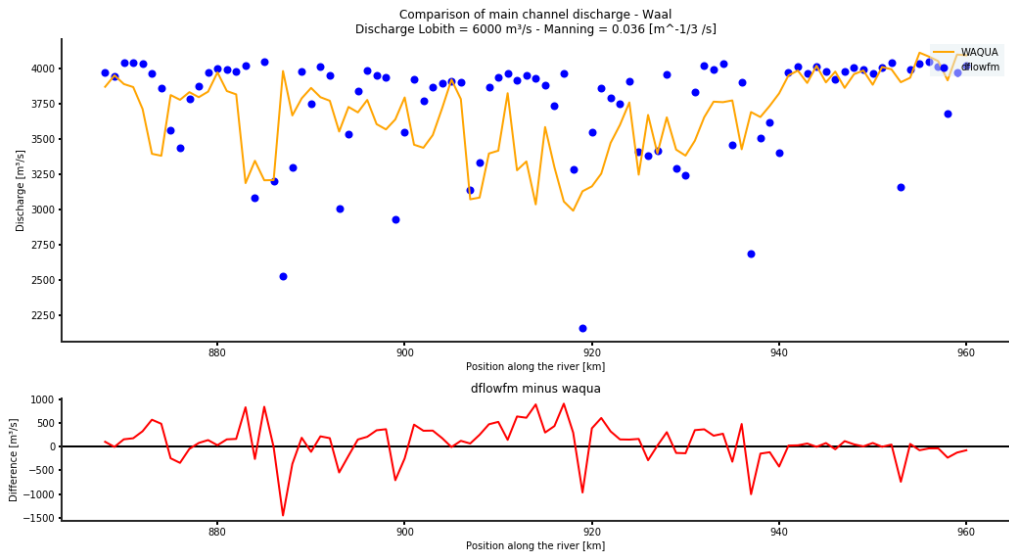
Figure 117 Comparison main channel discharge D-FLow FM 1D - WAQUA - Waal - Q=6000
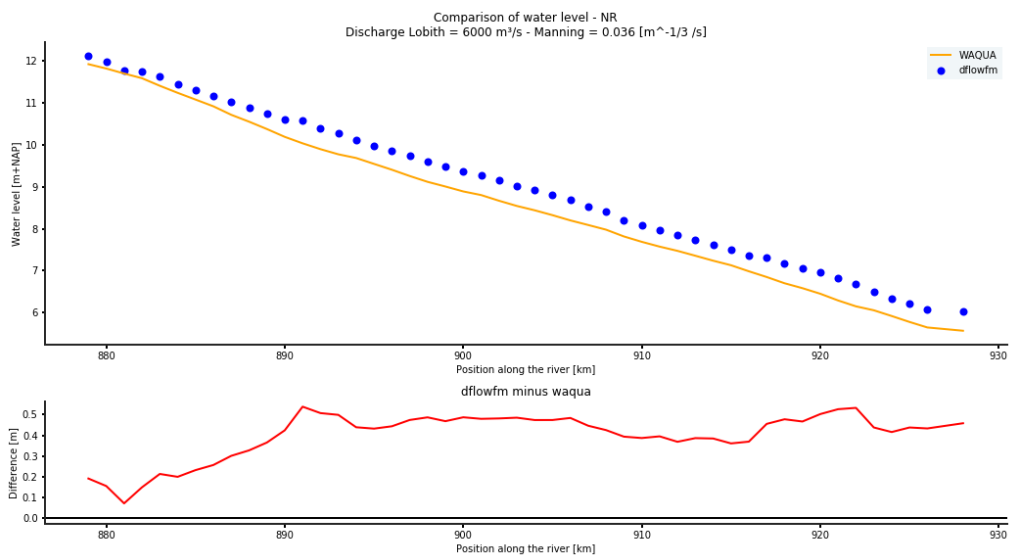
Figure 118 Comparison water level D-FLow FM 1D - WAQUA - Nederrijn - Q=6000

Morphological models for IRM
11203684-015-ZWS-0011_v1.0, Version 0.1, 2020-12-11, Final

Deltares
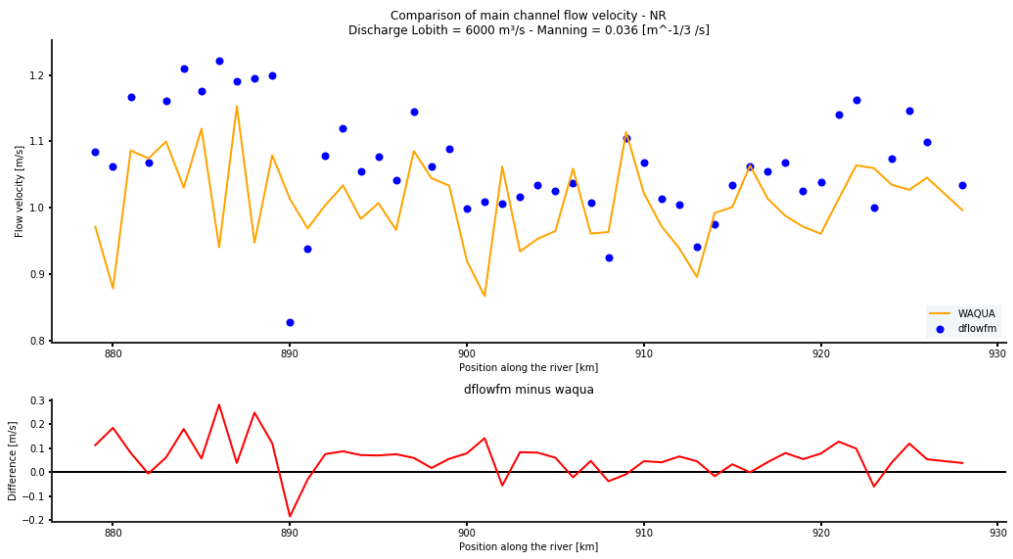
Figure 119 Comparison main channel flow velocity D-Flow FM 1D - WAQUA - Nederrijn - Q=6000
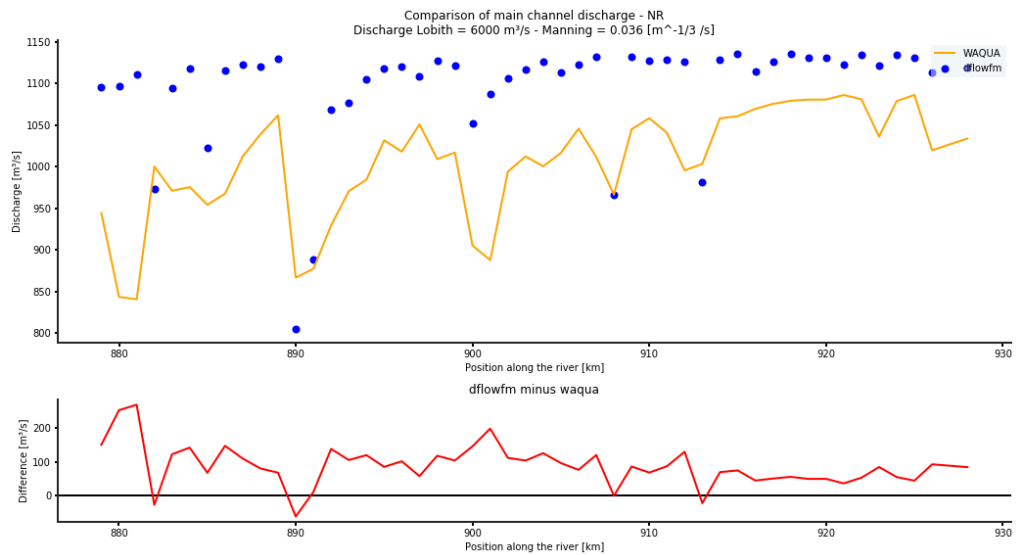
Figure 120 Comparison main channel discharge D-Flow FM 1D - WAQUA - Nederrijn - Q=6000

Morphological models for IRM
11203684-015-ZWS-0011_v1.0, Version 0.1, 2020-12-11, Final

Deltares
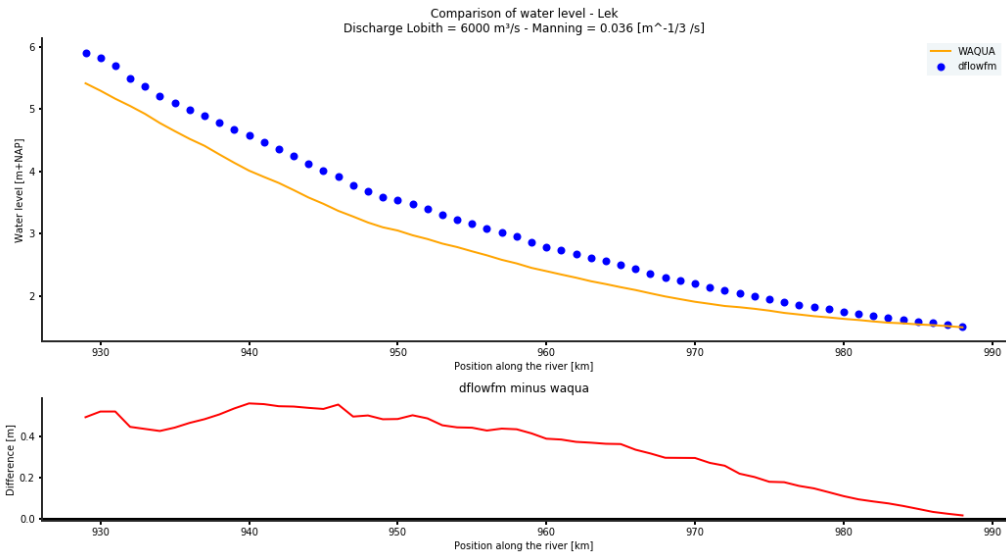
Figure 121 Comparison water level D-Flow FM 1D - WAQUA - Lek - Q=6000
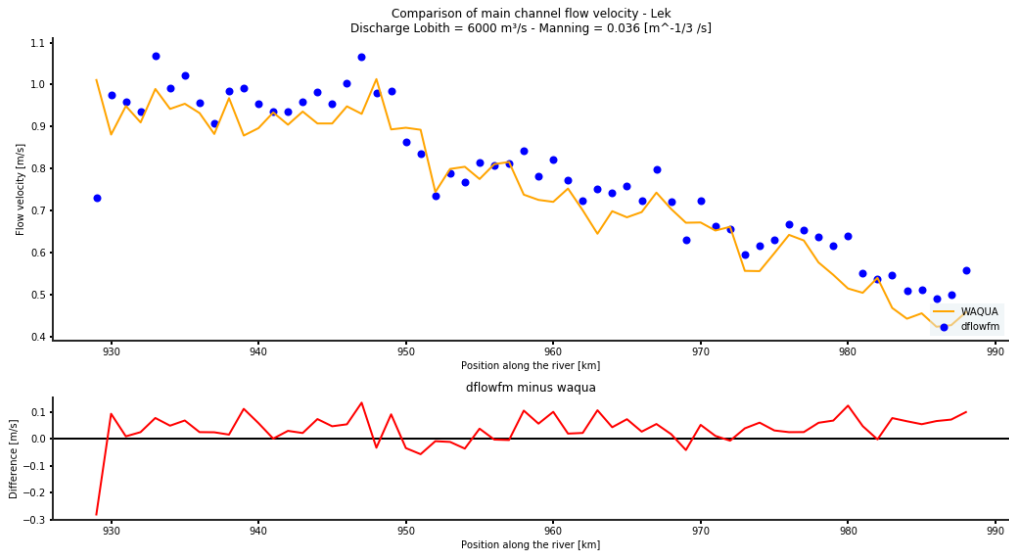
Figure 122 Comparison main channel flow velocity D-Flow FM 1D - WAQUA - Lek - Q=6000

Deltares
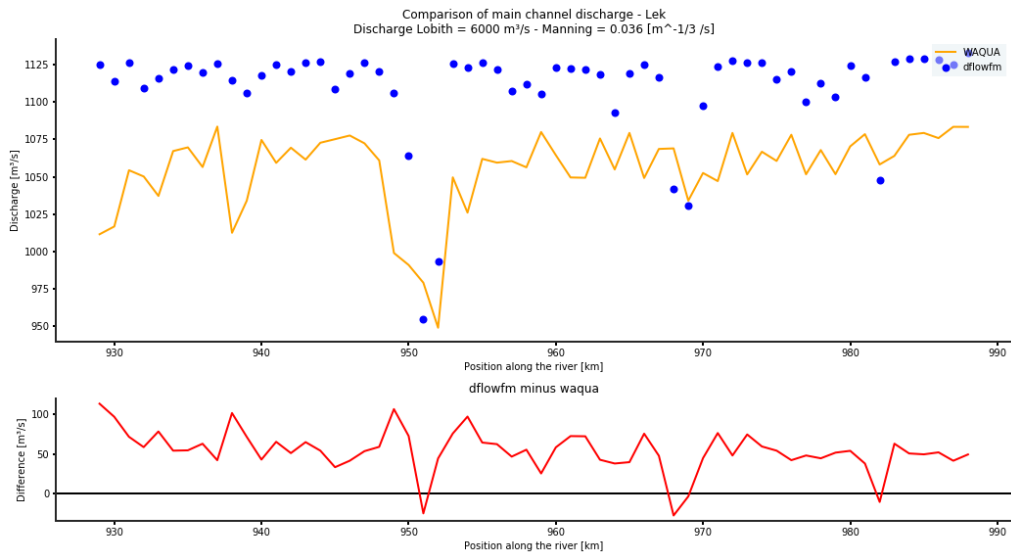
Figure 123 Comparison main channel discharge D-Fʟᴏᴡ FM 1D - WAQUA - Lek - Q=6000
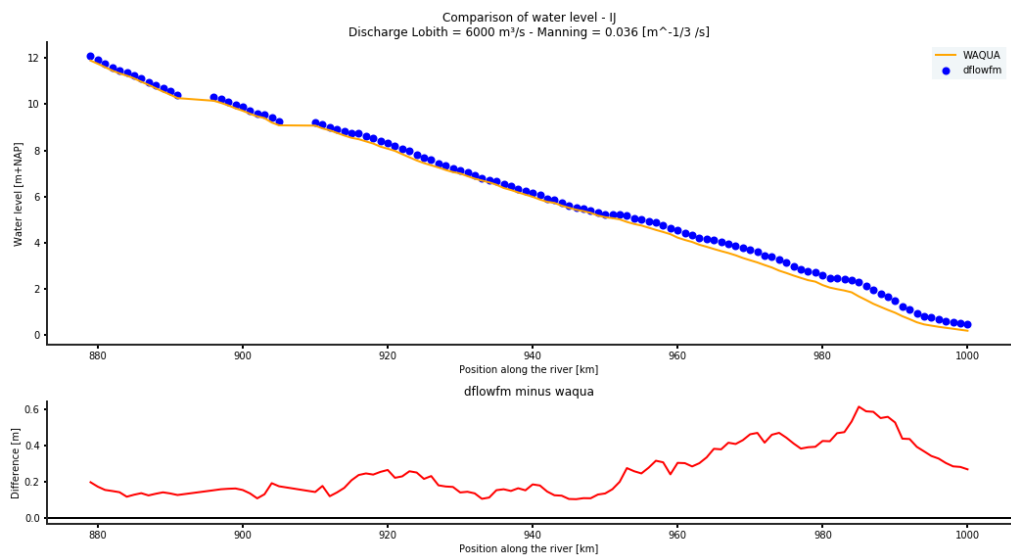
Figure 124 Comparison water level D-Fʟᴏᴡ FM 1D - WAQUA - IJssel - Q=6000

Morphological models for IRM
11203684-015-ZWS-0011_v1.0, Version 0.1, 2020-12-11, Final

Deltares
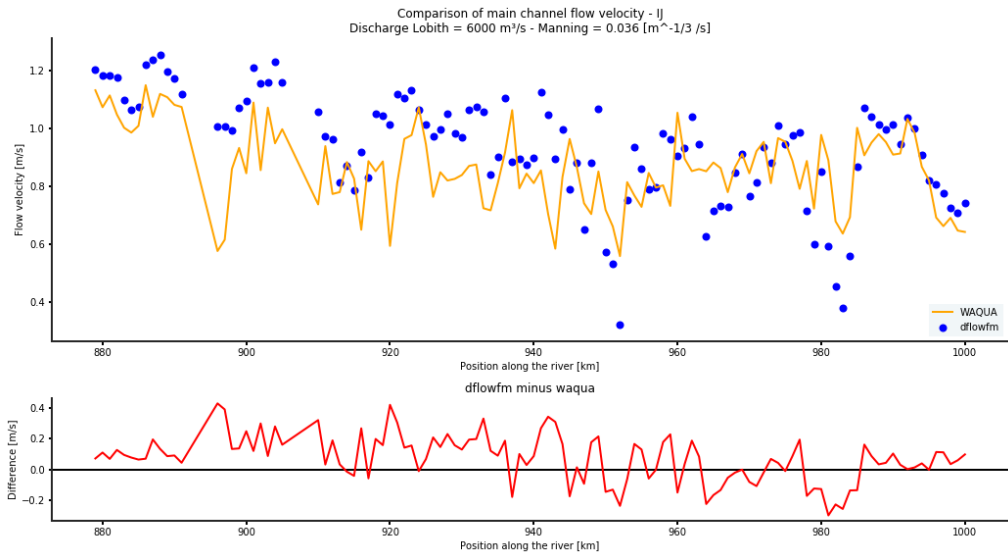
Figure 125 Comparison main channel flow velocity D-Fʟᴏᴡ FM 1D - WAQUA - IJssel - Q=6000
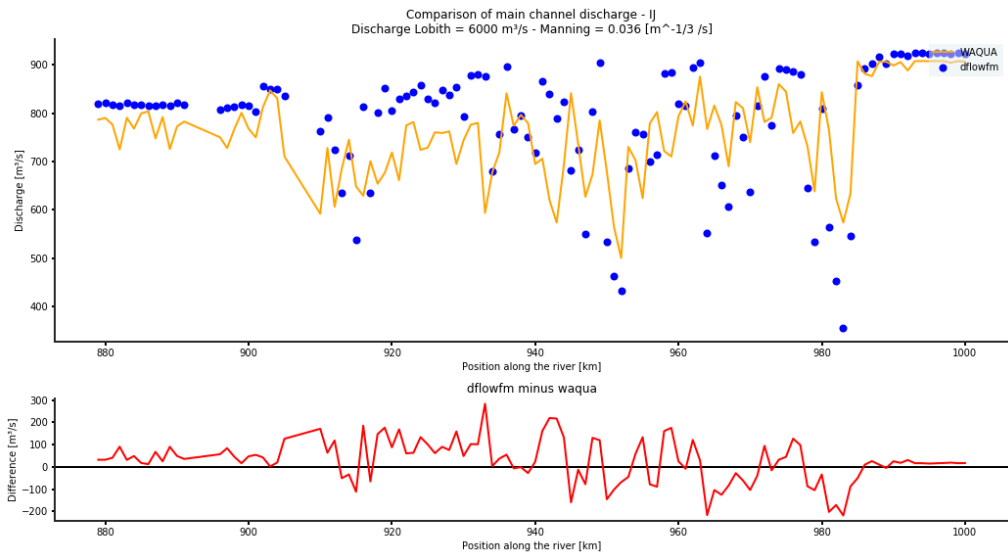
Figure 126 Comparison main channel discharge D-Fʟᴏᴡ FM 1D - WAQUA - IJssel - Q=6000

Deltares

H Comparison between WAQUA and D-Flow FM 1D for a discharge equal to 8000 m³/s

Comparison of water level - BR
Discharge Lobith = 8000 m³/s - Manning = 0.036 [m^-1/3 /s]
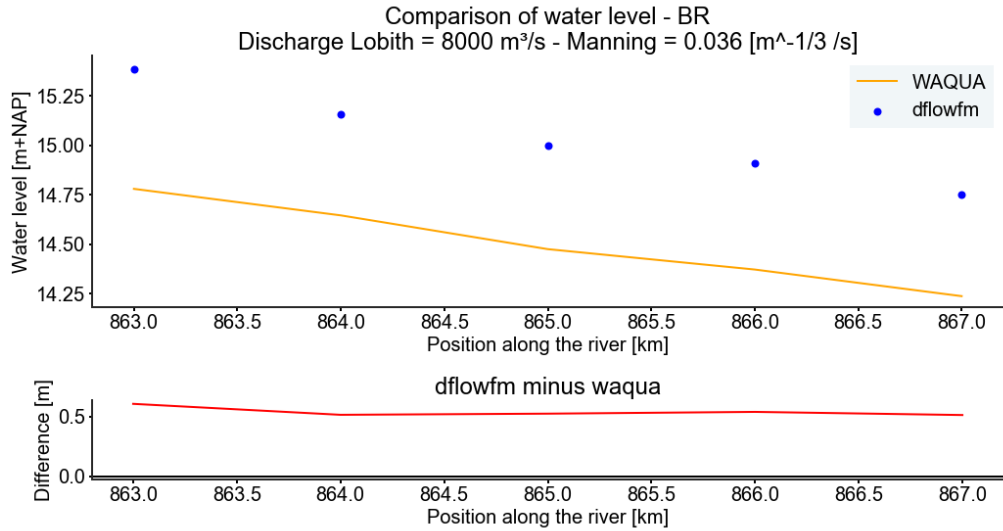
Figure 127 Comparison water level D-Flow FM 1D - WAQUA - Boven-Rijn - Q=8000

Comparison of main channel flow velocity - BR
Discharge Lobith = 8000 m³/s - Manning = 0.036 [m^-1/3 /s]
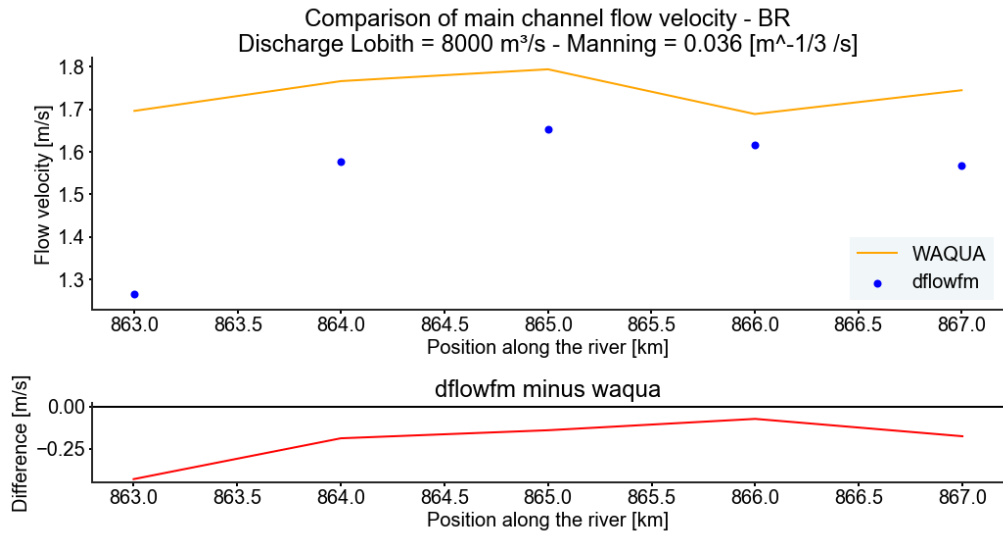
Figure 128 Comparison main channel flow velocity D-Flow FM 1D - WAQUA - Boven-Rijn - Q=8000

Deltares
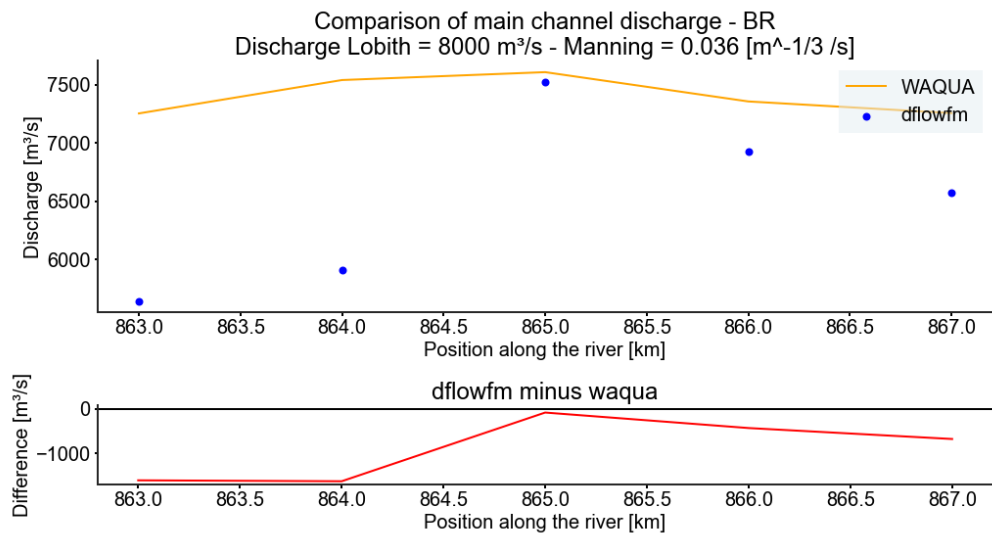
Figure 129 Comparison main channel discharge D-Flow FM 1D - WAQUA - Boven-Rijn - Q=8000
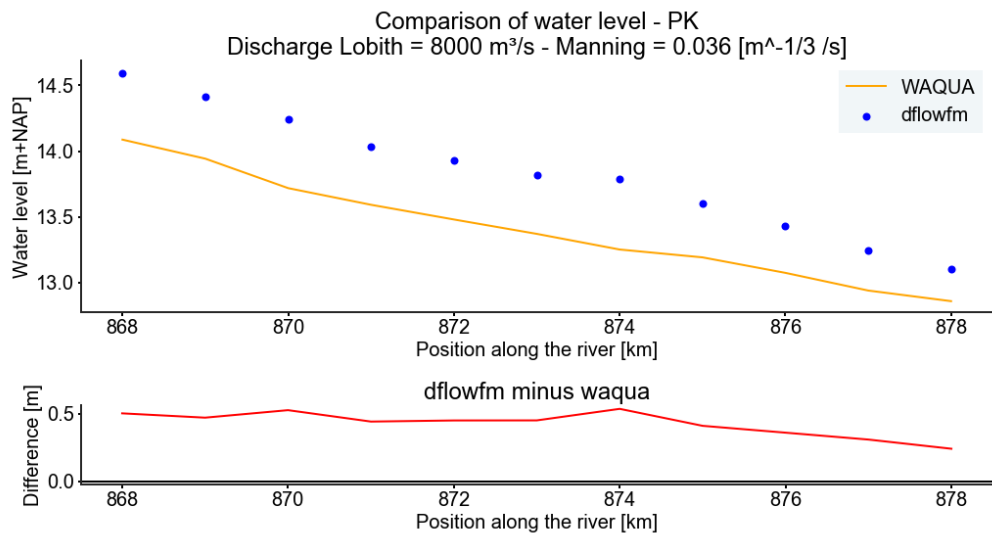
Figure 130 Comparison water level D-Flow FM 1D - WAQUA - Pannerdensch Kanaal - Q=8000
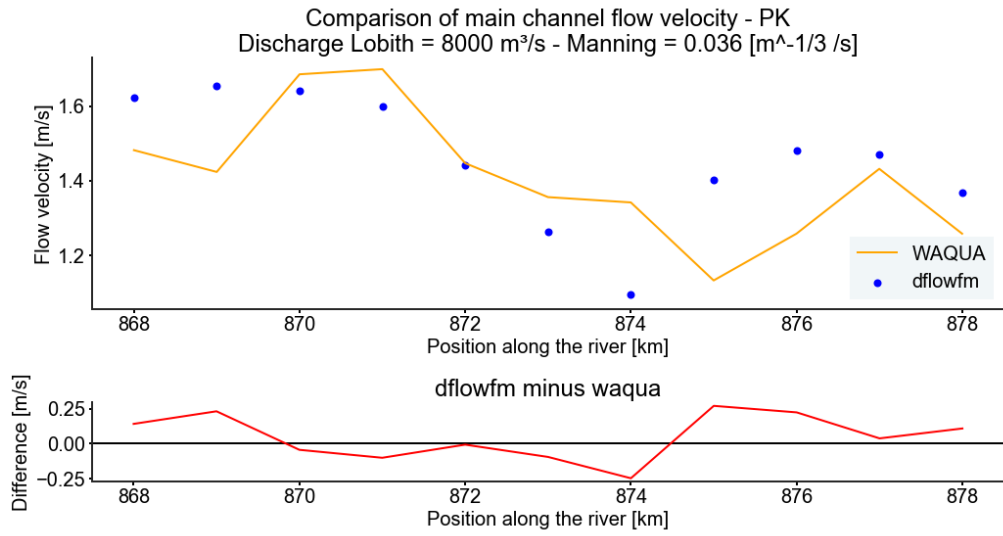
Figure 131 Comparison main channel flow velocity D-FLOW FM 1D - WAQUA - Pannerden-sch Kanaal - Q=8000
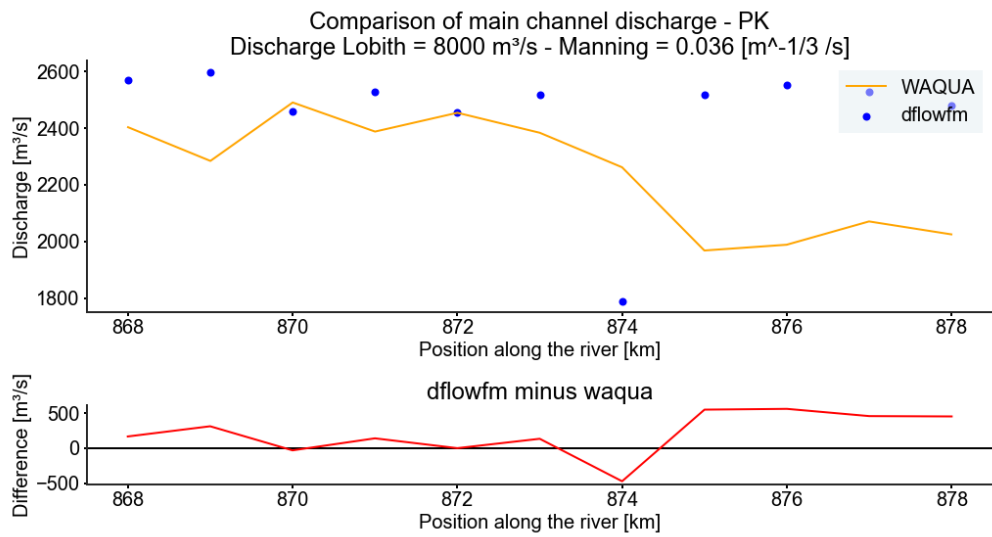
Figure 132 Comparison main channel discharge D-FLOW FM 1D - WAQUA - Pannerdensch Kanaal - Q=8000

Morphological models for IRM
11203684-015-ZWS-0011_v1.0, Version 0.1, 2020-12-11, Final

Deltares
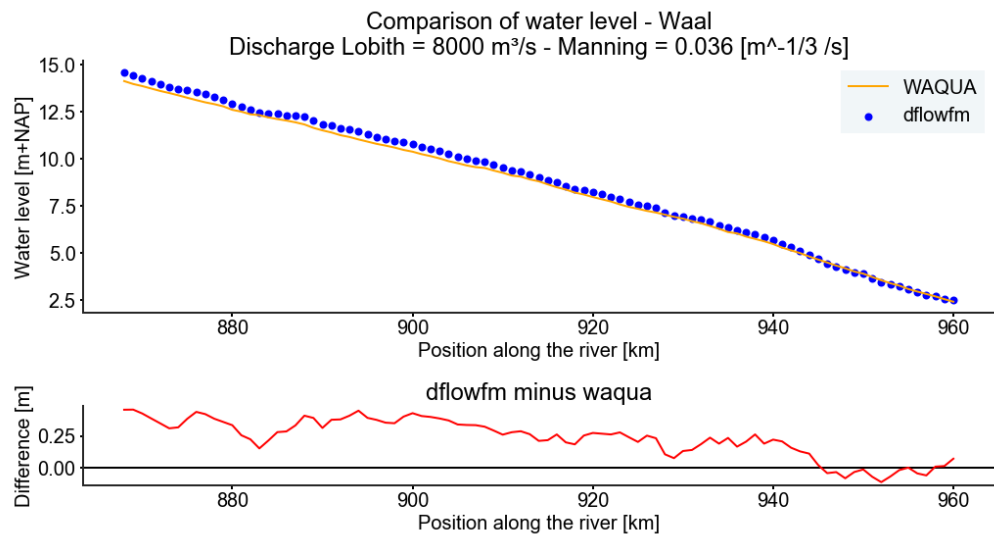
Figure 133 Comparison water level D-FLOW FM 1D - WAQUA - Waal - Q=8000
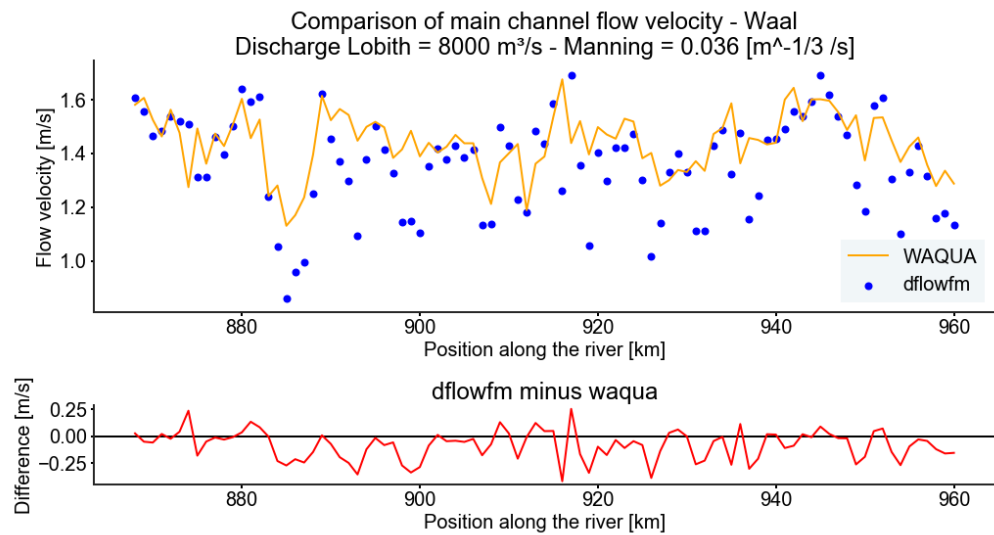
Figure 134 Comparison main channel flow velocity D-FLOW FM 1D - WAQUA - Waal - Q=8000

Deltares
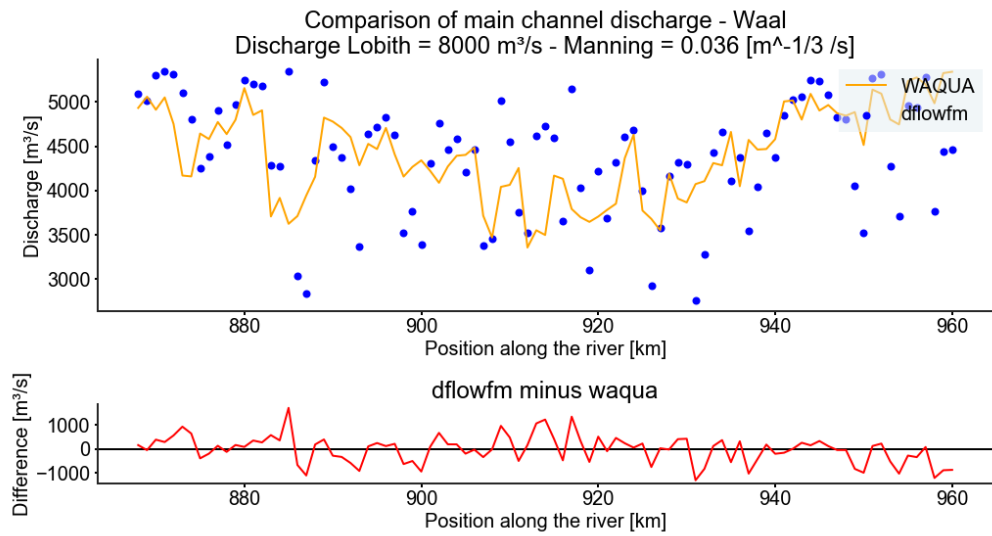
Figure 135 Comparison main channel discharge D-Flow FM 1D - WAQUA - Waal - Q=8000
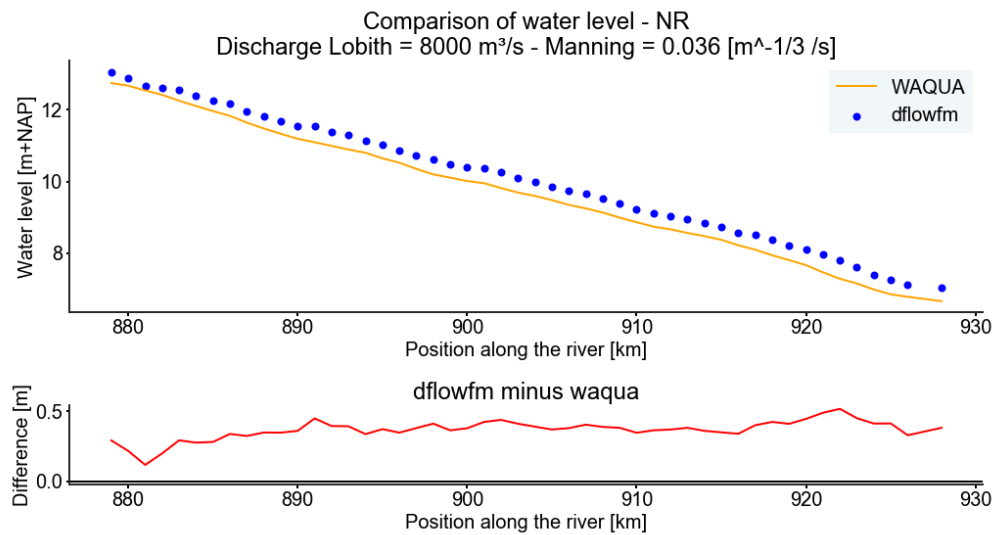
Figure 136 Comparison water level D-Flow FM 1D - WAQUA - Nederrijn - Q=8000

Deltares
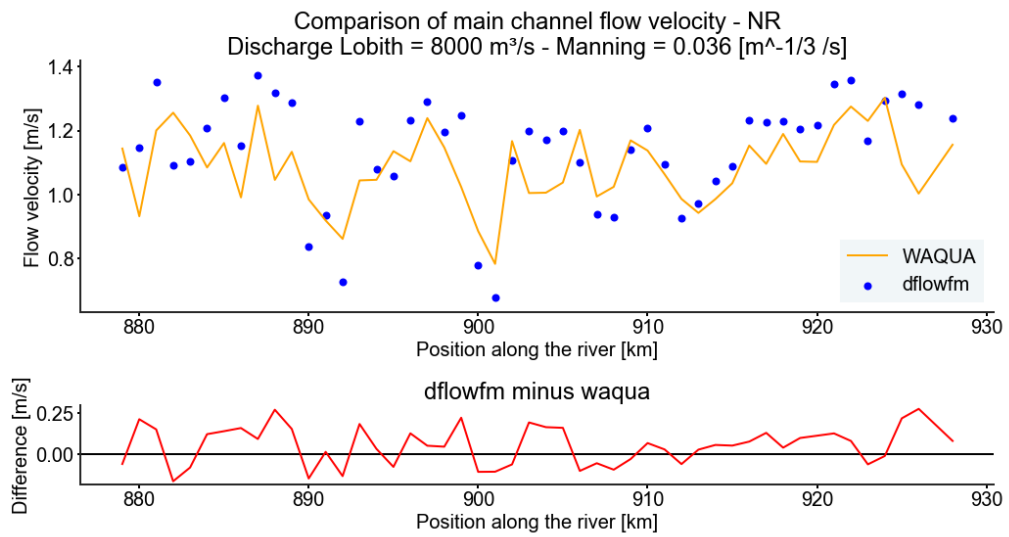
Figure 137 Comparison main channel flow velocity D‑Flow FM 1D - WAQUA - Nederrijn - Q=8000
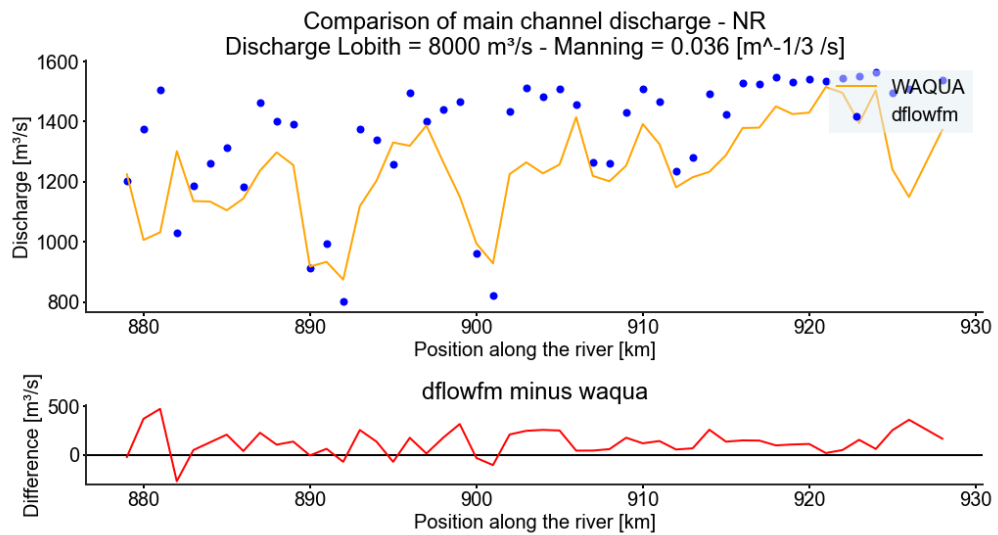
Figure 138 Comparison main channel discharge D‑Flow FM 1D - WAQUA - Nederrijn - Q=8000
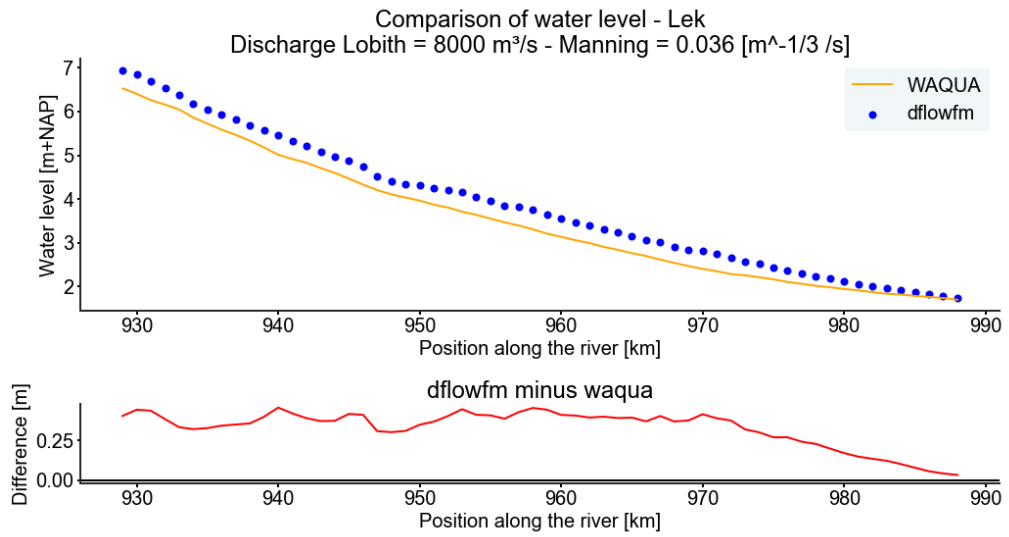
Figure 139 Comparison water level D-Flow FM 1D - WAQUA - Lek - Q=8000
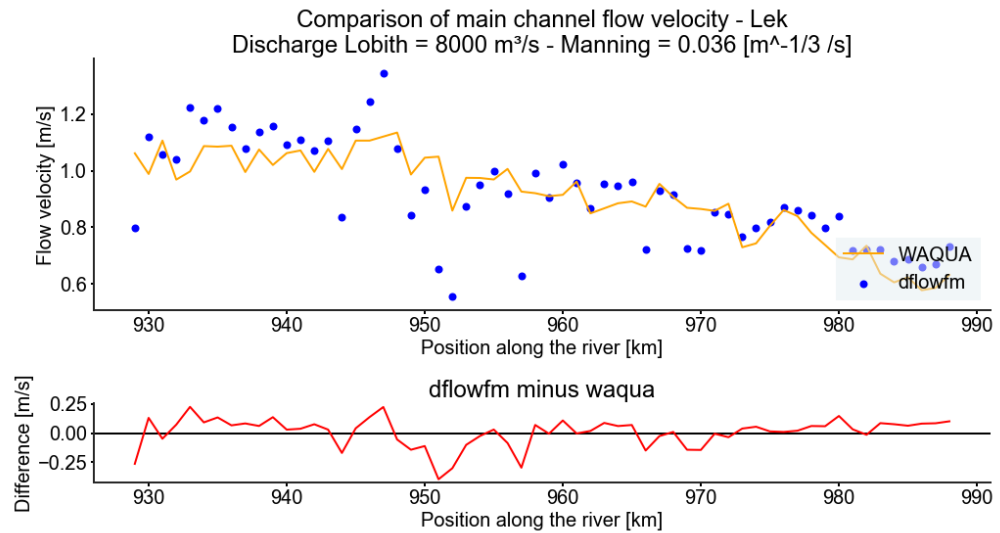
Figure 140 Comparison main channel flow velocity D-Flow FM 1D - WAQUA - Lek - Q=8000

Deltares
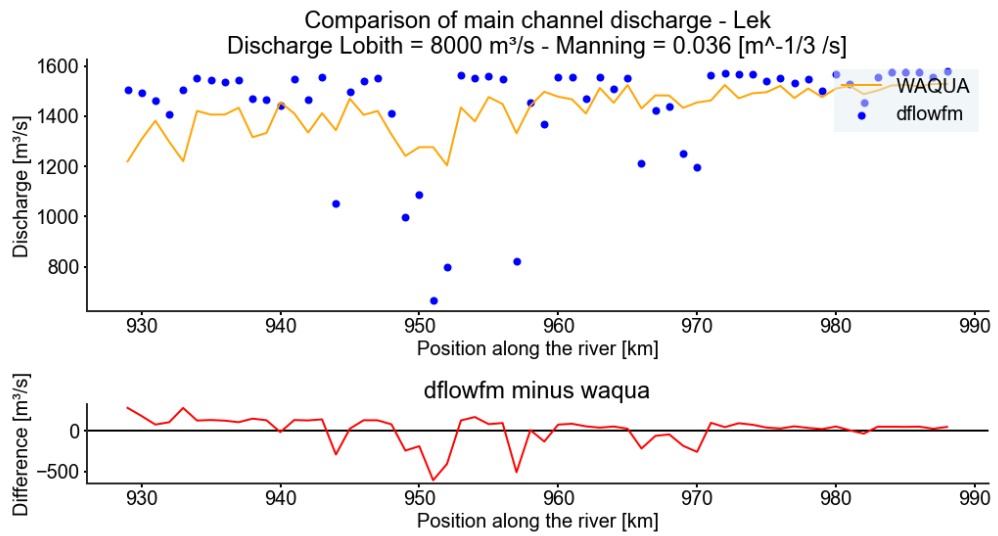
Figure 141 Comparison main channel discharge D-Flow FM 1D - WAQUA - Lek - Q=8000
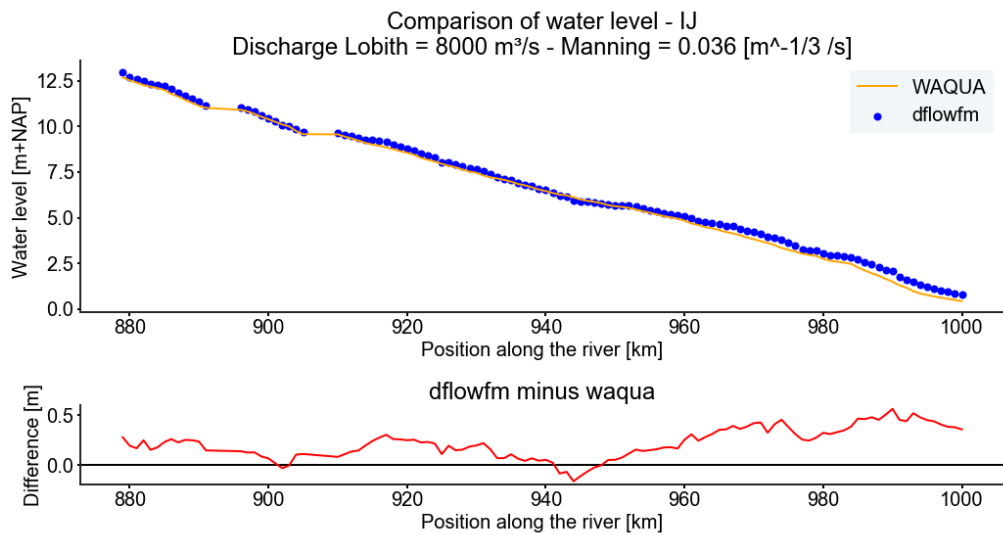
Figure 142 Comparison water level D-Flow FM 1D - WAQUA - IJssel - Q=8000

Deltares
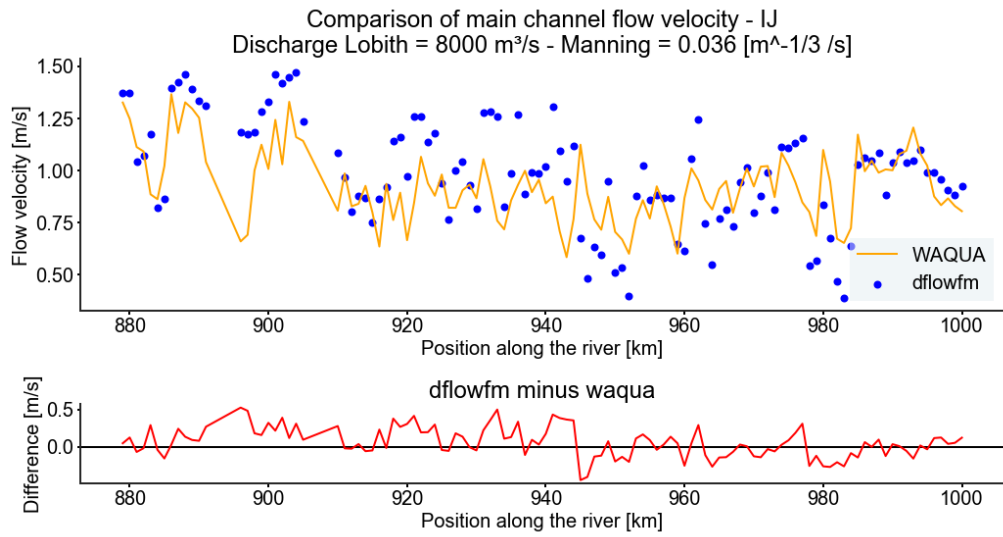
Figure 143 Comparison main channel flow velocity D-Flow FM 1D - WAQUA - IJssel - Q=8000
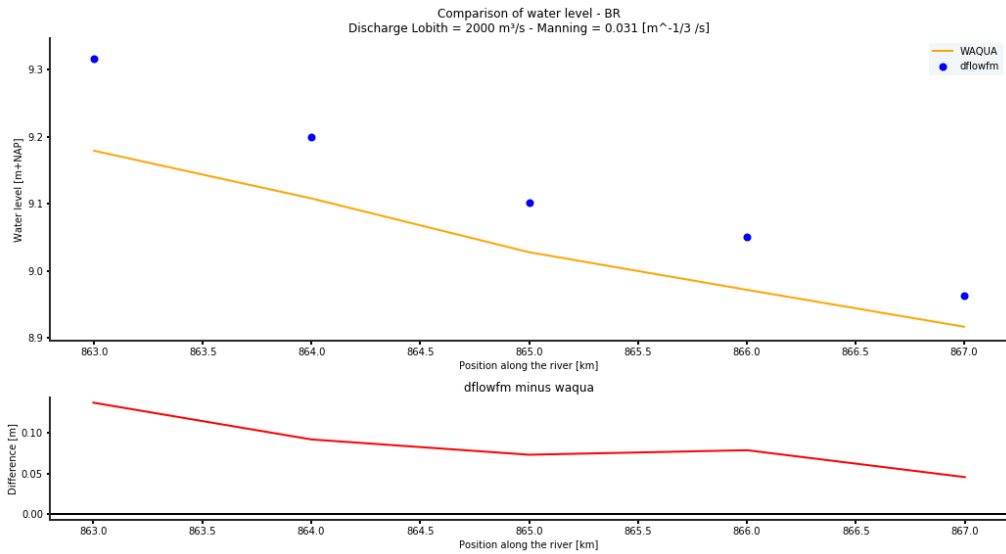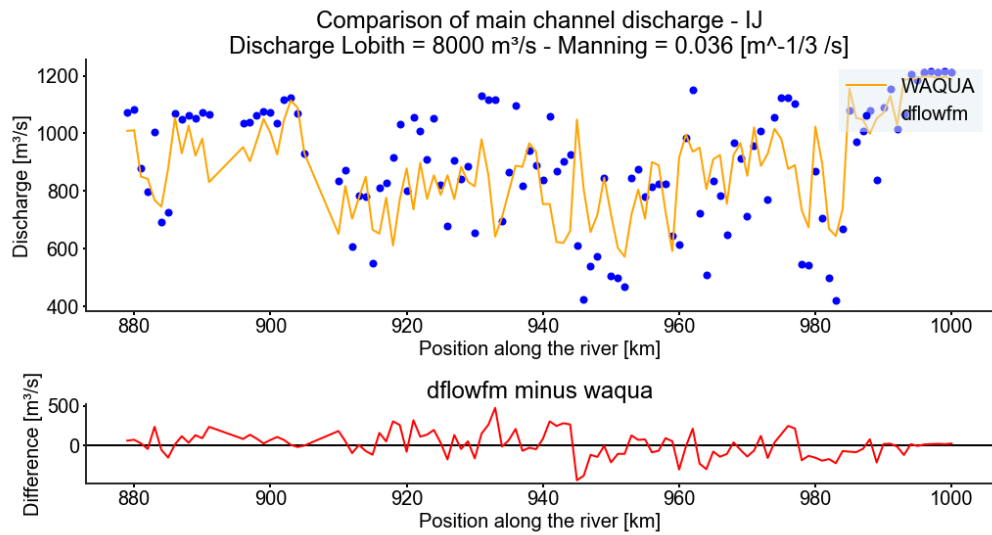
Figure 144 Comparison main channel discharge D-Flow FM 1D - WAQUA - IJssel - Q=8000

Deltares

I Comparison between WAQUA and D-FLOW FM 1D for a discharge equal to 1020 m³/s

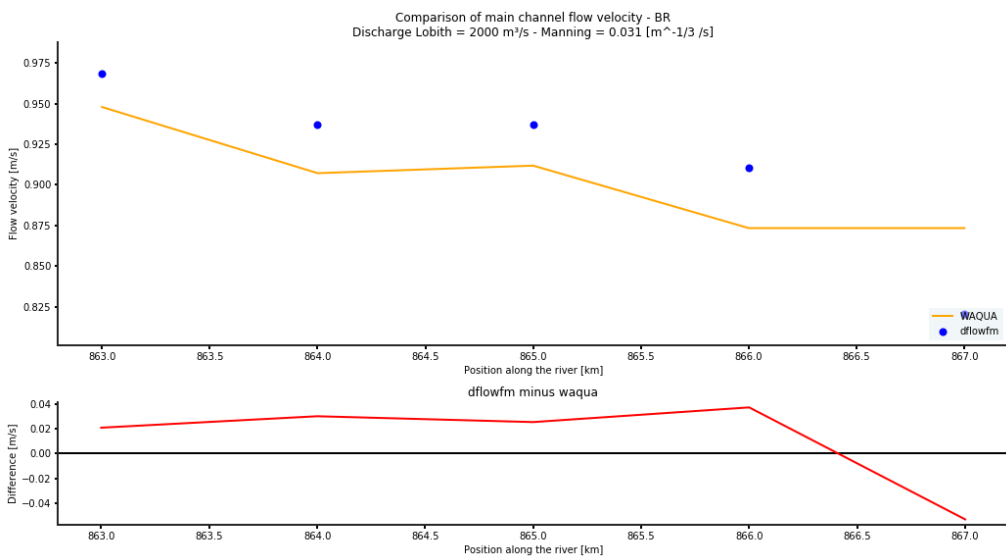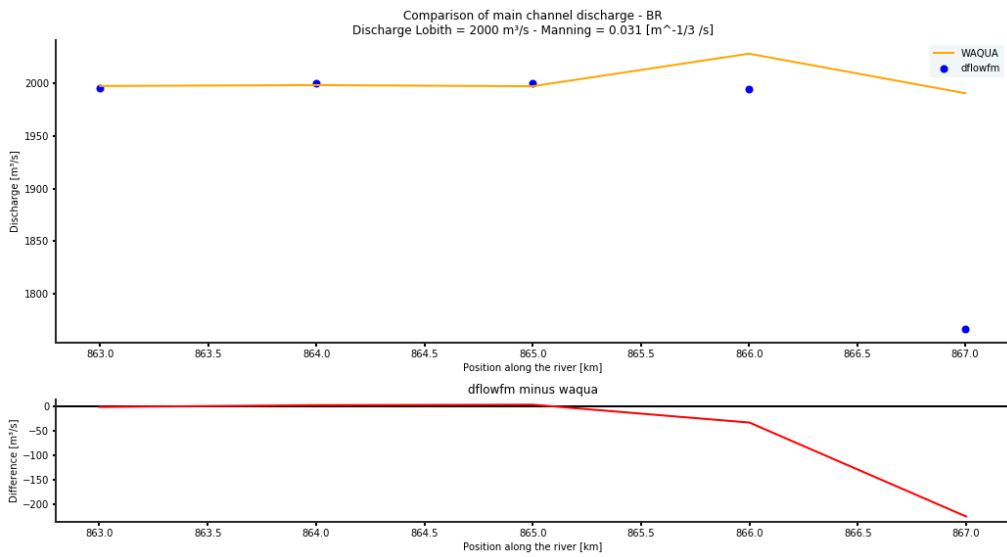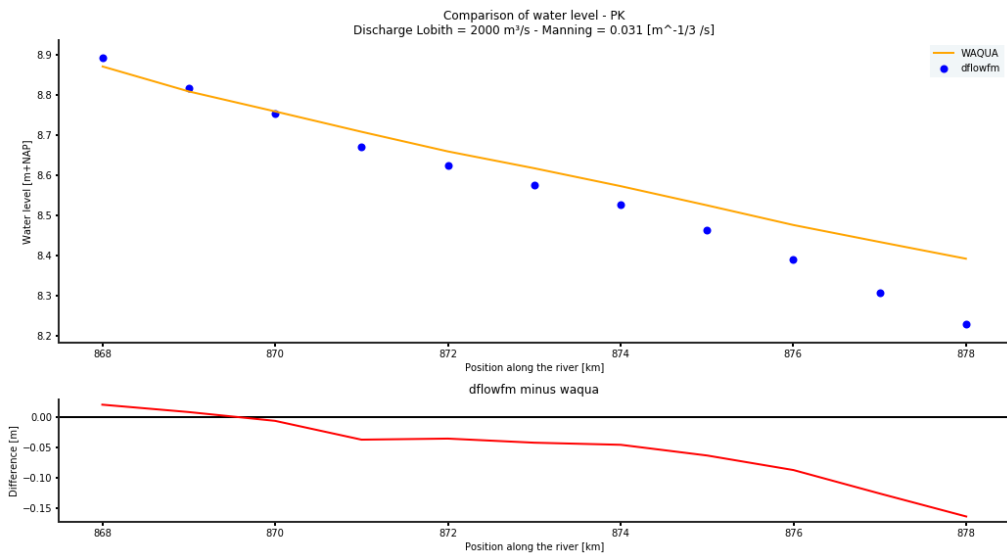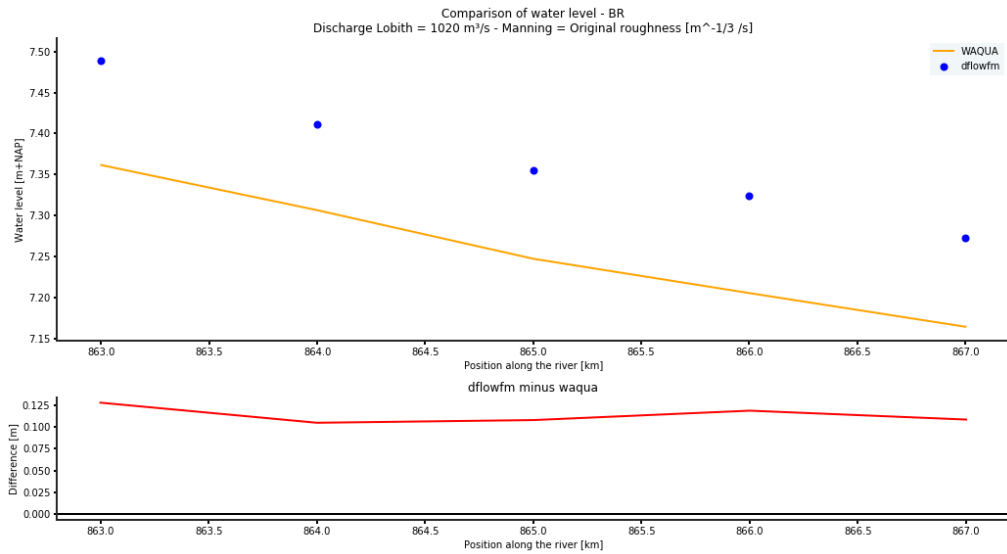**Figure 145** Comparison water level D-FLOW FM 1D - WAQUA - Boven-Rijn - Q=1020
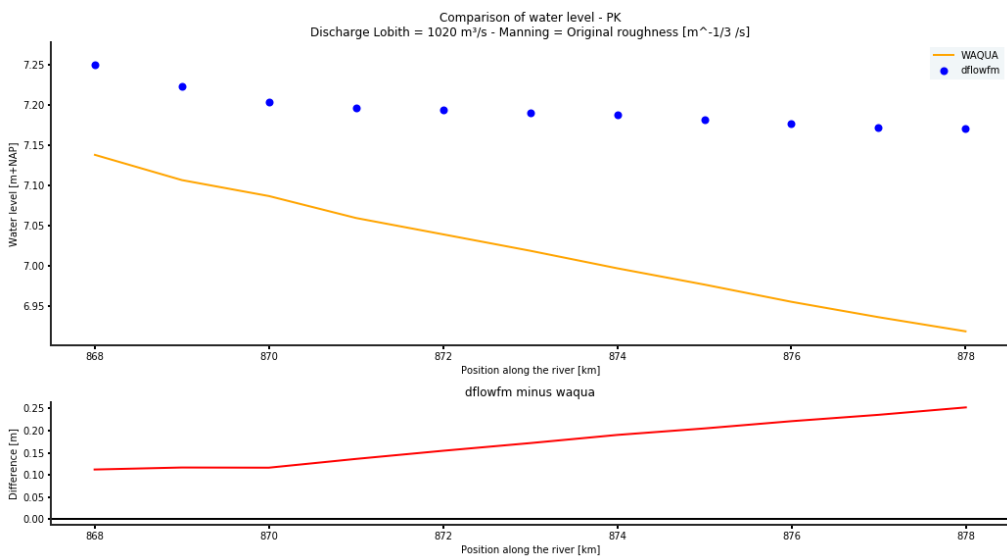
Figure 146 Comparison water level D-FLOW FM 1D - WAQUA - Pannerdensch Kanaal - Q=1020
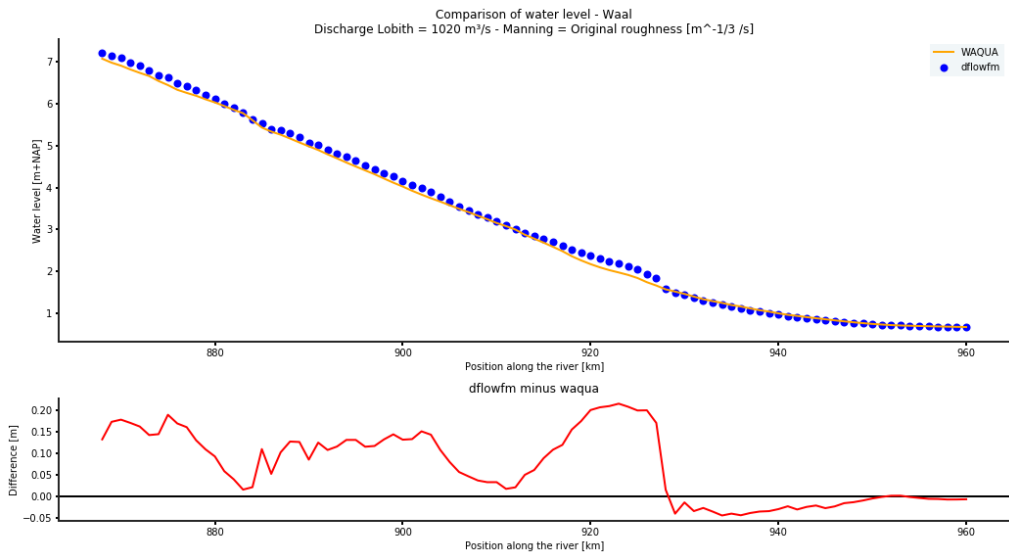
Figure 147 Comparison water level D-Flow FM 1D - WAQUA - Waal - Q=1020
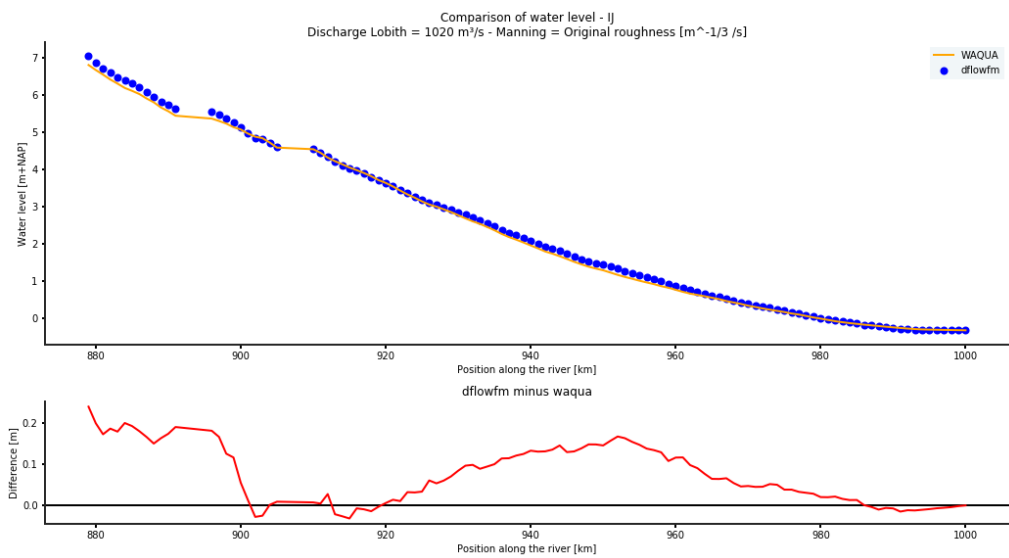
Figure 148 Comparison water level D-Flow FM 1D - WAQUA - IJssel - Q=1020
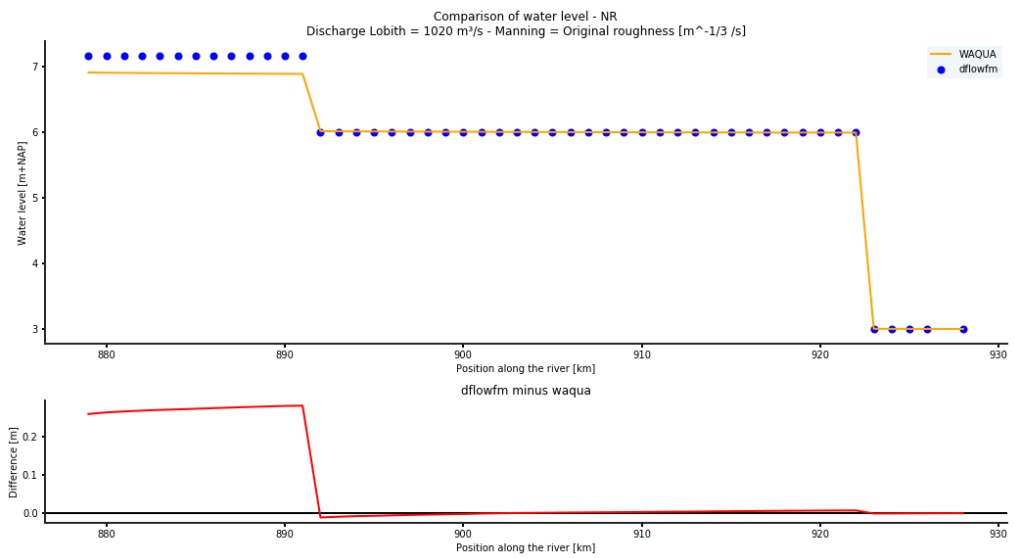
Figure 149 Comparison water level D-Flow FM 1D - WAQUA - Nederrijn - Q=1020
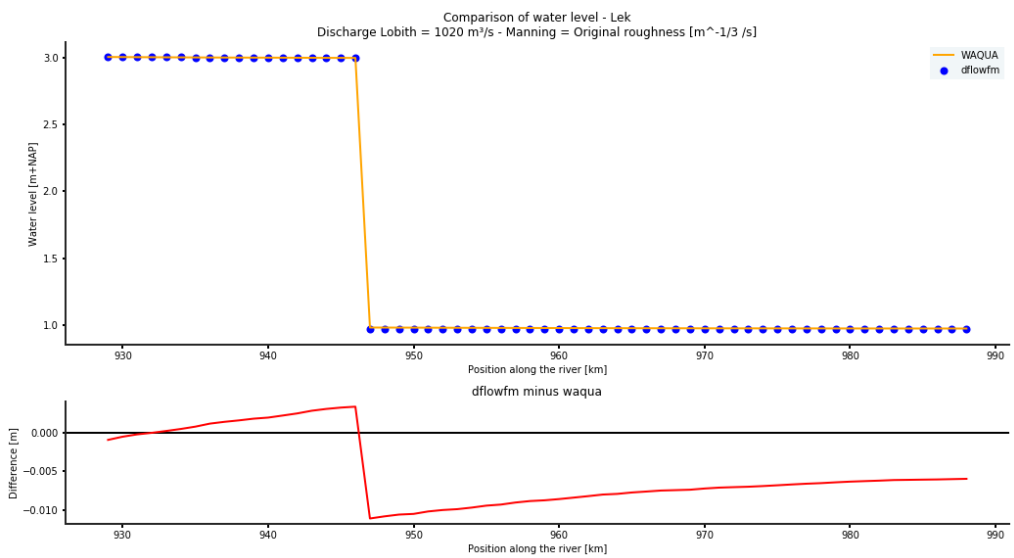
Figure 150 Comparison water level D-Flow FM 1D - WAQUA - Lek - Q=1020

Morphological models for IRM
11203684-015-ZWS-0011_v1.0, Version 0.1, 2020-12-11, Final

Deltares

J Annual sediment transport rate for different sediment transport relations

In this section the figures showing the annual sediment transport rate computed by neglecting morphodynamic changes for different sediment transport relations are presented.

Deltares
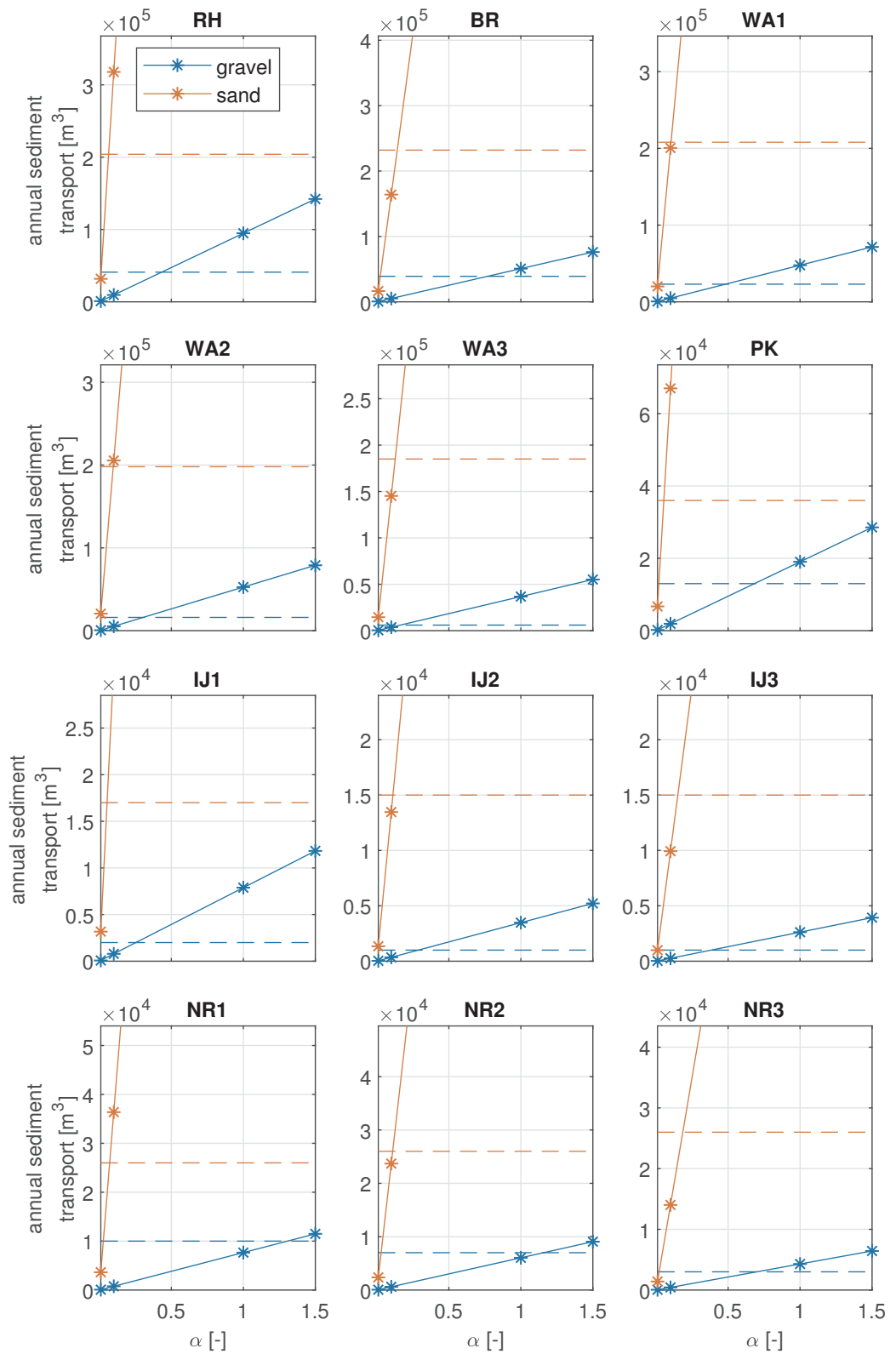
Figure 151 Mean annual gravel and sand sediment transport predicted using Engelund and Hansen (1967) sediment transport relation for a varying calibration coefficient. The dashed line represents the measured transport. Each panel corresponds to a river section (see text for a description).
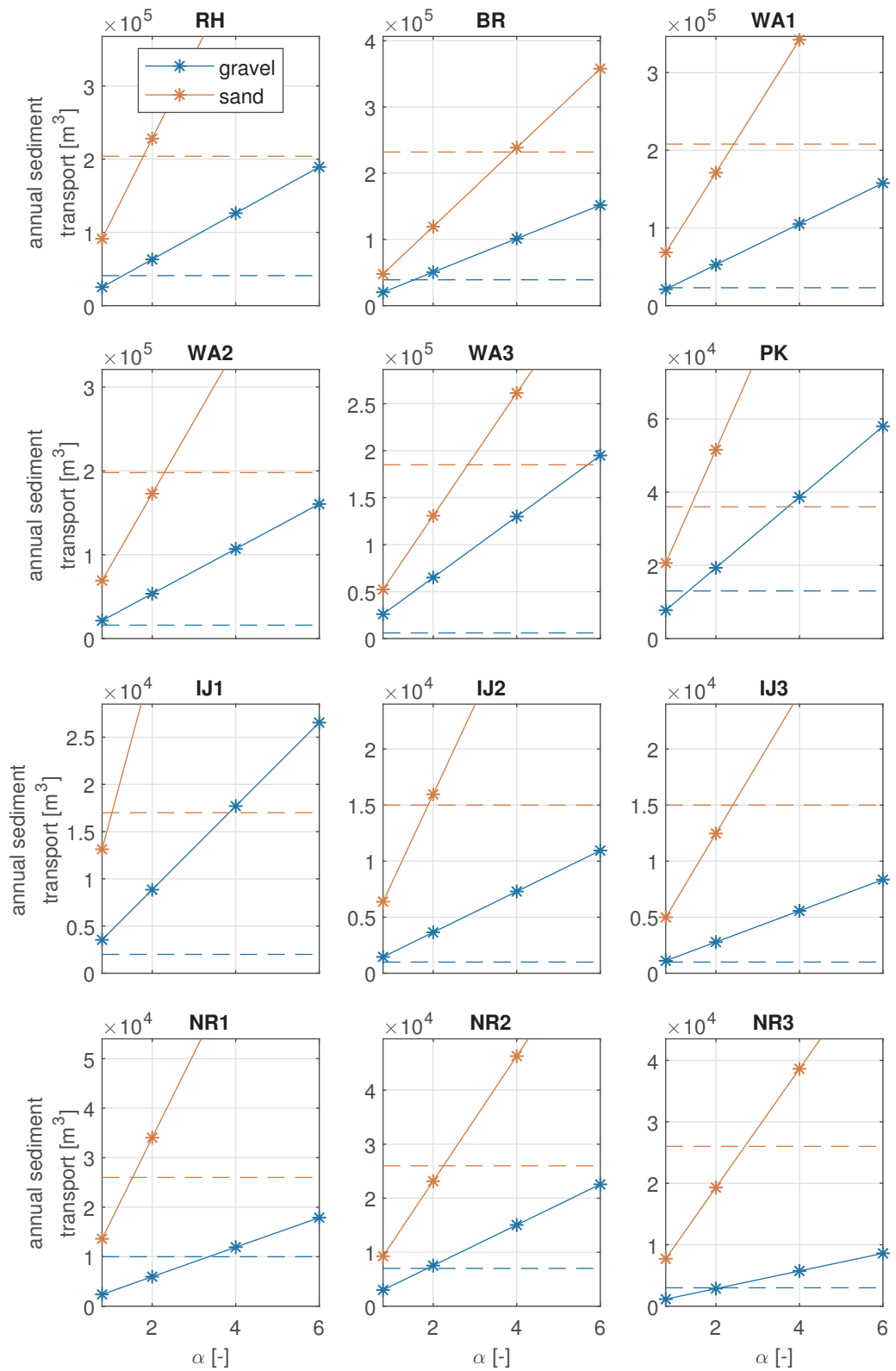
Figure 152 Mean annual gravel and sand sediment transport predicted using Meyer-Peter and Müller (1948) sediment transport relation for a varying factor. The dashed line represents the measured transport. Each panel corresponds to a river section (see text for a description).

Morphological models for IRM
11203684-015-ZWS-0011_v1.0, Version 0.1, 2020-12-11, Final

Deltares
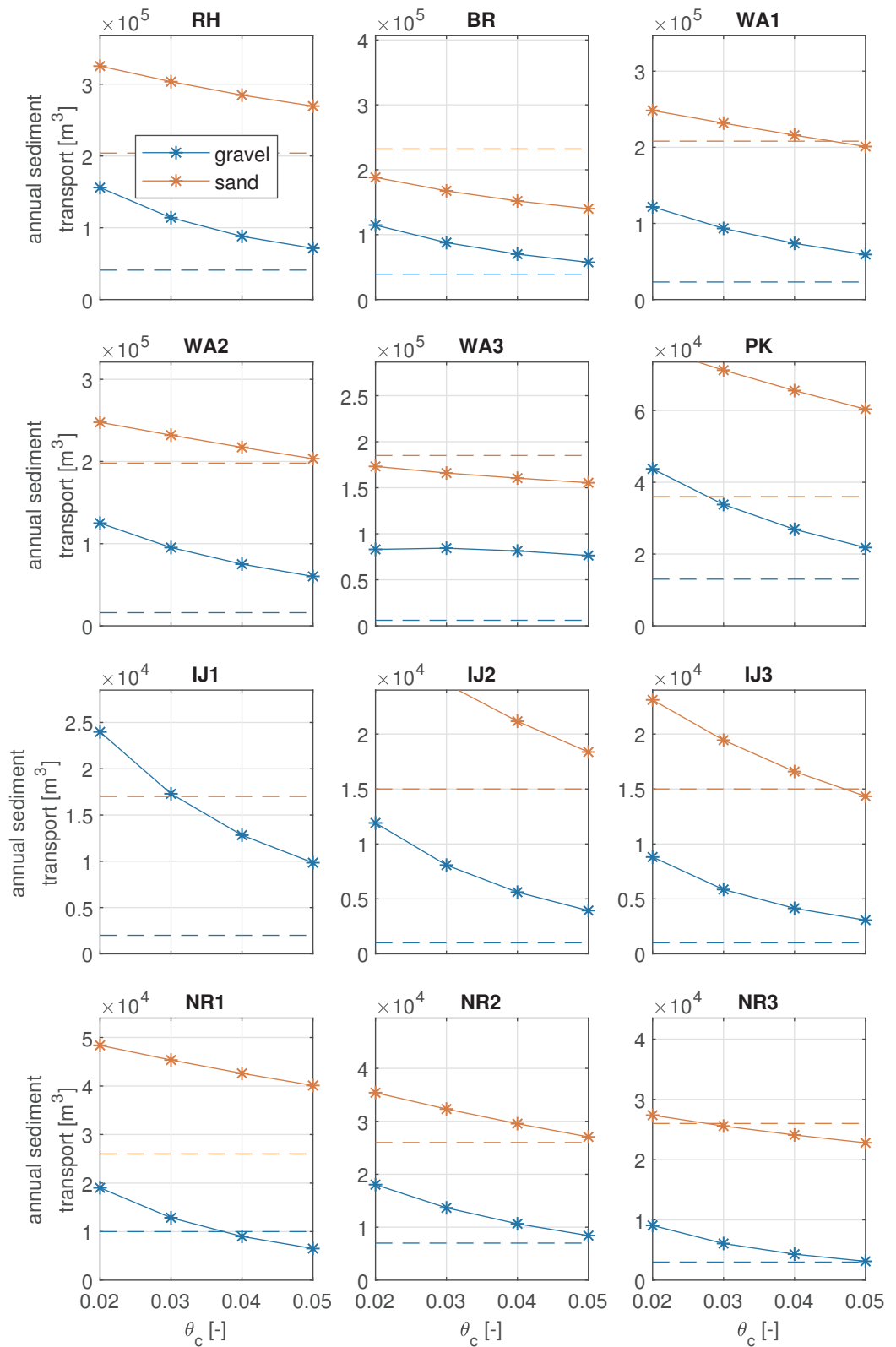
Figure 153 Mean annual gravel and sand sediment transport predicted using Meyer-Peter and Müller (1948) sediment transport relation for a varying critical bed shear stress. The dashed line represents the measured transport. Each panel corresponds to a river section (see text for a description).

Deltares
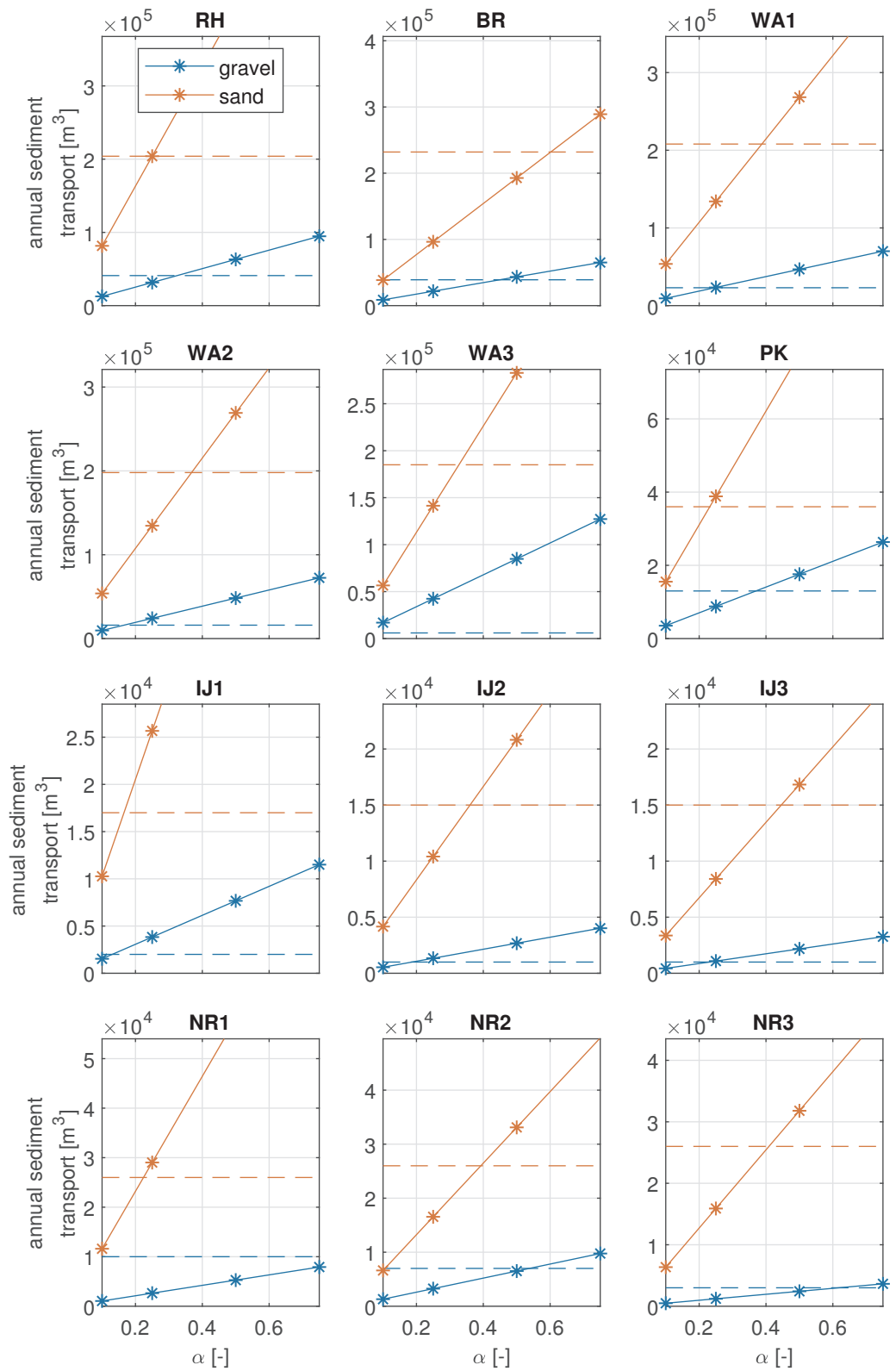
Figure 154 Mean annual gravel and sand sediment transport predicted using Wilcock and Crowe (2003) sediment transport relation for a varying calibration coefficient. The dashed line represents the measured transport. Each panel corresponds to a river section (see text for a description).

Deltares
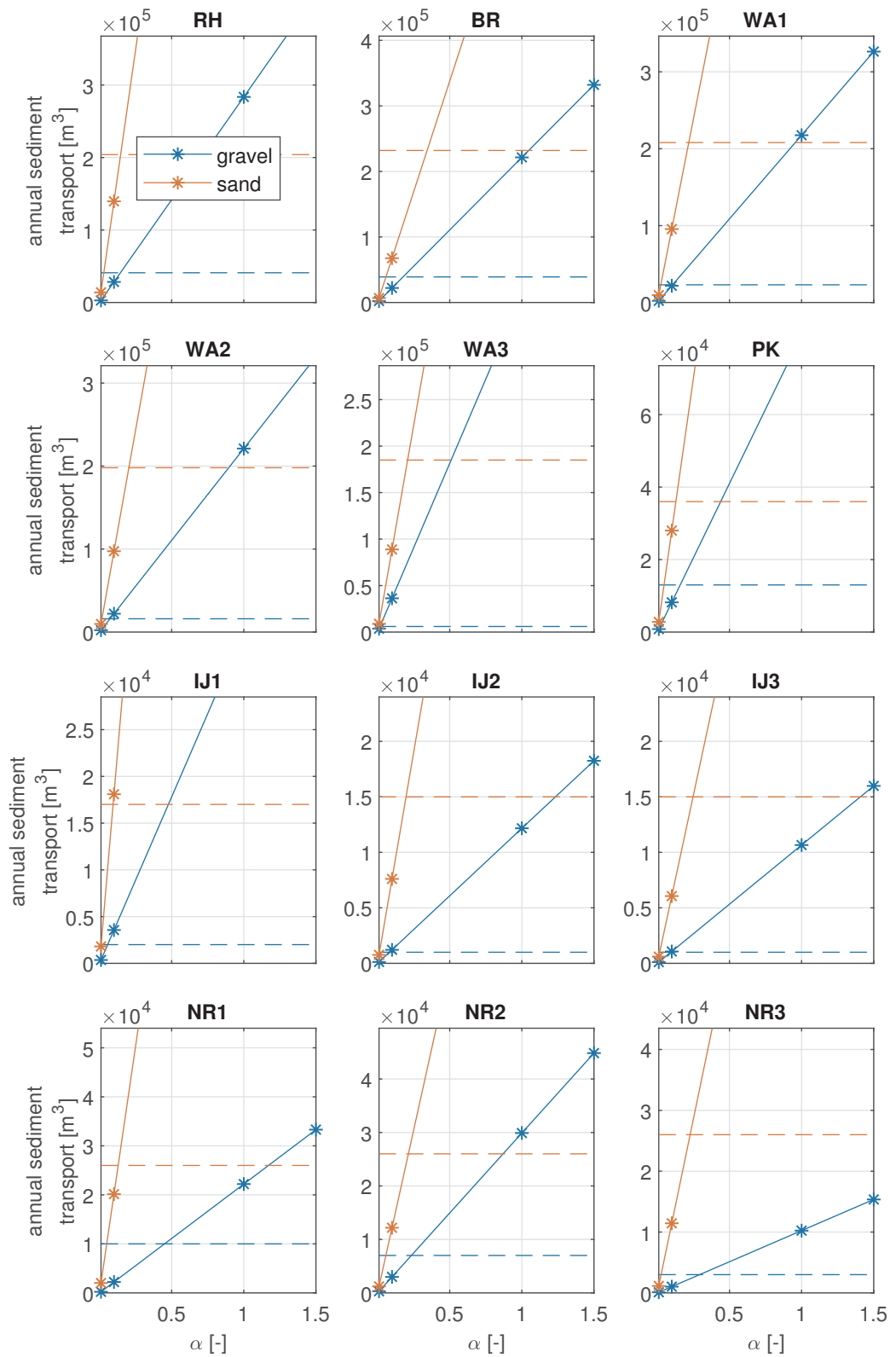
Figure 155 Mean annual gravel and sand sediment transport predicted using Ashida and Michiue (1972) sediment transport relation for a varying calibration coefficient. The dashed line represents the measured transport. Each panel corresponds to a river section (see text for a description).

Deltares

K   Details of the calibration run

```
[General]
Program                             = D-Flow FM          # Program
Version                             = 1.2.102.66429M     # Version number of computational kernel
fileType                            = modelDef           # File type. Do not edit this.
fileVersion                         = 1.09               # File format version (do not edit this)
AutoStart                           = 0                  # Autostart simulation after loading MDU
(0: no, 1: autostart, 2: autostartstop)
ModelSpecific
=                                                        # Optional 'model specific ID', to
enable certain custom runtime function calls (instead of via MDU name).
PathsRelativeToParent               = 0                  # Default: 0. Whether or not (1/0) to
resolve file names (e.g. inside the *.ext file) relative to their direct parent, instead of to the
toplevel MDU working dir.

[geometry]
NetFile                             = rijn-flow-model_net.nc# Unstructured grid file *_net.nc
GridEnclosureFile                   =                    # Enclosure file to clip outer parts from
the grid *.pol
BedlevelFile                        =                    # Bedlevels points file e.g. *.xyz, only
needed for bedlevtype not equal 3
DryPointsFile                       =                    # Dry points file *.xyz (third column
dummy z values), or dry areas polygon file *.pol (third column 1/-1: inside/outside)
CrossDefFile                        = CrossSectionDefinitions.ini# 1D Cross section definition file
(*.ini)
CrossLocFile                        = CrossSectionLocations.ini# 1D Cross section location file
(*.ini)
StorageNodeFile                     =                    # 1D Storage node/manhole file (*.ini)
frictFile                           =
roughness-Main.ini;roughness-FloodPlain1.ini;roughness-FloodPlain2.ini# 1D Roughness files (*.ini)
StructureFile                       = Structures.ini     # Hydraulic structure file (*.ini)
WaterLevIniFile                     =                    # Initial water levels sample file *.xyz
LandBoundaryFile                    =                    # Land boundaries file *.ldb, used for
visualization
ThinDamFile                         =                    # Polyline file *_thd.pli, containing thin
dams
Cutcelllist                         =                    # File with names of cutcell polygons,
e.g. cutcellpolygons.lst
FixedWeirFile                       =                    # Polyline file *_fxw.pliz, containing
fixed weirs with rows x, y, crest level, left ground level, right ground level
PillarFile                          =                    # Polyline file *_pillar.pliz, containing
four colums with x, y, diameter and Cd coefficient
Gulliesfile                         =                    # Polyline file *_gul.pliz, containing
lowest bed level along talweg x, y, z level
Roofsfile                           =                    # Polyline file *_rof.pliz, containing
roofgutter heights x, y, z level
VertplizFile                        =                    # Vertical layering file *_vlay.pliz with
rows x, y, Z, first Z, nr of layers, second Z, layer type
ProflocFile                         =                    # Channel profile location file
*_proflocation.xyz with rows x, y, z, profile number ref
ProfdefFile                         =                    # Channel profile definition file
*_profdefinition.def with definition for all profile numbers
ProfdefxyzFile                      =                    # Channel profile definition file
_profdefinition.def with definition for all profile numbers
IniFieldFile                        = initialFields.ini  # Initial values and parameter fields file
UseCaching                          = 0                  # Use caching for
geometrical/network-related items (0: no, 1: yes)
Uniformwidth1D                      = 1.                 # Uniform width for channel profiles not
specified by profloc
Uniformheight1D                     = 1.                 # Uniform height for channel profiles not
specified by profloc
Uniformtyp1Dstreetinlets            = -2                 # Uniform type street inlets
Uniformtyp1Droofgutterpipes         = -2                 # Uniform type roof gutter pipes
1D2DLinkFile                        =                    # File *.ini containing custom parameters
for 1D2D links
Dxwuimin2D                          = 0.                 # Smallest fraction dx/wu , set dx >
Dxwuimin2D*wu, Default = 0.1
ManholeFile                         =                    # File *.ini containing manholes
PipeFile                            =                    # File *.pliz containing pipe-based
'culverts'
ShipdefFile                         =                    # File *.shd containing ship definitions
WaterLevIni                         = -999.              # Initial water level at missing s0 values
BedlevUni                           = -5.                # Uniform bed level used at missing z
values if BedlevType > 2
BedlevType                          = 1                  # Bathymetry specification
```

```
                                                     # 1: at cell centers (from BathymetryFile)
                                                     # 2: at faces (from BathymetryFile)
                                                     # 3: at nodes, face levels mean of node
                                                     values
                                                     # 4: at nodes, face levels min. of node
                                                     values
                                                     # 5: at nodes, face levels max. of node
                                                     values
                                                     # 6: at nodes, face levels max. of
                                                     cell-center values
Blmeanbelow                      = -999.            # If not -999d0, below this level the cell
center bed level is the mean of surrouding net nodes
Blminabove                       = -999.            # If not -999d0, above this level the cell
center bed level is the min. of surrouding net nodes
Groundlayerthickness             = -999.            # Only in pipes: groundlayer thickness (m)
PartitionFile                    =                  # Domain partition polygon file *_part.pol
for parallel run
AngLat                           = 0.               # Angle of latitude S-N (deg), 0: no
Coriolis
AngLon                           = 0.               # Angle of longitude E-W (deg), 0:
Greenwich, used in solar heat flux computation.
Conveyance2D                     = -1               # -1: R=HU,0: R=H, 1: R=A/P, 2:
K=analytic-1D conv, 3: K=analytic-2D conv
Nonlin1D                         = 1                # Non-linear 1D volumes, 1 = Preisman
slot, 2 = pipes closed (Nested Newton)
Slotw2D                          = 0.               # -
Sillheightmin                    = 0.5              # Weir treatment only if both sills larger
than this value (m)
Makeorthocenters                 = 0                # Switch from circumcentres to
orthocentres in geominit (i>=1: number of iterations, 0: do not use)
Dcenterinside                    = 1.               # Limit cell center (1.0: in cell, 0.0: on
c/g)
Bamin                            = 1.d-6            # Minimum grid cell area, in combination
with cut cells
OpenBoundaryTolerance            = 3.               # Search tolerance factor between boundary
polyline and grid cells, in cell size units
AllowBndAtBifurcation            = 0                # Allow 1d boundary node when connecting
branch leads to bifurcation (1: yes, 0: no)
CreateLinks1D2D                  = 0                # Ruecksichtslos create links between 1D
nodes and 2D cells when initializing model (1: yes, 0: no)
RenumberFlowNodes                = 1                # Renumber the flow nodes (1: yes, 0: no)
dxDoubleAt1DEndNodes             = 1                # Extend 1D end nodes by 0.5 dx (1: yes,
0: no).
Kmx                              = 0                # Maximum number of vertical layers
Layertype                        = 1                # Vertical layer type (1: all sigma, 2:
all z, 3: use VertplizFile)
Numtopsig                        = 0                # Number of sigma layers in top of z-layer
model
SigmaGrowthFactor                = 1.               # Layer thickness growth factor from bed up
StretchType                      = -1               # Type of layer stretching, 0 = uniform, 1
= user defined, 2 = fixed level double exponential

[numerics]
CFLMax                           = 0.7              # Maximum Courant number
Lincontin                        = 0                # Default 0; Set to 1 for linearizing
d(Hu)/dx; link to AdvecType
AdvecType                        = 33               # Advection type (0: none, 1: Wenneker, 2:
Wenneker q(uio-u), 3: Perot q(uio-u), 4: Perot q(ui-u), 5: Perot q(ui-u) without itself)
TimeStepType                     = 2                # Time step handling (0: only transport,
1: transport + velocity update, 2: full implicit step-reduce, 3: step-Jacobi, 4: explicit)
maxNonlinearIterations           = 100              # Maximal iterations in non-linear
iteration loop before a time step reduction is applied
setHorizontalBobsFor1d2d         = 0                # bobs are set to 2D bedlevel, to prevent
incorrect storage in sewer system (0: no, 1:yes).
Icoriolistype                    = 5                # 0=No, 5=default, 3,4 no weights, 5-10
Kleptsova hu/hs, 25-30 Ham hs/hu, odd: 2D hs/hu, even: hsk/huk
Newcorio                         = 0                # 0=prior to 27-11-2019, 1=no normal
forcing on open bnds, plus 12 variants )
Limtyphu                         = 0                # Limiter type for waterdepth in
continuity eqn. (0: none, 1: minmod, 2: van Leer, 3: Kooren, 4: monotone central)
Limtypmom                        = 4                # Limiter type for cell center advection
velocity (0: none, 1: minmod, 2: van Leer, 3: Kooren, 4: monotone central)
Limtypsa                         = 4                # Limiter type for salinity transport (0:
none, 1: minmod, 2: van Leer, 3: Kooren, 4: monotone central)
```

```
TransportMethod                       = 1                    # Transport method (0: Herman's method, 1:
transport module)
TransportTimestepping                 = 1                    # Timestepping method in Transport module,
0 = global, 1 = local (default)
TransportAutoTimestepdiff             =
Vertadvtypsal                         = 6                    # Vertical advection type for salinity (0:
none, 1: upwind explicit, 2: central explicit, 3: upwind implicit, 4: central implicit, 5: central
implicit but upwind for neg. stratif., 6: higher order explicit, no Forester)
Vertadvtyptem                         = 6                    # Vertical advection type for temperature
(0: none, 1: upwind explicit, 2: central explicit, 3: upwind implicit, 4: central implicit, 5: central
implicit but upwind for neg. stratif., 6: higher order explicit, no Forester)
Vertadvtypmom                         = 6                    # Vertical advection type for u1: 0: No,
3: Upwind implicit, 4: Central implicit, 5: QUICKEST implicit., 6: centerbased upwind expl
Vertadvtypmom3onbnd                   = 0                    # vert. adv. u1 bnd UpwimpL: 0=follow
javau , 1 = on bnd, 2= on and near bnd
Cffacver     (0d0: no, 1d0: yes)      = 0.                   # Factor for including (1-CFL) in HO term
vertical
Jarhoxu                               = 0                    # Inlcude density gradient in advection
term (0: no, 1: yes, 2: Also in barotrop and baroclin pressure term)
Horadvtypzlayer                       = 0                    # Horizontal advection treatment of
z-layers (1: default, 2: sigma-like)
Zlayercenterbedvel                    = 1                    # reconstruction of center velocity at
half closed bedcells (0=no, 1: copy bed link velocities)
Zlayeratubybob                        = 0                    # Lowest connected cells governed by bob
instead of by bL L/R
Icgsolver                             = 4                    # Solver type (1: sobekGS_OMP, 2:
sobekGS_OMPthreadsafe, 3: sobekGS, 4: sobekGS + Saadilud, 5: parallel/global Saad, 6: parallel/Petsc, 7:
parallel/GS)
Maxdegree                             = 6                    # Maximum degree in Gauss elimination
Noderivedtypes                        = 5                    # 0=use der. types. , 1 = less, 2 =
lesser, 5 = also dealloc der. types
jposhchk                              = 2                    # Check for positive waterdepth (0: no, 1:
0.7*dts, just redo, 2: 1.0*dts, close all links, 3: 0.7*dts, close all links, 4: 1.0*dts, reduce au, 5:
0.7*dts, reduce au)
FixedWeirScheme                       = 0                    # Fixed weir scheme (0: none, 1: compact
stencil, 2: whole tile lifted, full subgrid weir + factor)
FixedWeirContraction                  = 1.                   # Fixed weir flow width contraction factor
Fixedweirfrictscheme                  = 0                    # Fixed weir friction scheme (0: friction
based on hu, 1: friction based on subgrid weir friction scheme)
Fixedweirtopwidth                     = 3.                   # Uniform width of the groyne part of
fixed weirs
Fixedweirtopfrictcoef                 = -999.                # Uniform friction coefficient of the
groyne part of fixed weirs
Fixedweirtalud                        = 4.                   # Uniform talud slope of fixed weirs
Izbndpos                              = 0                    # Position of z boundary (0: D3Dflow, 1:
on net boundary, 2: on specified polyline)
Tlfsmo                                = 0.                   # Fourier smoothing time (s) on water
level boundaries
Logprofatubndin                       = 1                    # ubnds inflow: 0=uniform U1, 1 = log U1,
2 = user3D
Logprofkepsbndin                      = 0                    # inflow: 0=0 keps, 1 = log keps inflow, 2
= log keps in and outflow
Slopedrop2D                           = 0.                   # Apply drop losses only if local bed
slope > Slopedrop2D, (<=0: no drop losses)
Drop1D                                = 0                    # Apply drop losses in 1D (0: no, 1:yes)
Drop3D                                = 1.                   # Apply droplosses in 3D if z upwind below
bob + 2/3 hu*drop3D
Chkadvd                               = 0.1                  # Check advection terms if depth <
chkadvdp, => less setbacks
Trsh_u1Lb                             = 0.                   # 2D bedfriction in 3D below this
threshold (m)
Epshstem                              = 1.d-3                # Only compute heatflx + evap if depth >
epshstem
Zwsbtol                               = 0.                   # tolerance for zws(kb-1) at bed
Keepzlayeringatbed                    = 1                    #  bedlayerthickness = zlayerthickness at
bed 0 or 1
Teta0                                 = 0.55                 # Theta of time integration (0.5 < theta <
1)
Qhrelax                               = 1.d-2                # Relaxation on Q-h open boundaries
Jbasqbnddownwindhs                    = 0                    # Water depth scheme at discharge
boundaries (0: original hu, 1: downwind hs)
cstbnd                                = 0                    # Delft-3D type velocity treatment near
boundaries for small coastal models (1: yes, 0: no)
Maxitverticalforestersal              = 0                    # Forester iterations for salinity (0: no
```

```
vertical filter for salinity, > 0: max nr of iterations)
Maxitverticalforestertem                = 0                          # Forester iterations for temperature (0:
no vertical filter for temperature, > 0: max nr of iterations)
Turbulencemodel                         = 3                          # Turbulence model (0: none, 1: constant,
2: algebraic, 3: k-epsilon, 4: k-tau)
Turbulenceadvection                     = 3                          # Turbulence advection (0: none, 3:
horizontally explicit and vertically implicit)
Eddyviscositybedfacmax                  = 0.                         # Limit eddy viscosity at bed )
AntiCreep                               = 0                          # Include anti-creep calculation (0: no,
1: yes)
Maxwaterleveldiff                       = 0.                         # upper bound (in m) on water level
changes (<= 0: no bounds). Run will abort when violated.
Maxvelocitydiff                         = 0.                         # upper bound (in m/s) on velocity changes
(<= 0: no bounds). Run will abort when violated.
Maxvelocity                             = 0.                         # upper bound (in m/s) on velocity (<= 0:
no bounds). Run will abort when violated.
Waterlevelwarn                          = 0.                         # warning level (in m) on water level (<=
0: no check).
Velocitywarn                            = 0.                         # warning level (in m/s) on velocity u1
(<= 0: no check).
Velmagnwarn                             = 0.                         # warning level (in m/s) on velocity
magnitude (<= 0: no check).
MinTimestepBreak                        = 0.                         # smallest allowed timestep (in s),
checked on a sliding average of several timesteps. Run will abort when violated.
Epshu                                   = 1.d-4                      # Threshold water depth for wet and dry
cells
SobekDFM_umin                           = 0.                         # Minimal velocity treshold for weir
losses in Sobek-DFM coupling.
SobekDFM_umin_method                    = 0                          # Method for minimal velocity treshold for
weir losses in Sobek-DFM coupling.
SobekDFM_Minimal_1d2d_Embankment        = 1.d-2                      # Minimal crest height of 1D2D SOBEK-DFM
embankments.
sobekDFM_relax                          = 0.1                        # Relaxation factor for SOBEK-DFM coupling
algorithm.
jaupwindsrc                             = 1                          # 1st-order upwind advection at
sources/sinks (1) or higher-order (0)
jasfer3D                                = 0                          # corrections for spherical coordinates
HorizontalMomentumFilter                = 0                          # apply horizontal filter (1:explicit,
2,3:implicit) or not (0)
checkerboardmonitor                     = 0                          # compute and output checkerboard monitor
(1) or not (0)
LocSaltLev                              = 1.                         # salinity level for case of lock exchange
LocSaltMin                              = 5.                         # minimum salinity for case of lock exchange
LocSaltMax                              = 10.                        # maximum salinity for case of lock exchange
Numlimdt_baorg                          = 0                          # if previous numlimdt > Numlimdt_baorg
keep original cell area ba in cutcell
Baorgfracmin                            = 0.                         # Cell area =
max(orgcellarea*Baorgfracmin, cutcell area)

[physics]
UnifFrictCoef                           = 50.                        # Uniform friction coefficient (0: no
friction)
UnifFrictType                           = 0                          # Uniform friction type (0: Chezy, 1:
Manning, 2: White-Colebrook, 3: idem, WAQUA style)
UnifFrictCoef1D                         = 50.                        # Uniform friction coefficient in 1D links
(0: no friction)
UnifFrictCoef1D2D                       = 50.                        # Uniform friction coefficient in 1D links
(0: no friction)
UnifFrictCoefLin                        = 0.                         # Uniform linear friction coefficient (0:
no friction)
UnifFrictCoef1DgrLay                    = 5.d-2                      # Uniform ground layer friction
coefficient for ocean models (m/s) (0: no friction)
Umodlin                                 = 1.                         # Linear friction umod, for ifrctyp=4,5,6
Vicouv                                  = 1.                         # Uniform horizontal eddy viscosity (m2/s)
Dicouv                                  = 1.                         # Uniform horizontal eddy diffusivity (m2/s)
Vicoww                                  = 5.d-5                      # Uniform vertical eddy viscosity (m2/s)
Dicoww                                  = 5.d-5                      # Uniform vertical eddy diffusivity (m2/s)
Vicwminb                                = 0.                         # Minimum visc in prod and buoyancy term
(m2/s)
Xlozmidov                               = 0.                         # Ozmidov length scale (m), default=0.0,
no contribution of internal waves to vertical diffusion
Smagorinsky                             = 0.                         # Smagorinsky factor in horizontal
turbulence, e.g. 0.15
Elder                                   = 0.                         # Elder factor in horizontal turbulence
```

```
irov                               = 0                 # 0=free slip, 1 = partial slip using
wall_ks
wall_ks                            = 0.                # Wall roughness type (0: free slip, 1:
partial slip using wall_ks)
Rhomean                            = 1000.             # Average water density (kg/m3)
Idensform                          = 2                 # Density calulation (0: uniform, 1:
Eckart, 2: Unesco, 3: baroclinic case)
Ag                                 = 9.81              # Gravitational acceleration
TidalForcing                       = 0                 # Tidal forcing, if jsferic=1 (0: no, 1:
yes)
SelfAttractionLoading              = 0                 # Self attraction and loading (0=no,
1=yes, 2=only self attraction)
SelfAttractionLoading_correct_wl_with_ini = 0          # correct water level with initial water
level in Self attraction and loading (0=no, 1=yes)
ITcap                              = 0.                # Upper limit on internal tides
dissipation (W/m^2)
Doodsonstart                       = 55.565            # TRIWAQ: 55.565, D3D: 57.555
Doodsonstop                        = 375.575           # TRIWAQ: 375.575, D3D: 275.555
Doodsoneps                         = 3.d-2             # TRIWAQ = 0.0   400 cmps , D3D = 0.03    60
cmps
VillemonteCD1                      = 1.                # Calibration coefficient for Villemonte.
Default = 1.0.
VillemonteCD2                      = 10.               # Calibration coefficient for Villemonte.
Default = 10.0.
Salinity                           = 0                 # Include salinity, (0=no, 1=yes)
InitialSalinity                    = 0.                # Uniform initial salinity concentration
(ppt)
Sal0abovezlev                      = -999.             # Vertical level (m) above which salinity
is set 0
DeltaSalinity                      = -999.             # for testcases
Salimax                            = -999.             # Limit the salinity
Salimin                            = 0.                # Limit the salinity
Backgroundsalinity                 = 30.               # Background salinity for eqn. of state
(psu) if salinity not computed
Backgroundwatertemperature         = 20.               # Background water temperature for eqn. of
state (deg C) if temperature not computed
Temperature                        = 0                 # Include temperature (0: no, 1: only
transport, 3: excess model of D3D, 5: composite (ocean) model)
InitialTemperature                 = 6.                # Uniform initial water temperature (degC)
Secchidepth                        = 1.                # Water clarity parameter (m)
Stanton                            = -1.               # Coefficient for convective heat flux, if
negative, Ccon = abs(Stanton)*Cdwind
Dalton                             = -1.               # Coefficient for evaporative heat flux,
if negative, Ceva = abs(Dalton)*Cdwind
Tempmax                            = -999.             # Limit the temperature
Tempmin                            = 0.                # Limit the temperature
Surftempsmofac                     = 0.                # Hor . Smoothing factor for surface water
in heatflx comp. (0.0-1.0), 0=no
Soiltempthick                      = 0.1               # Use soil temperature buffer if > 0, e.g.
0.2 (m)
Heat_eachstep                      = 1                 # 1=heat each timestep, 0=heat each
usertimestep
SecondaryFlow                      = 0                 # Secondary flow (0: no, 1: yes)
BetaSpiral                         = 0.                # Weight factor of the spiral flow
intensity on flow dispersion stresses
Equili                             = 0                 # Equilibrium spiral flow intensity (0:
no, 1: yes)

[sediment]
Sedimentmodelnr                    = 4                 # Sediment model nr, (0=no, 1=Krone,
2=SvR2007, 3=E-H, 4=MorphologyModule)
SedFile                            = sed.sed           # Sediment characteristics file (*.sed)
MorFile                            = mor.mor           # Morphology settings file (*.mor)
DredgeFile                         =                   # Dredging/dumping settings file (*.dad)
TransportVelocity                  = 1                 # Velocities for sediment transport,
0=Lagr bed+sus, 1=Eul bed + Lagr sus, 2=Eul bed+sus
MorCFL                             = 0                 # Use CFL condition for morphologic
updating 1=true, 0=false (default)
DzbDtMax                           = 0.1               # Maximum bed level change (m) per time
step for the case MorCFL=1 (default=0.1 m)

[veg]
Vegetationmodelnr                  = 0                 # Vegetation model nr, (0=no, 1=Baptist DFM)
Clveg                              = 0.8               # Stem distance factor, default 0.8 ()
```

```
Cdveg                               = 0.7                   # Stem Cd coefficient , default 0.7 ()
Cbveg                               = 0.                    # Stem stiffness coefficient , default 0.7
()
Rhoveg                              = 0.                    # Stem Rho, if > 0, -> bouyant stick
procedure, default 0.0 ()
Stemheightstd                       = 0.                    # Stem height standard deviation fraction,
e.g. 0.1  ()
Densvegminbap                       = 0.                    # Minimum vegetation density in Baptist
formula  (1/m2)

[wind]
ICdtyp                              = 2                     # Wind drag coefficient type (1=Const;
2=Smith&Banke (2 pts); 3=S&B (3 pts); 4=Charnock 1955, 5=Hwang 2005, 6=Wuest 2005, 7=Hersbach 2010 (2 pts)
Cdbreakpoints                       = 6.3d-4 7.23d-3        # Wind drag coefficient break points
Windspeedbreakpoints                = 0. 100.               # Wind speed break points (m/s)
Relativewind                        = 0                     # Wind speed relative to top-layer water
speed, 1=yes, 0 = no)
Windpartialdry                      = 0                     # Reduce windstress on water if link
partially dry, only for bedlevtyp=3, 0 = no, 1 = yes = default
Rhoair                              = 1.2                   # Air density (kg/m3)
PavBnd                              = 0.                    # Average air pressure on open boundaries
(N/m2) (only applied if > 0)
Pavini                              = 0.                    # Average air pressure for initial water
level correction (N/m2) (only applied if > 0)
Stericcorrection                    = 0                     # Steric correction on waterlevel bnds,
for which sal + temp should be prescribed

[grw]
groundwater                         = 0                     # 0=No (horizontal) groundwater flow,
1=With groundwater flow
Infiltrationmodel                   = 0                     # 0=No infiltration,
1=infiltration=interceptionlayer (with grw), 2=infiltration=Infiltrationcapacity, 3=model
unsaturated/saturated (with grw), 4=Horton
Hinterceptionlayer                  = 0.                    # Intercept this amount of rain (m)
UnifInfiltrationCapacity            = 0.                    # Uniform maximum infiltration capacity
(m/s)
Conductivity                        = 0.                    # non dimensionless K conductivity
saturated (m/s), Q = K*A*i (m3/s)
h_aquiferuni                        = 20.                   # bgrw = bl - h_aquiferuni (m), if
negative, bgrw = bgrwuni
h_unsatini                          = 0.200000002980232     # initial level groundwater is bedlevel -
h_unsatini (m), if negative, sgrw = sgrwini

[waves]
Wavemodelnr                         = 0                     # Wave model nr. (0: none, 1: fetch/depth
limited hurdlestive, 2: Young-Verhagen, 3: SWAN, 5: uniform
Wavenikuradse                       = 1.d-2                 # Wave friction Nikuradse ks coefficient
(m), used in Krone-Swart
Rouwav                              = FR84                  # Friction model for wave induced shear
stress: FR84 (default) or: MS90, HT91, GM79, DS88, BK67, CJ85, OY88, VR04
Gammax                              = 1.                    # Maximum wave height/water depth ratio
uorbfac                             = 1                     # Orbital velocities: 0=D3D style; 1=Guza
style
jahissigwav                         = 1                     # 1: sign wave height on his output; 0:
hrms wave height on his output. Default=1.
jamapsigwav                         = 0                     # 1: sign wave height on map output; 0:
hrms wave height on map output. Default=0 (legacy behaviour).
hminlw                              = 0.2                   # Cut-off depth for application of wave
forces in momentum balance

[time]
RefDate                             = 19940101              # Reference date (yyyymmdd)
Tzone                               = 0.                    # Time zone assigned to input time series
DtUser                              = 3600.                 # Time interval (s) for external forcing
update
DtNodal                             = 60.                   # Time interval (s) for updating nodal
factors in astronomical boundary conditions
DtMax                               = 600.                  # Maximal computation timestep (s)
Dtfacmax                            = 1.1                   # Max timestep increase factor ( )
DtInit                              = 1.                    # Initial computation timestep (s)
Timestepanalysis                    = 0                     # 0=no, 1=see file *.steps
Autotimestepvisc                    = 0                     # 0 = no, 1 = yes (Time limitation based
on explicit diffusive term)
AutoTimestepNoStruct                = 0                     # 0 = no, 1 = yes (Exclude structure links
```

```
(and neighbours) from time step limitation)
Tunit                                = S                     # Time unit for start/stop times (D, H, M
or S)
TStart                               = 47174400.            # Start time w.r.t. RefDate (in TUnit)
TStop                                = 536457600.           # Stop  time w.r.t. RefDate (in TUnit)

[restart]
RestartFile                          =                      # Restart netcdf-file, either *_rst.nc or
*_map.nc
RestartDateTime                      = yyyymmddhhmmss        # Restart date and time (yyyymmddhhmmss)
when restarting from *_map.nc

[external forcing]
ExtForceFile                         =                      # Old format for external forcings file
*.ext, link with tim/cmp-format boundary conditions specification
ExtForceFileNew                      = rijn-flow-model.ext # New format for external forcings file
*.ext, link with bc-format boundary conditions specification
Rainfall                             = 0                    # Include rainfall, (0=no, 1=yes)
QExt                                 = 0                    # Include user Qin/out, externally
provided, (0=no, 1=yes)
Evaporation                          = 0                    # Include evaporation in water balance,
(0=no, 1=yes)
WindExt                              = 0                    # Include wind, externally provided,
(0=no, 1=reserved for EC, 2=yes)

[trachytopes]
TrtRou                               =                      # Include alluvial and vegetation
roughness (trachytopes) (Y: yes, N: no)
TrtDef                               =                      # File (*.ttd) including trachytope
definitions
TrtL                                 =                      # File (*.arl) including distribution of
trachytope definitions
DtTrt                                = 3600.                # Trachytope roughness update time
interval (s)
TrtMxR                               = 8                    # Maximum recursion level for combined
trachytope definitions
TrtCll                               =                      # Calibration factor file for roughness
from trachytopes (see also [calibration] block)
TrtMnH                               = 0.1                  # Minimum water depth for roughness
computations
TrtMth                               = 1                    # Area averaging method, (1=Nikuradse k
based, 2=Chezy C based (parallel and serial))

[calibration]
UseCalibration                       = 0                    # Activate calibration factor friction
multiplier (1 = yes, 0 = no)
DefinitionFile                       =                      # File (*.cld) including calibration
definitions
AreaFile                             =                      # File (*.cll) including area distribution
of calibration definitions

[output]
OutputDir                            =                      # Output directory of map-, his-, rst-,
dat- and timings-files, default: DFM_OUTPUT_<modelname>. Set to . for current dir.
FlowGeomFile                         =                      # Flow geometry NetCDF *_flowgeom.nc
ObsFile                              = ObservationPoints.ini# Points file *.xyn with observation
stations with rows x, y, station name
CrsFile                              = ObservationPoints_crs.ini# Polyline file *_crs.pli defining
observation cross sections
FouFile                              =                      # Fourier analysis input file *.fou
FouUpdateStep                        = 0                    # Fourier update step type: 0=every user
time step, 1=every computational timestep.
HisFile                              =                      # HisFile name *_his.nc
MapFile                              =                      # MapFile name *_map.nc
HisInterval                          = 86400. 47174400. 536457600.# History times (s), interval,
starttime, stoptime (s), if starttime, stoptime are left blank, use whole simulation period
XLSInterval                          = 0.                   # Interval (s) XLS history
MapInterval                          = 2629800. 47174400. 536457600.# Map times (s), interval,
starttime, stoptime (s), if starttime, stoptime are left blank, use whole simulation period
RstInterval                          = 0. 47174400. 536457600.# Restart times (s), interval,
starttime, stoptime (s), if starttime, stoptime are left blank, use whole simulation period
MbaInterval                          = 0.                   # Mass balance area output interval (s)
WaqOutputDir                         =                      # Output directory of WAQ communication
files (flowgeom, vol, flo, etc.), default: DFM_DELWAQ_<modelname>. Set to . for current dir.
```

```
WaqInterval                           = 0. 47174400. 536457600.# DELWAQ output times, given as
"interval" "start period" "end period" (s)
WaqHorAggr                            =                          # DELWAQ output horizontal aggregation
file (*.dwq)
WaqVertAggr                           =                          # DELWAQ output vertical aggregation file
(*.vag)
ClassMapInterval                      = -999. 47174400. 536457600.# Class map times (s), interval,
starttime, stoptime (s), if starttime, stoptime are left blank, use whole simulation period
ClassMapFile                          =                          # ClassMapFile name *_clm.nc
WaterlevelClasses                     =                          # Class map's list of class values for
water levels
WaterDepthClasses                     =                          # Class map's list of class values for
water depths
VelocityMagnitudeClasses              =                          # Class map's list of class values for
velocity magnitudes
VelocityDirectionClassesInterval      =                          # Class map's step size of class values
for velocity direction
StatsInterval                         = -60.                     # Screen step output interval in seconds
simulation time, if negative in seconds wall clock time
WriteBalancefile                      = 0                        # Write balance file (1: yes, 0: no)
TimingsInterval                       = 0.                       # Timings statistics output interval
TimeSplitInterval                     = 0 s                      # Time splitting interval, after which a
new output file is started. value+unit, e.g. '1 M', valid units: Y,M,D,h,m,s.
MapFormat                             = 4                        # Map file format, 1: netCDF, 2: Tecplot,
3: netCFD and Tecplot, 4: NetCDF-UGRID
NcFormat                              = 3                        # Format for all NetCDF output files (3:
classic, 4: NetCDF4+HDF5)
NcWriteLatLon                         = 0                        # Write extra lat-lon coordinates for all
projected coordinate variables in each NetCDF file (for CF-compliancy).
Wrihis_balance                        = 1                        # Write mass balance totals to his file
(1: yes, 0: no)
Wrihis_sourcesink                     = 1                        # Write sources-sinks statistics to his
file (1: yes, 0: no)
Wrihis_structure_gen                  = 1                        # Write general structure parameters to
his file (1: yes, 0: no)
Wrihis_structure_dam                  = 1                        # Write dam parameters to his file (1:
yes, 0: no)
Wrihis_structure_pump                 = 1                        # Write pump parameters to his file (1:
yes, 0: no)
Wrihis_structure_gate                 = 1                        # Write gate parameters to his file (1:
yes, 0: no)
Wrihis_structure_weir                 = 1                        # Write weir parameters to his file (1:
yes, 0: no)
Wrihis_structure_orifice              = 1                        # Write orifice parameters to his file (1:
yes, 0: no)
Wrihis_structure_bridge               = 1                        # Write bridge parameters to his file (1:
yes, 0: no)
Wrihis_structure_culvert              = 1                        # Write culvert parameters to his file (1:
yes, 0: no)
Wrihis_structure_damBreak             = 1                        # Write dam break parameters to his file
(1: yes, 0: no)
Wrihis_structure_uniWeir              = 1                        # Write universal weir parameters to his
file (1: yes, 0: no)
Wrihis_structure_compound             = 1                        # Write compound structure parameters to
his file (1: yes, 0: no)
Wrihis_turbulence                     = 1                        # Write k, eps and vicww to his file (1:
yes, 0: no)
Wrihis_wind                           = 1                        # Write wind velocities to his file (1:
yes, 0: no)
Wrihis_rain                           = 1                        # Write precipitation to his file (1: yes,
0: no)
Wrihis_temperature                    = 0                        # Write temperature to his file (1: yes,
0: no)
Wrihis_waves                          = 1                        # Write wave data to his file (1: yes, 0:
no)
Wrihis_heat_fluxes                    = 0                        # Write heat fluxes to his file (1: yes,
0: no)
Wrihis_salinity                       = 0                        # Write salinity to his file (1: yes, 0: no)
Wrihis_density                        = 1                        # Write density to his file (1: yes, 0: no)
Wrihis_waterlevel_s1                  = 1                        # Write water level to his file (1: yes,
0: no)
Wrihis_bedlevel                       = 1                        # Write bed level to his file (1: yes, 0:
no)
Wrihis_waterdepth                     = 0                        # Write waterd epth to his file (1: yes,
```

```
                                                                 0: no)
Wrihis_velocity_vector                    = 1                    # Write velocity vectors to his file (1:
yes, 0: no)
Wrihis_upward_velocity_component          = 0                    # Write upward velocity to his file (1:
yes, 0: no)
Wrihis_sediment                           = 1                    # Write sediment transport to his file (1:
yes, 0: no)
Wrihis_constituents                       = 1                    # Write tracers to his file (1: yes, 0: no)
Wrihis_zcor                               = 1                    # Write vertical coordinates to his file
(1: yes, 0: no)
Wrimap_waterlevel_s0                      = 0                    # Write water levels for previous time
step to map file (1: yes, 0: no)
Wrimap_waterlevel_s1                      = 1                    # Write water levels to map file (1: yes,
0: no)
Wrimap_evaporation                        = 0                    # Write evaporation to map file (1: yes,
0: no)
Wrimap_volume1                            = 0                    # Write volumes to map file (1: yes, 0: no)
Wrimap_waterdepth_hu                      = 0                    # Write water depths on u-points to map
file (1: yes, 0: no)
Wrimap_ancillary_variables                = 0                    # Write ancillary_variables attributes to
map file (1: yes, 0: no)
Wrimap_flowarea_au                        = 0                    # Write flow areas au to map file (1: yes,
0: no)
Wrimap_velocity_component_u0              = 0                    # Write velocity component for previous
time step to map file (1: yes, 0: no)
Wrimap_velocity_component_u1              = 1                    # Write velocity component to map file (1:
yes, 0: no)
Wrimap_velocity_vector                    = 1                    # Write cell-center velocity vectors to
map file (1: yes, 0: no)
Wrimap_velocity_magnitude                 = 1                    # Write cell-center velocity vector
magnitude to map file (1: yes, 0: no)
Wrimap_velocity_vectorq                   = 0                    # Write cell-center velocity vectors
(discharge-based) to map file (1: yes, 0: no)
Wrimap_upward_velocity_component          = 0                    # Write upward velocity component on cell
interfaces (1: yes, 0: no)
Wrimap_density_rho                        = 1                    # Write flow density to map file (1: yes,
0: no)
Wrimap_horizontal_viscosity_viu           = 1                    # Write horizontal viscosity to map file
(1: yes, 0: no)
Wrimap_horizontal_diffusivity_diu         = 1                    # Write horizontal diffusivity to map file
(1: yes, 0: no)
Wrimap_flow_flux_q1                        = 1                    # Write flow flux to map file (1: yes, 0:
no)
Wrimap_flow_flux_q1_main                   = 1                    # Write flow flux in main channel to map
file (1: yes, 0: no)
Wrimap_numlimdt                           = 1                    # Write the number times a cell was
Courant limiting to map file (1: yes, 0: no)
Wrimap_taucurrent                         = 1                    # Write the shear stress to map file (1:
yes, 0: no)
Wrimap_chezy                              = 1                    # Write the chezy roughness to map file
(1: yes, 0: no)
Wrimap_sediment                           = 1                    # Write sediment fractions to map file (1:
yes, 0: no)
Wrimap_turbulence                         = 0                    # Write vicww, k and eps to map file (1:
yes, 0: no)
Wrimap_rain                               = 0                    # Write rainfall rates to map file (1:
yes, 0: no)
Wrimap_wind                               = 0                    # Write wind velocities to map file (1:
yes, 0: no)
Wrimap_windstress                         = 0                    # Write wind stress to map file (1: yes,
0: no)
Writek_CdWind                             = 1                    # Write wind friction coeffs to tek file
(1: yes, 0: no)
Wrimap_DTcell                             = 0                    # Write time step per cell based on CFL
(1: yes, 0: no)
Wrimap_wet_waterdepth_threshold           = 2.d-5                # Waterdepth threshold above which a grid
point counts as 'wet'. Used for Wrimap_time_water_on_ground.
Wrimap_time_water_on_ground               = 0                    # Write cumulative time when water is
above ground level to map file, only for 1D nodes (1: yes, 0: no)
Wrimap_freeboard                          = 0                    # Write freeboard to map file, only for 1D
nodes (1: yes, 0: no)
Wrimap_waterdepth_on_ground               = 0                    # Write waterdepth that is above ground
level to map file, only for 1D nodes (1: yes, 0: no)
Wrimap_volume_on_ground                   = 0                    # Write volume that is above ground level
```

```
                                       to map file, only for 1D nodes (1: yes, 0: no)
Wrimap_total_net_inflow_1d2d           = 0                        # Write current total 1d2d net inflow
(discharge) and cumulative total 1d2d net inflow (volume) to map file, only for 1D nodes (1: yes, 0: no)
Wrimap_total_net_inflow_lateral        = 1                        # Write current total lateral net inflow
(discharge) and cumulative total net lateral inflow (volume) to map file, only for 1D nodes (1: yes, 0: no)
Wrimap_water_level_gradient            = 0                        # Write water level gradient to map file,
only on 1D links (1: yes, 0: no)
Writepart_domain                       = 1                        # Write partition domain info. for
postprocessing
Richardsononoutput                     = 0                        # Write Richardson numbers (1: yes, 0: no)
Wrishp_crs                             = 0                        # Write grid-snapped cross sections to
shapefile (1: yes, 0: no)
Wrishp_obs                             = 0                        # Write grid-snapped observation stations
to shapefile (1: yes, 0: no)
Wrishp_weir                            = 0                        # Write grid-snapped weirs to shapefile
(1: yes, 0: no)
Wrishp_thd                             = 0                        # Write grid-snapped thin dams to
shapefile (1: yes, 0: no)
Wrishp_gate                            = 0                        # Write grid-snapped gates to shapefile
(1: yes, 0: no)
Wrishp_emb                             = 0                        # Write grid-snapped 1d2d embankments to
shapefile (1: yes, 0: no)
Wrishp_fxw                             = 0                        # Write grid-snapped fixed weirs to
shapefile (1: yes, 0: no)
Wrishp_src                             = 0                        # Write grid-snapped source-sinks to
shapefile (1: yes, 0: no)
Wrishp_pump                            = 0                        # Write grid-snapped pumps to shapefile
(1: yes, 0: no)
Wrishp_dryarea                         = 0                        # Write a shape file for dry areas
wrishp_genstruc                        = 0                        # Write a shape file for general structures
WriteDFMinterpretedvalues              = 0                        # Write DFMinterpretedvalues (1: yes, 0: no)
MapOutputTimeVector                    =                         # File (*.mpt) containing fixed map output
times (s) w.r.t. RefDate
FullGridOutput                         = 0                        # Full grid output mode (0: compact, 1:
full time-varying grid data)
EulerVelocities                        = 0                        # Euler velocities output (0: GLM, 1:
Euler velocities)
Wrirst_bnd                             = 1                        # Write waterlevel, bedlevel and
coordinates of boundaries to restart files
Wrimap_bnd                             = 0                        # Write boundary points to map file (1:
yes, 0: no)

[particles]
ParticlesFile                          =
ParticlesReleaseFile                   =
AddTracer                              = 0                        # add tracer (1) or not (other)
StartTime                              = 0.                       # starttime (if >0)
TimeStep                               = 0.                       # time step (>0) or every computational
time step
3Dtype                                 = 0                        # 3D type: depth averaged (0) or free
surface (1)

[processes]
SubstanceFile                          =                         # substance file
AdditionalHistoryOutputFile            =                         # extra history output file
StatisticsFile                         =                         # statistics file
ThetaVertical                          = 0.                       # theta vertical for waq
DtProcesses                            = 0.                       # waq processes time step
DtMassBalance                          = 0.                       # waq mass balance output time step
ProcessFluxIntegration                 = 1                        # Process fluxes integration option (1:
WAQ, 2: D-Flow FM)
VolumeDryThreshold                     = 1.d-3
DepthDryThreshold                      = 1.d-3
** INFO    : **
** INFO    : Modelinit finished   at: 06:48:44, 11-06-2020
** INFO    :
** INFO    :
** INFO    : nr of netnodes         ( )  :                        767
** INFO    : nr of netlinks         ( )  :                        766
** INFO    : nr of flownodes        ( )  :                        772
** INFO    : nr of openbnd cells    ( )  :                          5
** INFO    : nr of 1D-flownodes     ( )  :                        767
** INFO    : nr of flowlinks        ( )  :                        771
** INFO    : nr of internal links   ( )  :                        766
```

```
** INFO    : nr of 1D links           ( )  :                         766
** INFO    : nr of closed walls       ( )  :                           0
** INFO    :
** INFO    :
** INFO    : my model area            (m2) :          0.3859920925E+06
** INFO    : my model volume          (m3) :          0.4255698115E+09
** INFO    :
** INFO    :
** INFO    :
** INFO    :
** INFO    :
** INFO    :
** INFO    : extra timer:Flow geometry                          0.0156250000
** INFO    : extra timer:Sed/mor                                2.0312500000
** INFO    : extra timer:Flow init                             26.9531250000
** INFO    : extra timer:Observations init 2                    0.0156250000
** INFO    : extra timer:initime setbnd                        94.2656250000
** INFO    : extra timer:initime sethuau                     1754.5625000000
** INFO    : extra timer:initime setdt                         10.7500000000
** INFO    : extra timer:initime advec                         90.6250000000
** INFO    : extra timer:initime u0u1                           5.1250000000
** INFO    : extra timer:initime setumod                       74.9531250000
** INFO    : extra timer:initime cfuhi                          5.5312500000
** INFO    : extra timer:initime structactual                   4.4687500000
** INFO    :
** INFO    :
** INFO    :
** INFO    : nr of timesteps          ( )  :        2307601.0000000000
** INFO    : average timestep         (s)  :            212.0311093642
** INFO    : nr of setbacks           ( )  :              0.0000000000
** INFO    :
** INFO    :
** INFO    : simulation period        (d)  :           5663.0000000000
** INFO    : total computation time   (d)  :              0.3412594039
** INFO    : time modelinit           (d)  :              0.3409174262
** INFO    : time steps (+ plots)     (d)  :              0.0003419777
** INFO    :
** INFO    : simulation period        (h)  :         135912.0000000000
** INFO    : total computation time   (h)  :              8.1902256944
** INFO    : time modelinit           (h)  :              8.1820182292
** INFO    : time steps (+ plots)     (h)  :              0.0082074653
** INFO    :
** INFO    : simulation period        (s)  :      489283200.0000000000
** INFO    : total computation time   (s)  :              8.1902256944
** INFO    : time modelinit           (s)  :              8.1820182292
** INFO    : time steps (+ plots)     (s)  :              0.0082074653
** INFO    :
** INFO    :
** INFO    : time iniexternalforc.    (s)  :             22.8906250000
** INFO    :
** INFO    : time inistep             (s)  :           2068.8281250000
** INFO    : time setumod             (s)  :             67.8906250000
** INFO    : time furu                (s)  :             73.4375000000
** INFO    : time solve               (s)  :            158.7500000000
** INFO    : time setexternalforc.    (s)  :             40.5937500000
** INFO    : time setexternalfbnd.    (s)  :             91.2031250000
** INFO    : time steps               (s)  :          28308.6406250000
** INFO    : fraction solve/steps     ( )  :              0.0056078284
** INFO    : total/(dnt*ndx)          (s)  :              0.0000165509
** INFO    : av nr of cont. it s1it   ( )  :              3.0745540175
** INFO    : time transport [s]             :             35.0789999996
** INFO    : time debug     [s]             :              0.0000000000
** INFO    :
** INFO    :
** INFO    :
** INFO    : Computation started  at: 06:48:44, 11-06-2020
** INFO    : Computation finished at: 15:13:01, 11-06-2020
** INFO    :
** INFO    : simulation period        (h)  :         135912.0000000000
** INFO    : total time in timeloop   (h)  :              0.0082074653
** INFO    : MPI    : no.
** INFO    : OpenMP : yes.          #threads max : 1
```

L   Space-time changes of the calibration simulation

change in main channel averaged bed level [m] (wrt initial)
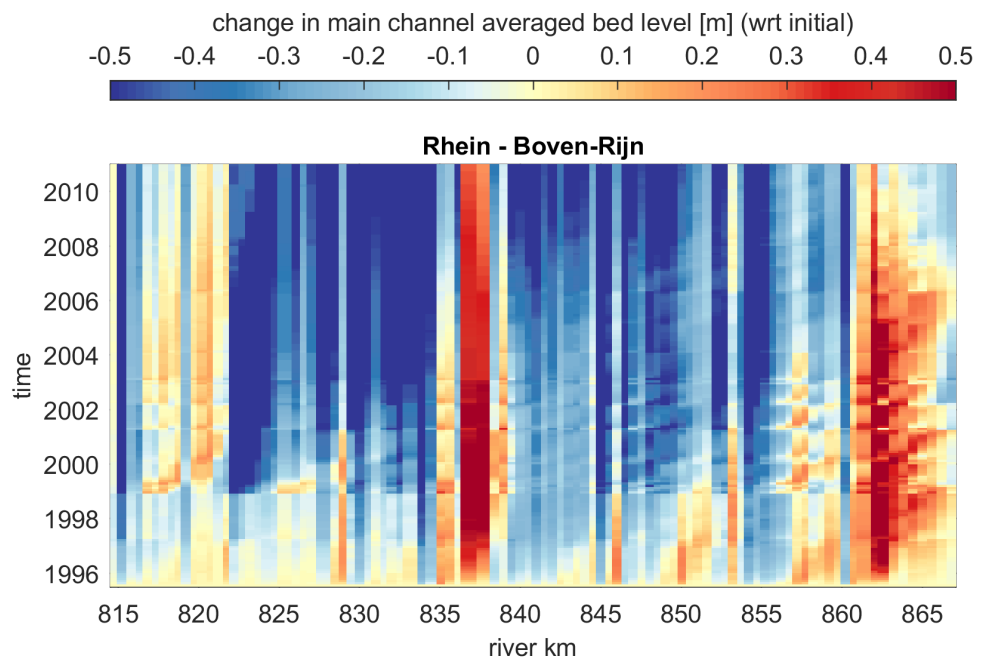
Figure 156 Bed level changes in time with respect to the initial conditions along the Rhein - Boven-Rijn
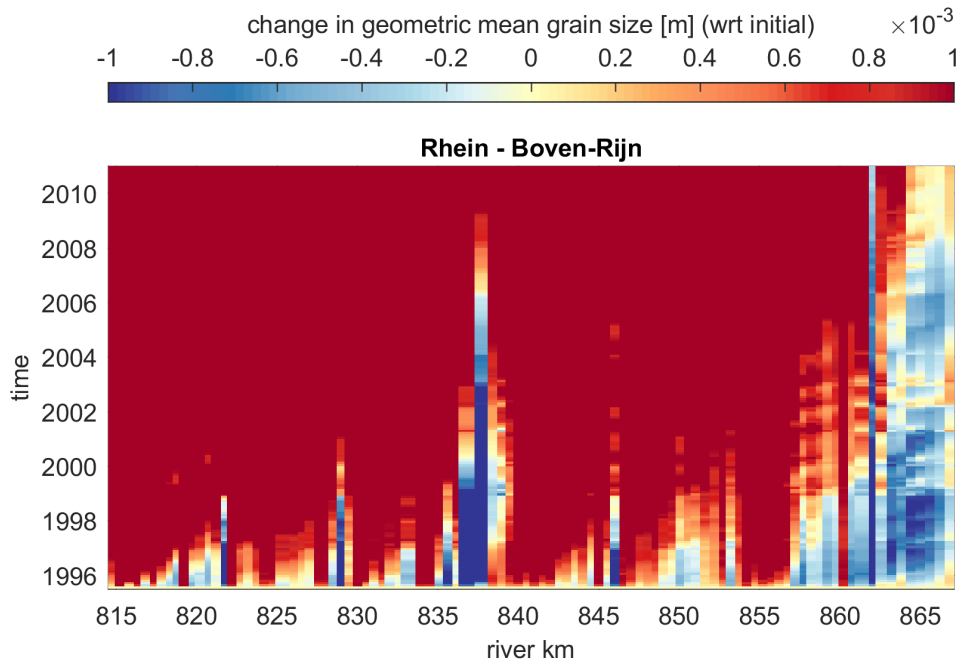
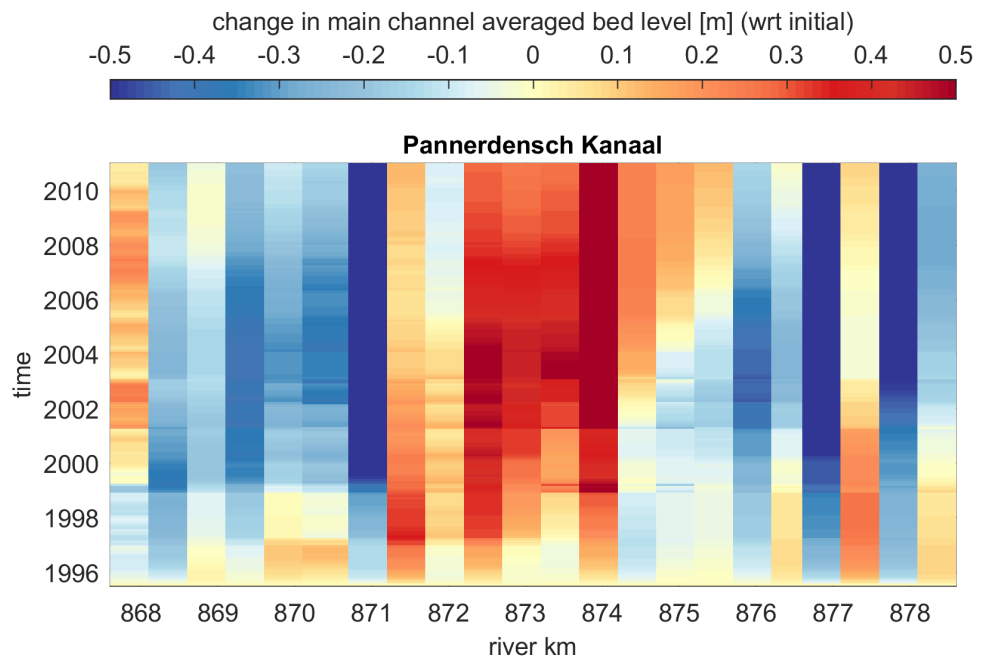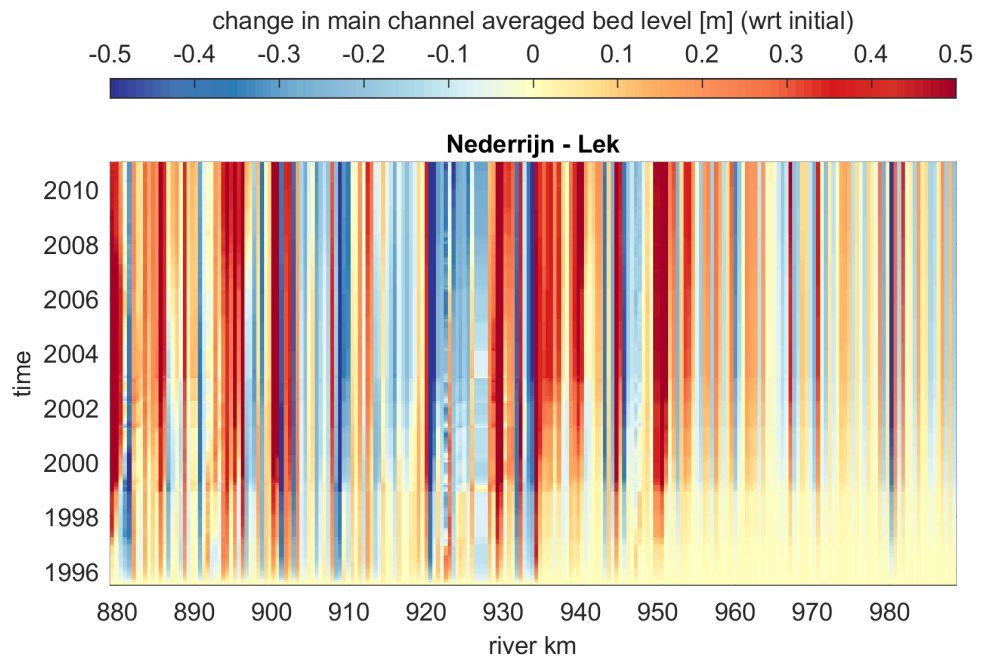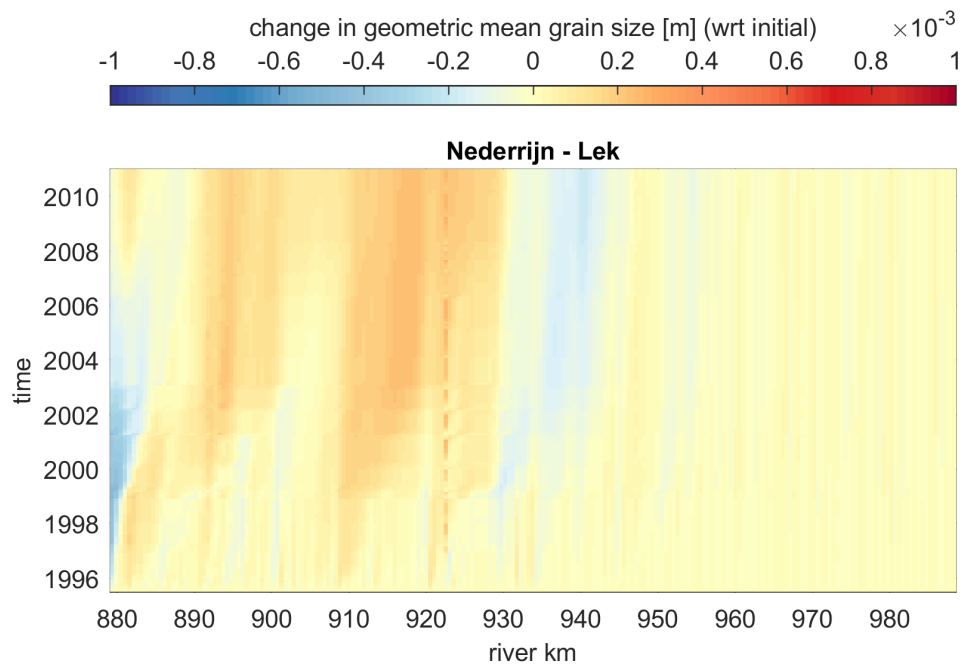**Figure 157** Grain size changes in time with respect to the initial conditions along the Rhein - Boven-Rijn
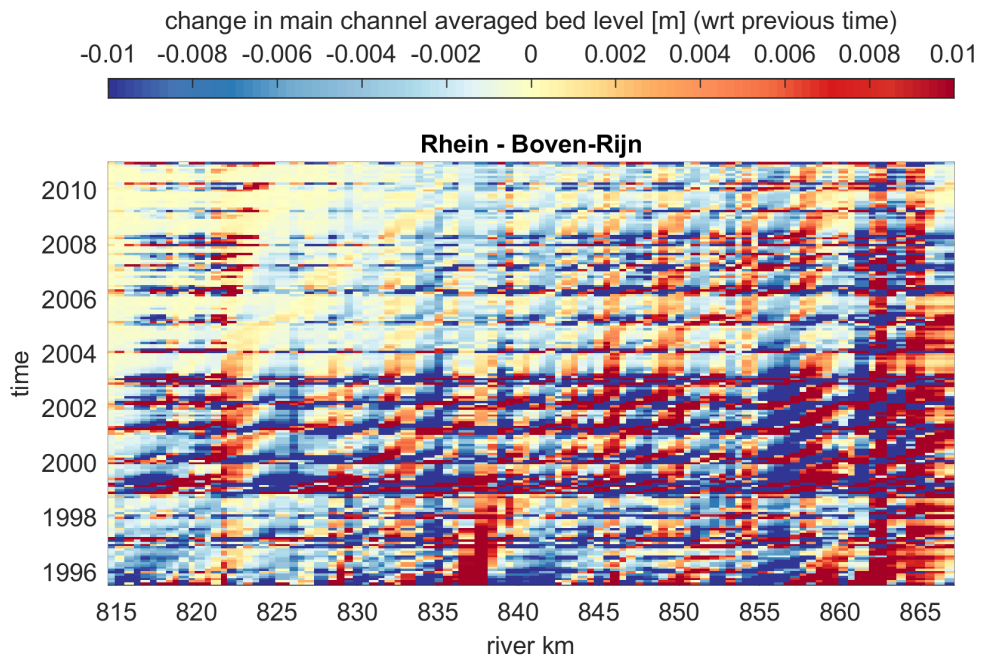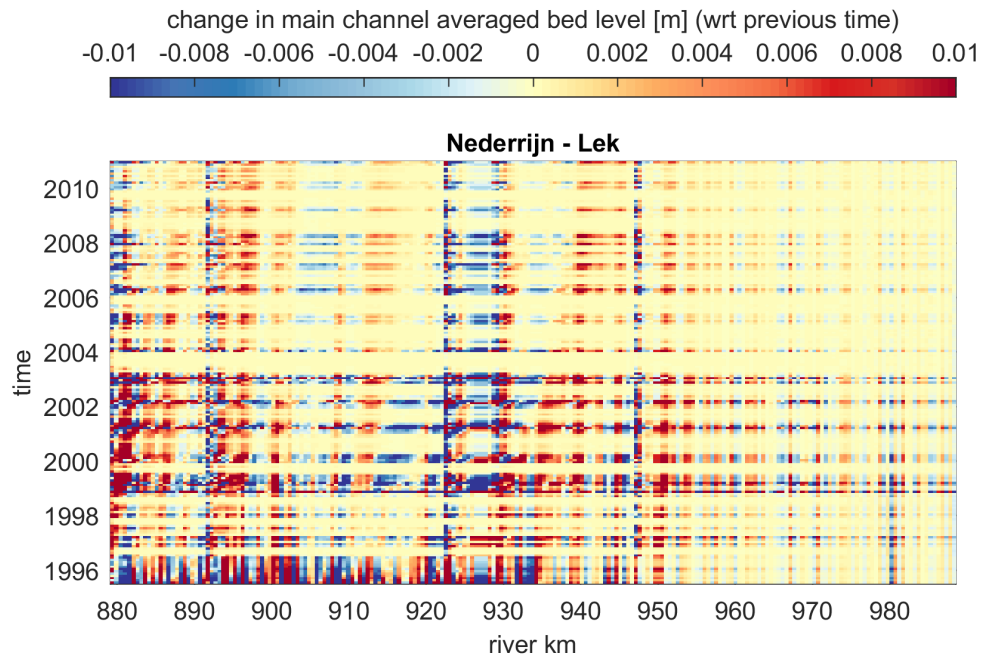

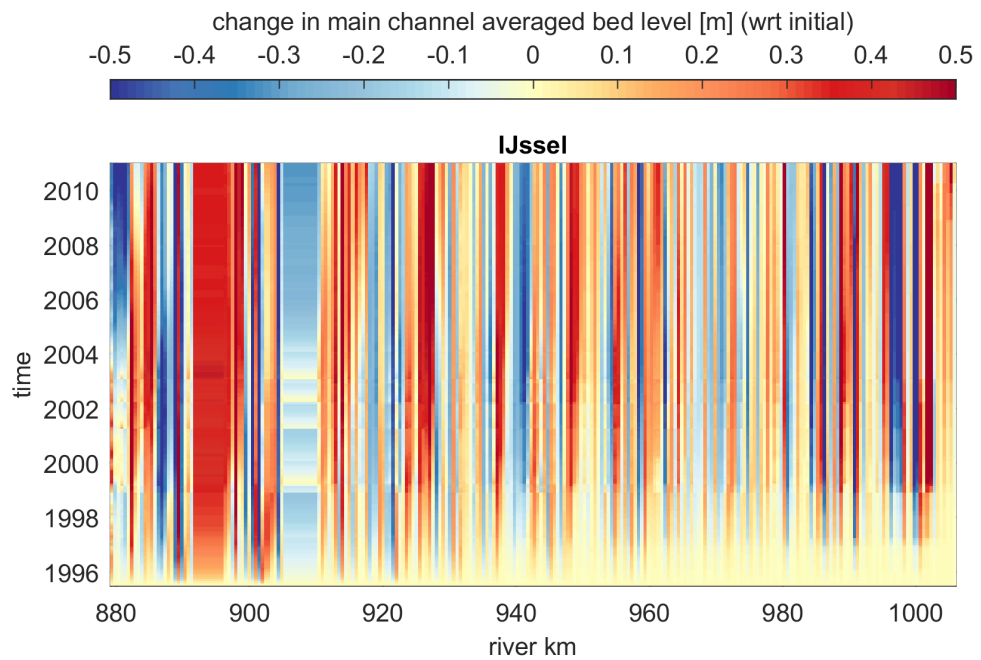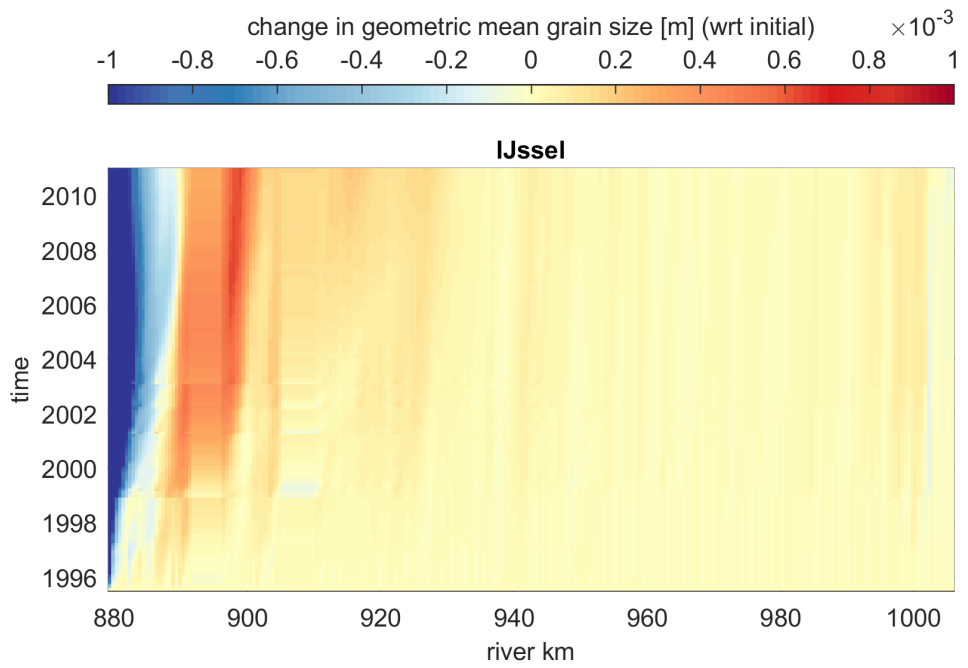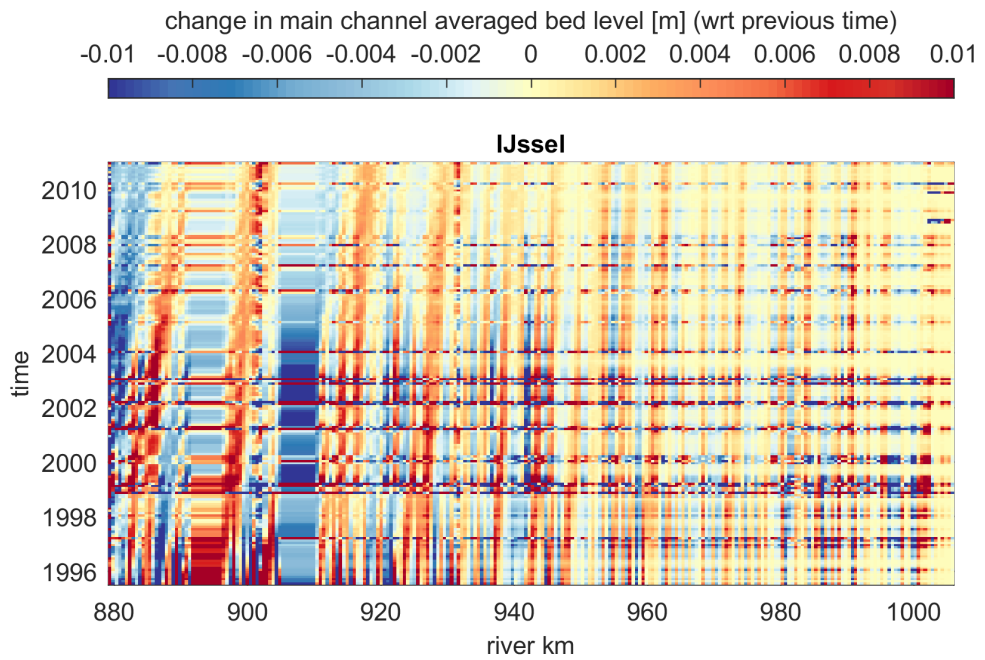**Figure 158** Bed level changes in time with respect to the previous output time along the Rhein - Boven-Rijn

Deltares

change in main channel averaged bed level [m] (wrt initial)

-0.5 -0.4 -0.3 -0.2 -0.1 0 0.1 0.2 0.3 0.4 0.5
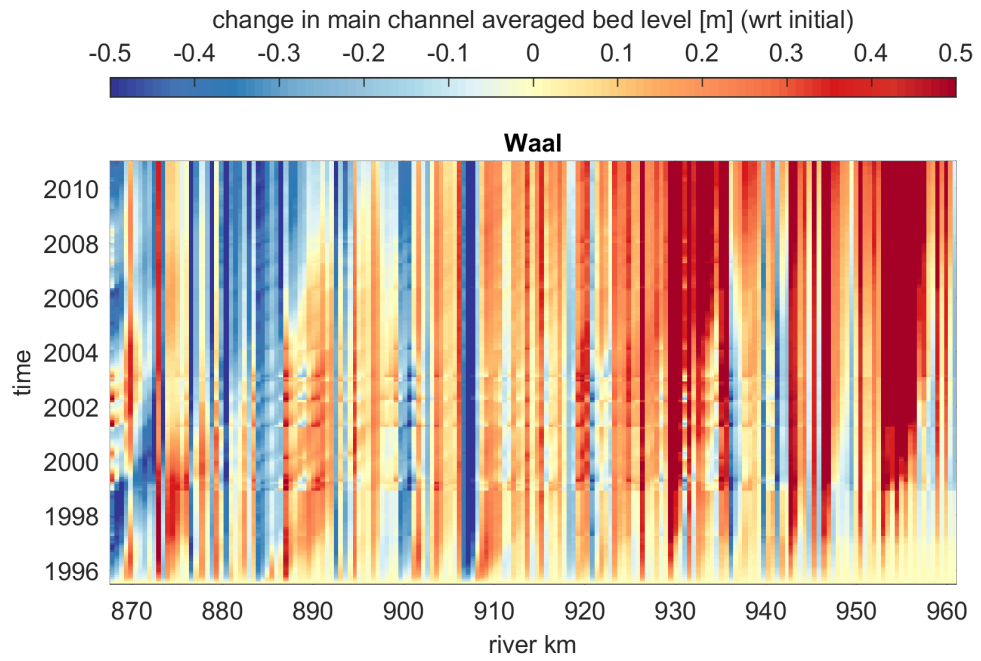
Waal

Figure 159 Bed level changes in time with respect to the initial conditions along the Waal

change in geometric mean grain size [m] (wrt initial) $\times 10^{-3}$

-1 -0.8 -0.6 -0.4 -0.2 0 0.2 0.4 0.6 0.8 1
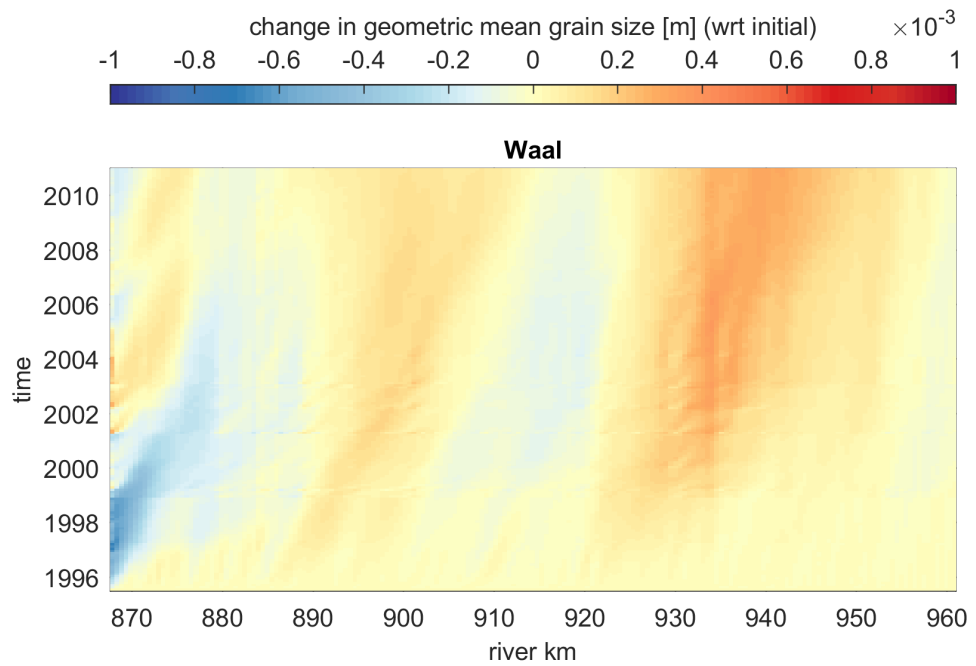
Waal

Figure 160 Grain size changes in time with respect to the initial conditions along the Waal

Deltares

change in main channel averaged bed level [m] (wrt previous time)

-0.01 -0.008 -0.006 -0.004 -0.002   0   0.002 0.004 0.006 0.008 0.01
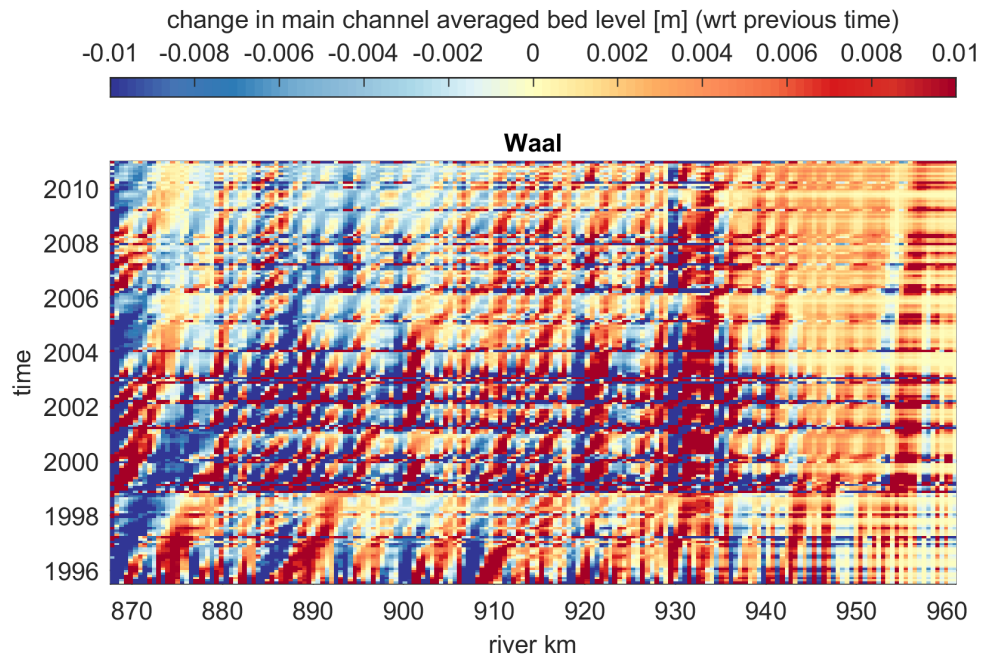
Waal

Figure 161 Bed level changes in time with respect to the previous output time along the Waal

change in main channel averaged bed level [m] (wrt initial)

-0.5   -0.4   -0.3   -0.2   -0.1   0   0.1   0.2   0.3   0.4   0.5

Pannerdensch Kanaal

Figure 162 Bed level changes in time with respect to the initial conditions along the Pannerdensch Kanaal

Deltares
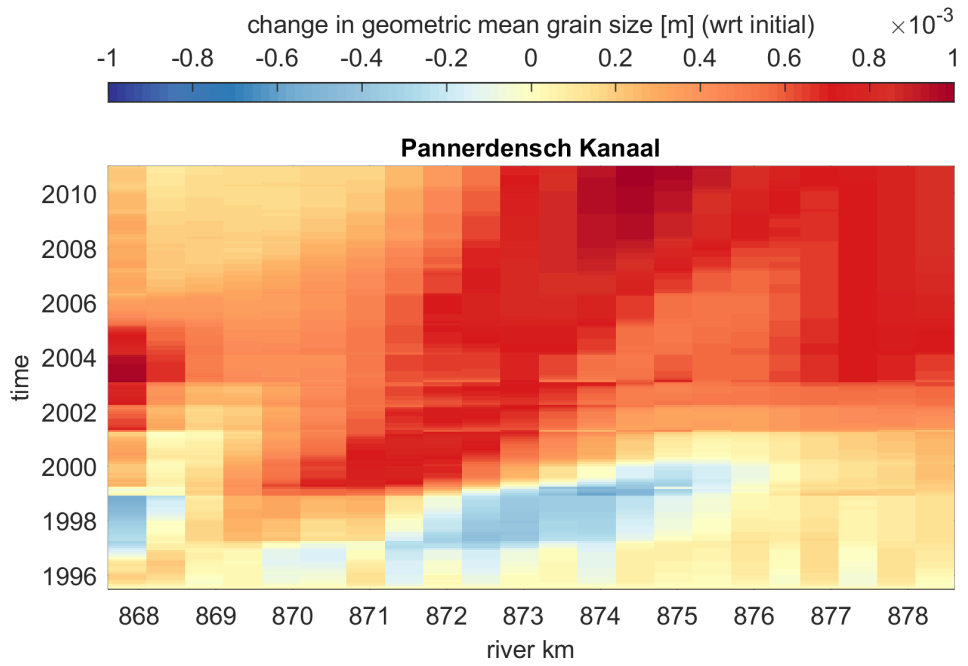
Figure 163 Grain size changes in time with respect to the initial conditions along the Pannerdensch Kanaal
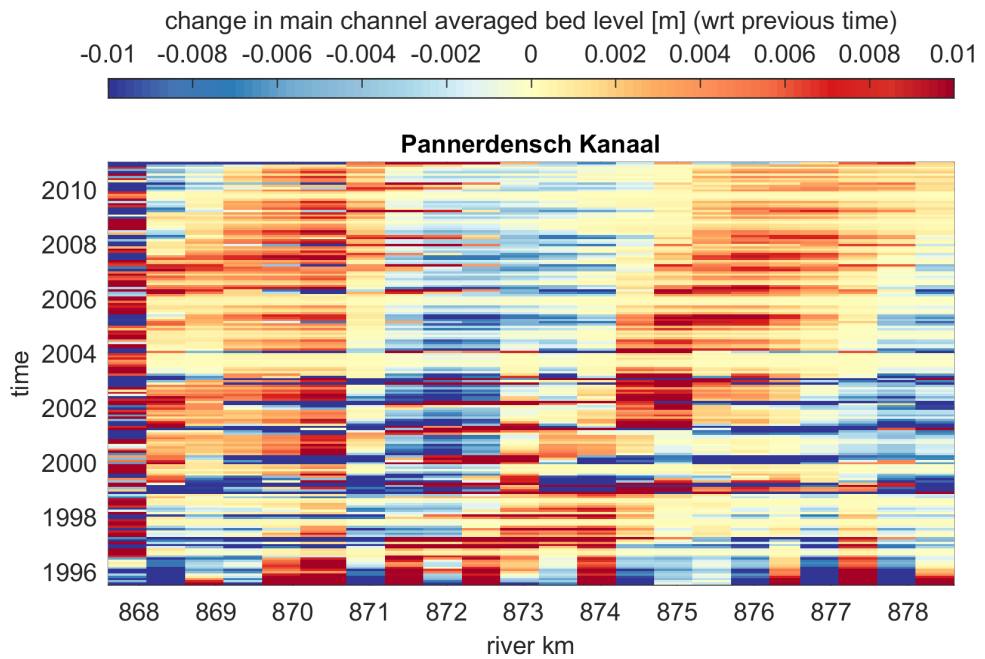
Figure 164 Bed level changes in time with respect to the previous output time along the Pannerdensch Kanaal

Deltares

change in main channel averaged bed level [m] (wrt initial)

Nederrijn - Lek

Figure 165 Bed level changes in time with respect to the initial conditions along the Nederrijn - Lek

change in geometric mean grain size [m] (wrt initial) $\times 10^{-3}$

Nederrijn - Lek

Figure 166 Grain size changes in time with respect to the initial conditions along the Nederrijn - Lek

Deltares

change in main channel averaged bed level [m] (wrt previous time)

Figure 167 Bed level changes in time with respect to the previous output time along the Nederrijn - Lek

change in main channel averaged bed level [m] (wrt initial)

Figure 168 Bed level changes in time with respect to the initial conditions along the IJssel

Deltares

Figure 169 Grain size changes in time with respect to the initial conditions along the IJssel

Figure 170 Bed level changes in time with respect to the previous output time along the IJssel

Deltares

M Verification results of the period 1995-2011

M.1 Mean annual load at bifurcations
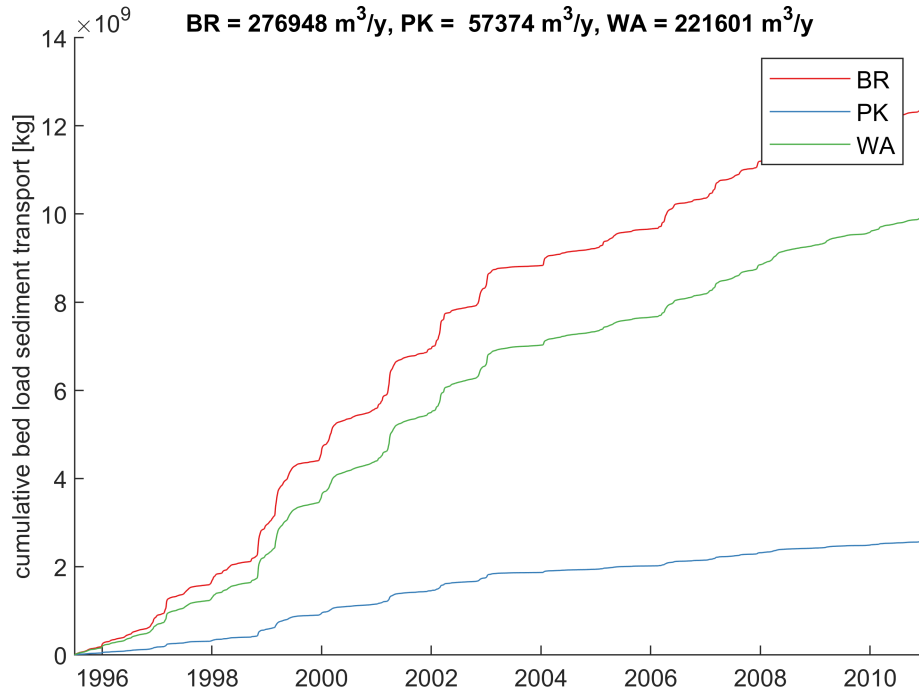
Figure 171 Total (gravel and sand) sediment transport at the Pannerdensche Kop.

Deltares
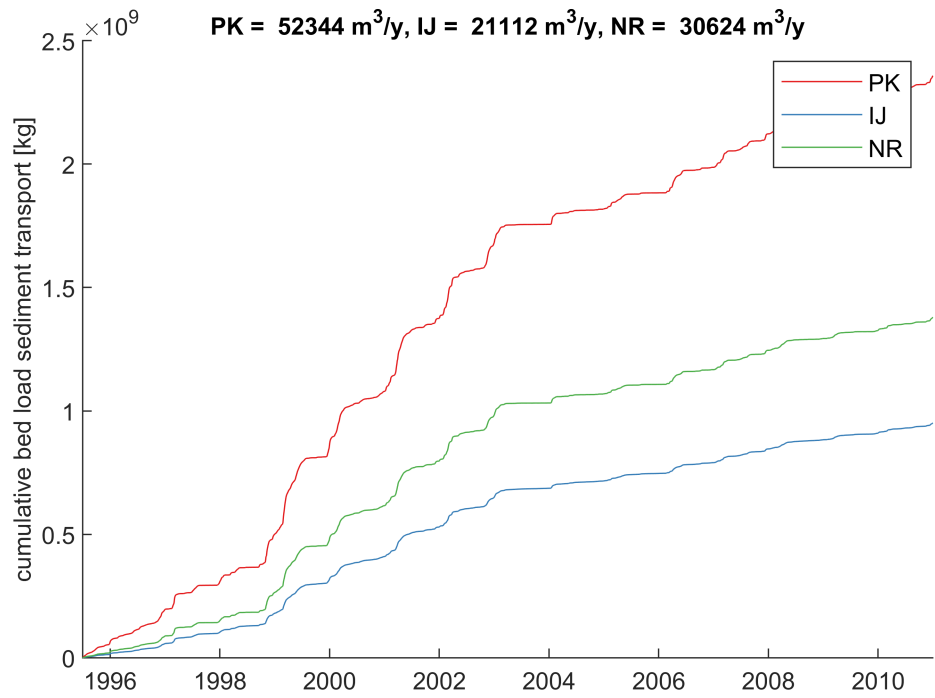
Figure 172 Total (gravel and sand) sediment transport at the IJssel Kop.
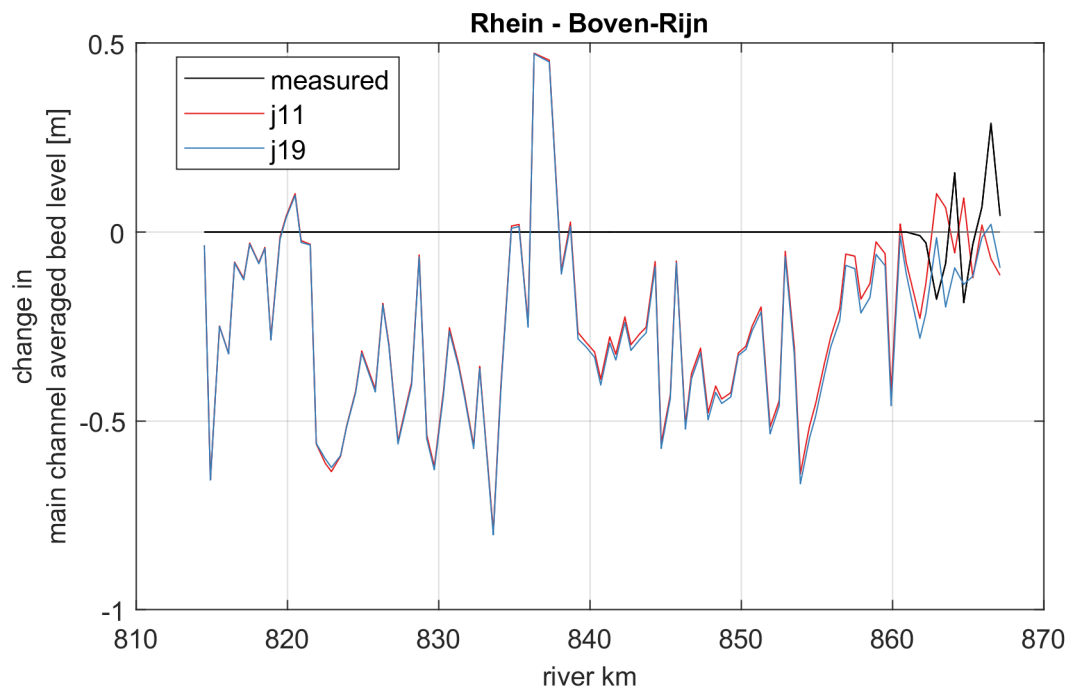
M.2   Bed elevation changes

Deltares
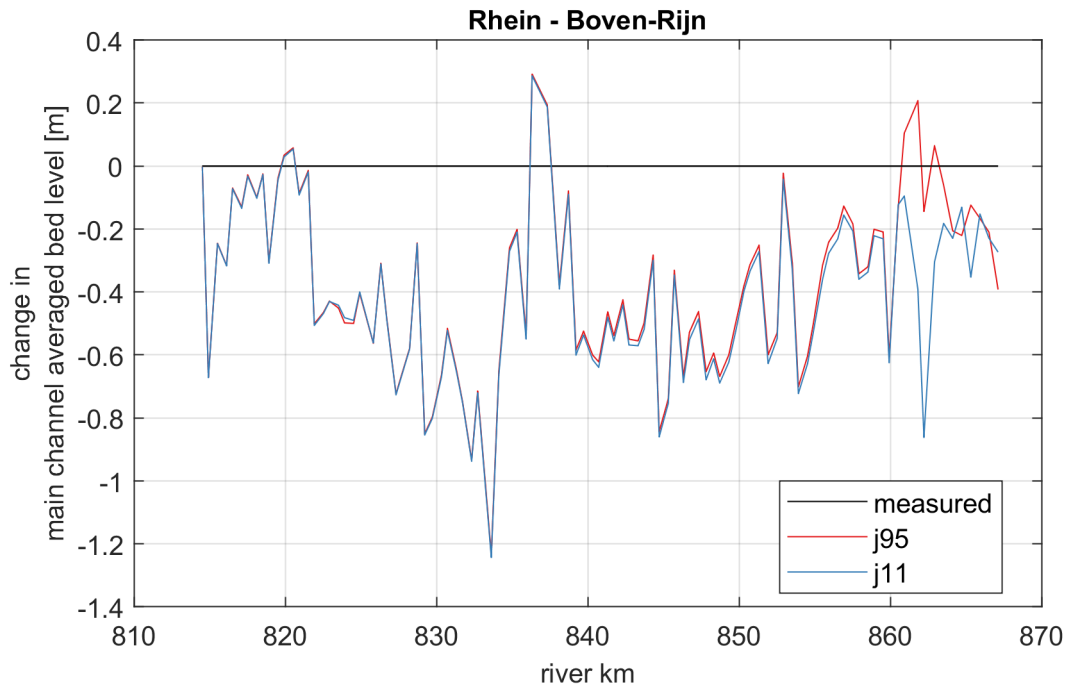
Figure 173 Bed elevation changes for the period 1995-2011 along the Rhein - Boven-Rijn
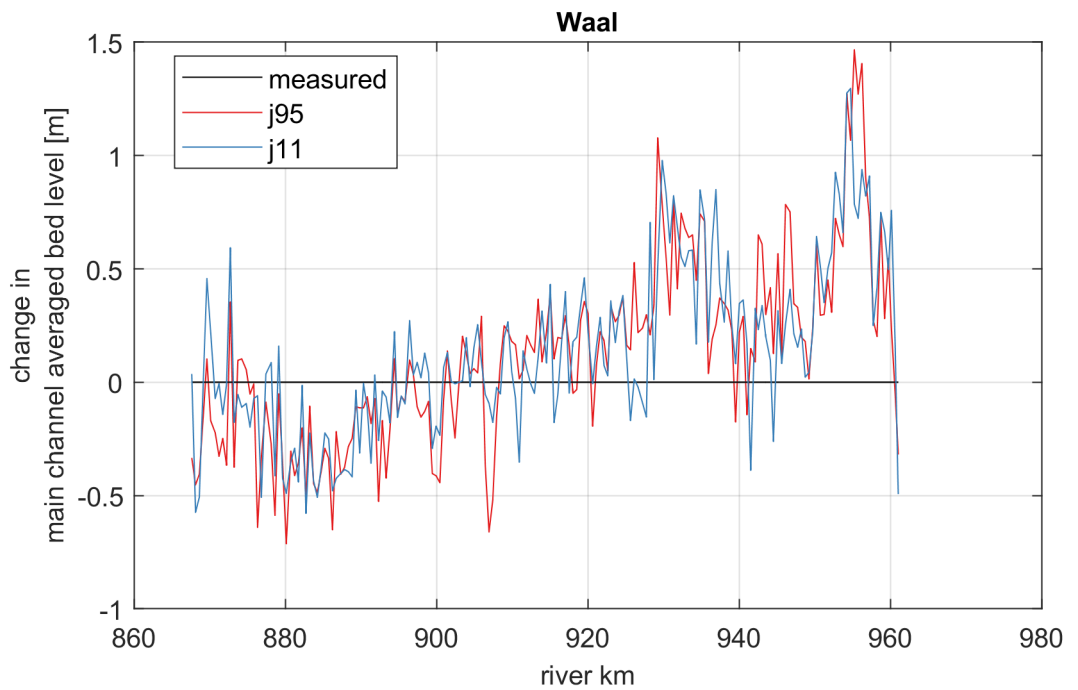
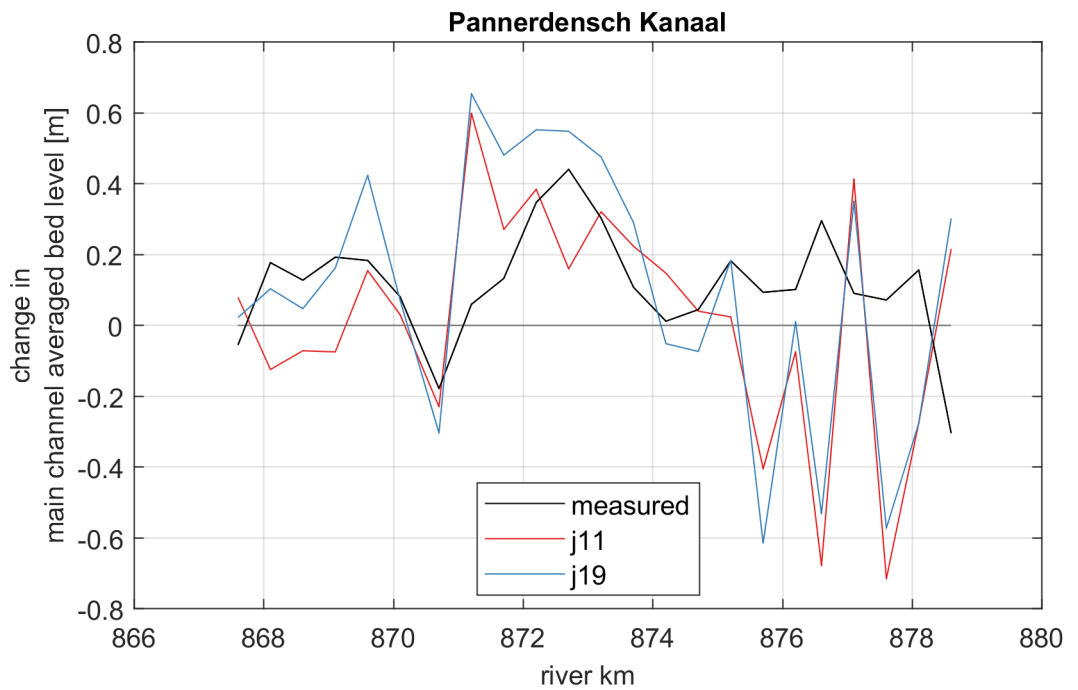**Figure 174** Bed elevation changes for the period 1995-2011 along the Waal

Deltares
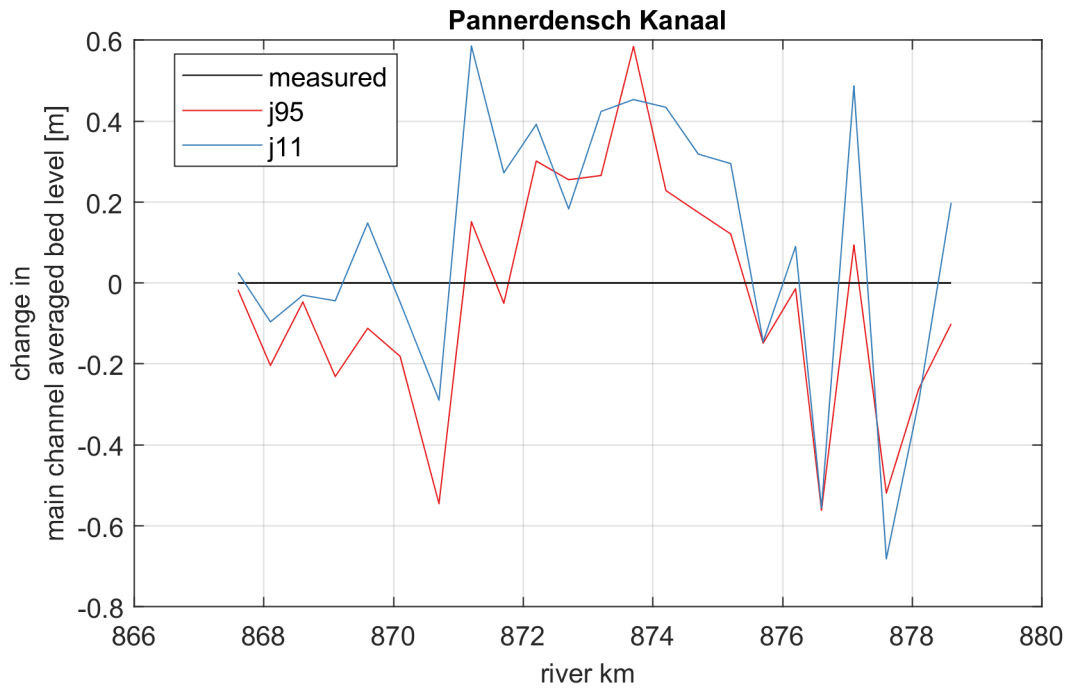
Figure 175 Bed elevation changes for the period 1995-2011 along the Pannerdensch Kanaal
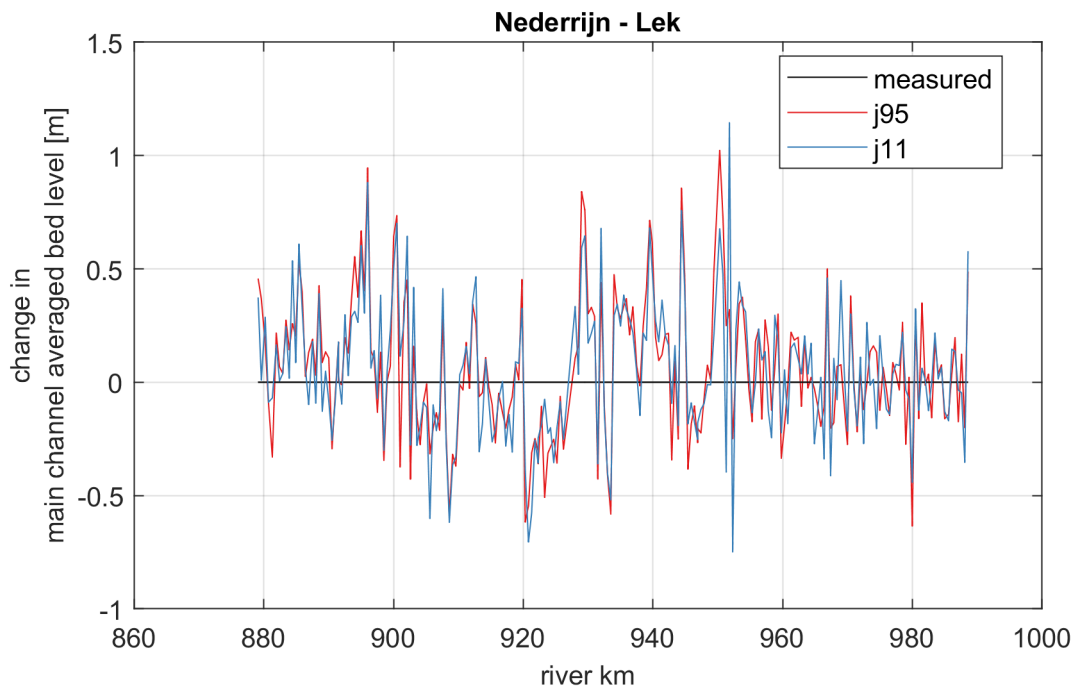
Figure 176 Bed elevation changes for the period 1995-2011 along the Niederrijn - Lek
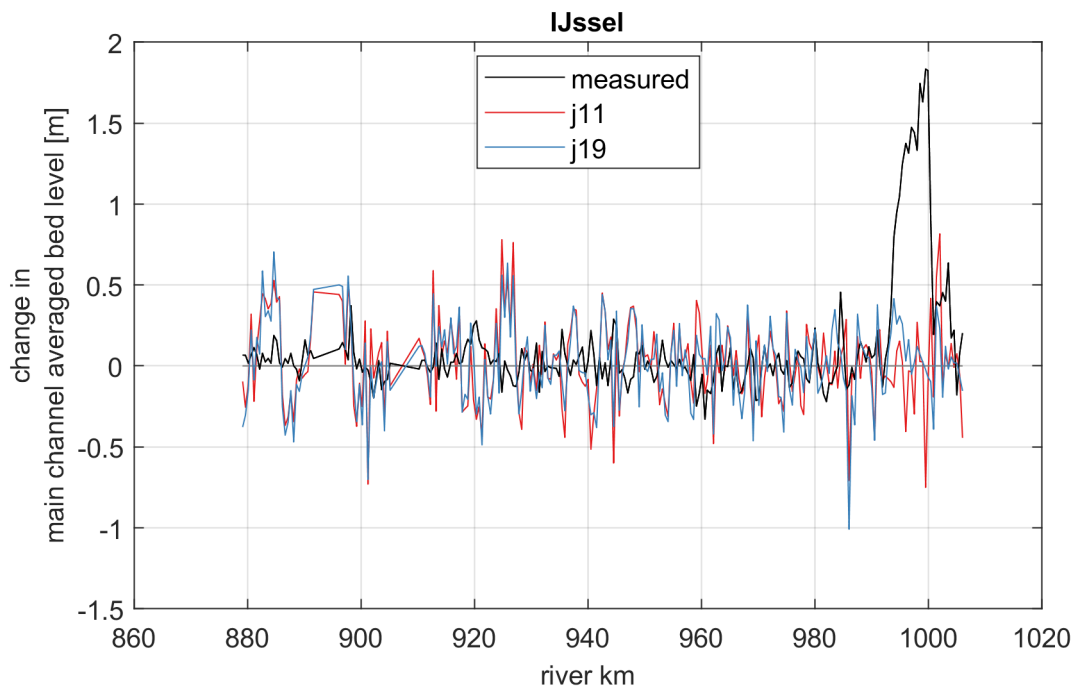
Deltares
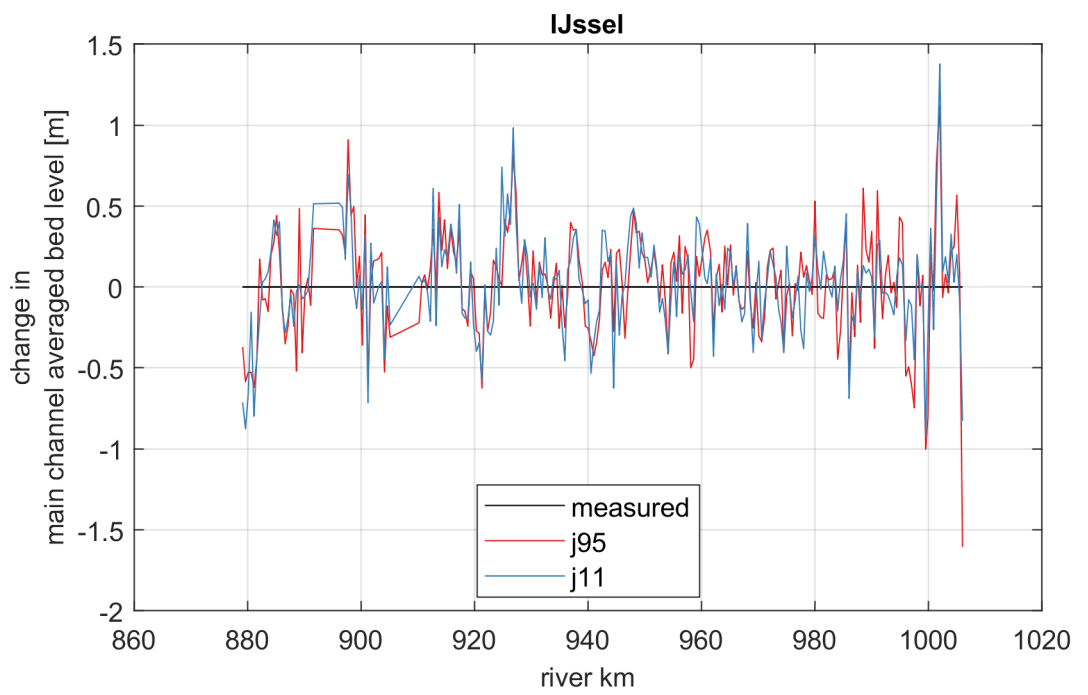
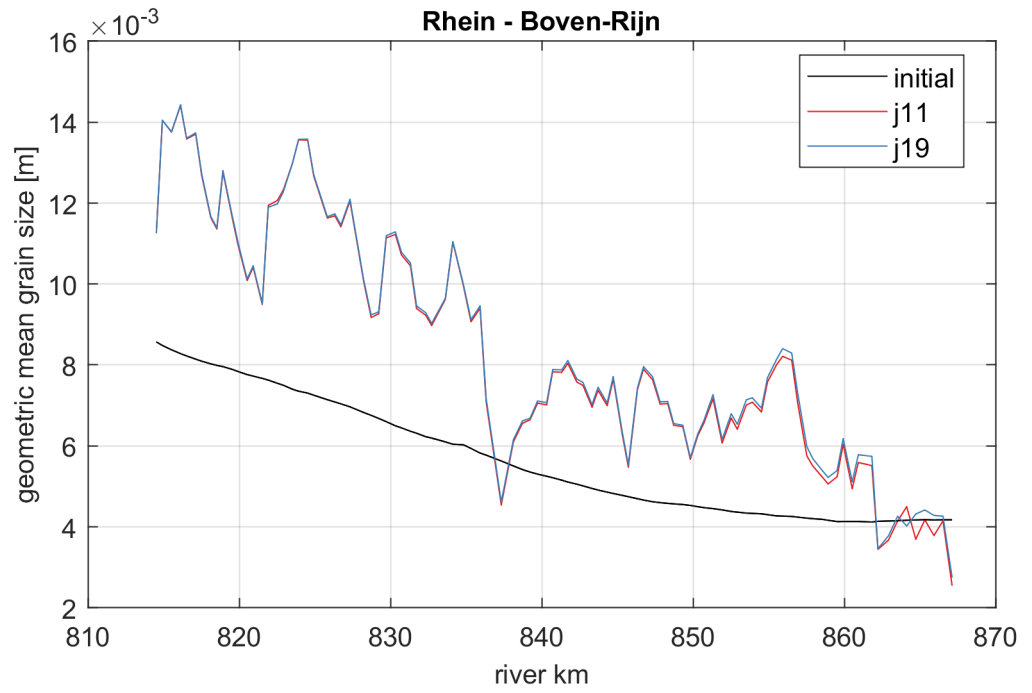**Figure 177** Bed elevation changes for the period 1995-2011 along the IJssel
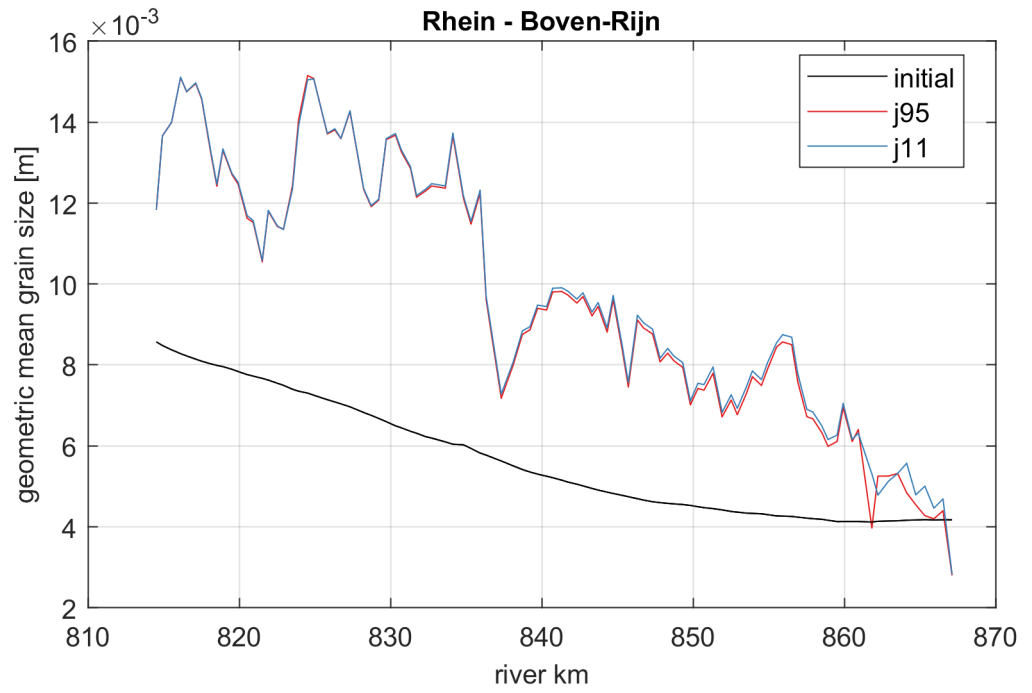
Figure 178 Grain size distribution changes for the period 1995-2011 along the Rhein - Boven-Rijn
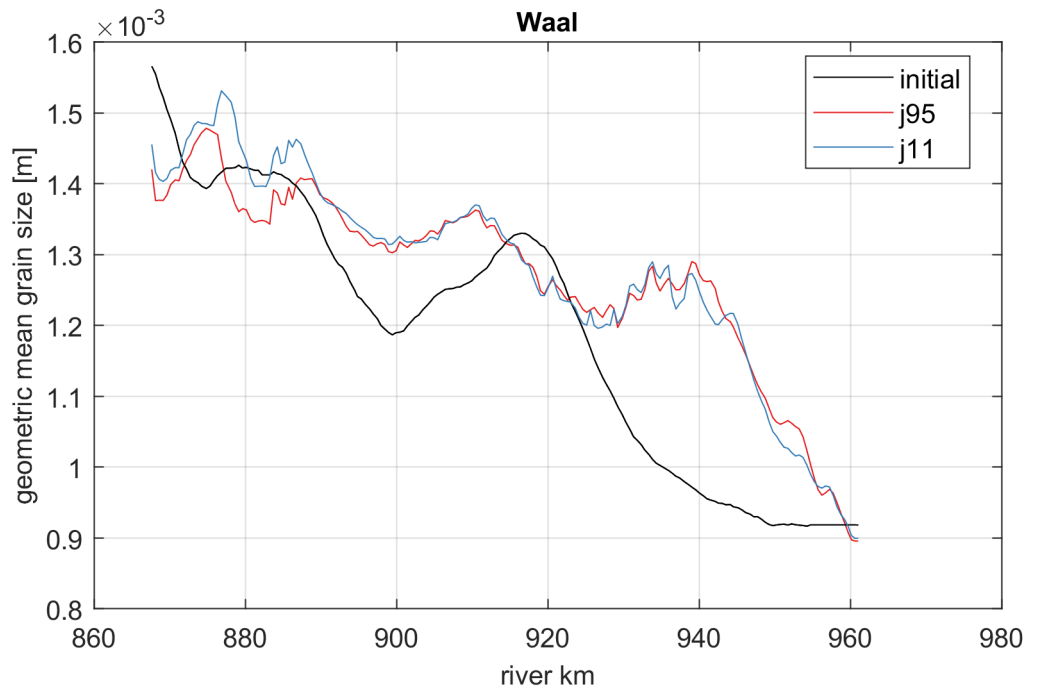
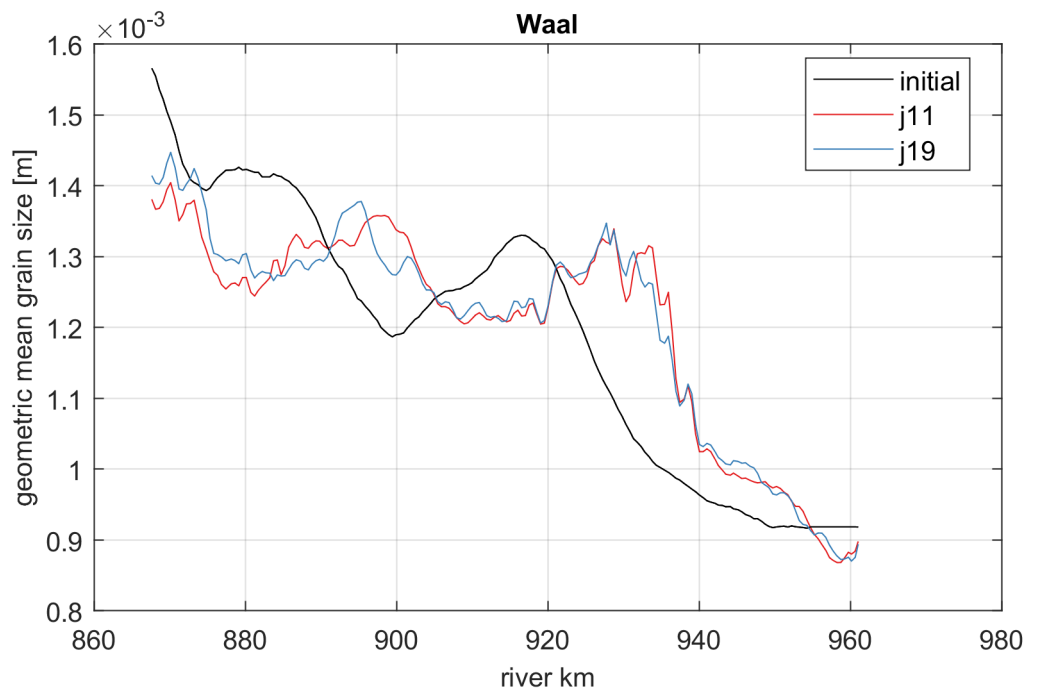**Figure 179** Grain size distribution changes for the period 1995-2011 along the Waal
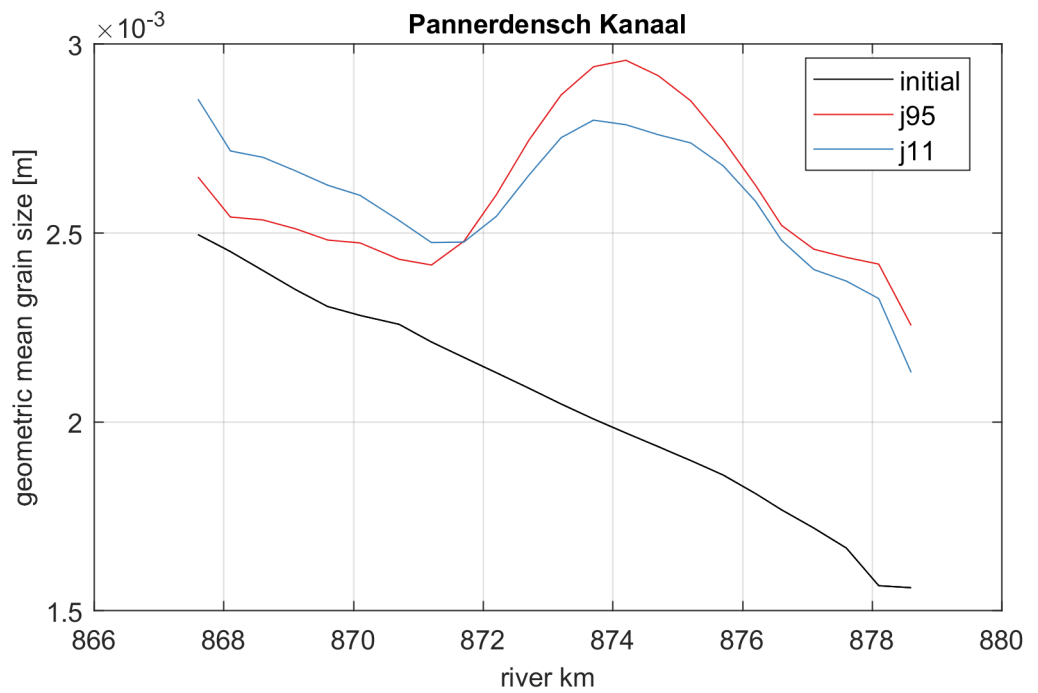
Figure 180 Grain size distribution changes for the period 1995-2011 along the Pannerdensch Kanaal

Deltares
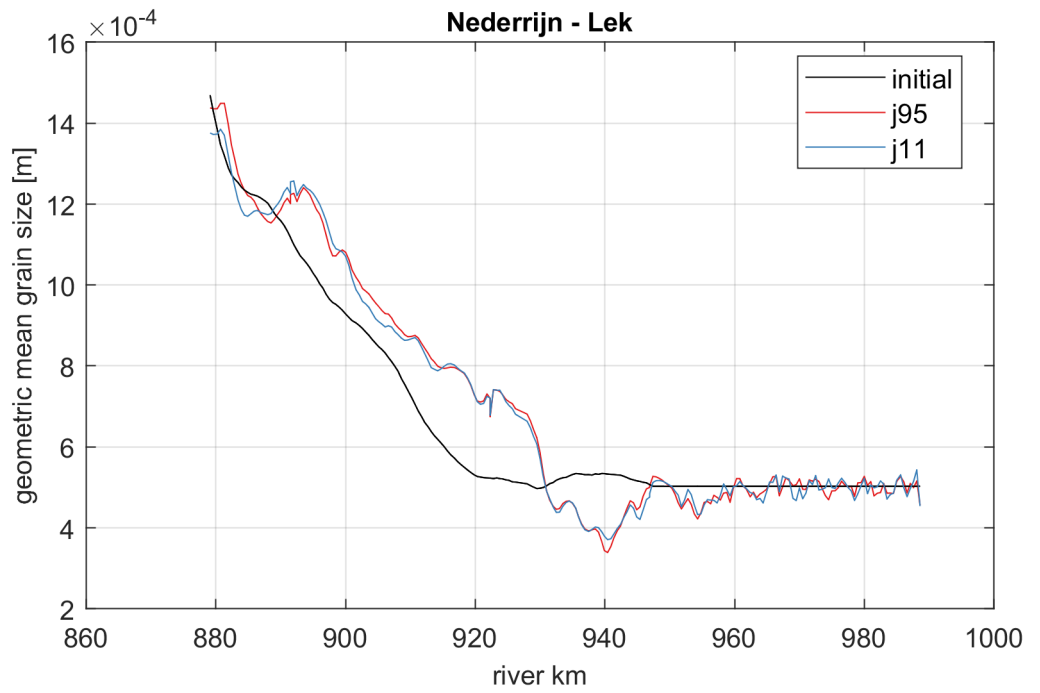
Figure 181 Grain size distribution changes for the period 1995-2011 along the Niederrijn - Lek
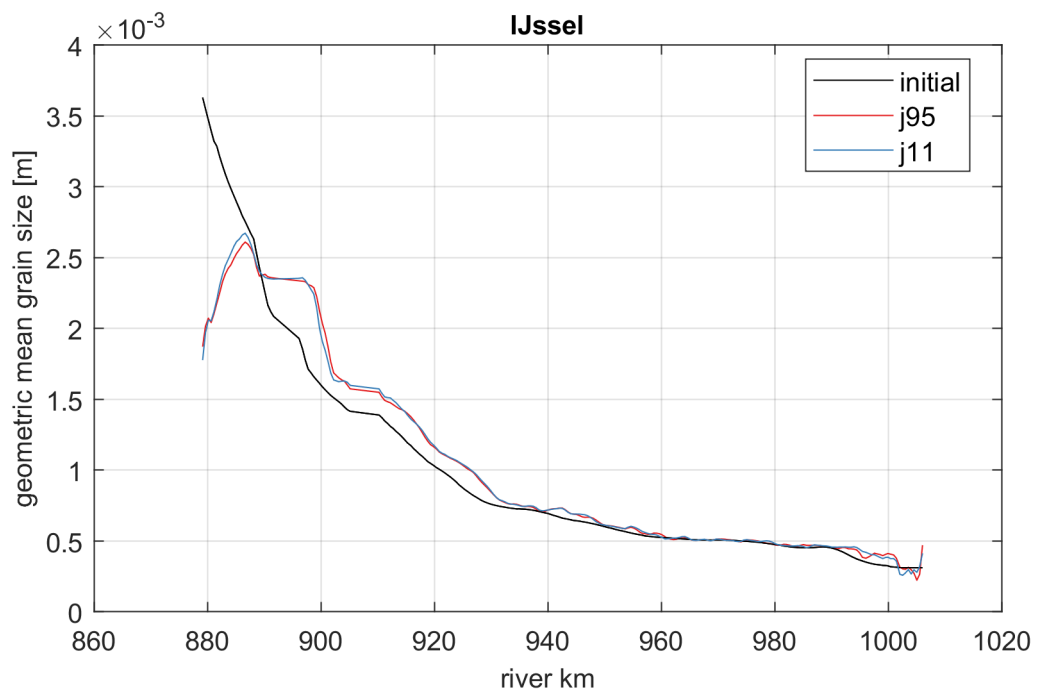
Figure 182 Grain size distribution changes for the period 1995-2011 along the IJssel

Deltares

N Verification results of the period 2011-2019

N.1 Mean annual load at bifurcations
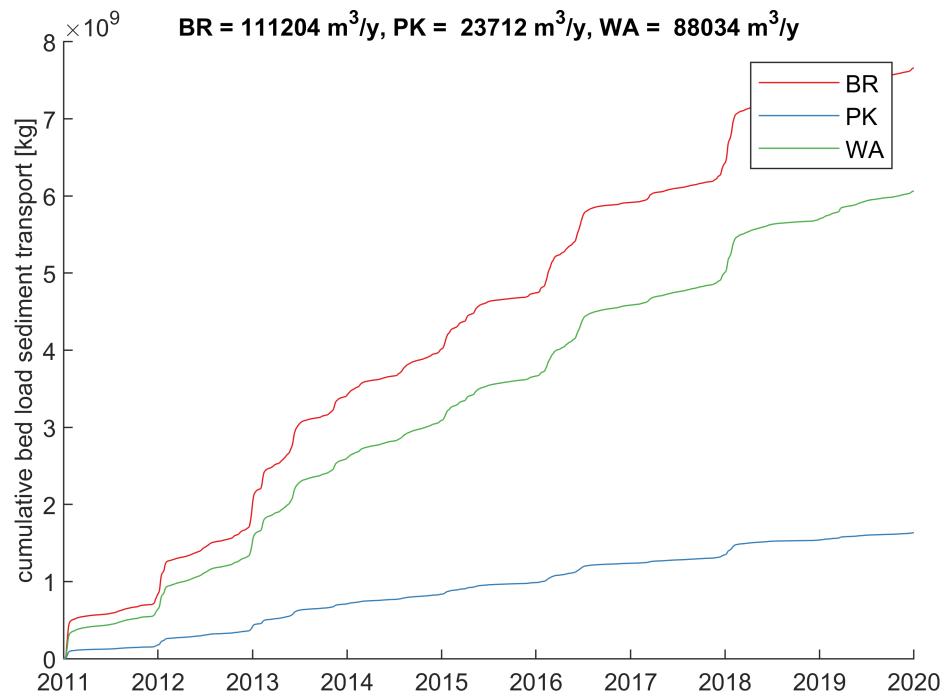
Figure 183 Total (gravel and sand) sediment transport at the Pannerdensche Kop for the period 2011-2019 using the schematization from 2011.
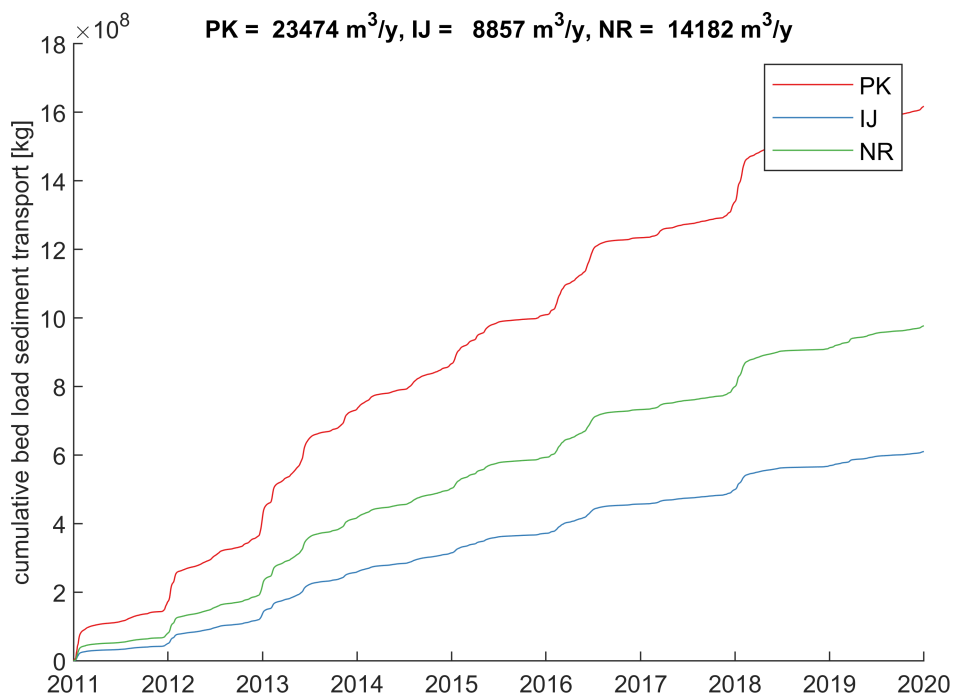
Figure 184 Total (gravel and sand) sediment transport at the IJssel Kop for the period 2011-2019 using the schematization from 2011.
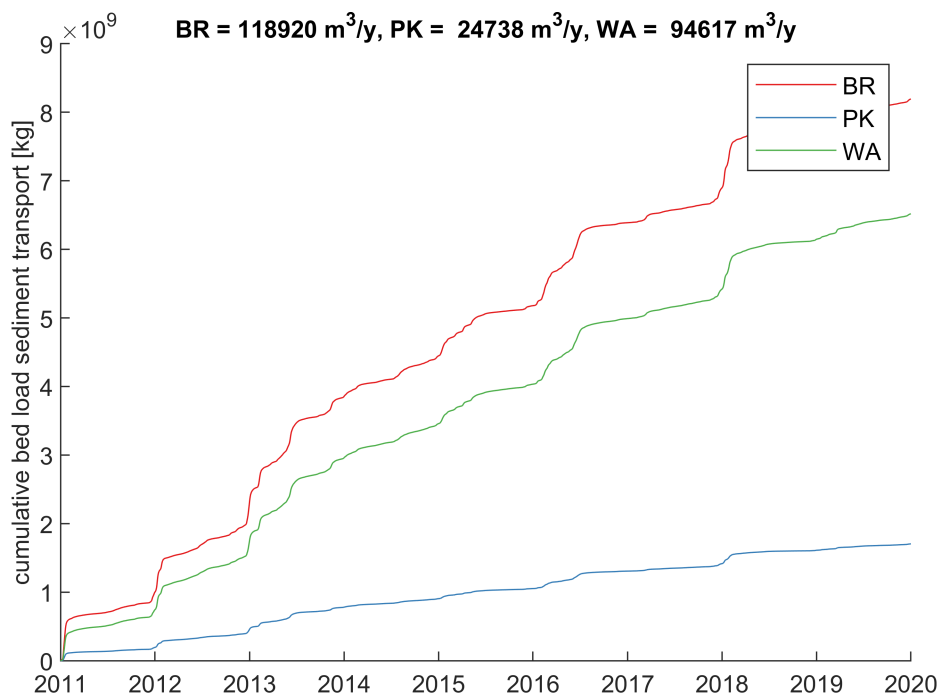
Figure 185 Total (gravel and sand) sediment transport at the Pannerdensche Kop for the period 2011-2019 using the schematization from 2019.

Deltares
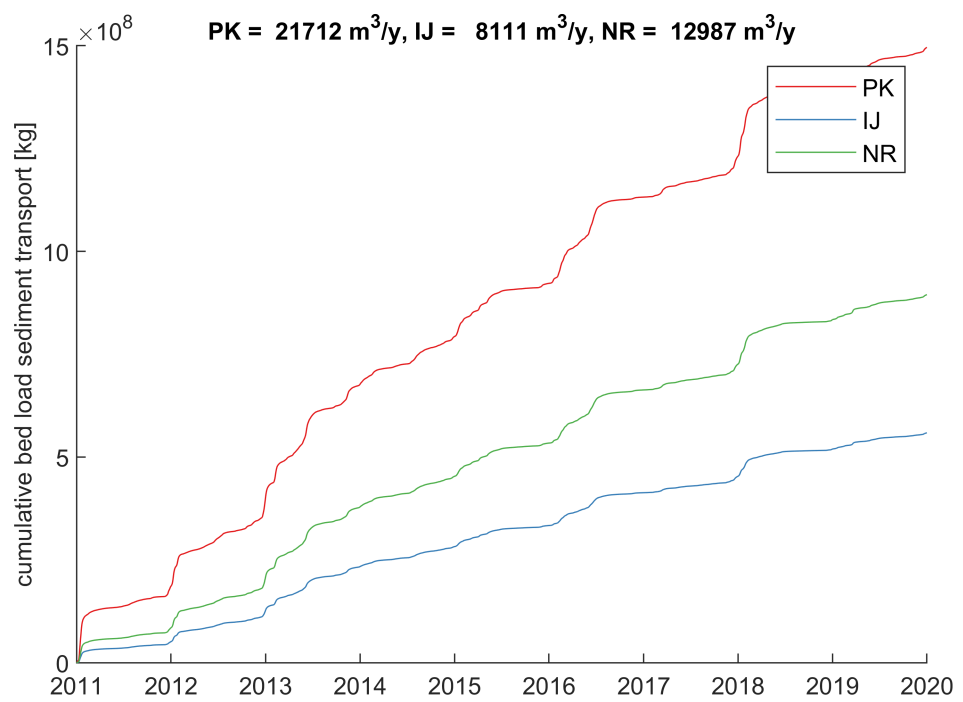
Figure 186 Total (gravel and sand) sediment transport at the IJssel Kop for the period 2011-2019 using the schematization from 2019.

Deltares

N.2 Bed elevation changes

Figure 187 Bed elevation changes for the period 2011-2019 along the Rhein - Boven-Rijn
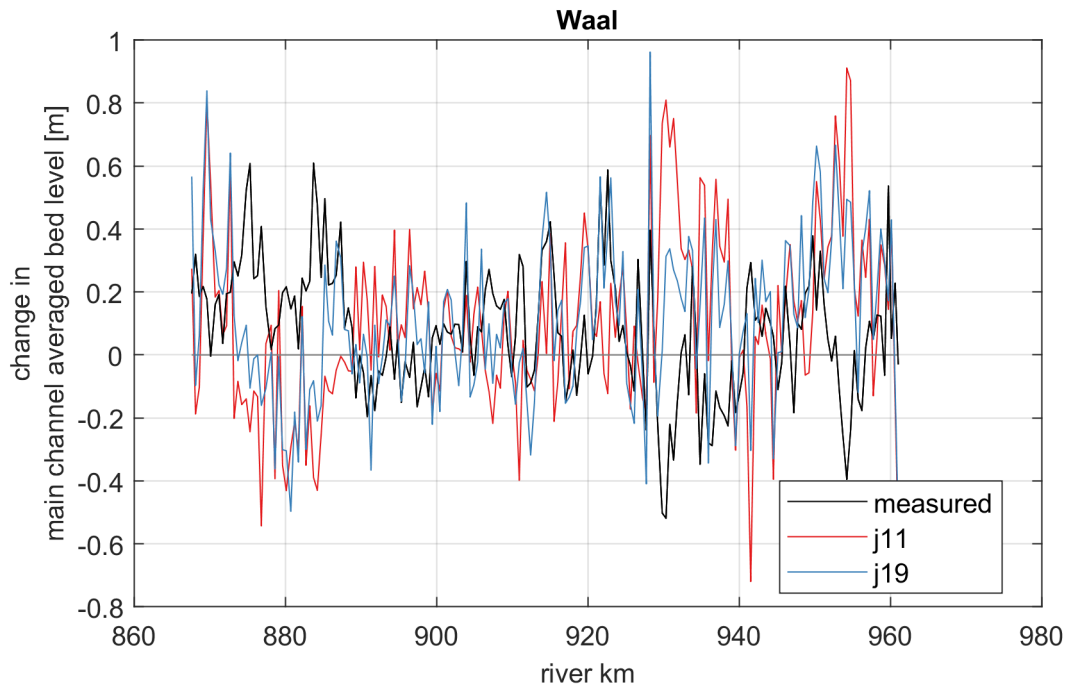
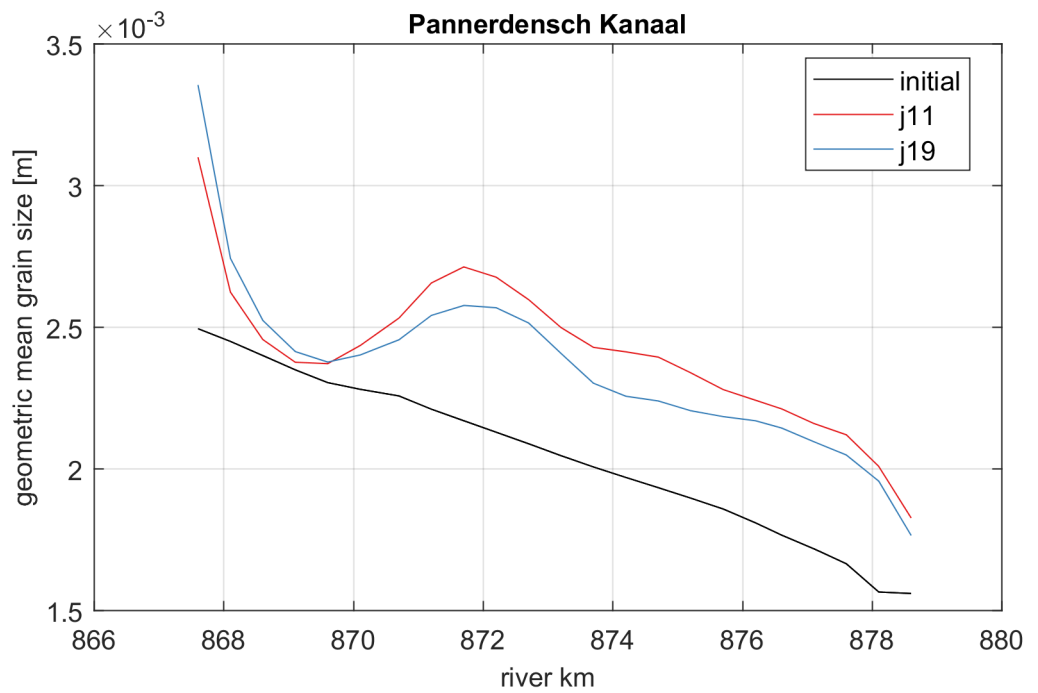**Figure 188** Bed elevation changes for the period 2011-2019 along the Waal

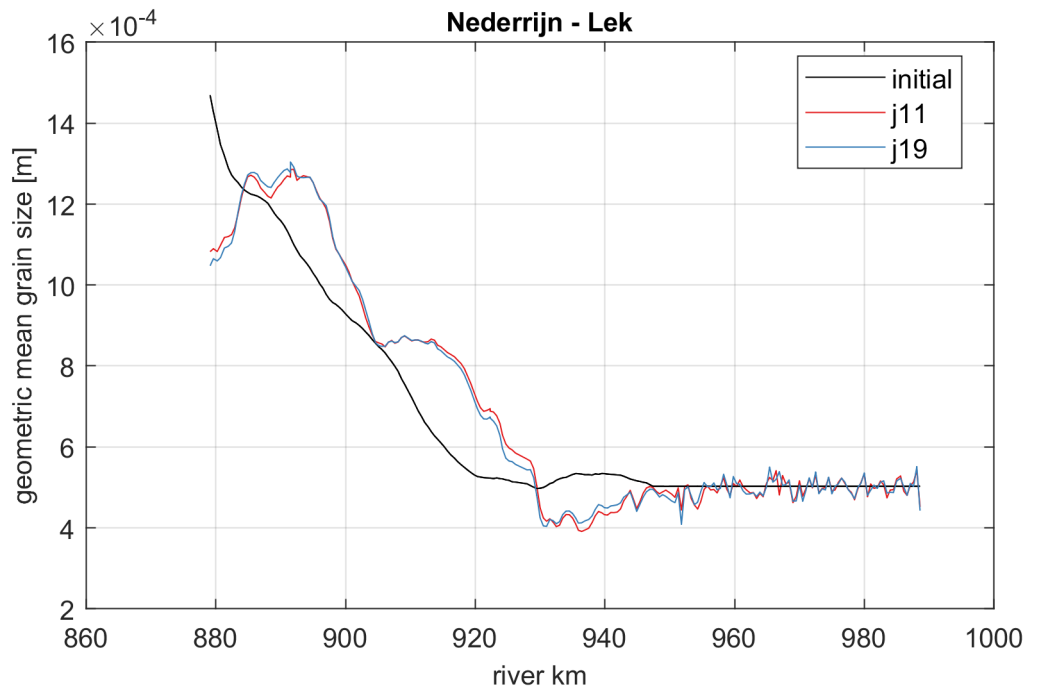**Figure 189** Bed elevation changes for the period 2011-2019 along the Pannerdensch Kanaal

Deltares
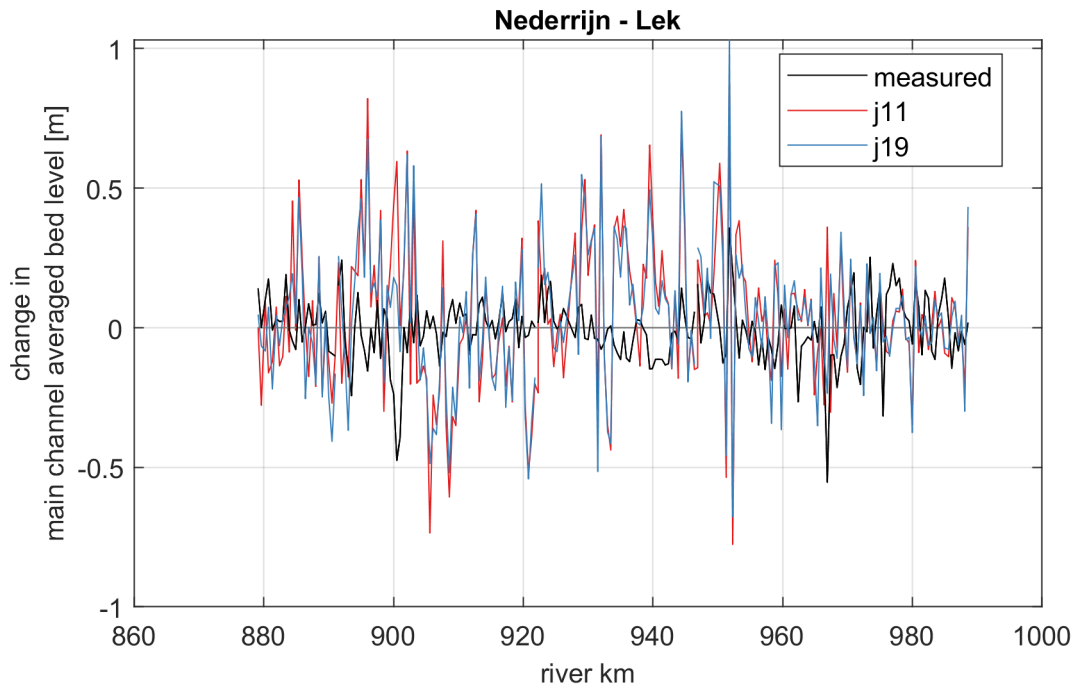
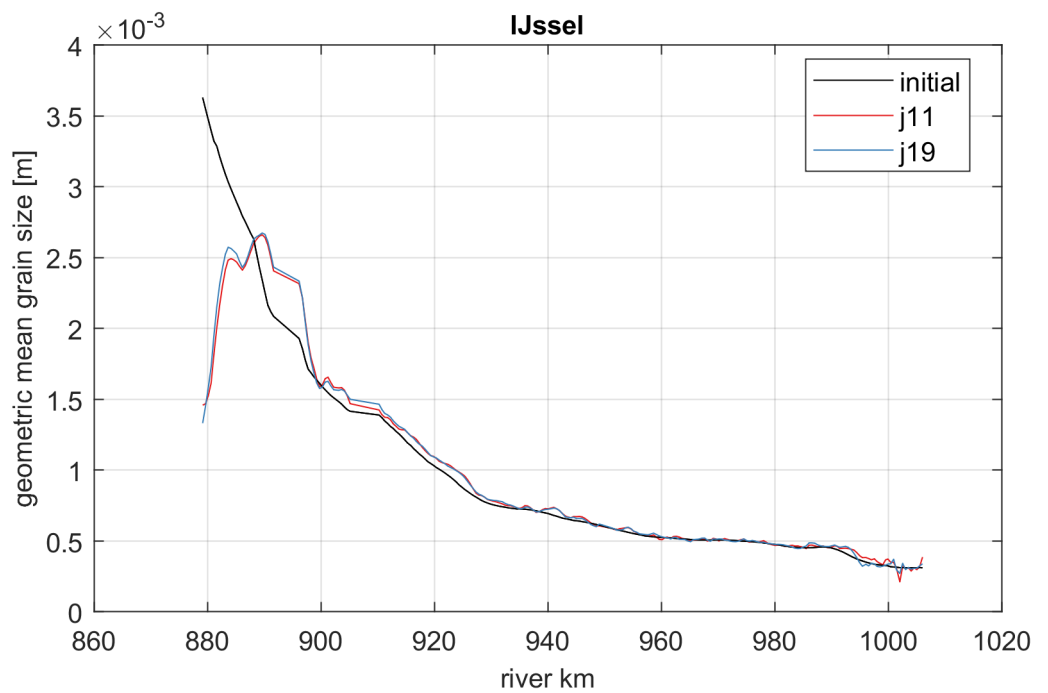**Figure 190** Bed elevation changes for the period 2011-2019 along the Niederrijn - Lek

Figure 191 Bed elevation changes for the period 2011-2019 along the IJssel

Morphological models for IRM
11203684-015-ZWS-0011_v1.0, Version 0.1, 2020-12-11, Final

Deltares

Figure 192 Grain size distribution changes for the period 2011-2019 along the Rhein - Boven-Rijn

Deltares

Figure 193 Grain size distribution changes for the period 2011-2019 along the Waal

Figure 194 Grain size distribution changes for the period 2011-2019 along the Pannerdensch Kanaal

Deltares

Figure 195 Grain size distribution changes for the period 2011-2019 along the Niederrijn - Lek

Figure 196 Grain size distribution changes for the period 2011-2019 along the IJssel

Morphological models for IRM
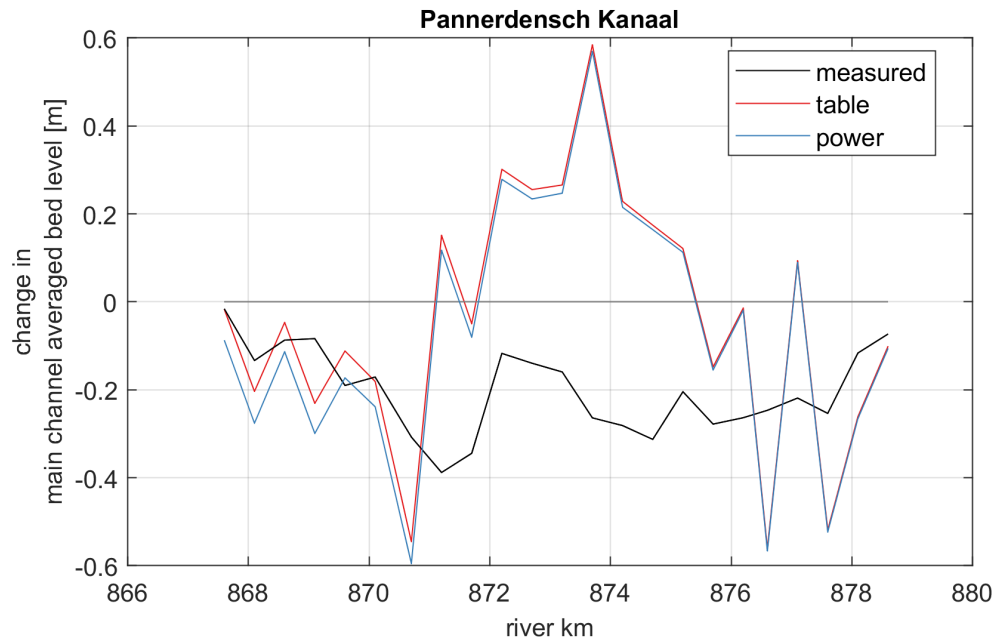11203684-015-ZWS-0011_v1.0, Version 0.1, 2020-12-11, Final

Deltares
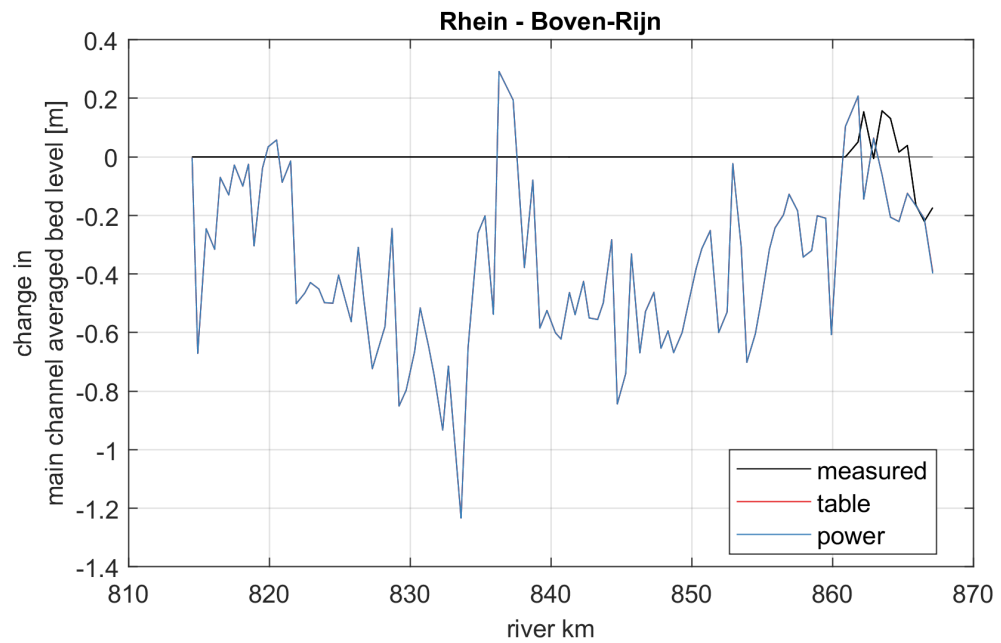
Figure 197 Bed elevation changes of the calibration run along the Rhein - Boven-Rijn using an unstable nodal-point relation ("table") and a stable one ("power").
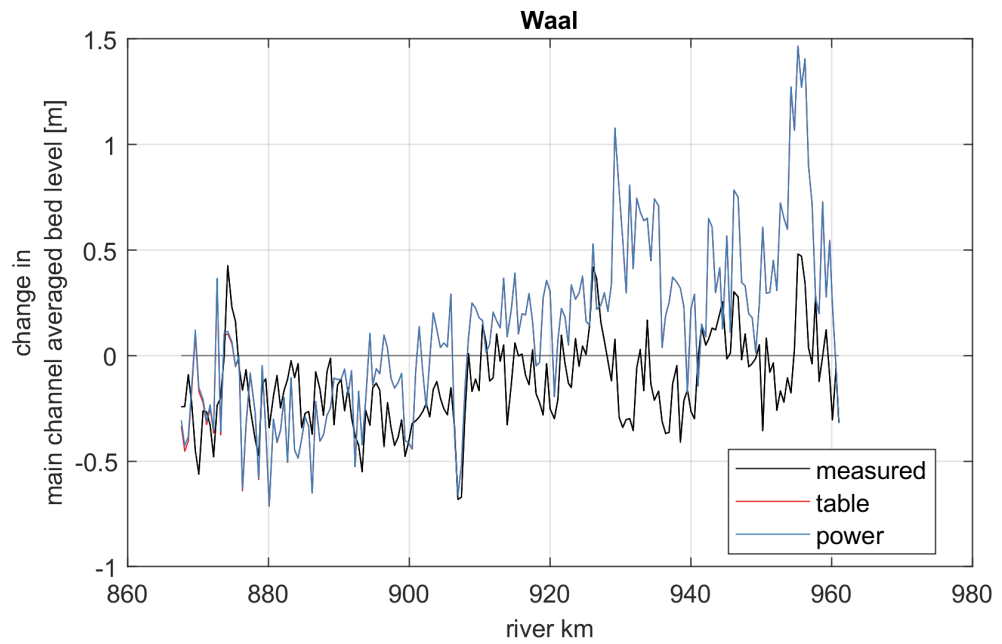
Figure 198 Bed elevation changes of the calibration run along the Waal using an unstable nodal-point relation ("table") and a stable one ("power").
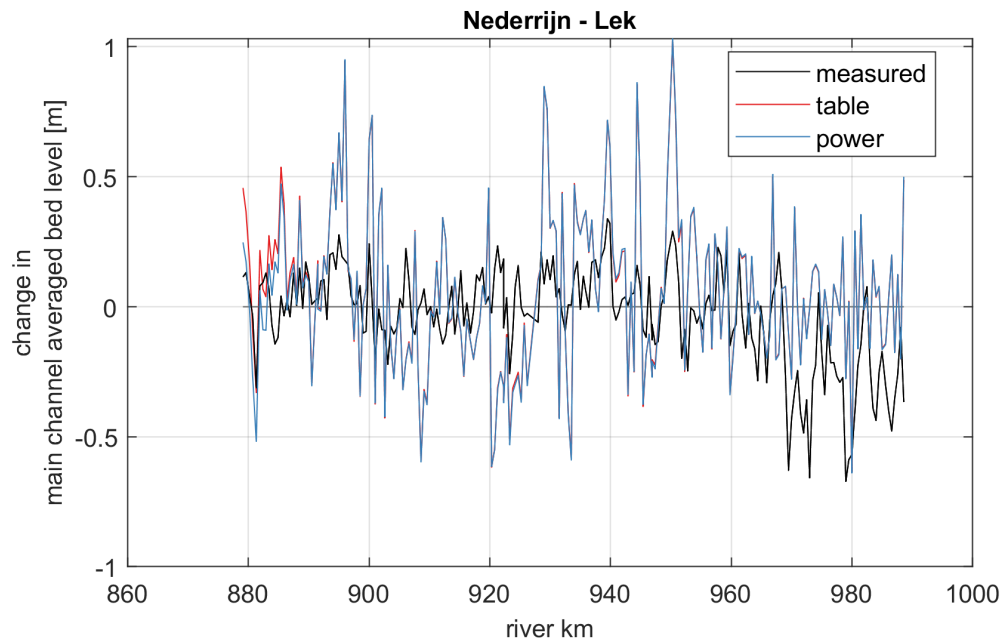

Figure 199 Bed elevation changes of the calibration run along the Pannerdensch Kanaal using an unstable nodal-point relation ("table") and a stable one ("power").

Deltares

Figure 200 Bed elevation changes of the calibration run along the Nederrijn-Lek using an unstable nodal-point relation ("table") and a stable one ("power").
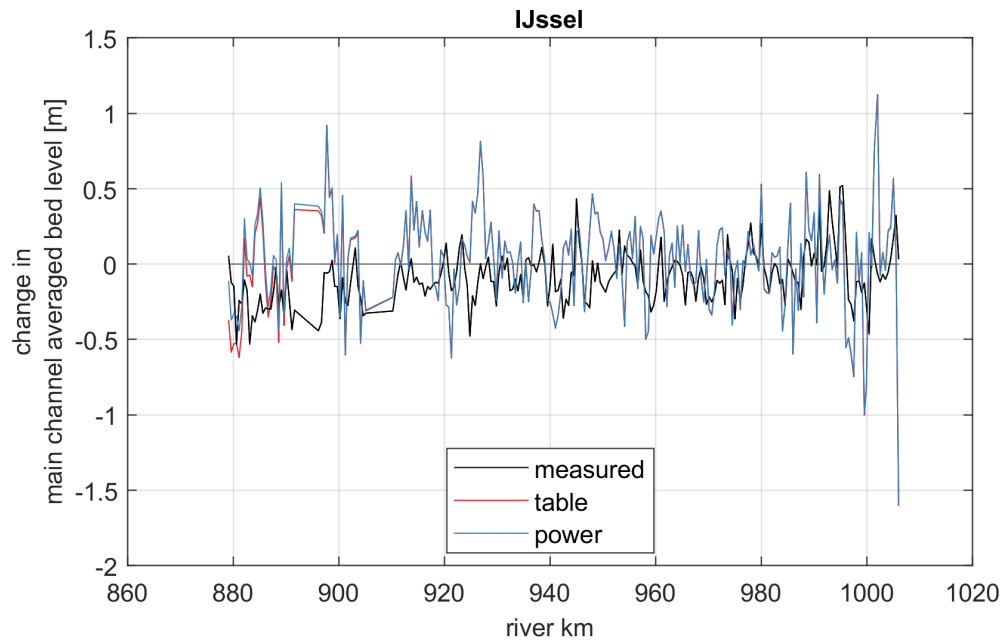

Figure 201 Bed elevation changes of the calibration run along the IJssel using an unstable nodal-point relation ("table") and a stable one ("power").
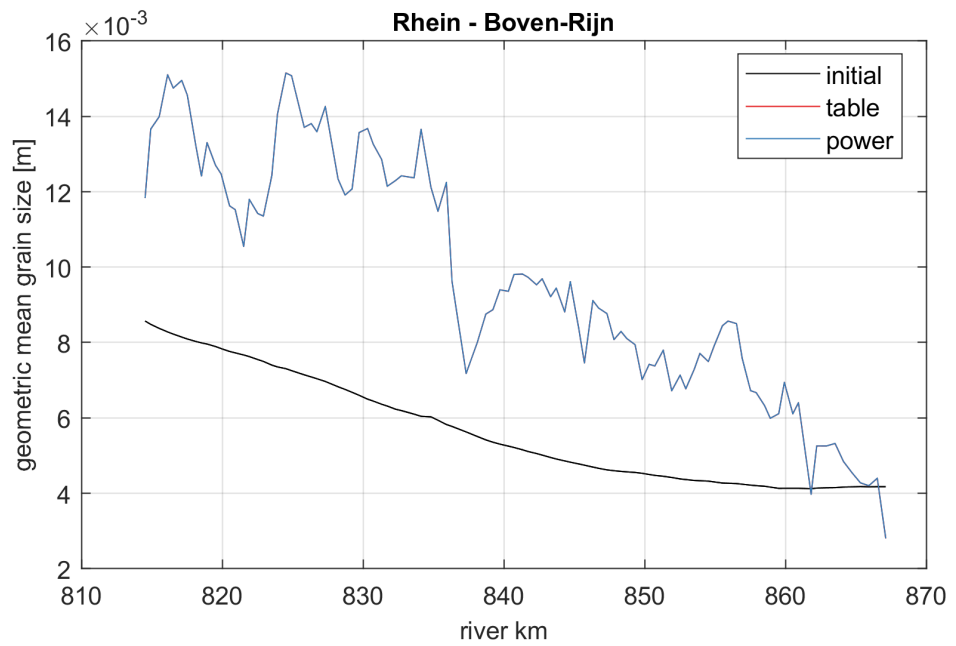
Morphological models for IRM
11203684-015-ZWS-0011_v1.0, Version 0.1, 2020-12-11, Final

Deltares

Figure 202 Mean grain size changes of the calibration run along the Rhein - Boven-Rijn using an unstable nodal-point relation ("table") and a stable one ("power").
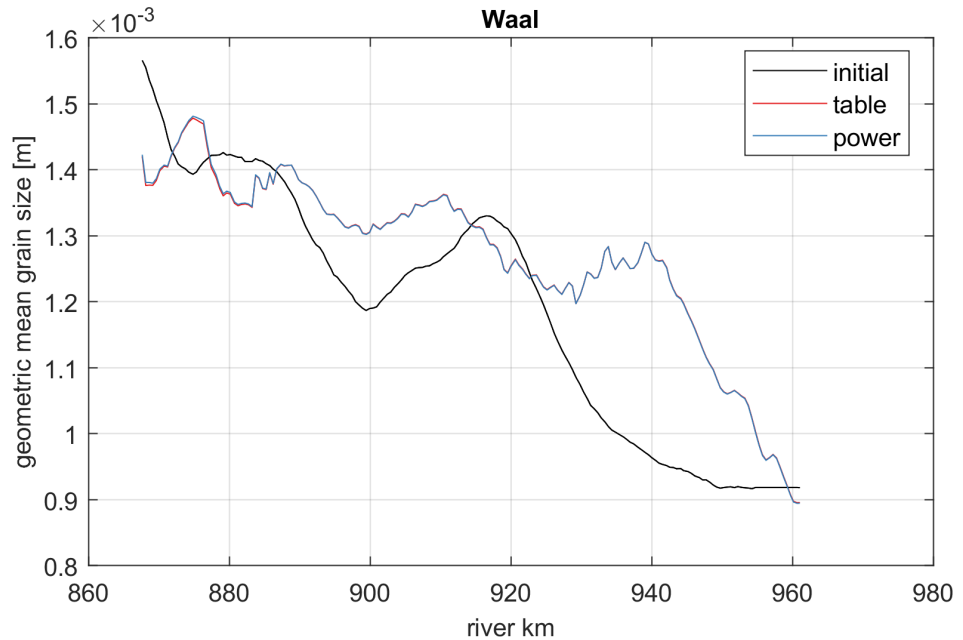

Figure 203 Mean grain size changes of the calibration run along the Waal using an unstable nodal-point relation ("table") and a stable one ("power").
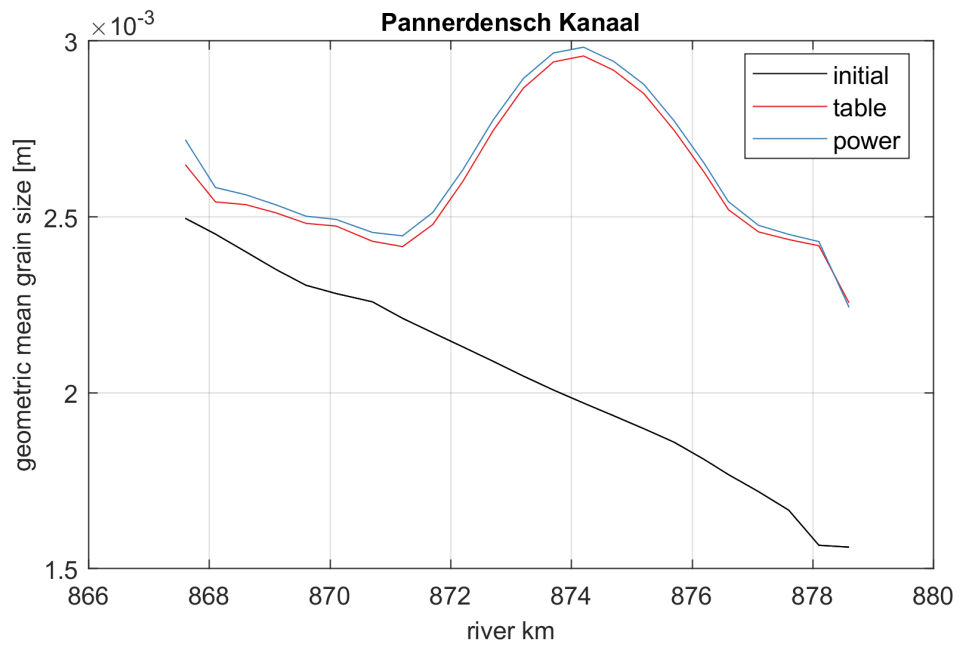
Deltares

Figure 204 Mean grain size changes of the calibration run along the Pannerdensch Kanaal using an unstable nodal-point relation ("table") and a stable one ("power").
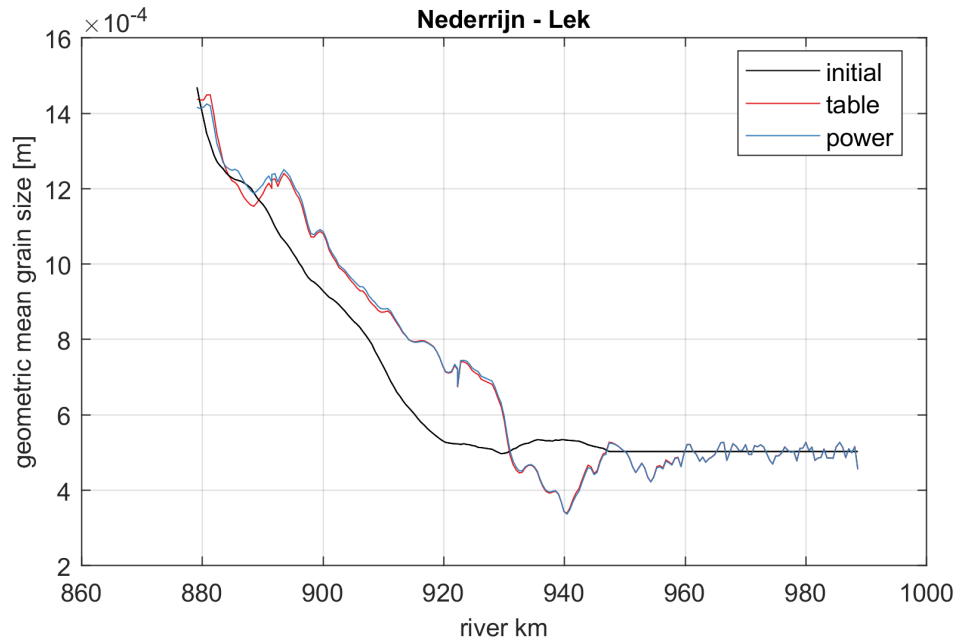

Figure 205 Mean grain size changes of the calibration run along the Nederrijn-Lek using an unstable nodal-point relation ("table") and a stable one ("power").

Morphological models for IRM
11203684-015-ZWS-0011_v1.0, Version 0.1, 2020-12-11, Final
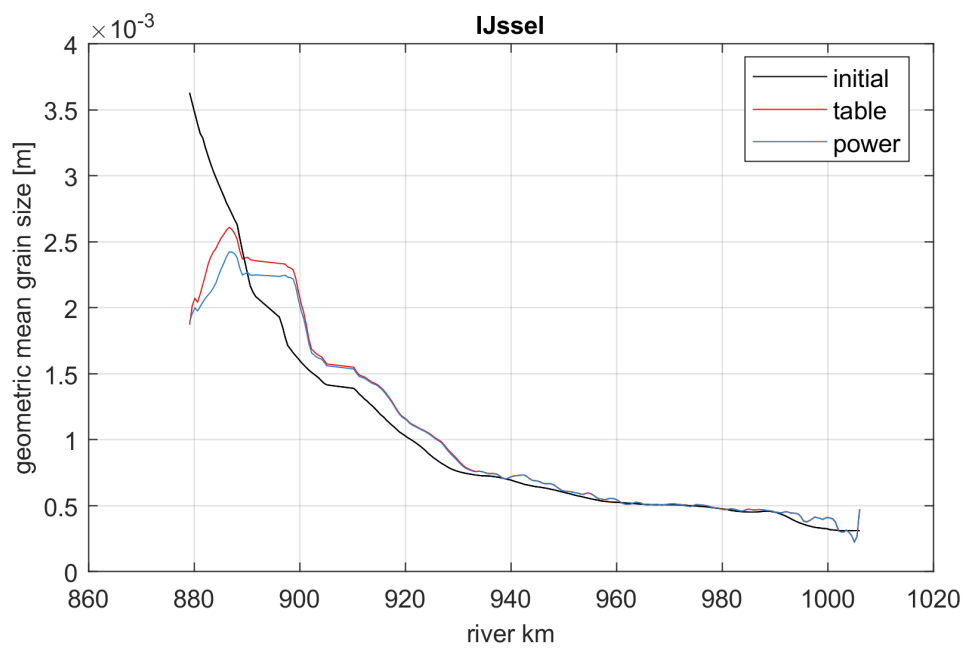
Deltares

Figure 206 Mean grain size changes of the calibration run along the IJssel using an unstable nodal-point relation ("table") and a stable one ("power").